Chitosan-Sericin Blend Membranes for Controlled Release of Drugs

by

Shahabedin Eslami

A thesis

presented to the University of Waterloo

in fulfillment of the

thesis requirement for the degree of

Master of Applied Science

in

Chemical Engineering

Waterloo, Ontario, Canada, 2011

AUTHOR'S DECLARATION

I hereby declare that I am the sole author of this thesis. This is a true copy of the thesis, including any required final revisions, as accepted by my examiners.

I understand that my thesis may be made electronically available to the public.

Abstract

The peak and valley problems caused by oral administration, injection or other conventional methods, call for developing systems that can deliver therapeutics more effectively. As one of the techniques, diffusion-controlled drug release membranes have significant interest due to great ease with which they can be designed to achieve near-zeroth-order release kinetics. Since diffusion is the rate-limiting step in these systems, determining the permeability and diffusivity of drug molecules in the membrane is therefore important in evaluating drug release performance.

This study focuses on the Membrane Permeation Controlled Release (MPC) system, which involves a non-porous (dense) membrane, comprising of two biopolymers, sericin and chitosan. *Ciprofloxacin hydrochloride* and *(+)-cis-diltiazem hydrochloride* were used as hydrophilic model drugs, and *nitro-2-furaldehyde semicarbazone (Nitrofurazon)* was used as a hydrophobic model drug. Permeation experiments were carried out in a semi-infinite reservoir/receptor system to simulate in-vitro drug release.

The intrinsic permeability and diffusivity (P, D) of the drugs through the membranes were determined using a modified time-lag method based on short time permeation and mass balance method based on long time permeation. The partition coefficients K_d of the drugs in the membranes and the swelling degree of the membranes were determined by sorption/desorption experiments. The diffusivities of the drugs were also determined from the sorption/desorption kinetics. Over the experimental ranges tested, the drug concentration and

membrane cross-linking did not have significant effects on these parameters presumably due to the relatively low drug concentrations and mild crosslinkings of the membranes. The diffusivity coefficients of *ciprofloxacin hydrochloride, (+)-cis-diltiazem hydrochloride* and *nitrofurazon* in the membranes were found to be in the range of $(2.0-2.6)\times10^{-9}\pm2.6\times10^{-10}$ cm^2/s, $(2.5-2.6)\times10^{-9}\pm1.1\times10^{-10}$ and $(38-134)\times10^{-9}\pm33.1\times10^{-9}$ (cm^2/s), respectively, and their permeability coefficients were in the range of $(24-29)\times10^{-8}$, $(51-52)\times10^{-8}$ and $(131-169)\times10^{-8}$ (cm^2/s), respectively. The partition coefficients were determined to be around 0.91 ± 0.21, 25 ± 0.12 and 26 ± 0.31, respectively. The diffusivity coefficients determined from sorption experiments for ciprofloxacin hydrochloride, diltiazem hydrochloride and nitrofurazon were found to be in the range of $(3.2-7.6)\times10^{-9}\pm6.3\times10^{-8}$, $(6-10)\times10^{-9}\pm2.6\times10^{-8}$ and $(15-18)\times10^{-9}\pm2.7\times10^{-7}$ (cm^2/s), respectively. Also the diffusivity coefficients determined from sorption experiments for ciprofloxacin hydrochloride, diltiazem hydrochloride and nitrofurazon were in the range of $(20-47)\times10^{-9}$, $(12-24)\times10^{-9}$ and $(11-20)\times10^{-9}$ (cm^2/s), respectively. Nonetheless the differences in the diffusivities calculated from permeation and sorption/desorption experiments are considered to be acceptable, in view of the different experimental techniques used in this work, for the purpose of comparison of the membrane diffusivity and permeability.

Acknowledgements

I would like to express my heart full thanks to my supervisor, Dr. Xianshe Feng for his support, invaluable guidance, constructive criticism, and encouragement throughout my two years of study.

I would also like to extend my gratitude to all my lab coworkers and students who have provided me with support, assistance, and enthusiasm during my research studies. I would like to acknowledge Dr. Gil J. Francisco and Charlie Ulloa, who supported me by all means during the course of studying and research in the lab.

Last but not least, I am very grateful for endless support from my lovely wife, Hengameh, who is always standing beside me at any circumstances. I could not complete this study without her understanding and caring. I wish to express my immense gratitude for her patience and moral support.

I wish to thank the University of Waterloo for providing me the opportunity to conduct meaningful research during my graduate studies and for providing financial support to pursue this research project.

To my Parents Moluk and Hassan who have been encouraging and supporting me during my life

May God give them health and blessings

Table of Contents

List of Figures

.

List of Tables

Chapter 1 Introduction

Controlled drug release technologies have been emerging in the past three decades and have been commercialized in some administrative pharmaceutical therapies. The safety and therapeutic efficiency of drugs are improved by controlling the rate of release, biodegradation and targeting the specific site. These technologies help avoid the "peak and valley" problems caused by oral or injection therapy and provide more effective treatment by delivering drugs steadily in the body over a long period of time (Jin and Song, 2006).

There are two main physical methods of controlled release using polymeric systems controlled release studies, including Membrane Permeation Controlled (MPC) release and Matrix Diffusion Controlled (MDC) release. In the latter, the release profile of drugs usually depends upon such parameters as initial drug loading, size of the matrix, pH of medium and type of mechanism involved (Singh and Ray, 1999). In the membrane permeation controlled (MPC) systems, where the drug is surrounded by a polymeric membrane and diffusion of the drug through the membrane is the rate limiting step, determining the intrinsic permeation parameters such as diffusivity, permeability and partition coefficients is therefore important for evaluation and analysis of drug release profiles (Chen et al., 2010).

Using of polymeric materials either stand alone or as blends for controlled drug release systems have many major advantages, including facilitating and adjustment of a desired drug release pattern, improvement in mechanical properties and controlling drug release mechanisms, improving film formation, protecting the chemical stability of drug, and developing strategies for site targeting(Langer and Peppas, 1981).

Sericin is a natural macromolecular protein derived from silkworm *Bombyx mori*. Sericin protein is very useful because of its unique properties. Resistance to oxidation, and UV radiation, absorbance and releases of moisture and its antibacterial effects made this protein unique and widely applicable. Sericin has the ability to be cross-linked, copolymerized, and blended with other macromolecular materials (e.g. chitosan), to provide materials with improved properties. The materials modified or blended with sericin or sericin composites are well-known as biodegradable and biocompatible materials that can be used for forming articles, functional membranes, fibers, and fabrics (Zhang, 2002).

Chitosan, a modified natural biopolymer with a special structure contains more than 5,000 glucosamine units and is commercially produced from shrimp, shell fish, and crab shell by alkaline deacetylation. Because of the chemical nature of chitosan, it is ready for covalent and ionic modifications which allow extensive adjustment of mechanical and biological properties. Chitosan is an interesting biopolymer, and it can easily be made into a variety of forms including membranes, sponges, fibers, beads, powders and solutions. This biomaterial has a specific chemical structure as a linear polyelectrolyte with a high charge density as well as reactive hydroxyl and amino groups (Muzzarelli et al., 1999, Stoilova et al., 2001, Wang et al., 2003, Zhang M. et al., 2003, Kenawy et al., 2005).

Diltiazem-HCl is one of the calcium channel blockers and is used clinically as a drug choice for cure of hypertension and angina pectoris. Ciprofloxacin-HCl is a synthetic chemotherapeutic antibiotic and used for bacterial infections. Nitrofurazon is also an

antibiotic used most commonly in the form of ointments. The drugs were used as model drug compounds in this study.

This research focused on the preparation and application of novel sericin/chitosan blend membranes for controlled release of drugs. This sericin/chitosan blend was tested for controlled release of drugs for the first time and the main objective of this work was to evaluate the intrinsic permeation properties (e.g. diffusivity, permeability and partition coefficients) of three model drugs using different measurement techniques, including modified time-lag and mass balance methods as well as sorption and desorption kinetic studies.

Scope of Thesis

This thesis work covers the following aspects to provide a systematic study of controlled release of model drugs using sericin/chitosan blend membranes:

Chapter 1 gives an introduction to polymeric controlled release systems, polymeric materials used in controlled release of drugs, and the model drugs used in this study.

Chapter 2 is a review of the background of controlled release of drugs, polymers and biopolymers used for controlled release, and methods for evaluating the intrinsic permeation parameters of drugs in the membranes.

Chapter 3 deals with the materials, experimental setup and procedures used in this study

Chapter 4 presents the results obtained from this study and discussion of the results.

Finally, the general conclusions derived from the study, and recommendations of future work to be done for further studies are presented in chapters 5 and 6, respectively. The sample calculations and some additional experimental data are presented in the appendix.

Chapter 2 Literature Review

2.1 Controlled Release Systems

Recent controlled-release applications include a vast variety of areas including medical, agricultural, food and household products**.** Controlled-release is very important in many fields. For instance, in agriculture, the controlled release of pesticides and fertilizer using polymeric films makes it possible to shorten treatment times, which leads to labor saving and the prevention of phytotoxicity and excess release of agrochemicals into the environment.

The history of controlled release of drugs goes back to the mid 1960s when Judah Folkman, a MD at University of Harvard, discovered that a silicone tube could be implanted in rabbits and acted as a constant-rate drug delivery device. It was the first time that zeroth-order controlled drug delivery implant *in-vivo* was suggested (Hoffman, 2008). For a long period of time, researchers have been focusing on the synthesis or discovery of potent drugs with new or improved biological activity. While this continues to be an important area of research, increasing attention is being devoted to the manner in which these drugs are delivered. One of the areas in which chemists and chemical engineers are contributing to is the design and development of systems which controls drug delivery. Such delivery systems offer numerous advantages over conventional methods. Since the 1980s, a major focus of drug-related research has been devoted to drug delivery. Recent growth of significant interest in controlled-release relates to solving the general dose-delivery problems. The “peak and

valley" problems, caused by oral administration, injection or other conventional methods, call for developing systems that can deliver therapeutics more effectively.

In the past three decades, many polymer- drug systems were investigated. Using polymeric carriers for drugs may lead to a continuous release of drug for a long period of time. One way that has been considered as a means of controlling drug delivery is the incorporation of drugs in solid polymers. Controlled-release polymeric systems can be classified based on the mechanism of drug release. Diffusion of drug molecules in the polymer may be the rate limiting step of the release process. The systems designed based on the diffusion of drugs in polymers are called diffusion-controlled systems. If chemical reaction at the interface of the polymer and the dissolution medium can be the rate controlling step it will be called a chemically-controlled system. Countercurrent diffusion of dissolution medium at constant penetration rate in the polymer matrix can also be the rate limiting factor, and such a system is called swelling-controlled system. Sometimes an external field is responsible for the release of drugs and magnetically-controlled release systems are an example of such systems (Langer and Peppas, 1981).

2.2 Diffusion-Controlled Systems

Diffusion-controlled systems are the most widely used. Several diffusion controlled release systems have been developed and marketed since the 1970s, though first trace of these studies goes back to the early 1960s. There are two types of diffusion controlled release systems, including Matrix Diffusion Controlled systems (MDC) and Membrane Permeation

Controlled systems (MPC) or Reservoir systems. MDCs may be divided into two categories: (i) degrading polymer matrix, which degrades or dissolves in the system, and (ii) non-degrading polymer matrix where drug molecules diffuse through the polymer. MPCs may also be divided into two categories depending whether non-porous membranes or micro-porous membranes are used in the controlled release systems (Jain et al., 2003; Langer and Peppas, 1981). Figure 2-1 illustrates the diffusion controlled systems schematically.

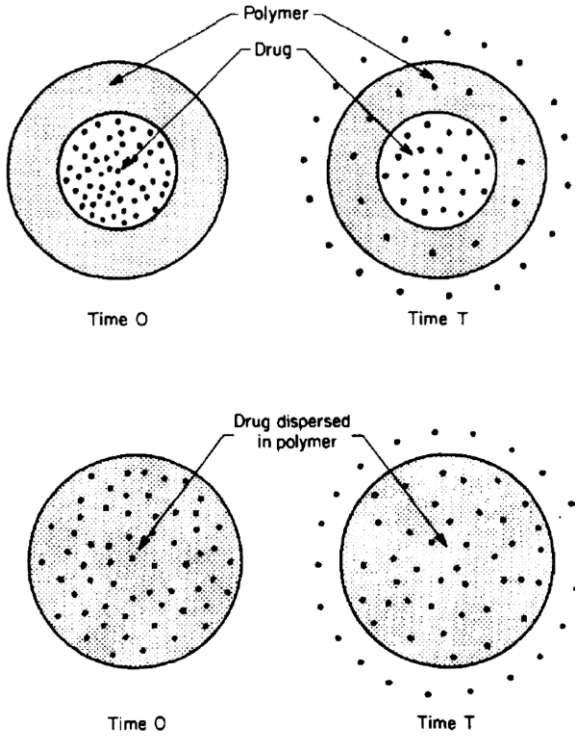

Figure 2-1 Idealized diffusion-controlled reservoir release system (top),
Idealized diffusion-controlled matrix release system (bottom)(Langer and Peppas, 1981)

2.3 Reservoir Systems (Membrane Controlled Permeation)

In such systems, a polymeric film surrounds the drug and the diffusion of the drug through the film is the rate limiting step controlling the release rate (See Figure2-1). Membranes, capsules, microcapsules, and hollow fibers can be used in these systems as the surrounding polymer. Among these, membranes and polymeric films have proven to be of greatest value and attracted most attentions in controlled-release applications. In fact, most products developed or marketed to date are membrane-enclosed reservoir systems. At present, a wide range of polymers (both synthetic and natural biopolymers) are used for this type of release systems. These polymers must be relatively inert, do not readily biodegrade, be nontoxic, have good tissue biocompatibility, and be generally permeable only to low molecular weight solutes, in order to be suitable for clinical use. A key problem in design of such a system, from a pharmaceutical point of view, is to reach the zeroth-order release rate. The most important advantage of membrane controlled permeation systems is the ease with which they can be designed to achieve the zeroth-order release kinetics. Diffusion through membranes has been investigated extensively and many reviews have been published (Crank, 1975; Crank and Park 1968).

2.4 Polymers Used for Controlled Drug Release

Because of the vast variety of polymer structures, classifying polymers for controlled release applications is not an easy job. Generally, the polymers may be classified into biodegradable and non-biodegradable. Biodegradable polymers have attracted significant attention for drug

delivery systems because of their excellent biocompatibility. On the other hand, for in vivo applications non-biodegradable polymers need retrieval after introduction into the body. Table 2-1 summarizes the polymers mostly used in controlled release systems recently.

Table 2-1 Summary of Polymers Based on their Application in Controlled Release of Drugs (Uhrichetal., 1999)

Polymer	Applications
Polyethylene	Zeroth-order controlled by diffusion from matrix.
Polypropylene	Ophthalmic drug delivery applications.
Polyvinyl chloride	Membrane devices for controlled release of volatiles in the air and non-volatile into solutions.
Polyvinyl alcohol	Bioadhesive hydrogels.
Polyethylene-vinyl acetate	Ultrasound-stimulated release for cancer chemotherapy
Polyacrylic acid	Bioadhesive polymer.
Polyacrylamide	Component of photosensitive delivery
Polyethylene glycol	Used as Polymer-drug conjugates
Poly(dimethyl siloxane)	Controlled release of rifampicin
Poly (L-lactic acid)	Biomedical application (biodegradable)
Cyclodextrin	Drug penetration enhancer-Drug shell
Chitosan	Tablet coatings-Transdermal patches
Sericin	Wound healing-cosmetics
Poly(methyl methacrylate)	Drug reservoir gel

2.5 Sericin

Sericin is a natural silk protein, which is a highly hydrophilic macromolecule and derived from silkworm *Bombyx mori* cocoons in a process called degumming. Sericin is comprised of 18 amino acids. The molecular weights of sericin protein range from 24 to 400 kDa with predominant amino acid groups being serine (40%), glycine (16%), glutamic acid, aspartic acid, threonine and tyrosine. Thus it consists of polar side chains of hydroxyl, carboxyl and amino groups that enable easy cross-linking, copolymerization and blending with other polymers to form improved biodegradable materials (Takasu *et al*., 2002). Sericin represents 20-30% of total cocoon weight. The main role of sericin is to hold and bind the fibroin fibers together. Sericin occurs mainly in an amorphous random coil and to a lesser extent, in a β-sheet structure. The randomly coiled structure easily changes to β-sheet structure, as a consequence of repeated moisture absorption and mechanical stretching (Padamwar M. N. et al., 2005).

Sericin can be divided into three types, based on their solubility. Sericin type A is soluble in hot water. It is comprised of 17.32% of nitrogen and amino acids like, serine, threonine, glycine, and aspartic acid. Type B contains 16.8% of nitrogen and it turns to type A by acid hydrolysis. Sericin type C is the innermost layer, adjacent to fibroin and is insoluble in boiling water and can be removed from fibroin by treatment with hot dilute acid or alkali solutions. The most abundant molecular conformation of water soluble sericin is random coils, whereas the β-sheet structure is more difficult to dissolve in aqueous solutions.

Sericin proteins with lower molecular weights (<20 kDa) or sericin hydrolysates are usually used in cosmeticeutical products such as skincare and hair-care products, health products, and medications. Sericin with higher molecular weights (>20 kDa) are mostly used as medical biomaterials, degradable biomaterials, compound polymers, functional biomembranes, hydrogels, and functional fibers and fabrics (Dash *et al*., 2007).

The structure of sericin, especially in the two convertible forms (e. g. water-soluble and insoluble) gives it unique properties. Table 2-2 summarizes some properties of sericin.

Table 2-2 Properties of Sericin and Characteristics (Padamwar and Pawar, 2004)

Property	Characteristics
Gelling property	Sericin due to its solubility can be in the form of random coil or β-sheet structure. Random coil is soluble in boiling water and by decreasing the temperature the random coil turns to β-sheet structure. So it converts to a gel form.
Sol-Gel Transition	Sericin has shown a sol-gel property due to its ease of dissolution in water at 50-60°C and turning to gel form as cooled.
Isoelectric pH	As there are more acidic than basic amino acid residues the isoelectric point of sericin is about 4.0.
Solubility of sericin	By transforming of sericin structure from random coil into β sheet, its solubility in water decreases, and will increase by addition of poly(Na acrylate). Its solubility in water decreases as polyacrylamide, formaldehyde, or resin finishing agents are added.
Molecular Weight	Extracting sericin using hot water shows molecular weight of 24,000, whereas sericin extracted by spray-drying have the molecular weight of 5,000-50,000. Its molecular weight ranges 300-10,000 when it is enzymaticly treated, and ranges above 50,000 when it is extracted with aqueous urea at 100°C

Blending sericin with some resins may produce environment-friendly biodegradable polymers (Annamaria et al., 1998). Sericin blended with polyurethane foams gives excellent moisture absorbing and desorbing properties which turns it to a good sol-gel material (Nomura et al., 1995). The sericin/polyurethane blended foam has the moisture absorption/desorption capacity of 2-5 times greater than that of the control. The polyurethane/sericin blend contains biodegradable sericin segments, and is capable to turn into films, fibers, and molded objects (Fujita et al., 1998; Sumitomo et al., 1997; Zhang, 2002).

Membrane separation processes such as reverse osmosis (RO), dialysis, ultra filtration, and microfiltration are worldwide used in many industries including water desalination, production of pure water, and bioprocessing (Chisti, 1998). Sericin can be used to make membranes for use in separation processes. For instance, it's reported by Hirotsu and Nakajima (1988) that silk membrane can be used for dehydration of alcohol. It is hard to make a pure sericin membrane, but some membranes are reported to be made readily from sericin in a cross-linked form, blended with other polymers, or copolymerized with other substances. Due to a large number of amino acids with neutral polar functional groups in sericin, sericin-containing films are highly hydrophilic. Sericin composite membranes are generally permselective for water in an aqueous-organic liquid mixture.

As mentioned above pure sericin film is difficult to form, but sericin based films can be prepared by attaching to another matrix. Nakajima (1994) showed that sericin films used in a liquid crystal can uniformly orient the liquid crystal molecules to provide better quality liquid

crystal displays. Also, it is reported that the surfaces of refrigeration equipment can be coated by sericin to achieve its antifrosting action (Tanaka, 2001).

A silk based wound dressing has been developed by (Tsubouchi, 1999a), which has healing effects and can be peeled off without damaging the new tissue. Subsequently, the wound dressing was made with a mixture of fibroin and sericin (Tsubouchi, 1999b). Membranes made of sericin and fibroin, are as an effective substrate for cell proliferation and adhesion in animal cells culture and can be used as in tissue engineering. Minoura et al. (1995) and Tsukada et al. (1999) investigated the cell attachment and growth of mammalian cells on the films made of sericin and fibroin.

2.6 Chitosan

Chitosan is a natural polycationic polymer with properties and characteristics. It contains more than 5,000 glucosamine units and is commercially produced from chitin by alkaline deacetylation. Chitosan is also found in some microorganisms, yeast and fungi. Chitin, a naturally abundant mucopolysaccharide, and the supporting material of crustaceans, insects, etc., is well known to consist of 2-acetamido-2-deoxy-β-D-glucose through a β (1→4) linkage. Chitin is a white, hard, non-elastic, nitrogenous polysaccharide (Rabea et al, 2003). Chitosan, from deacetylation of chitin, is a linear polysaccharide, composed of glucosamine and N-acetyl glucosamine units linked by β (1–4) glycosidic bonds. The content of glucosamine is related to the degree of deacetylation. Chitosan is available in a wide range of molecular weights and degrees of deacetylation. Depending on the source and preparation

procedure, its molecular weight may vary from 300 to over 1,000 kDa with a deacetylation degree from 30% to 95% (Dornish et al., 2001; VandeVord et al., 2002). The schematic structures of chitin and chitosan and the preparation of chitosan from chitin are illustrated in Figure 2-2.

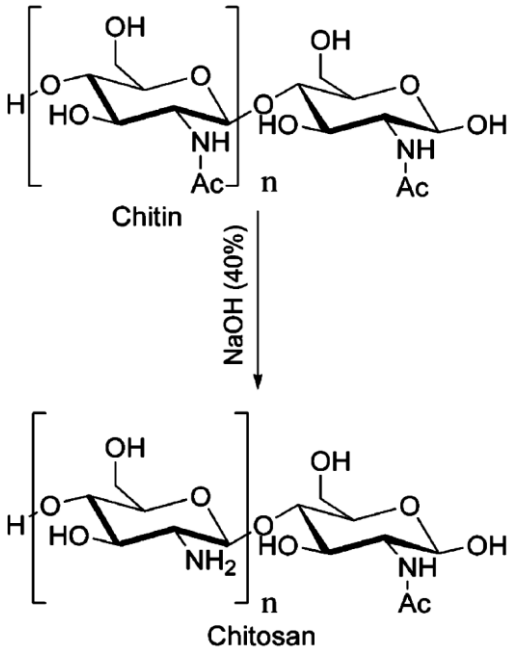

Figure 2-2 Preparation of chitosan from chitin (Rabea et al., 2003)

Chitosan in a crystalline form is normally insoluble in aqueous solutions above pH 7. However, it is soluble in most dilute organic acidic solutions at pH<6.0, including acetic, formic, tartaric and citric acids. The protonated free amino groups on glucosamine facilitate solubility of the molecule. Chitosan has three types of reactive functional groups, an amino group and a primary and secondary hydroxyl groups. These functional groups allow modification of chitosan by graft copolymerization for specific applications. Chitosan may

also be subjected to covalent and ionic modifications which allow for extensive adjustment of mechanical and biological properties. Chitosan is an interesting biopolymer since it is readily available and can be made into a variety of forms (e. g. membranes, sponges, fibers, beads, powders and solutions). Chitosan is a linear polyelectrolyte with a high charge density, having reactive hydroxyl and amino groups (Muzzarelli et al., 1999; Stoilova et al., 2001; Wang et al., 2003; Zhang et al., 2003; Kenawy et al., 2005). Chitosan has also been reported for a wound healing biomaterial (Malette et al., 1983). It can also reduces serum cholesterol levels (Nagyvary et al., 1987) and stimulate the immune system. Chitosan is an excellent flocculent, adhering to negatively charged surfaces with biocompatible, non-toxic, biodegradable and fungicidal activities. Furthermore, it is possible to modify chitosan as an antimicrobial polymer, making it a very attractive biomaterial.

Controlled release technology and drug delivery systems are the emerging sciences of the 1980s, and they are commercially available for certain therapeutics applications. Designing a release system for a target agent into a specific medium for a long time is a key factor for the controlled delivery system. Chitosan a natural biopolymer appears to be an ideal candidate for controlled release applications. There is a great deal of work reported in literature confirming that chitosan is one of the best choices for drug delivery systems.

Nakatsuka and Andrady (1992) used chitosan blended with poly(vinyl alcohol) (PVA) with different degrees of crosslinking in the form of membranes, and they evaluated their applications in controlled release of *Vitamin B-12*. These chitosan membranes showed acceptable permeability, diffusivity, and hydrogel properties when crosslinked or blended

with PVA. Their results showed that the hydration of chitosan hydrogels as measured by the swelling ratio can be altered over a wide range, either by crosslinking or by blending with PVA. Kim et al. (1992) used crosslinked PVA/chitosan blend membranes for controlled release of *Riboflavin* and *Insulin*. It is shown that the permeability and diffusivity of the blended membranes have pH dependencies and increase with an increase in the glucose concentration. In controlled release of Insulin using the membranes, the desired release rate can be achieved by means of crosslinking. Jin and Song (2006) reported that the chitosan and chitosan/poly(ethylene oxide) blend films crosslinked by genipin are pH sensitive and have desirable mechanical properties. These characteristics and film's non-toxic nature make it ideal for use in controlled release of drugs. *Vitamin* B_{12} and *Eleutherococcus Sentisocus* were used as model drugs. Silva et al. (2006) used fosfosal, an anionic model drug, to study the permeability of chitosan membranes to small molecular-weight water-soluble molecules. They reported that chitosan modification have a strong influence on the permeability of the anionic model drug. Thacharodi and Rao (1993) studied the permeability characteristics of a chitosan membrane using an anti-hypertensive drug nifedipine, and they investigated the effect of crosslinking on the permeability of membrane. Singh and Ray (1999) modified a chitosan membrane by graft copolymerization and used it to study the controlled release of glucose as a model drug. They studied the release characteristics of glucose as a function of the degree of grafting in the chitosan membranes. The permeability coefficient of glucose through the grafted membranes is reported to be in the order of $10^{-6} – 10^{-7}$ cm^2/s. Berthold et al. (1996) used chitosan in a microsphere form as the drug carriers and the release kinetics of

model drugs from the microspheres was studied. They found that the drug release from the microspheres is dependent on the drug-polymer ratio. Wang et al. (2007) studied the controlled release of *ciprofloxacin hydrochloride* from chitosan/poly(ethylene glycol) blend films. Chemical and morphological characterizations confirmed that there is a good compatibility between the membrane matrix and ciprofloxacin hydrochloride because of their strong interactions (e.g. hydrogen bonding and ionic interactions). The mechanical property of the membrane was also good. Their research showed that the loading amount of the drug to the membrane can be controlled by the ratio of chitosan/PEG and the degree of crosslinking.

The main properties of chitosan and its potential applications are summarized the Table 2-3.

Table 2-3 Principal properties of chitosan in relation to its application (Marguerite Rinaudo, 2006)

Principal applications	Principal characteristics
Surgical sutures	Biocompatible
Dental implants	Biodegradable
Artificial skin	Renewable
Rebuilding of bone	Film forming
Corneal contact lenses	Hydrating agent
Time release drugs for animals and humans	Nontoxic, biological tolerance
Encapsulating material	Hydrolyzed by lyzosyme, Wound healing properties, Efficient against bacteria, viruses, fungi
Agriculture	Defensive mechanism in plants, Stimulation of plant growth, Seed coating, Frost protection, Time release of fertilizers and nutrients into the soil.
Water & waste treatment	Flocculant to clarify water (drinking water, pools), Removal of metal ions, Ecological polymer (eliminate synthetic polymers), Reduce odors
Food & beverages	Not digestible by human (dietary fiber), Bind lipids (reduce cholesterol), Preservative, Thickener and stabilizer for sauces, Protective, Fungi static, antibacterial coating for fruit
Cosmetics & toiletries	Maintain skin moisture, Treat acne, Improve suppleness of hair, Reduce static electricity in hair, Tone skin, Oral care (toothpaste, chewing gum)
Biopharmaceutics	Immunologic, anti tumor, Hemostatic and anticoagulant, Healing, bacterio static

2.7 Sericin and Chitosan Blend Film

Srihanam et al. (2009) have attempted to investigate films from chitosan/sericin blends as well as the native sericin and chitosan films. The morphologies of the films were observed using Scanning Electron Microscope (SEM). They analyzed the secondary structures of the films by FTIR spectroscopy. Also they investigated the transparency of the films using UV-Visible spectroscopy. The native sericin film showed absorption bands of at 1684 cm^{-1} (amide I), 1559 cm^{-1} (amide II), while the blend sericin/chitosan film showed wide absorption bands at about 1640 cm^{-1} (amide I), 1534 cm^{-1} (amide II) and 1100-1080 cm^{-1}. For pure chitosan film, the FTIR spectrum showed an absorption band at 1650 cm^{-1} with shoulder bands at 1578 and 1103 cm^{-1}. These results indicate that the blend film composed of sericin and chitosan has an amide I band in the range of the carbonyl groups. It is illustrated in their work that sericin and chitosan are compatible. Also they showed that two materials are miscible together. The FTIR results indicated that most of the films were composed of random coils and β-sheets. It appears that the blend film of sericin and chitosan did not change the interamolecular structure when compared to the native films.

Sericin-based film properties are dependent on components used to form film, which can used to tailor the desired film flexibility and controlling the permeability of the films. Sericin is removed as waste during the degumming process of the silk manufacturing. Sericin can be utilized to make biofilms as a value-added product developed from the wastes. Therefore it represents a significant source of profit, not only having beneficial effect of waste reduction for pollution prevention but also having healing effect which accelerates the wound healing

process and improving the moisture adsorption of the film. Sericin based film also have shown good oxygen permeability which is an essential characteristic for wound dressing or drug loaded patches that will be placed on top of skin for long hours (Zhang, 2002).

2.8 Diffusion in Membranes

The mathematical model of diffusion in polymers, more specifically in membranes is based on the hypothesis that the rate of diffusion through a unit area of the membrane is proportional to the concentration gradient of diffusing substance across the membrane. The diffusion rate of the penetrant through a membrane is determined by the Fick's law of diffusion. Consider drug diffusion through a flat membrane, shown in Figure 2-3

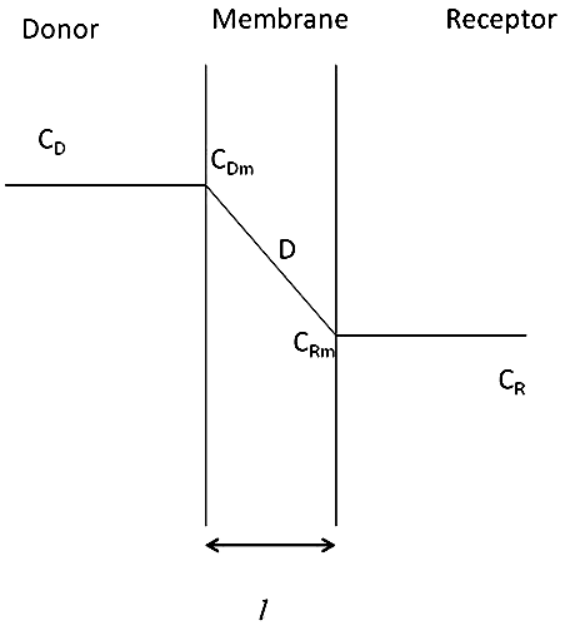

Figure 2-3 Concentration profile of drug across a membrane

$$\boldsymbol{J = -D\frac{\partial C}{\partial x}} \qquad (\mathbf{2-1})$$

where J is the rate of molar flux per unit area of the membrane, $\frac{\partial C}{\partial x}$ is the concentration gradient across the membrane, and D is the diffusion coefficient in the membrane. By considering the mass balance of an element of volume it can be shown that the differential equation of diffusion takes the form:

$$\frac{\partial C}{\partial t} = D\left(\frac{\partial^2 C}{\partial^2 x} + \frac{\partial^2 C}{\partial^2 y} + \frac{\partial^2 C}{\partial^2 z}\right) \qquad (2-2)$$

where D is constant and independent of concentration.

Often diffusion occurs effectively in one direction only. Assuming the concentration gradient is one dimensional along the *x*-axis, the Equation 2-2 reduces to:

$$\frac{\partial C}{\partial t} = D\left(\frac{\partial^2 C}{\partial^2 x}\right) \qquad (2-3)$$

Equations 2-1 and 2-3 are referred to as Fick's first and second laws of diffusion respectively.

For a constant diffusion coefficient and constant membrane thickness (i.e., there is no change in membrane thickness when drug concentration changes during the course of permeation), equation 2-1 can be integrated to yield:

$$J = -D\frac{\Delta C}{l} \qquad (2-4)$$

where l is the membrane thickness. To maintain a constant flux, the trans-membrane concentration difference, ΔC must be kept constant. This can be done by maintaining a constant, high drug concentration at the donor side ($C_D \gg C_R$) of the membrane and keep the receptor side at sink condition($C_R \cong 0$). To accomplish these conditions, the drug must be loaded at a high level. As long as the drug concentration is high enough at the donor side compared to receptor, zeroth-order release will occur. Since diffusion is a key step which controls the rate of release in such systems, determination of intrinsic permeation and diffusion coefficients of the drug molecules in the membrane is important in design of controlled release systems (Langer and Peppas, 1981; Chen et al., 2010).

The diffusion of drugs through a membrane can be divided into three stages. At an initial stage of permeation, the diffusion is at an unsteady-state and the mass transfer rate and concentration profile in the membrane vary with time. This stage is followed by a pseudo-steady-state permeation when the concentration gradient across the membrane is fully developed and both the concentration profile in the membrane and the rate of flow across the membrane become constant. The last stage is again an unsteady-state permeation during which the drug concentration at the receptor side builds up significantly and the concentration gradient in the membrane begins to decreases significantly with time. At this stage, the zeroth-order diffusion kinetics does not hold anymore.

2.8.1 Time-Lag Method

At the instant that the diffusion starts at one side of the membrane and prior to establishment of a constant concentration gradient across the film, both concentration profile in and the diffusion rate across the membrane vary with time. Assume that the diffusion coefficient of the drug in the membrane is constant and independent of concentration. If the membrane is initially free of any drug molecules and the drug diffused to the receptor side is continuously removed, the total amount of drug Q passing through the membrane at time t is given by (Crank and Park 1968):

$$\frac{Q}{A\ l\ C_{Dm}} = \frac{Dt}{l^2} - \frac{1}{6} - \frac{2}{\pi^2}\sum_{1}^{\infty}\frac{(-1)^n}{n^2}\exp\left(\frac{-Dn^2\pi^2 t}{l^2}\right) \qquad (2-5)$$

where l is the membrane thickness, C_{Dm} is drug concentration in the membrane at the donor side, and A is the membrane area.

The graph of Q versus t is illustrated in Figure 2-4, which shows the accumulative amount of drug released at different times. As time passes the permeation gradually reaches the steady-state and the exponential terms in the equation 2-5 will be negligible.

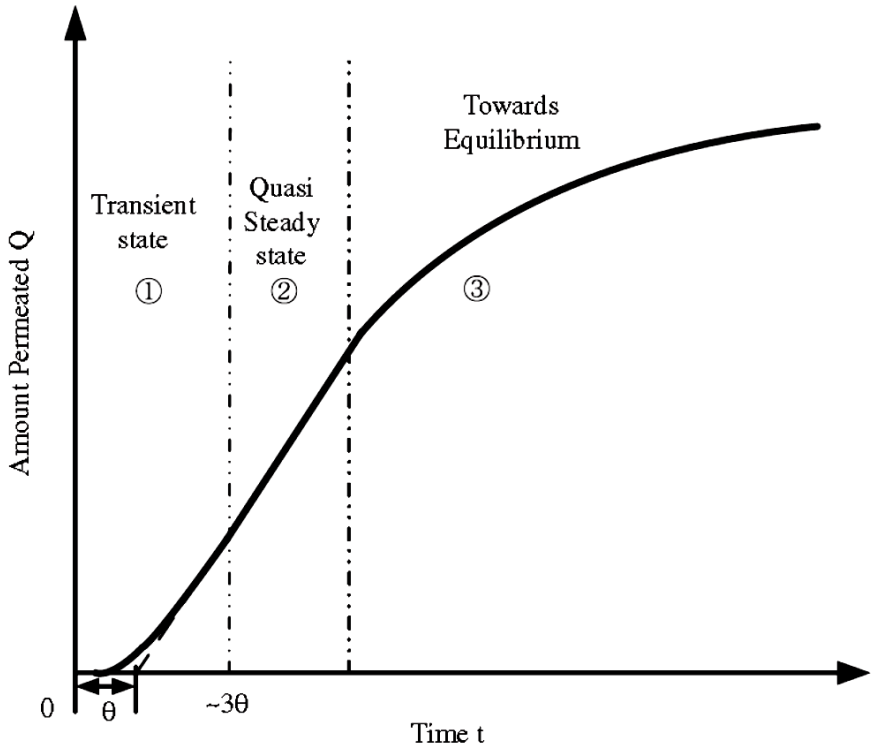

Figure 2-4 Quantity of permeant received in the receptor side of the membrane to illustrate the time-lagθ due to initial transient permeation (Chen et al., 2010)

The rate of pseudo steady state permeation through the membrane thus becomes

$$Q = \frac{ADC_{Dm}}{l}\left(t - \frac{l^2}{6D}\right) \qquad (2-6)$$

which yields a straight line, with an intercept, θ, when interpolated on the *t*-axis. θ is called time-lag (Crank and Park 1968), and is given by

$$\theta = \frac{l^2}{6D} \qquad (2-7)$$

In non-porous polymer films (dense membranes), drug transport across the film occurs via a solution-diffusion mechanism. The drug passes through the membrane by a mechanism

involving drug dissolution on the membrane surface, followed by drug diffusion across the membrane and then drug release to the receptor side. Assuming a linear relationship between the drug concentration in the membrane at donor side C_{Dm} and the equilibrium drug concentration in the solution C_D, that is, $C_{Dm} = KC_D$, then Equation 2-7 can be rewritten as

$$Q = \frac{PAC_D}{l}\left(t - \frac{l^2}{6D}\right) \qquad (2-8)$$

where, P is the permeability coefficient of the drug through the membrane at the steady state and it is equal to product of diffusivity coefficient and partition coefficient of the drug in the membrane:

$$P = DK \qquad (2-9)$$

The permeability coefficient P can therefore be determined from the slope of pseudo steady-state segment of the (Q vs. t) plot. The partition coefficient K can further be calculated from Equation 2-9. It must be mentioned that the time-lag calculated using Equations 2-7 is the intercept of the (Q vs. t) plot on the t-axis obtained by extrapolation of steady state permeation data based on Equation 2-8. As mentioned earlier, Equations 2-7 and 2-8 are based on the following assumptions: (i) the diffusion coefficient of the drug in membrane is constant and independent of concentration, (ii) the membrane initially is completely free of any drug molecules, (iii) The drug concentration at the donor side ($C_D \gg C_R$) is constant, and (iv) The concentration at the receptor side is kept at sink condition($C_R \cong 0$).

2.8.2 Mass Balance Method

For systems in which finite conditions hold at both source and receptor side of the membrane, there is an alternative method for the determination of permeability coefficient. This method is in fact based on mass balance. The concentrations at the donor and receptor sides of the membrane vary with time, and applying mass balance for the permeant at both sides of the membrane

$$V_D(C_0 - C_D) = V_R C_R \qquad (2-10)$$

where V_D is the volume of the donor side, V_R is the volume of the receptor side and C_0 is the initial concentration of the drug in the donor. As mentioned above, if the system has finite donor/receptor conditions, the drug concentrations at both sides of the membrane change with time. Further, the rate of drug permeation through the membrane is given by

$$V_R \frac{dC_R}{dt} = \frac{AP}{l}(C_D - C_R) \qquad (2-11)$$

Integrating Equation 2-11 from $t = 0$ to $t = t$ and rearranging the equation we will have

$$-\ln\left[1 - \left(1 + \frac{V_R}{V_D}\right)\frac{C_R}{C_D}\right] = \frac{PA}{l}\left(\frac{1}{V_D} + \frac{1}{V_R}\right)t \qquad (2-12)$$

This equation is widely used in the literature using a setup with equal volumes of donor and receptor (i.e. $V_D = V_R$), namely the Franz Diffusion Cell. Equation 2-12 can be rewritten as

$$-\ln\left(\frac{m_0 - V_t C_R}{m_0}\right) = \frac{PA}{l}\left(\frac{1}{V_D} + \frac{1}{V_R}\right)t \qquad (2-13)$$

where V_t is the total volume of the donor and the receptor compartment, $V_t = (V_D + V_R)$, and $m_0 (= V_D C_0)$ is the total initial amount of the drug at donor side. The permeability coefficient P can be calculated by plotting the logarithmic term of Equation 2-11 versus time, t which gives a straight line. The permeability can be determined from the slope of this straight line. The mass balance method is a more general form for determination of permeability coefficient. This method is also based on some assumptions such as (i) the amount of drug molecules within membrane is negligible, and (ii) the drug molecules is received in the receptor instantly as it leaves the donor compartment. In other words, membrane should be thin enough so that the time required to establish a steady concentration gradient across the membrane neglected (Chen et al., 2010; Tavelin et al., 2002; Jin and Song, 2006).

Chen et al., (2010) investigated both methods (i.e. time-lag and mass balance) for determination of intrinsic permeation parameters. By examining the assumptions underlying both methods, they attempt to show that a violation of those assumptions will lead to a significant error in determination of permeation parameters. They pointed out that the time lag is neither the time that the drug molecules take to pass through membrane nor the time to reach steady state as misperceived by other researchers. It is also stressed that the permeation experiments should be conducted for a sufficient long time, because the time lag is calculated

by extrapolating the steady-state permeation data, which occurs in theory after three times of time-lag. Otherwise at a shorter time of permeation test, the diffusivity coefficient might be underestimated. Chen et al., (2010) also clarified that for calculation of permeability coefficient using the mass balance method, the data at the early stage of permeation (which are affected by transient permeation significantly), must be excluded. Otherwise the permeability coefficient would be underestimated. Figure 2-5 shows how the slope of the logarithmic term in the Equation 2-13 changes with time at transient permeation stage.

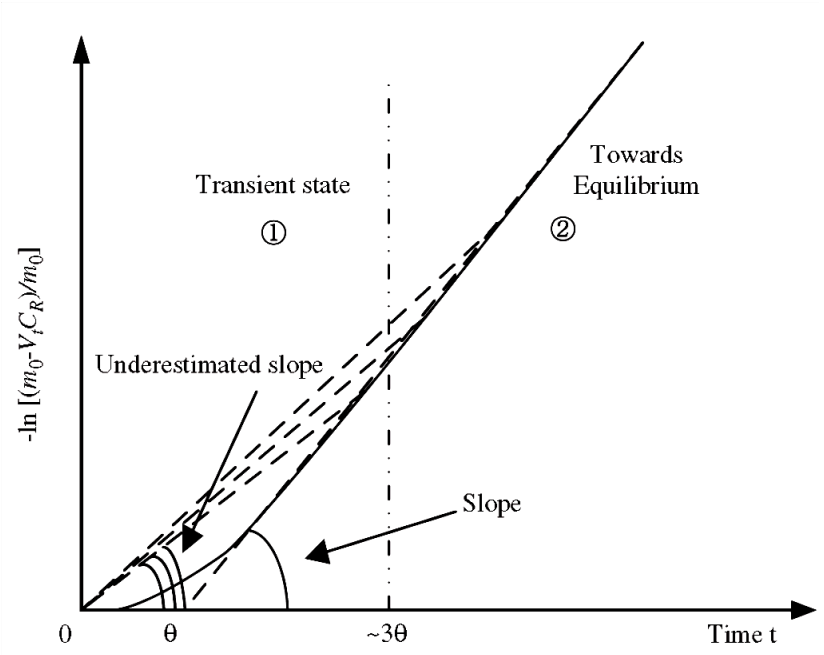

Figure 2-3 Illustration of underestimation in permeability calculated on the basis of the conventional mass balance method (Chen et al., 2010)

In view of what discussed the above, they proposed an improved approach for determination of intrinsic permeability and diffusivity relevant to controlled release by combining the two methods and taking advantages of the complementary characteristics of the time-lag and the

mass balance techniques. Basically the short-time permeation data are analyzed using the time-lag method, and the long-term permeation data are evaluated with the mass balance method. First, one needs to determine an upper limit of time beyond which the concentration variation is no longer valid for time-lag method which requires infinite source and sink conditions. A plot of Q vs. t should be constructed excluding the long term permeation data. An upper limit η must be assigned below which a small change in trans-membrane concentration is acceptable to relax the assumptions underlying the time-lag method:

$$\left(1 - \frac{C_D - C_R}{C_D - C_0}\right) \leq \eta \qquad (2-14)$$

Combining Equation 2-14 with Equation 2-10 gives

$$C_R \leq \eta\, C_\infty \qquad (2-15)$$

where $C_\infty (= {}^{m_0}/_{V_t})$ is the equilibrium concentration that will be reached at an infinite time. A series of η values (e.g., 2%, 5%, 10%) may be set to define an upper limit of C_R by Equation 2-15.

The next step in the evaluation of permeability coefficient from the long time permeation data is based on the time-lag obtained from the short term permeation data. An onset point should be determined at which the impact of transient permeation at early stage no longer affects the validity of the mass balance analysis. The effect of transient permeation is considered to be vanished after more than three times of time-lag ($t_0 > 3\theta$). The mass balance for the drug across the membrane after ($t_0 > 3\theta$) yields:

$$V_D(b - C_D) = V_R(C_R - a) \qquad (2-16)$$

where a and b are two parameters describing the onset point concentrations. Integrating Equation 2-11 from $t = t_0$ to $t = t$ will give

$$-\ln\left[1-\left(1+\frac{V_R}{V_D}\right)\frac{(C_R-a)}{(b-a)}\right]=\frac{PA}{l}\left(\frac{1}{V_D}+\frac{1}{V_R}\right)(t-t_0) \quad (2-17)$$

Based on data points from $t = 0$ to $t = t_0$, Equation 2-17 can be rewritten as

$$-\ln\left(\frac{m_0-V_tC_R}{m_0-V_ta}\right)=\frac{PA}{l}\left(\frac{1}{V_D}+\frac{1}{V_R}\right)(t-t_0) \qquad (2-18)$$

By setting a proper reference point and plotting the logarithmic term in Equation 2-18 versus time, a straight line is obtained and the permeability coefficient P can be calculated from its slope.

2.8.3 Sorption and Desorption Kinetics

Another method for determination of diffusivity and permeability coefficients is based on the sorption and desorption kinetics of the drug molecules through membrane sheets. Assuming that diffusion coefficient of drug through membrane is constant and independent of drug concentration, the amount of drug sorbed in the membrane M_t at time t is given by (Crank and Park 1968):

$$\frac{M_t}{M_\infty} = 4\left(\frac{\sqrt{Dt}}{l}\right)\left(\frac{1}{\sqrt{\pi}} + 2\sum_{n=0}^{\infty}(-1)^n ierfc\frac{nl}{2\sqrt{Dt}}\right) \quad (2-19)$$

where M_∞ is the equilibrium uptake after infinite time ($t \to \infty$). The sorption rate is considered to be controlled by diffusion and the diffusion coefficient D is assumed to be constant. Another underlying assumption is that the membrane thickness does not change during sorption or desorption. Equation 2-19 is also valid for desorption of drug from a membrane (Crank and Park, 1968). The value of diffusivity coefficient D can be determined by plotting $\frac{M_t}{M_\infty}$ for initial gradient of M_t against the $\sqrt{t}/_l$. Equation 2-19 is based on the assumption that the concentration of the drug is constant at the surface of the membrane. If, however, only a finite amount of drug is present initially, the concentration of drug will fall substantially during the sorption process as drug enters the membrane and Equation 2-19 will no longer be valid. In this case the drug uptake in the membrane should be determined from the concentration change of the drug solution. The appropriate equation expressing the total

amount of drug M_t in the membrane at time t as a fraction of M_∞ is developed by Crank (1975):

$$\frac{M_t}{M_\infty} = 1 - \sum_{n=1}^{\infty} \frac{2\alpha(1+\alpha)}{1+\alpha+\alpha^2 q_n^2} e^{-4Dq_n^2 t/l^2} \qquad (2-20)$$

where the q_n's are the non-zero positive roots of $\tan q_n = -\alpha q_n$ and α is the ratio of the volumes of drug solutions and the membrane.

2.8.4 Partition Coefficient

In definition, a partition coefficient is the ratio of concentrations of a solute in two immiscible solvents at equilibrium and can be related to dimensionless forms of Henry's law constant (see Equation 2-21). The partition coefficient in other words is a measure of differential solubility of the solute in two immiscible solvents. A partition coefficient can also be used when one or both solvents are in a solid phase (Leo et al., 1971).

$$\frac{C_2}{C_1} = K \qquad (2-21)$$

where C_2 is the concentration of solute in the solvent II, C_1 is the concentration of solute in the solvent I, and K is the Henry's law constant.

The partition coefficient of drugs in a membrane can be determined by solute uptake experiments (Chen et al., 2010). The membrane sheet is swollen in the drug solution, and after equilibrium, the concentration of the solution (C_1) reaches a constant value. Then by performing the desorption process with same membrane, taken out from the drug solution of

known volume (V) and desorption of drug in a solution free of drug with the same volume occurs till the concentration of drug released in the solution reaches a constant value (C_2) after equilibrium. The partition coefficient of drug K_d is given by

$$K_d = \frac{C_2 V}{V_P(C_1 - C_2)} \qquad (2-22)$$

where V_P refers to the volume of the swollen membrane.

Using Equation 2-9 the permeation coefficient is obtained by diffusivity and partition coefficients determined by sorption/desorption method.

$$P = K_d D \qquad (2-23)$$

Chapter 3 Experimental

3.1 Materials

3.1.1 Model Drugs

Ciprofloxacin hydrochloride, *(+)-cis-diltiazem hydrochloride*, and *5-nitro-2-furaldehyde, semicarbazone (Nitrofurazon)* were chosen to be used in this work as model drugs to test the controlled released system. *Diltiazem hydrochloride* and *nitrofurazon* were purchased from Sigma-Aldrich Co. Ltd., and used as received. *Ciprofloxacin hydrochloride* was obtained by reacting *ciprofloxacin* (purchased from Fluka BioChemica Co. Ltd.) with excess hydrogen chloride (molar ratio 1:10) at room temperature. Both ciprofloxacin and hydrogen chloride solution (2.0 M in diethyl ether) were supplied by Sigma-Aldrich. The reaction product was a light yellow suspension, which was filtered and then washed extensively with anhydrous diethyl ether to remove excess hydrogen chloride. After drying in air, the purified *ciprofloxacin hydrochloride* was an off-white powder. Figure 3-1 shows the chemical structure of model drugs.

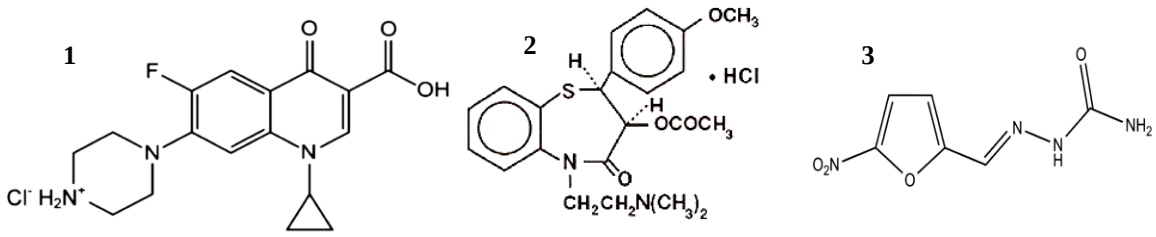

Figure 3-1 Molecular Structure of 1. Ciprofloxacin-HCl, 2. Diltiazem-HCl, 3. Nitrofurazon

Ciprofloxacin hydrochloride and *diltiazem hydrochloride* are water soluble, whereas *nitrofurazon* is partially soluble in water. To prepare drug solutions, *ciprofloxacin –HCl* and *diltiazem-HCl* were dissolved in deionized water. In order to dissolve *nitrofurazon* completely in deionized water, a 5 wt% β-cyclodextrin dissolved in deionized water is prepared and heated to 40°C. *Nitrofurazon* is dissolved completely in this solution. Aqueous nitrofurazon solutions in 5 wt% β-cyclodextrin were prepared. The drug concentration used in this study was in the range of 100-400 ppm.

3.1.2 Chitosan

Chitosan with a deacetylation degree of 99% and a molecular weight of 100 kDa, were supplied from Kyowa Technos, Chiba, Japan. It was dissolved in 2 wt% aqueous acetic acid solutions to form 1wt% chitosan solution. Then the chitosan solution was filtered to remove undissolved particles and impurities. This solution is preserved in bottle at room temperature for further use in membrane casting.

3.1.3 Sericin

Sericin was extracted from silk worm *Bombyx mori* cocoons. To facilitate the extraction, the cocoons were cut into small pieces, washed thoroughly in de-ionized water and kept in water for 4 hours. In order to obtain the fraction of sericin proteins having relatively large molecular weights, the extraction was carried out in a two step process. In the first step, the cocoons were transferred into warm de-ionized water at 40 °C for 2 hours. During this period, small molecular-sized sericin proteins were dissolved in water. The aqueous solution

was discarded and cocoons were subjected to the second step of extraction to obtain the high molecular weight sericin. In this step the cocoons were transferred to boiling water for 2 hours. After filtration and partial evaporation at about 80 °C, the thick sericin solution turned into a gel upon cooling. The percentage of sericin present in the gel was estimated by drying a known amount of gel to a constant weight. The percentage of sericin in the gel varied between 8.8-12 % from batch to batch. The sericin gel was kept in refrigerator for further use.

3.2 Chitosan/Sericin Blend Membrane Preparation

Initially, it was tried to prepare the only sericin based film and sericin/chitosan based film using low molecular weight sericin. The dried films were treated with 5% NaOH aqueous solution. The membranes obtained from pure sericin were glassy and brittle that were not possible to peel off the plate. Also low molecular weight sericin and chitosan blend membranes were gel like and easily broke away while holding. Therefore sericin cannot be used to form films alone low molecular weight sericin also does not turn to a gel by cooling, neither can make a film as blended by chitosan.

Homogeneous chitosan/sericin membranes were prepared by the solution casting technique. The sericin-chitosan blend membranes were prepared by slowly warming up the sericin gel in the presence of small amount of water to turn it into a clear liquid, which was then blended with 1 wt % solution of chitosan in 2% (v/v) aqueous acetic acid solution. After a thorough mixing, a pre-determined amount of crosslinking agent glutaraldehyde (GA) was added and

mixed thoroughly for 30 minutes. The membranes were prepared by casting about 25 ml of the polymer solution in plastic Petri dishes, which were dried at room temperature for 24 hours followed by heat treatment at 60 °C for 1 h. The blend compositions are given in Table 3-1. After drying, the membranes were treated with 5 %wt NaOH dissolved in a 1:1 ethanol aqueous solution for 24h to convert the cationic amine groups of chitosan ($-NH_3^+$) to the free amine form ($-NH_2$). The membranes were rinsed thoroughly with deionized water prior to use. The resulting membranes were dense and homogeneous, and thus the drug release was by diffusion in the membrane, and not by diffusive or convective transport in pores as in a porous matrix. However, not all the membranes were suitable for controlled release studies because the membranes with higher degrees of crosslinkings were easily cracked when placed in the membrane holder. It was realized that the high percentage of GA (i.e. 2.5-4.5%) is responsible for the membrane cracking while holding. In order to save the sericin, membrane were casted by using only chitosan and GA in different percentages to get a suitable membrane. It was found that the chitosan membranes prepared using 0.08- 0.4% of GA were quite good in all respects. So the next batch of sericin/chitosan based membranes were prepared by using the 0.08-0.4% of GA. The sericin/chitosan based membranes with GA in 0.08-0.4% are quite stable membranes and would be a good starting point to test these membranes for controlled drug release studies and to study the effect of GA on the membrane structure towards controlled drug release.

Table 3-1 Compositions of sericin/chitosan blend membranes

Membrane	sericin/chitosan blend ratio	GA (%)	Remarks
1	1:10	4.5	After drying, the membranes were easily peeled off in 5% NaOH aqueous ethanol solution. The membranes were cracked while placing in the membrane holder due to high degree of crosslinking.
2	1:3	3.7	
3	1:2	3.3	
4	1:1	2.5	
5	1:4	0.4	After drying, the membranes were easily peeled off in 5% NaOH aqueous ethanol solution. The thin membranes can be hold easily without breaking. All these membranes seem to be suitable for the application of controlled drug release.
6	1:4	0.24	
7	1:4	0.16	
8	1:4	0.08	

Glutaraldehyde content (GA%) is with respect to the mass of the sericin/chitosan blend.

The sericin/chitosan membranes with blend ratio of 1:4 have been found to work well at varying concentration of crosslinking agent in terms of membrane stability and integrity. In all the permeation and sorption/desorption experiment, membranes with this composition were used.

3.3 Permeation experiments

The experimental apparatus for permeation experiments is shown schematically in Figure 3-2. It was comprised of a source compartment of 100 ml capacity and a receiving compartment of 2,500 ml capacity. The membrane, which had been stored in deionized water, was mounted horizontally at the bottom of the source compartment, which was

suspended on top of the receiving compartment. Then the receiving compartment was filled with 2,000 ml of deionized water, and the source compartment was lowered to be partially immersed in water. At time zero, the source compartment was filled with 80 ml of the drug solution at a predetermined concentration (ranging from 0.1 to 0.4 mg/ml) so that permeation started to occur. Vigorous agitations were provided mechanically in both compartments to eliminate the boundary layer effect, and this was confirmed by the fact that the measured permeability and diffusivity remained constant when membranes with different thickness were used to study the boundary layer resistance effect. The concentration of the drug in the receptor side during the course of permeation was measured using a Shimadzu UV–Vis spectrophotometer. The effective area of the membrane for permeation was 12 cm^2.The thicknesses of the membranes were determined by a digital micrometer at several spots and the average thickness was recorded. The experiments were carried out at room temperature (22 °C).

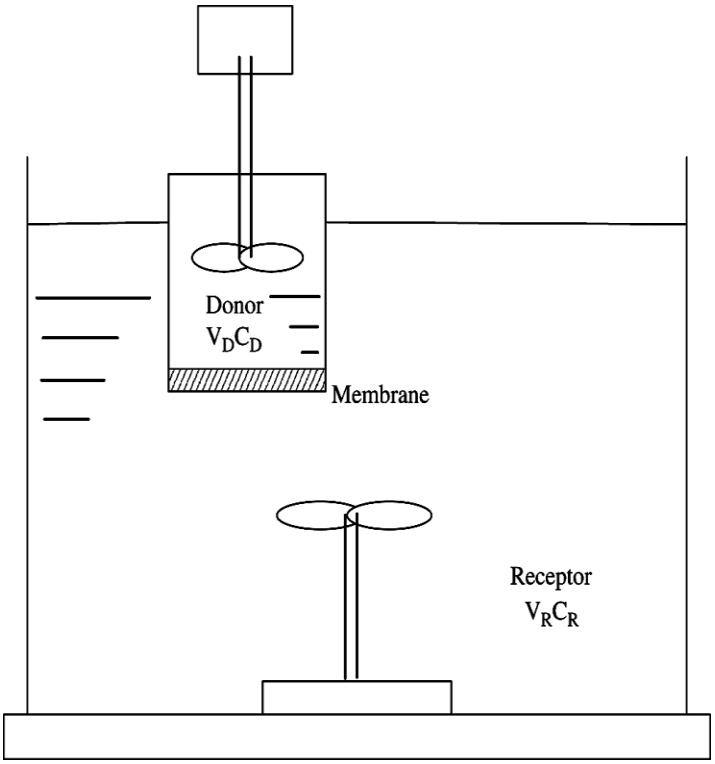

Figure 3-2 Schematic apparatus for permeation test (Chen et al., 2010)

3.4 Sorption and Desorption

The sorption experiments were conducted by immersing pre-swollen membrane samples in deionized water, then into 50 ml aqueous solutions of drugs at various known concentrations maintained at room temperature. The concentration of drug compounds in the solutions varied in the range of 100 to 400 ppm. The equilibrium sorption uptake was determined after the membrane sample was submerged in the liquid for a sufficiently long time (at least 24 h) and no further increase in the sorption uptake was observed. The quantity of the sorption uptake with time was determined from the concentration change of the drug solutions as measured by the spectrophotometric method. Desorption experiments were also carried out immediately after the swollen membrane was weighed using a digital balance. Desorption experiments were carried out by putting the drug-loaded membrane, in 50ml of deionized water. The concentration change of the drug released to the deionized water at different times time was monitored spectrophotometricly.

3.4.1 Determination of partition coefficient

The partition coefficients of drugs in the membranes were also determined by sorption/desorption experiments, where the concentration of the drug solution at equilibrium in sorption C_1, and the desorbed concentration of drug in the deionized water after reaching the equilibrium C_2 were determined spectrophotometricly. The partition coefficients K_d of drugs in the membranes were calculated using Equation 2-22.

3.5 Degree of Swelling

The degrees of swelling (R_{sw}) of the membrane drug solutions were determined at 22 °C from mass uptake using the following equation:

$$R_{sw} = \frac{W_{sw}}{W_d} \times 100 \qquad (3-1)$$

where W_d is the weight of a dry membrane sample and W_{sw} the weight of the swollen membrane.

3.6 Effect of boundary layer

To study whether there was a boundary layer resistance in the permeation system, the release of ciprofloxacin hydrochloride through the membrane, was determined using membranes of different thickness. The membranes have the same compositions.

Chapter 4 Results and Discussion

4.1 Effect of boundary layer

The flux of solute across the membrane (J), derived from Fick's law of diffusion, can be expressed as:

$$J = \frac{1}{A}\frac{dm}{dt} = \frac{P\Delta C}{l} \qquad (4-1)$$

where $\frac{dm}{dt}$ is the amount of solute that permeates through the membrane in unit time and ΔC is the concentration difference between the donor and receptor chamber. At steady state of permeation, the permeation flux (J_s) is inversely proportional to the thickness of the membrane. However in systems where a boundary layer is not negligible on either surface of the membrane, the boundary layer will contribute to an additional resistance to drug transport. In this case, Equation 4-1 can be modified based on the resistance in series model:

$$\frac{1}{J_s} = \frac{1}{P\Delta C}\,(l + PR_b\,) \qquad (4-2)$$

where R_b is the boundary layer resistance. It can be seen that a plot of $\frac{1}{J_s}$ versus l will yield a straight line with a positive intercept on the *y*- axis, and the boundary layer resistance can thus be determined from the intercept of the straight line.

The permeation flux of *ciprofloxacin hydrochloride* through the membranes of different thicknesses was measured to determine whether there is boundary layer effect in the test

system. An initial drug concentration of 0.1 $\frac{mg}{ml}$ was used in the tests. All the membrane thicknesses reported in this work were the thicknesses of swollen membranes. As expected, the steady-state permeation flux of the drug decreases as the thickness of the membrane increases. As illustrated in Figure 4-1, there is a linear relationship between the reciprocal of steady-state flux $\frac{1}{J_s}$ and thickness of the membrane *l*, with a *y-axis* intercept close to the point of origin. This indicates the negligible effects of boundary layers on both sides of the membrane in the system under the experimental conditions. Therefore the diffusivity and permeability coefficients determined for this system are the intrinsic kinetic values for drug transport through the membranes.

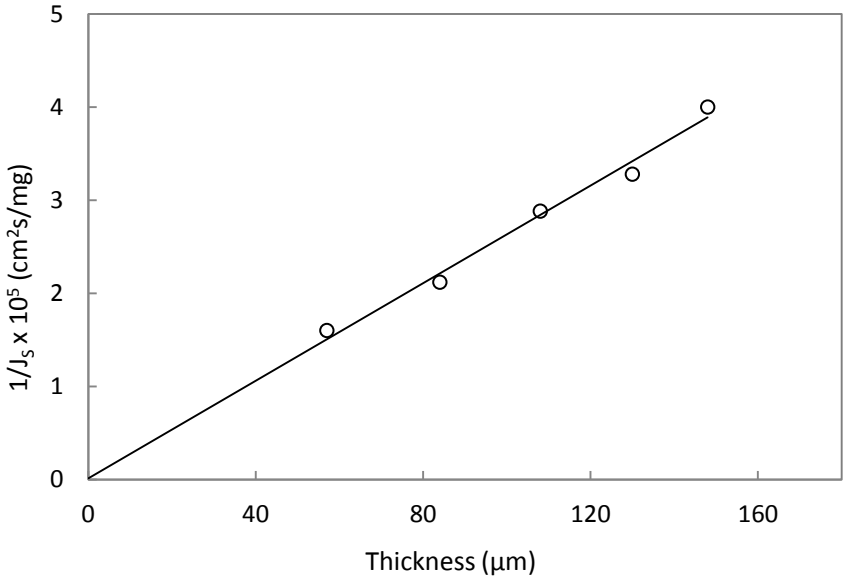

Figure 4-1 Relationship between the reciprocal of steady-state flux and membrane thickness, sericin/chitosan blend ratio in the membranes 1:4, amount of crosslinking agent 0.4% of sericin/chitosan in the membrane, Initial drug concentration 100 ppm

4.2 Swelling Degree of Membranes

The water sorption capacity of the sericin/chitosan membranes were determined by swelling the sericin/chitosan membranes in water and in drug solutions with concentrations ranging from 100 to 400 ppm at room temperature. The degree of swelling of a membrane is governed by its crosslinking density, temperature, composition of the solution, and interaction between the solution and the membrane (Thacharodi and Rao, 1993). Swelling can be altered over a wide range by crosslinking and concentration of the solution. However, the swelling behavior of the sericin/chitosan membranes, which were crosslinked with glutaraldehyde in water and the drug solutions, did not vary significantly. The degrees of swelling of the membranes are shown in Figure 4-2. The equilibrium swelling degrees in water were in the range of (265-272%) which is similar to degrees of membrane swelling in the drug solutions, presumably due to the low concentrations of the compounds in the solutions. As can be seen in Figure 4-2, there is no significant change in the swelling of the membranes due to change in the crosslinking density. This may be because of the high affinity of chitosan and sericin with water molecules as both polymers have strong hydrophilic groups, or probably the crosslinking times (i.e. 30 min) were sufficiently long to cover the crosslinking agent concentration effect on the degree of crosslinking in the membranes.

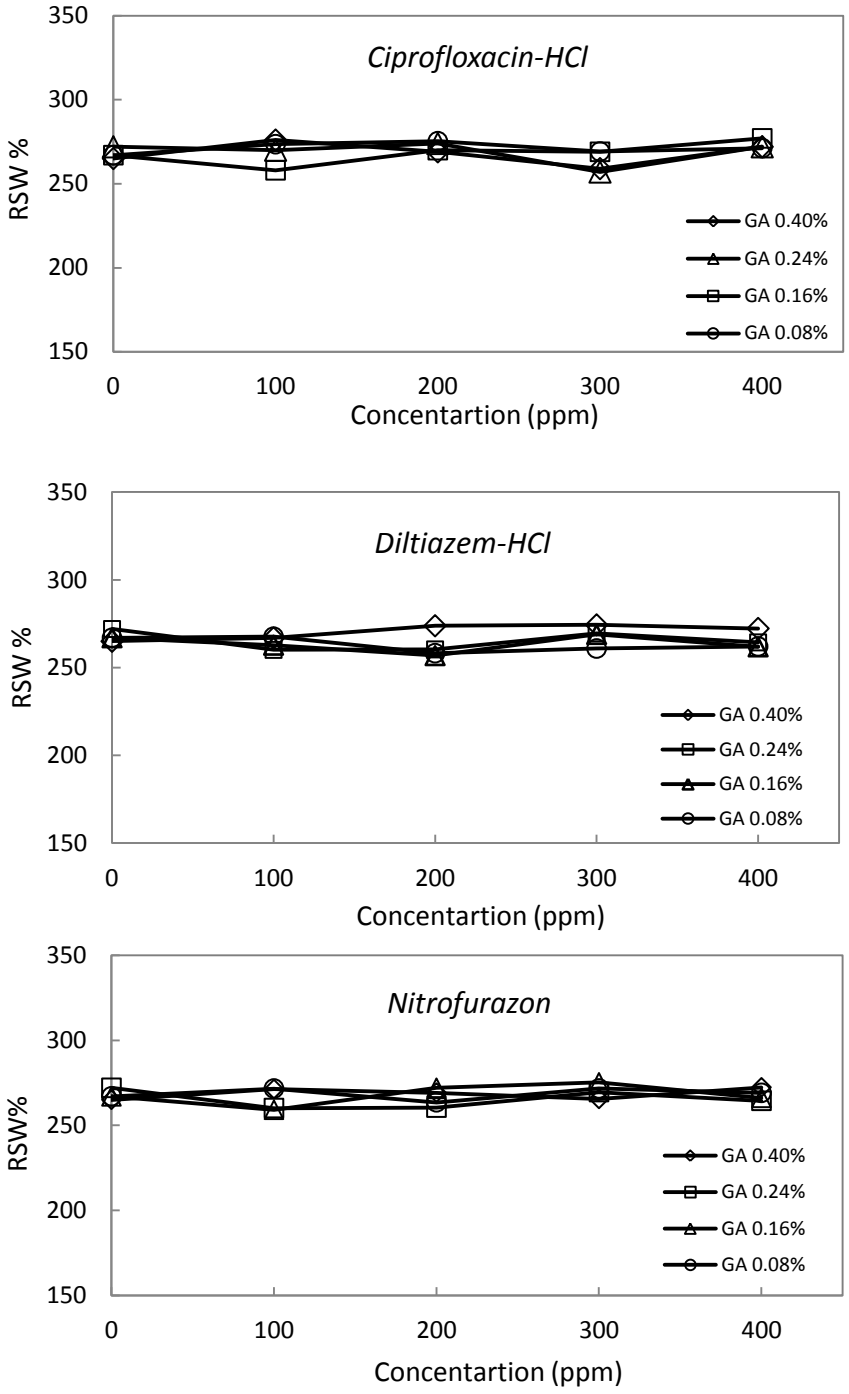

Figure 4-2 Swelling degrees of sericin/chitosan membranes of different degrees of crosslinking in drug solutions

Chen et al., (2010) have studied the swelling degree of pure chitosan membranes in ciprofloxacin-HCl solutions and their results also showed that the swelling degrees of the chitosan membranes are not affected by the change in the drug concentrations. They reported that the degrees of swelling of chitosan membranes was 164% which is consistent with the results obtained (i.e. 267% for *ciprofloxacin-HCl*) in view that a blend of sericin/chitosan membranes are used in this study.

4.3 Permeation Results

4.3.1 Time-lag analysis of short-time permeation data

A plot of the mass of drugs permeated Q versus time t was constructed for the three model drugs with initial concentrations varying in the range of 100-400 ppm for sericin/chitosan blend membranes with different crosslinking densities. The concentration difference across the membrane is driving force for permeation, and it changes from $(C_0 - 0)$ at beginning to $(C_D - C_R)$ at time t. The long time permeation data must be excluded in accordance with the criteria discussed earlier, to apply Equations 2-6 and 2-7 for calculation of time-lags. An upper limit $\eta = 5\%$ was assigned to allow a relative change in the trans-membrane concentration within 5% to relax the assumptions of constant source concentration and zero sink concentration. Obviously, smaller values of η lead to more accuracy in determination of the time lag, but on the other hand, there will be fewer data available for extrapolation (Chen et al., 2010). Different values of η have been tested (ranging from 5-15%) for the three drugs. The value of $\eta = 5\%$ was found to be the optimum for calculation of time-lags for the permeation of the three drugs.

The diffusion coefficients D_T of ciprofloxacin hydrochloride, diltiazem hydrochloride, and nitrofurazon through the sericin/chitosan membrane crosslinked with different concentrations of glutaraldehyde at four initial concentrations of drugs were determined from the time-lag. Figure 4-3 shows the diffusivities so determined from the time-lag based on short-time permeation data. The diffusivity coefficients of ciprofloxacin hydrochloride were in the range

of $(2.0 - 2.6) \times 10^{-9} \pm 2.6 \times 10^{-10}$ cm^2/s, which are well within the common range of drug diffusivities in various membranes. Furthermore, the diffusivity coefficients of diltiazem hydrochloride and nitrofurazon in the membranes were in the range of $(2.5 - 2.6) \times 10^{-9} \pm 1.0 \times 10^{-10}$ and $(55 - 104) \times 10^{-9} \pm 33.1 \times 10^{-9}$ (cm^2/s), respectively. These values also fall completely in the common range of diffusivities reported for different drugs in chitosan based membranes. The permeation of drug molecules through membranes may be explained by a process consisting of three steps: sorption, diffusion, and desorption. In the time-lag method, it is assumed that the diffusion is the rate controlling step, and the sorption and desorption of the drug on the surfaces of the membrane occur instantaneously. Therefore, the diffusivity of drug molecules in the membrane is affected by the chemical interactions between the drug molecules and the polymers forming the membrane, and the morphology of the membrane. No clear trend was observed for the influence of drug concentration on the permeability and diffusivity within the experimental error in the concentration ranges tested. This means that the underlying assumption of concentration independency of the diffusivity, used in the diffusivity measurements appears to be satisfactory in the experimental range studied. Compared to the diffusivity coefficients of two other drugs, the diffusivity of nitrofurazon in the membranes is much higher (i.e. 38-134 $\times 10^{-9} \pm 33.1 \times 10^{-9}$ cm^2/s) within the drug concentrations studied. This is due to the effect of presence of β-cyclodextrin added in the donor and receptor medium. β-cyclodextrin may act as a penetration enhancer. The effects of hydrophilic cyclodextrin on drug flux through various types of artificial and biological membranes have been studied extensively in the literature. It has been shown that

cyclodextrin enhances the penetration of lipophilic drugs by increasing the drug/cyclodextrin complex concentration in the donor side, thereby improving the interaction of permeating drug and the membrane (Loftsson et al., 2007). Therefore there is a significant difference in the diffusivity between nitrofurazon (a hydrophobic drug) and ciprofloxacin-HCl and diltiazem-HCl (two hydrophilic drugs). In fact, it is the enhancing effect of cyclodextrin that has been used to dissolve nitrofurazon in the aqueous solution, as discussed in the experimental section.

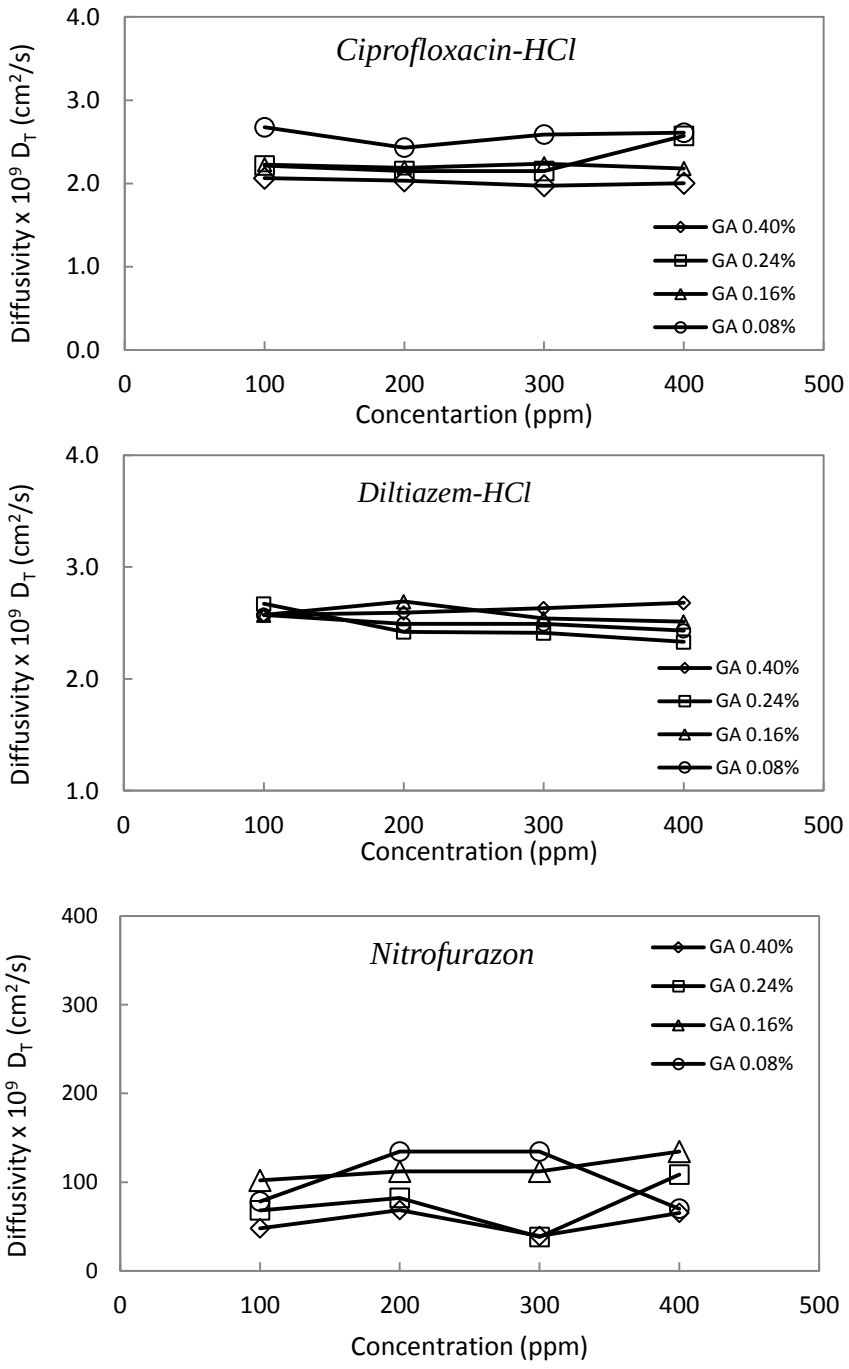

Figure 4-3 Diffusivity (D_T) determined from time lag using short-time permeation data (η=5%)

The pseudo-steady state permeability coefficient of the drugs through the membranes can be determined from the slope of Q vs. t plots using the permeation data at the early permeation stage. As discussed previously, the permeability coefficient calculated from the short-term permeation data may be affected by transient permeation leading to an underestimation in the permeability. However it will be beneficial to calculate the permeability using the time-lag method in order to compare with permeability coefficient obtained from the long-time permeation data bases on the mass balance method. The permeability coefficients determined from the short-term permeation data, $P_{T,}$ at different drug concentrations are shown in Figure 4-5. It is shown that the permeabilities of ciprofloxacin-HCl and diltiazem-HCl in the membranes are in the range of $(17 - 25) \times 10^{-8} \pm 2.3 \times 10^{-8}$, and $(4.7 - 5.4) \times 10^{-8} \pm 2.210^{-9} \times {\text{cm}^2}/{\text{s}}$, respectively. The permeability of nitrofurazon which is a hydrophobic drug in the membranes is in the range of $(91 - 216) \times 10^{-8} \pm 39.5 \times 10^{-8}\ {\text{cm}^2}/{\text{s}}$. Further, the permeabilities of the three drugs through the membranes are shown to be independent of their concentrations in the experimental range studied, in spite of the fluctuations in the permeability calculated due to experimental errors. The fluctuations in the permeability coefficients are much more significant for nitrofurazon. This might also be related to the presence of β-cyclodextrin in the drug solution at the donor compartment and the receptor side. Cyclodextrin is hydrophilic and has a cage structure, and its presence in the solution of nitrofurazon is expected to enhance the drug permeation. Cyclodextrins are good options to be used either for complexation or as functional carrier materials in drug delivery. A main characteristic of cyclodextrin is forming an inclusion

complex in solution which surrounds the hydrophobic substance within its cavity (Loftsson et al., 2007). The macrocyclic ring structure of β-cyclodextrin is presented in Figure 4-4. This is probably why the hydrophobic nitrofurazon exhibited higher permeability in the hydrophilic membranes than the hydrophilic drugs (i.e., ciprofloxacin hydrochloride and diltiazem hydrochloride) in the absence of cyclodextrin.

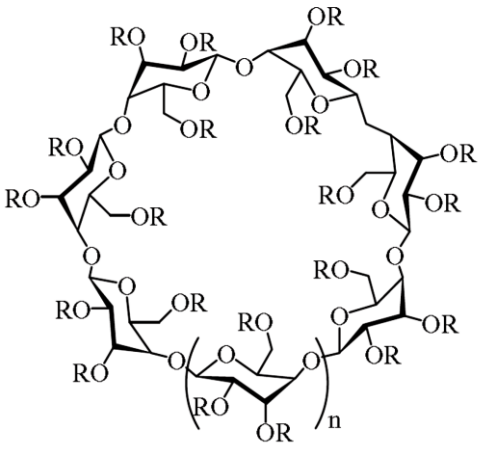

Figure 4-4 macrocyclic ring structure of β-cyclodextrin (Loftsson et al., 2007).

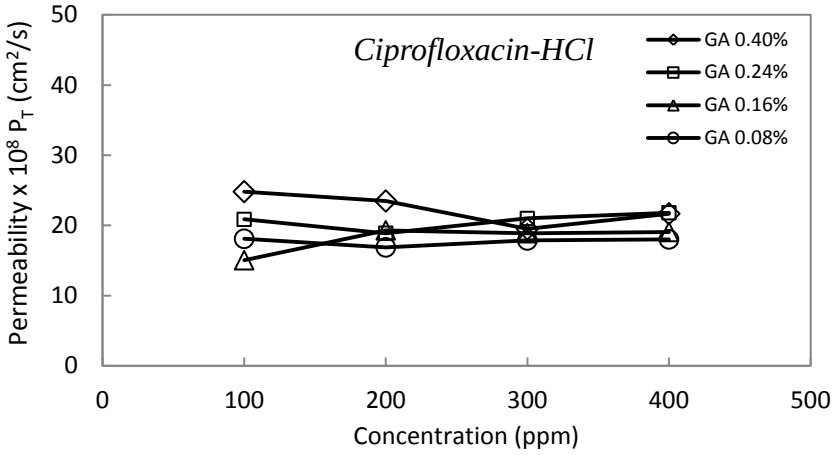

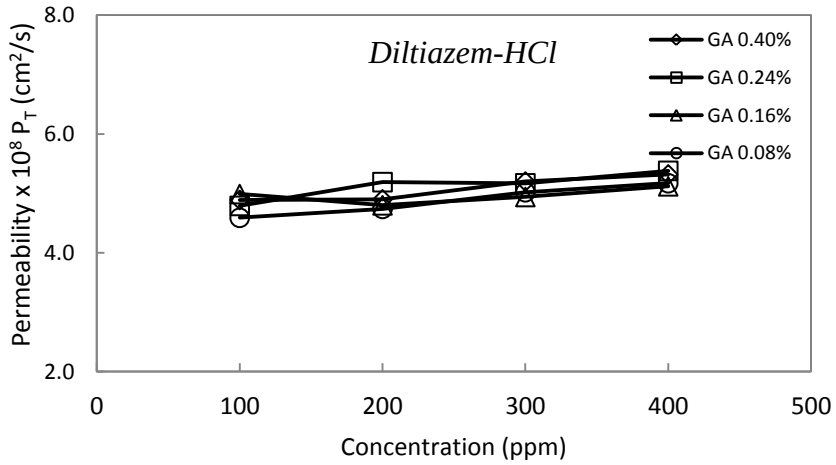

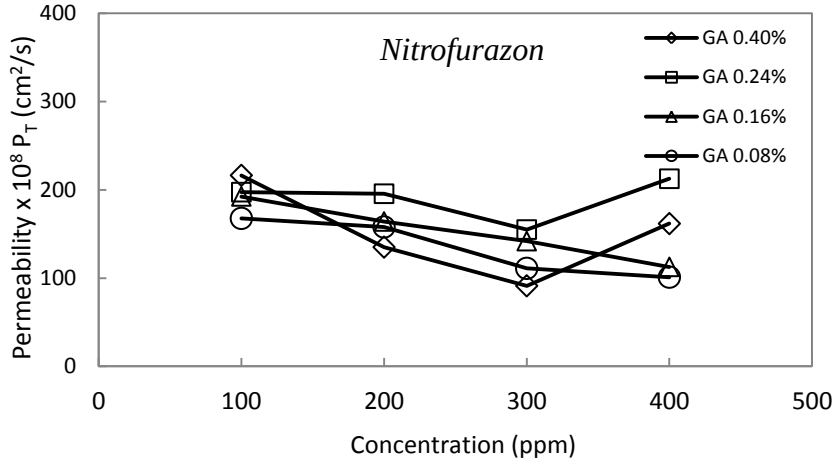

Figure 4-5 Permeability P_T determined on the basis of pseudo steady state permeation using short-time permeation data (η=5%)

Generally speaking, crosslinking will improve the chemical stability and mechanical strength of a membrane. Membrane crosslinking often causes a decrease in its permeability and diffusivity. However, over the crosslinking agent concentrations used in this study, no clear trend can be observed with respect to the effect of crosslinking on diffusivity and permeability. A relatively low concentration of glutaraldehyde was used for membrane crosslinking in this study, which may have just helped the stability of the membrane but did not change the membrane morphology or reduce the chemical functionality of chitosan and sericin significantly.

4.3.2 Long-time permeation data analysis with mass balance method

The impact of transient permeation is considered to have diminished after three times of the time-lag. Therefore, the long time $(t > 3\theta)$ permeation data are subjected to mass balance analysis. Based on Equation 2-18, by selecting an appropriate reference point t_0 and plotting $F(t) = -ln\,[(m_0 - V_t C_R)/(m_0 - V_t a)]$ against t, a straight line will be obtained and permeability coefficient P can be calculated from its slope.

After the time-lag was obtained from the short-time permeation data, we were able to set a reference point $t_0 \geq 3\theta$, and only the permeation data beyond this point were used to determine the permeability coefficient P_M of the drugs using the mass balance analysis (Chen et al., 2010). Using the long-time permeation data, the permeability coefficient, P_M, was calculated from the slope of the plot of $F(t)\ vs.\ t$ using Equation 2-18. The results are shown in Figure 4-6 for the three model drugs. The P_M values for ciprofloxacin-HCl and diltiazem-

HCl were shown to be in the range of $(16-33)\times10^{-8}\pm6.3\times10^{-8}$, $(4.7-5.6)\times10^{-8}\pm0.26\times10^{-8}\ {cm^2}/{s}$ respectively. Nitrofurazon was determined to have a permeability of $(94-201)\times10^{-8}\pm26.9\times10^{-8}\ {cm^2}/{s}$. In general the P_M values tend to be slightly greater than the P_T values obtained from the time-lag method and this is not unexpected because of the two different methods used. As discussed earlier, the effect of concentration variations on evaluation of P_T was neglected based on pseudo steady state permeation. Therefore, there is an underestimation in the permeability determined using the short-time data and P_M appears to be more realistic to measure the membrane permeability. As can be seen in Figure 4-5, a variation in initial concentration of the drugs has no significant effect on the P_M determined. This is expected considering the concentration independency of diffusivity and permeability coefficients of the permeation system. There is a more significant fluctuation in the P_M values for nitrofurazon when compared to the P_M values for ciprofloxacin-HCl and diltiazem-HCl. This can be explained by the presence of β-cyclodextrin in nitrofurazon permeation system. The concentration of crosslinking agent also did not show a clear trend in P_M in the test range studied here. Membrane crosslinking generally leads to a decrease in permeability, diffusivity and solubility of the drug in the membrane: (i) the crosslinked sites in the membrane polymer are more impermeable for the diffusion process, and the penetrating drug molecules have to migrate around the barrier sites which lengthen the path of diffusion relative to nominal dimension of the membrane, (ii) The chemical modification of the membrane matrix at crosslinking points changes the interaction between the membrane

polymer and the drugs (Thacharodi and Rao, 1993). The fluctuation in P_M values but no specific trend with respect to concentration of crosslinking agent may be attributed to the low concentrations of glutaraldehyde used in this study which helped improving the stability of the membranes but did not cause a change in the chemical functionality of chitosan and sericin.

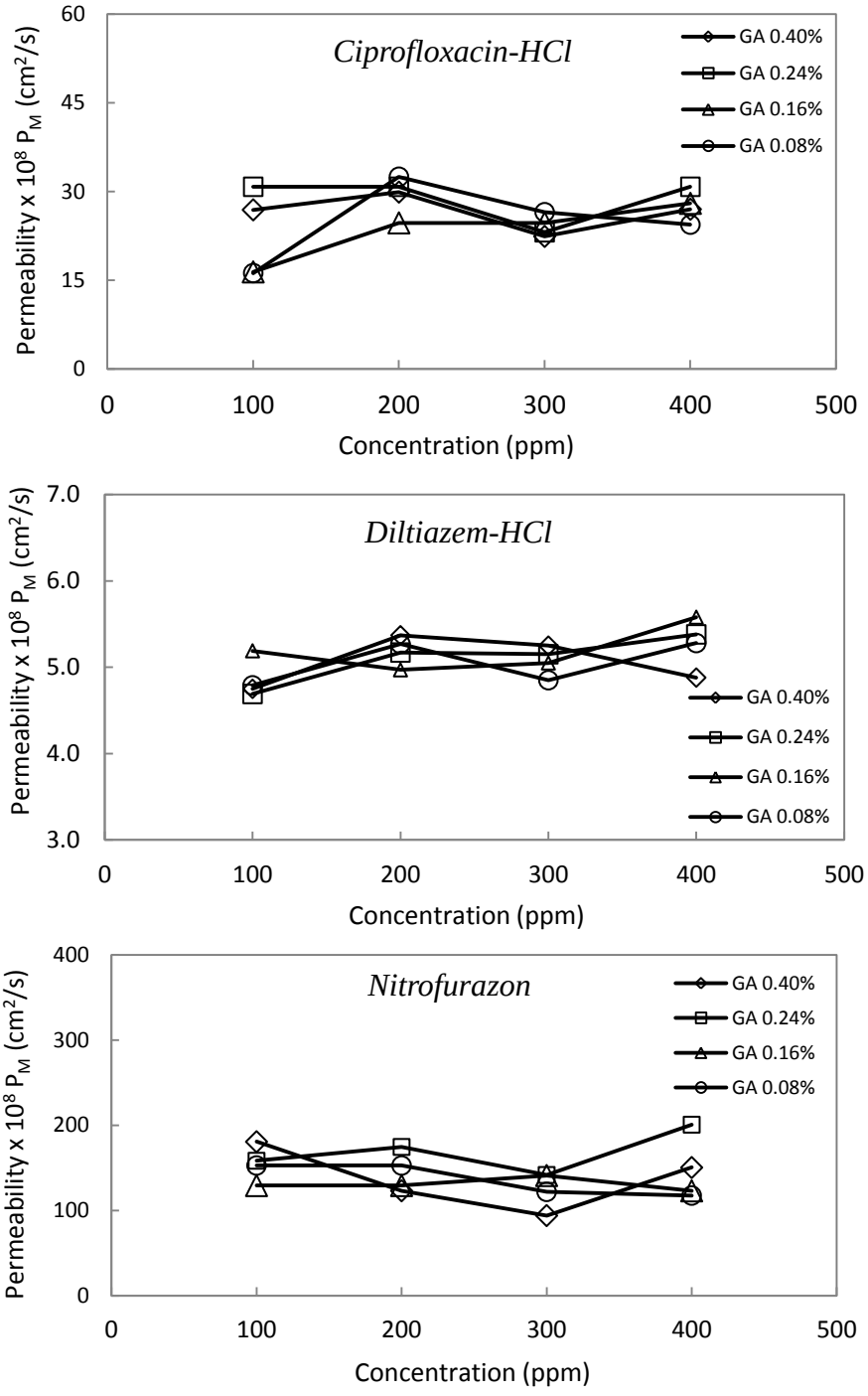

Figure 4-6 Permeability P_M determined from the log-time permeation data ($t_0 > 3\Theta$) based on mass balance method.

Since diffusivity and permeability coefficients D_T, P_T and P_M found to be independent of the drug concentration in the concentration ranges studied in this work, the average values of these permeation parameters are calculated for each drug penetrant through the sericin/chitosan membranes at different crosslinking degrees for better comparison. The results are summarized in Table 4-1.

Table 4-1 Average diffusivity and permeability of drugs in the sericin/chitosan membrane

Drug	GA %	D_T x 10^9(cm^2/s)	P_T x 10^8 (cm^2/s)	P_M x 10^8 (cm^2/s)
Ciprofloxacin-HCl	0.40	2.0	22.4	26.6
	0.24	2.3	20.6	28.9
	0.16	2.2	18.1	23.5
	0.08	2.6	17.7	24.9
Diltiazem-HCl	0.40	2.6	5.1	5.1
	0.24	2.5	5.1	5.1
	0.16	2.6	5.0	5.2
	0.08	2.5	4.9	5.0
Nitrofurazon	0.40	55.2	151.1	137.1
	0.24	74.2	190.0	168.8
	0.16	115.1	152.7	130.7
	0.08	104.3	134.3	136.2

D_T: diffusivity determined from time lag using short-time permeation data

P_T: permeability determined from pseudo steady state stage using short-time permeation data

P_M: permeability determined from the log-time permeation data based on mass balance method

4.4 Results from Sorption and Desorption Studies

The sorption and desorption studies provide information about sorption isotherms as well as the kinetics of sorption and desorption of drug permeation in the sericin/chitosan membranes. The amount of drug sorbed by the membrane at a given instant M_t was determined from concentration change in the drug solution measured by the UV-Vis spectrophotometer. Figures 4-7 and 4-8 show the typical $\frac{M_t}{M_\infty}$ $vs.$ t plots for the sorption and desorption of ciprofloxacin-HCl with an initial concentration of 100 ppm in a sericin/chitosan membrane. The membrane composition was 1:4 sericin/chitosan by weight, crosslinked by 0.40 wt% glutaraldehyde with respect to sericin/chitosan blend. Similar results are shown in Appendix for sorption and desorption of other drugs through the sericin/chitosan membranes with different degrees of crosslinking. The diffusion coefficients were evaluated by data fitting to Equation 2-20 with the assistance of Polymath 6.1. The diffusivity so determined from sorption and desorption experiments are shown in Figures 4-8 and 4-9, respectively.

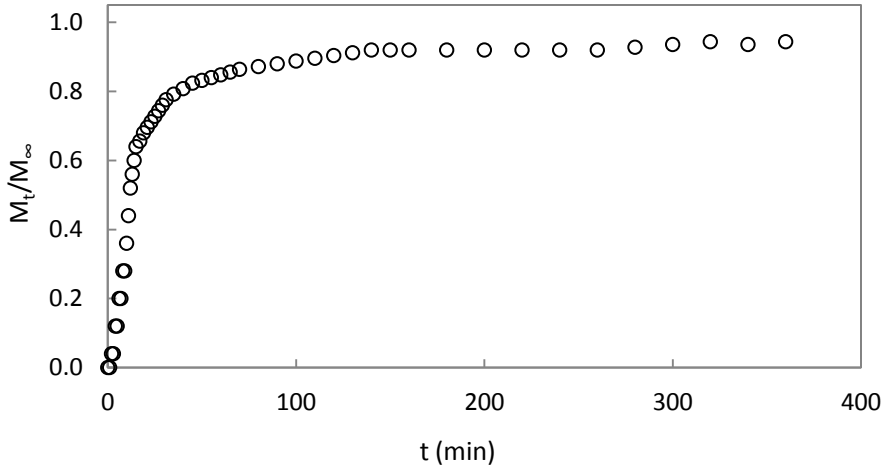

Figure 4-7 Sorption kinetics of ciprofloxacin-HCl. Initial drug concentration 100 ppm. Sericin/chitosan blend ratio 1:4; GA amount 0.40% wt with respect to the sericin/chitosan blend ratio

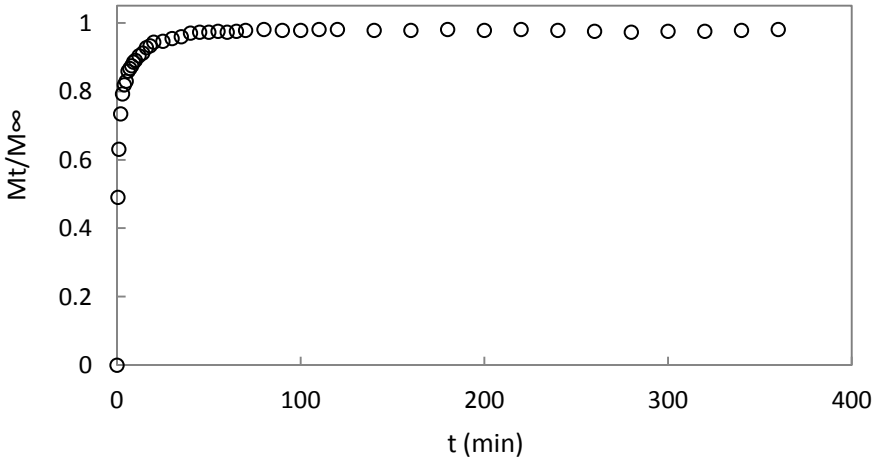

Figure 4-8 Desorption kinetics of ciprofloxacin-HCl. Initial drug concentration 100 ppm. Sericin/chitosan blend ratio 1:4; GA amount 0.40% wt with respect to the sericin/chitosan blend ratio

Figures 4-9 and 4-10 show the diffusivity of the three model drugs in the membranes as determined from sorption and desorption kinetics. It can be seen that the diffusion coefficient determined by the sorption and desorption experiments tend to be independent of the initial drug concentrations. Equation 2-20 for calculation of D_S and D_D, is based on the assumption of concentration independence of diffusivity in the system. Therefore, the results are clearly

in agreement with the assumption. The average diffusivities of the drugs in the membranes with different degrees of crosslinking are summarized in Table 4-2. The average diffusivities of the drugs, D_S and D_D, tend to decrease as the concentration of crosslinking agent increases. These results are in agreement with the theory; however, as discussed before, no specific trends in their permeabilities were observed with regard to the crosslinking degree of the membranes. Nonetheless the differences in the diffusivities calculated from permeation and sorption/desorption experiments are considered to be acceptable, in view of the different experimental techniques used in this work, for the purpose of comparison of the membrane diffusivity and permeability.

Table 4-2 Average diffusivity coefficients of drugs calculated from sorption and desorption kinetics

Drug	GA%	D_S ±error x 10^9(cm^2/s)	D_D ±error x 10^9(cm^2/s)
Ciprofloxacin-HCl	0.40	7.6±2.0	19.7±14.1
	0.24	7.2±2.0	35.0±14.1
	0.16	5.1±2.0	40.4±14.1
	0.08	3.2±2.0	46.9±14.1
Diltiazem-HCl	0.40	5.9±1.8	18.6±5.3
	0.24	6.2±1.8	21.7±5.3
	0.16	7.2±1.8	11.9±5.3
	0.08	10.1±1.8	23.7±5.3
Nitrofurazon	0.40	15.7±1.9	11.0±4.5
	0.24	15.2±1.9	16.3±4.5
	0.16	14.7±1.9	19.6±4.5
	0.08	18.2±1.9	19.7±4.5

D_S: diffusivity determined from sorption experimental data

D_D: diffusivity determined from desorption experimental data

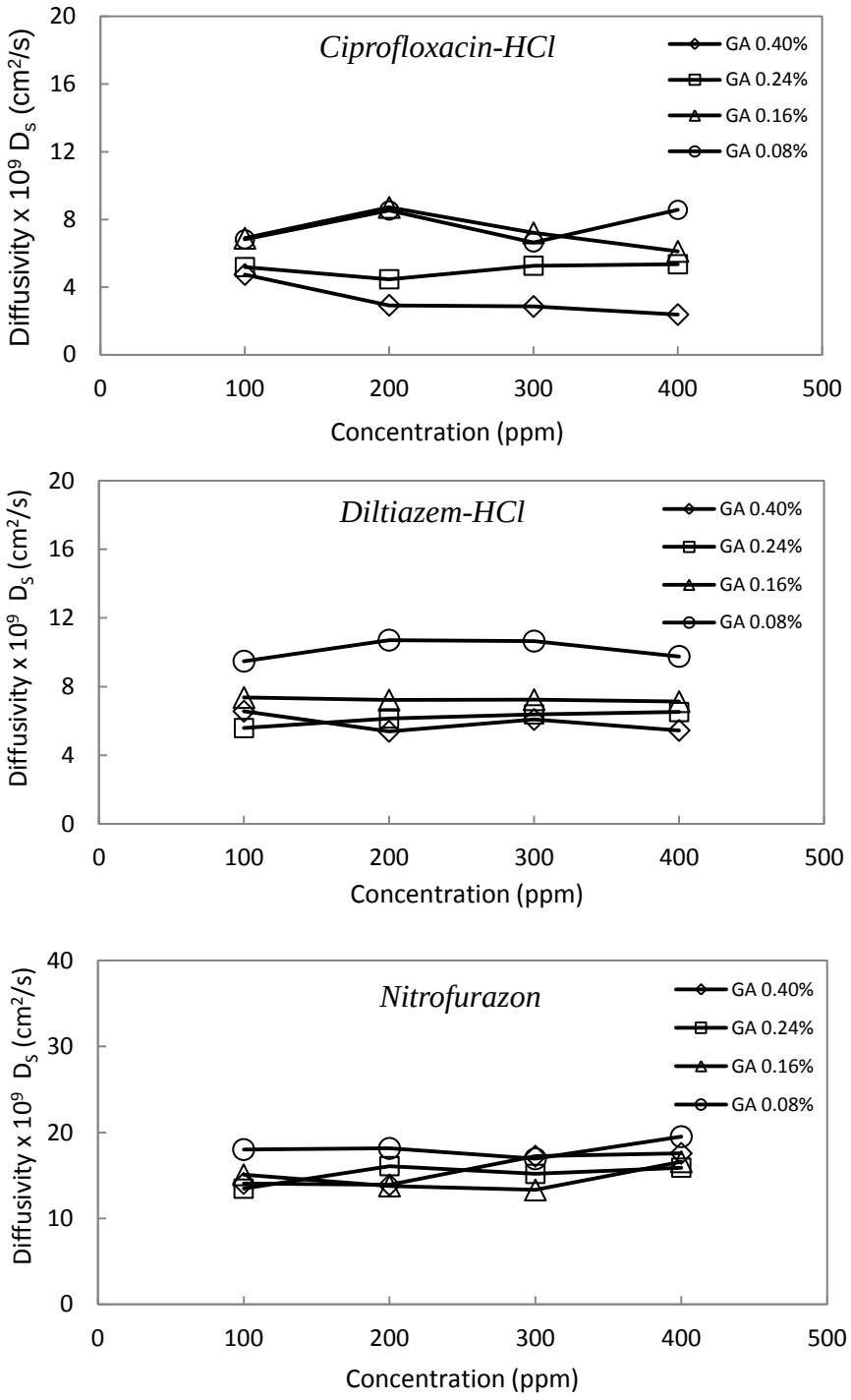

Figure 4-9 Diffusivity D_S determined from sorption kinetics; sericin/chitosan blend ratio 1:4; GA wt% with respect to the sericin/chitosan blend ratio

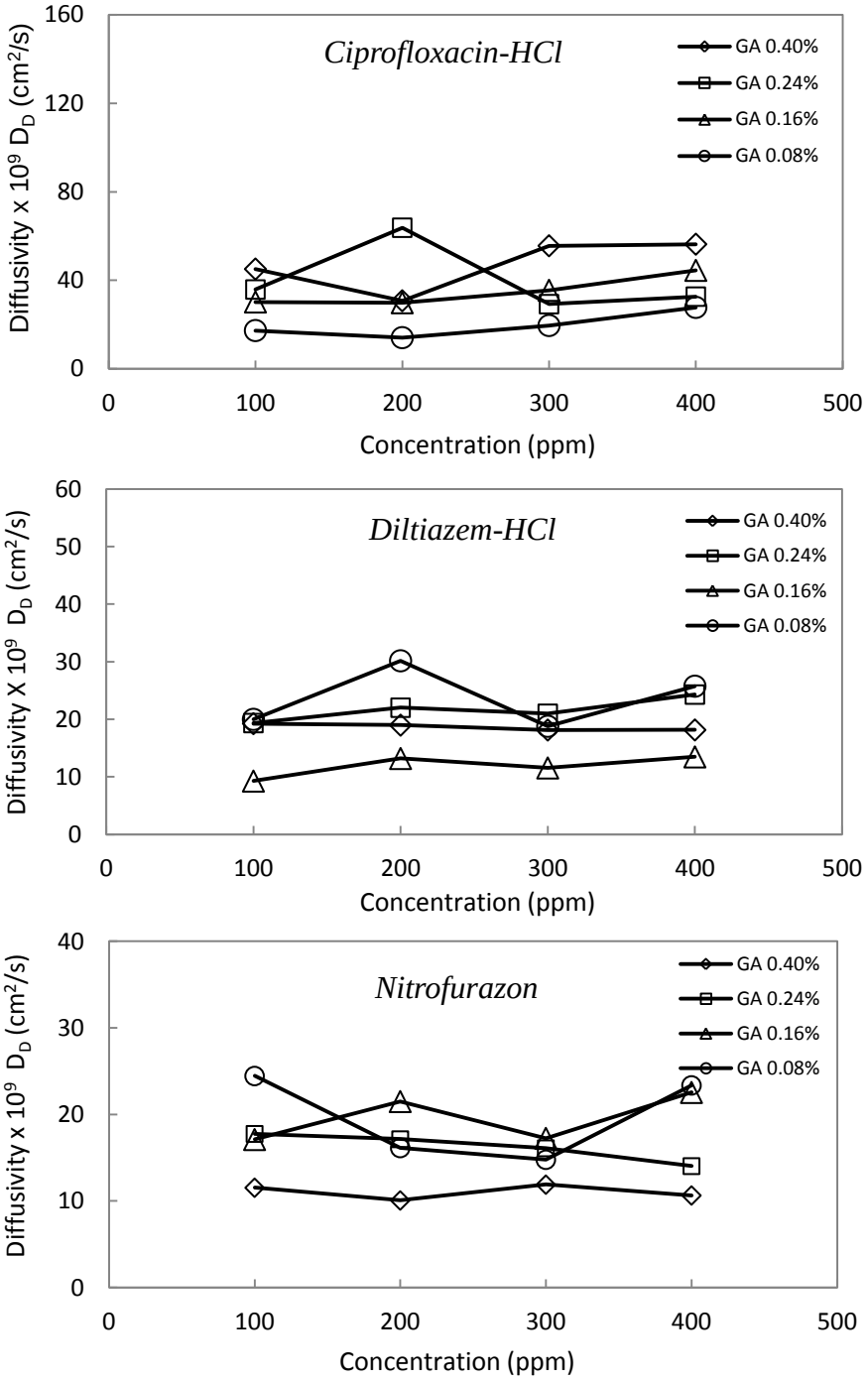

Figure 4-10 Diffusivity D_D determined from sorption kinetics; sericin/chitosan blend ratio 1:4; GA wt% with respect to the sericin/chitosan blend ratio

4.4.1 . Partition Coefficient

The permeation of drugs in the membranes can be described by solution-diffusion model. That is, the drug dissolves in the membrane and diffuses through membrane, and then desorbs from the membrane. The partition coefficients K_d for ciprofloxacin-HCl, diltiazem-HCl, and nitrofurazon were determined from sorption/desorption experiments using Equation 2-22. The partition coefficients for ciprofloxacin-HCl, diltiazem-HCl and nitrofurazon were found to be (0.9±0.21) and (25±0.12), and (26±0.31) respectively. As shown in Figure 4-11, the partition coefficients K_d of the drugs in the sericin/chitosan membranes is independent of the drug concentrations. Also, the partition coefficients are not affected by the degree of crosslinking in the membranes. Thacharodi and Rao (1993) have shown that transport of highly water soluble drugs such as propranolol hydrochloride through a chitosan membrane was by the pore mechanism where the drugs are transported through membranes microchannels, whereas the hydrophobic drugs or less water soluble drugs will be transported through the chitosan membranes by partition mechanism significantly. The K_d obtained for ciprofloxacin-HCl in the sericin/chitosan membrane was less than unity ($K_d \leq 1$), and the transport of this drug through the membrane appears to be influenced by microchannel transport mechanism. On the other hand, the transport of diltiazem-HCl and nitrofurazon (a hydrophobic drug), are governed by the partition mechanism.

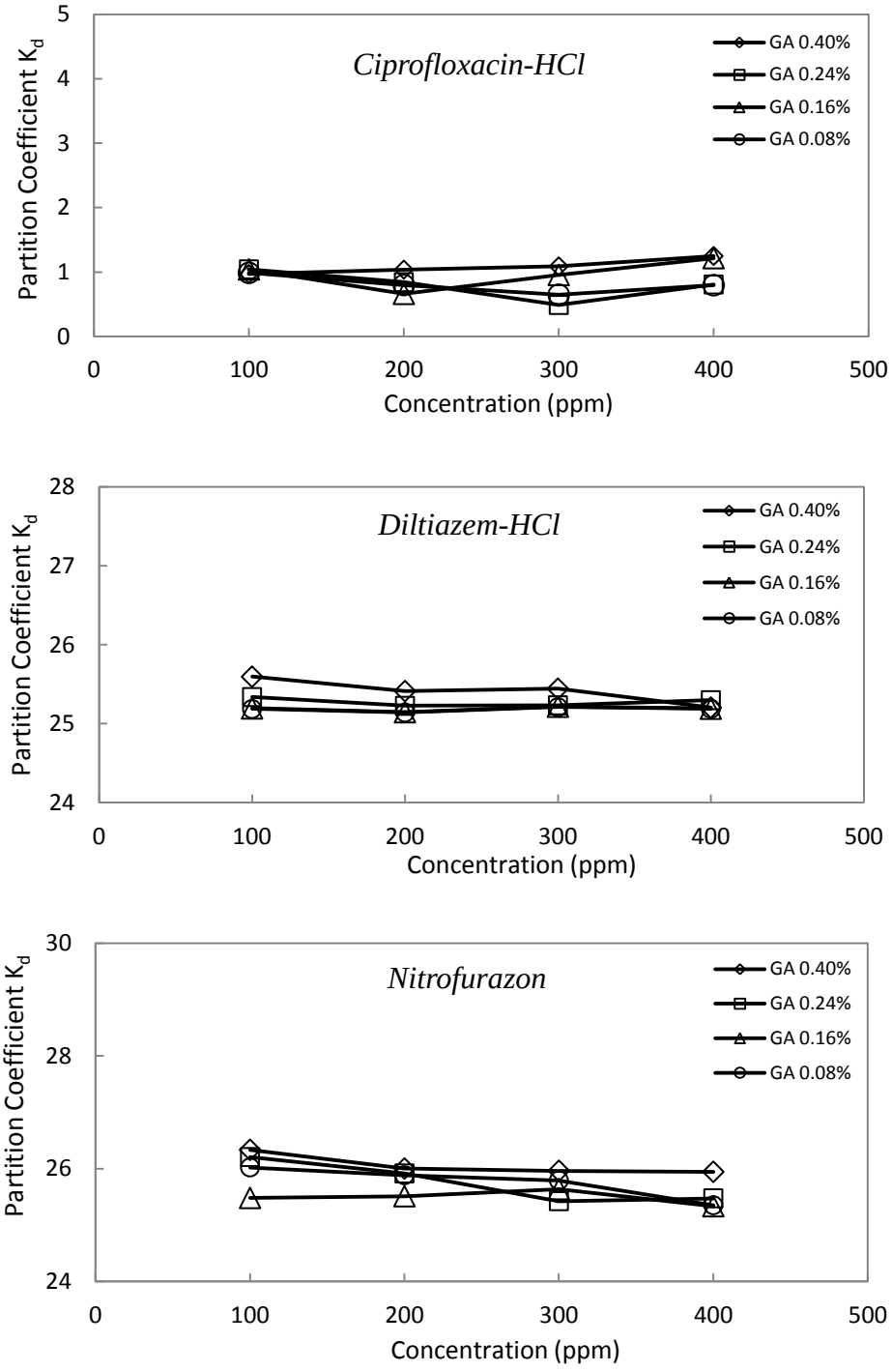

Figure 4-11 Partition coefficient K_d determined from sorption/desorption experiments; sericin/chitosan blend ratio 1:4; GA wt% with respect to the sericin/chitosan blend ratio

Chapter 5 Conclusions

In this work new membranes were prepared by blending sericin and chitosan for controlled release of drugs. The chitosan/sericin membranes were prepared by a solution casting technique, and the membranes were quite stable, homogeneous and transparent. These membranes were tested for controlled release of three model drugs including two hydrophilic (ciprofloxacin hydrochloride and diltiazem hydrochloride) and a hydrophobic (nitrofurazon). The intrinsic property parameters such as diffusivity, permeability and partition coefficients of the three drugs in the membranes were evaluated using permeation experiments and sorption/desorption tests. The setup for permeation experiments was found to have negligible boundary layer resistance.

The swelling degrees of the membranes with different degrees of crosslinking have been measured. The swelling degrees of the membranes were shown to be independent of drug concentrations and the degree of crosslinking over the experimental range tested in this work. Similarly, the drug concentration and membrane crosslinking did not exhibit significant effects on the diffusivity, permeability and partition coefficients of the three model drugs in the membranes. The diffusivity coefficients of the drugs in the membranes, were shown to be on the order of (10^{-9}-10^{-7} cm^2/s), and the permeability coefficients were on the order of (10^{-8}-10^{-6} cm^2/s). This is quite acceptable for controlled release applications when compared to the previous work.

The partition coefficients of the drugs were determined by sorption/desorption experiments. They were found to be (0.9±0.21) for ciprofloxacin-HCl, (25±0.12) for diltiazem-HCl and (26±0.31) for nitrofurazon, respectively. The permeation of ciprofloxacin-HCl, which is highly water soluble and has a strong interaction with amine groups in chitosan and sericin, appear to follow microchannel transport mechanism, while transport of less hydrophilic diltiazem-HCl and hydrophobic nitrofurazon appeared to be governed by the partition mechanism.

Chapter 6 Recommendations

Based on results obtained in this work, the following are recommended that may provide a further insight into controlled release of drugs using sericin/chitosan blend membranes:

This work deals mainly with the controlled release of ciprofloxacin-HCl, diltiazem-HCl and nitrofurazon using the newly developed chitosan/sericin blend membranes, and the diffusivity, permeability and partition coefficients of the drugs as well as swelling degree of the membranes were determined. In addition to the three model drugs investigated, these membranes should be tested with other different water soluble and insoluble drugs to gain further information on the general applicability of the membranes for controlled release. It is therefore recommended testing the membranes with other drugs, and if necessary modifying the composition and membrane crosslinking conditions. Further, the sericin/chitosan blend membrane may also be modified to achieve suitable structure for controlled release by matrix diffusion, and the following is recommended:

- Preparation of drug loaded films and evaluation of drug release profile and kinetics.
- Characterization of the membrane loaded by drugs and structural analysis in order to better understand the drug/membrane interactions
- Study of the effects of composition of drug loaded films and crosslinking degree as well as drug loading on the release profile
- Study of the effects of solution pH and ionic strength on the drug release profile

References

Annamaria S., Maria R., Tullia M., Silvio S, Orio C. The microbial degradation of silk: a laboratory investigation. Int. Biodeterior. Biodegrad. 1998; 42(4); 203–11

Berthold A., Cremer K., Kreuter j., Preparation and characterization of chitosan microspheres as drug carrier for prednisolone sodium phosphate as model for anti-inflammatory drugs, J. Ctrl. Rls., 1996; 39; 17-25

Chen Y., Zhang Y., Feng X., An improved approach for determining permeability and diffusivity relevant to controlled release, J. Chem. Eng. Sci. 2010; 65; 5921-5928

Chisti Y., Strategies in downstream processing, In: Subramanian G, editor. Bioseparation and bioprocessing: a handbook, vol. 2. New York, Wiley-VCH, 1998; 3–30

Crank, J., Park, G.S., Diffusion in Polymers, Academic Press, London. 1968

Crank, J., The Mathematics of Diffusion, Oxford University Press, Oxford. 1975

Dash R., Ghosh, S., Kaplan K. D. L., Kundu, S. C., Purification and biochemical characterization of a 70-kDa sericin from tropical tasar silkworm, Antheraea mylitta, Comp. Biochem. Physiol. B, 2007; 147; 129-134

Fujita T., Okubo M., Oonishi M., Production of natural organic polymer compound having polymerizability imparted here to. Japan Patent 10-195169A, 1998

Hoffman, A.S., The origins and evolution of controlled drug delivery systems. J. Ctrl. Rls. 2008; 132; 153–163

Hirotsu T., Nakajima S., Water–alcohol separation by pervaporation through silk fibroin membranes. sen-i Gakkaishi 1988; 44(2); 70–79

Jain S. K., Chourasia M. K., Sabitha M., Jain R., Jain A. K., and Ashawat M., Development and Characterization of Transdermal Drug Delivery Systems for Diltiazem Hydrochloride , J. Drug Delivery, 2003; 10; 169–177

Jin J. and Song M., Chitosan and Chitosan–PEO Blend Membranes Crosslinked by Genipin for Drug Release, J. Appl. Polym. Sci., 2006; 102; 436–444

Kenawy E., Abdel-Hay I., El-Magd A. A. and Mahmoud, Y., Biologically active polymers: Modification and anti-microbial activity of chitosan derivatives, J. Bioact. Comp. Polym. 2005; 20; 95-111

Kim J. H., Kim J. Y., Lee Y. M., and Kim K. Y., Controlled release of Riboflavin and Insulin through crosslinked poly(vinyl alcohol)/chitosan blend membrane, J. Appl. Polym. Sci., 1992; 44; 1823-1828

Langer, R.S., Peppas, N.A., Present and future applications of biomaterials in controlled drug delivery system. J. Biomat. 1981; 2; 201–214

Leo A., Hansch C., and Elkins D., Partition Coefficients and Their Uses, Chem. Rev., 1971; 71; 525-616

Loftsson T., Vogensen S. B., Brewster M. E., Konraosdottir F., Effects of Cyclodextrins on Drug Delivery Through Biological Membranes, J. Pharm. Sci., 2007; 96; 2532-2546

Malette W.G., Quigley H., Gaines R.D., Johnson N.D., Rainer G., Chitosan: a new hemostatic. Ann. Thorac. Surg. 1983; 36; 55–58

Minoura N., Aiba S., Gotoh Y., Tsukada M., Imai T., Attachment and growth of cultured fibroblast cells on silk protein matrices. J. Biomed. Mater. Res. 1995; 29; 1215–21

Muzzarelli R. A., Mattioli M., Pugnaloni A., Biagini G., Biochemistry, Histology and Clinical Uses of Chitins and Chitosans in Wound Healing, EXS, 1999; 87; 251-264

Nagyvary, J. J., Falk, J. D., Hill, M. L., Schmidt, M. L., Wilkins, A. K., Bradbury, E. L., The hypolipidemic activity of chitosan and other polysaccharides in rats, Nutri. Rep. Int., 1979; 20; 677–684

Nakajima Y. Liquid crystal element. Japan Patent 06-018892A, 1994

Nakatsuka S., and Andrady A. L., Permeability of Vitamin B-12 in Chitosan Membranes: Effect of Crosslinking and Blending with Poly(vinyl alcohol) on Permeability, J. Appl. Polym. Sci., 1992; 44; 17-28

Nomura M., Iwasa Y., Araya H., Moisture absorbing and desorbing polyurethane foam and its production. Japan Patent 07-292240A, 1995

Padamwar, M. N. and Pawar A. P., Silk sericin and its applications: A review, J. Sci. Ind. Res., 2004; 63; 323-329

Padamwar, M. N., Pawar, A. P., Daithankar, A. V., and Mahadik, K. R., Silk sericin as a moisturizer: an in vivo study. J. Cosmet. Dermatol., 2005; 4; 250-257

Rabea E. I., Badawy M. E.T., Stevens C. V., Smagghe G., Steurbaut W., Chitosan as Antimicrobial Agent: Applications and Mode of Action. Ame. Chem. Soci. 2003; 4; 1457-1465

Silva R. M. P., Mano J. F., Reis R. L., Study of the Fosfosal Controlled Permeation through Glutaraldehyde Crosslinked Chitosan Membranes, Materials Science Forum 2006; 514-516; 990-994

Singh D. K. and Ray A. R., Controlled release of glucose through modified chitosan membranes, J. Memb. Sci. 1999; 155; 107-112

Srihanam P., Simcheur W., Srihanam Y. S., Study on Silk Sericin and Chitosan Blend Film: Morphology and Secondary Structure Characterizations, Pakistan J. Biolog. Sci., 2009; 12; 1487-1490

Stoilova O., Koseva N., Petrova T.S., Manolova N., Rashkov I., Naydenov M., Hydrolysis of Chitosan, Chitosan-Polyoxyethylene and Chitosan-Poly(2-acryloylamido- 2-methyl propane sulfonic acid) by a Crude Enzyme Complex from Trichoderma viride J. Bioact. Comp. Polym., 2001; 16; 379

Sumitomo K., Yamagoshi K., Tsukiyama T., Hori T., Protein-containing polymer compound. Japan Patent 09-124796A, 1997

Takasu, Y., Yamada, H., Tsubouchi, K., Isolation of three main sericin components from the cocoon of the silkworm, Bombyx mori. Biosci. Biotechnol. Biochem., 2002; 66; 2715–2718

Tanaka T., Antifrosting method, antifrosting agent and snow melting agent. Japan Patent 2001 055562A, 2001

Tavelin, S., Grasjo J., Taipalensuu J., Ocklind G., Artursson P., Applications of epithelial cell culture in studies of drug transport, Methods Mol. Biol. 2002; 188; 233–272

Thacharodi D. and Rao P. K. D., Release of nifedipine through crosslinked chitosan membranes, Int. J. Pharm., 1993; 96; 33-39

Tsubouchi K. Wound covering material. US Patent US5951506, 1999a

Tsubouchi K. Occlusive dressing consisting essentially of silk fibroin and silk sericin and its production. Japan Patent 11-070160A, 1999b

Tsukada M., Hayasaka S., Inoue K., Nishikawa S., Yamamoto S., Cell culture bed substrate for proliferation of animal cell and its preparation. Japan Patent 11-243948A, 1999

Uhrich K. E., Cannizzaro S. M., Langer R. S., Shakesheff K.M., Polymeric systems for controlled drug release. Ind. Eng. Chem. Process Des. Dev. 1999; 10; 375–379

Vande Vord P.J., Matthew H.W., DeSilva S.P., Mayton L., Wu B., Wooley P.H., Evaluation of the biocompatibility of a chitosan scaffold in mice. J Biomed Mater Res 2002; 59; 58-58

Wang Q., Dong Z., Du Y., Kennedy J. F., Controlled release of ciprofloxacin hydrochloride from chitosan/polyethylene glycol bled films, Carbohyd. Polym. 2007; 69; 336-343

Wang X. H., Zhu Y., Feng Q. L., Cui F. Z., Ma J. B., Responses of Osteo- and Fibroblast Cells to Phosphorylated Chitin, J. Bioact. Comp. Polym., 2003; 18; 135-146

Zhang M., Tan T., Yuan H., Rui, Insecticidal and Fungicidal Activities of Chitosan and Oligo-chitosan, J. Bioact. Comp. Pol., 2003;18: 391-398

Zhang, Y. Q., Applications of natural silk protein sericin, Biomat. Biotechnol. Adv., 2002; 20; 91–100

Appendixes

Appendix A : Sample calculations

7.1.1. A.1. Permeation experiments

Determination of diffusivity and permeability using time-lag and mass balance method

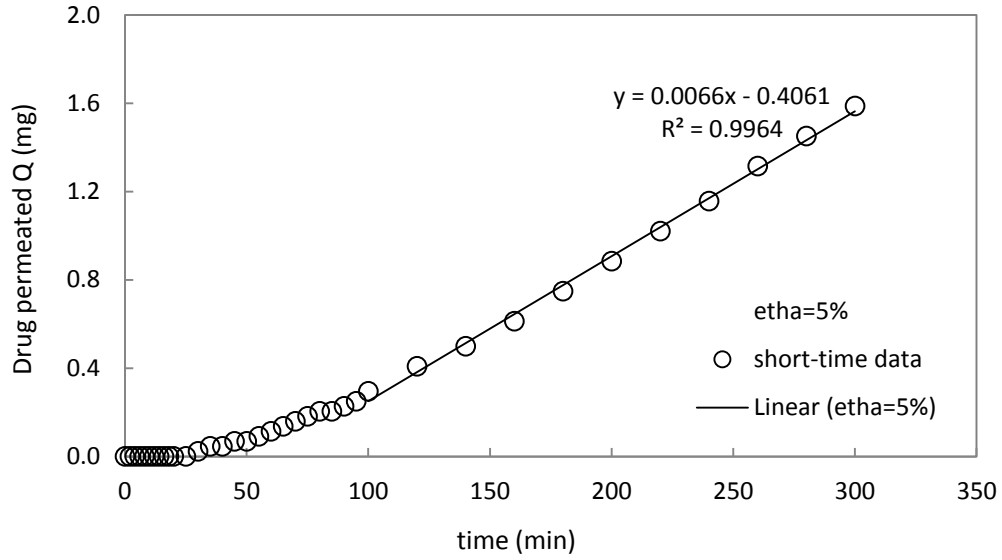

Figure 6-1 The permeated ciprofloxacin-HCl Q versus time through sericin/chitosan membrane, Initial drug concentration 400 ppm, GA%: 0.08, membrane thickness 76µm, η=5%

$time - lag\ \theta = 61\ min$

Membrane thickness l = 76 µm Membrane Area= 12 cm^2

$$Q = \frac{PAC_D}{l}(t - \frac{l^2}{6D})$$

$D_T = \frac{l^2}{6\theta}$ $D_T = \frac{0.0076^2}{6\times61\times60} = 2.6 \times 10^{-9}\ (^{cm^2}/_{s})$

$$P_T = \frac{slope \times l}{AC_D} = \frac{0.0066 \times 0.0076}{12 \times 0.409} \times \frac{1\ min}{60\ sec} = 1.8 \times 10^{-7} (^{cm^2}/_{s})$$

$t_0 \geq 3\theta; \qquad t_0 \geq 183\ min$

Plotting $F(t) = -ln\ [(m_0 - V_t C_R)/(m_0 - V_t a)]$ versus t

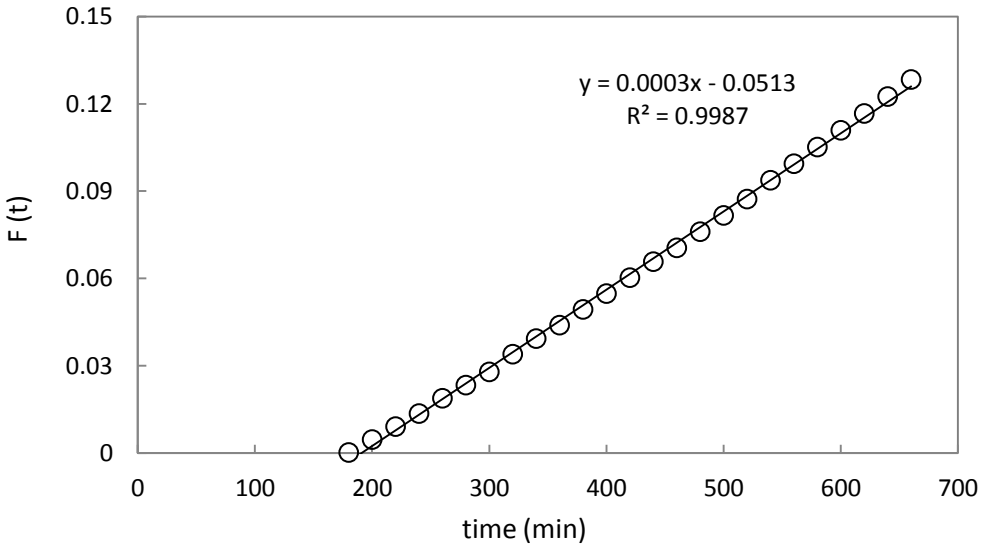

Figure 6-2 long time permeation data, F(t) vs. t, (t_0 >3 Θ) sericin/chitosan membrane, Initial drug concentration 400 ppm, GA%: 0.08, membrane thickness 76µm

$$-\ln\left(\frac{m_0 - V_t C_R}{m_0}\right) = \frac{PA}{l}\left(\frac{1}{V_D} + \frac{1}{V_R}\right) t$$

$$P_M = \frac{\frac{slope \times l}{A}}{\frac{1}{V_D} + \frac{1}{V_R}} = \frac{(0.0003 \times 0.0076)/12}{\frac{1}{2000} + \frac{1}{80}} \times \frac{1}{60} = 2.4 \times 10^{-7} (^{cm^2}/_{s})$$

7.1.2. A.2 Sorption and Desorption experiments

Determination of diffusivity using time-dependent sorption/desorption method

$$\frac{M_t}{M_\infty} = 1 - \sum_{n=1}^{\infty} \frac{2\alpha(1+\alpha)}{1+\alpha+\alpha^2 q_n^2} e^{-4Dq_n^2 t/l^2}$$

$$\tan q_n = \alpha q_n$$

Table 6-1 Non-zero positive roots of tan (q_n)=αq_n are illustrated in table below

q_n	αq_n	tan(q_n)
0	0	0
1.54491064	38.622766	38.622762
4.7038856	117.5971394	117.5971393
7.84888541	196.2221353	196.2221355
10.9919353	274.79838180	274.7983818
14.1343370	353.358424	353.3584241
17.2764443	431.9111077	431.9111077
20.4183932	510.4598308	510.4598325
23.5602471	589.0061782	589.0061782
26.7020395	667.5509886	667.5509886
29.8437899	746.0947474	746.0947474
32.9855102	824.6377552	824.6377552

$$\alpha = \frac{V}{V_p} = \frac{50\ ml}{2\ ml} = 25$$

Membrane thickness l = 76 µm Membrane Area= 12 cm^2

POLYMATH Report Ciprofloxacin –HCl desorption 400 ppm GA 0.1
Nonlinear Regression (L-M) 14-Nov-2011

Model: M = 1-0.85655*exp(-2.386749*A*t)-0.09383*exp(-22.12186*A*t)-0.0337407*exp(-61.60500*A*t)-0.01721*exp(-120.822641*A*t)-0.010409*exp(-199.7795*A*t)-0.0069678*exp(-298.4755*A*t)-0.00498858*exp(-416.91078*A*t)-0.0037469*exp(-555.085245*A*t)

Variable	Initial guess	Value	95% confidence
A	5.0E-08	0.1154553	0.0112184

Nonlinear regression settings
Max # iterations = 64

Precision

R^2	0.9754133
R^2adj	0.9754133
Rmsd	0.0066787
Variance	0.001518

General

Sample size	33
Model vars	1
Indep vars	1
Iterations	12

Source data points and calculated data points

	t	M	M calc	Delta M
1	0	0	-0.027443	0.027443
2	0.5	0.176056084	0.2265525	-0.0504965
3	1	0.306050982	0.3424306	-0.0363796
4	2	0.458564683	0.5058022	-0.0472376
5	3	0.644856585	0.625219	0.0196376
6	4	0.757450592	0.7155171	0.0419335

7	5	0.862879526	0.7840386	0.0788409
8	6	0.870044599	0.8360543	0.0339903
9	7	0.884374745	0.8755415	0.0088333
10	8	0.895634146	0.905518	-0.0098838
11	9	0.903822801	0.9282745	-0.0244517
12	10	0.910987874	0.9455499	-0.0345621
13	12	0.918152947	0.9686204	-0.0504674
14	14	0.924294439	0.9819159	-0.0576215
15	16	0.931459512	0.9895781	-0.0581186
16	18	0.936577421	0.9939939	-0.0574164
17	20	0.938624585	0.9965387	-0.0579141
18	25	0.944766076	0.9991273	-0.0543612
19	30	0.952954731	0.99978	-0.0468252
20	35	0.957049059	0.9999445	-0.0428955
21	40	0.960119805	0.999986	-0.0398662
22	45	0.962166968	0.9999965	-0.0378295
23	50	0.964214132	0.9999991	-0.035785
24	55	0.967284878	0.9999998	-0.0327149
25	60	0.970355623	0.9999999	-0.0296443
26	80	0.977520697	1.	-0.0224793
27	90	0.981615024	1.	-0.018385
28	100	0.985709352	1.	-0.0142906
29	120	0.994921589	1.	-0.0050784
30	180	0.996968752	1.	-0.0030312
31	240	0.996968752	1.	-0.0030312
32	300	0.997992334	1.	-0.0020077
33	360	0.997992334	1.	-0.0020077

$$A = \frac{4D}{l^2}; \rightarrow \quad D = \frac{A.l^2}{4}$$

$$D = \frac{0.1154553 \times 0.0076^2}{4} \times \frac{1min}{60\ sec} = 27.8\ \times 10^{-9}\ (\frac{cm^2}{s})$$

Appendix B: Experimental Data

7.1.3. Permeation experiments

Ciprofloxacin-HCl

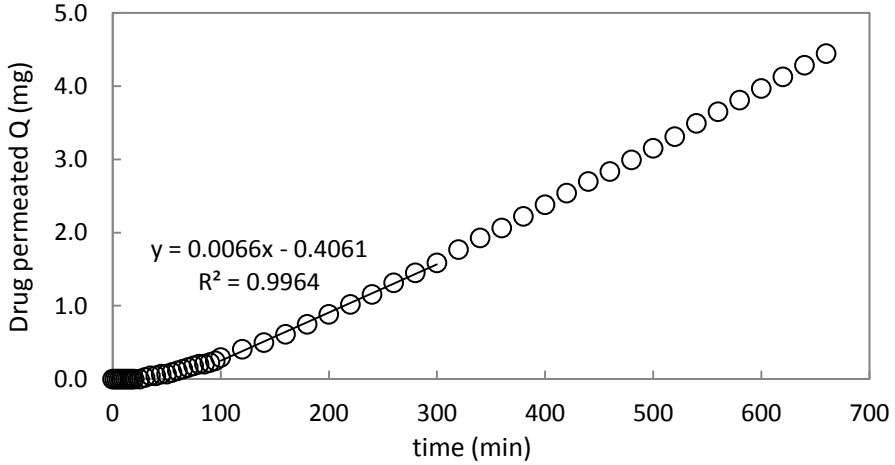

Figure 6-3 short-time permeation data, ciprofloxacin-HCl : 400 ppm, sericin/chitosan 1:4, GA: 0.08%

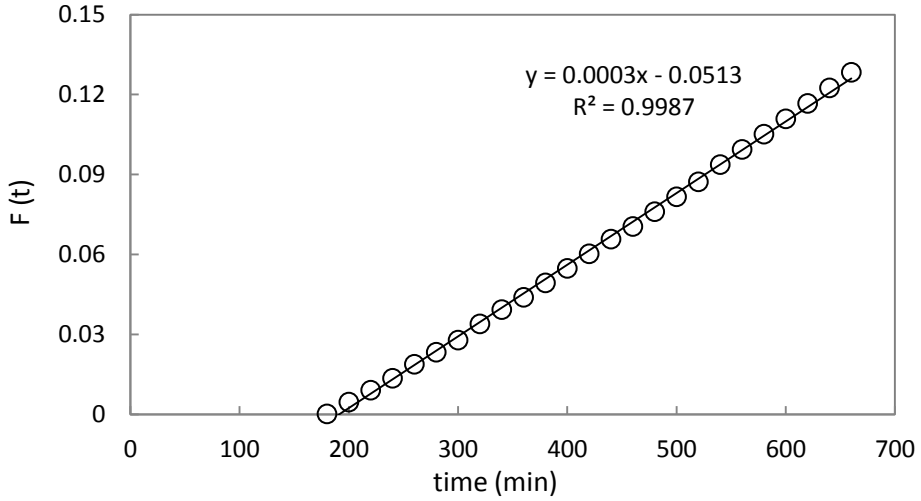

Figure 6-4 long-time permeation data. Ciprofloxacin-HCl : 400 ppm, sericin/chitosan 1:4, GA: 0.08%

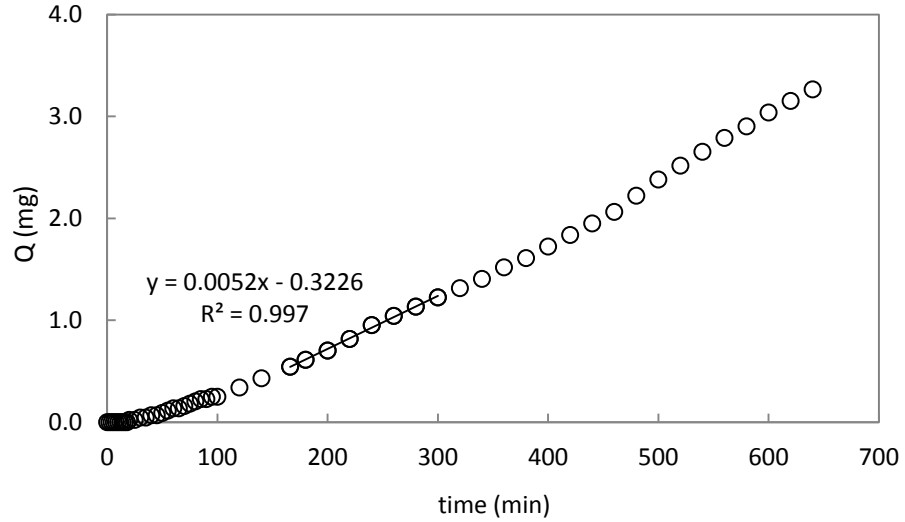

Figure 6-5 short-time permeation data, ciprofloxacin-HCl : 300 ppm, sericin/chitosan 1:4, GA: 0.08%

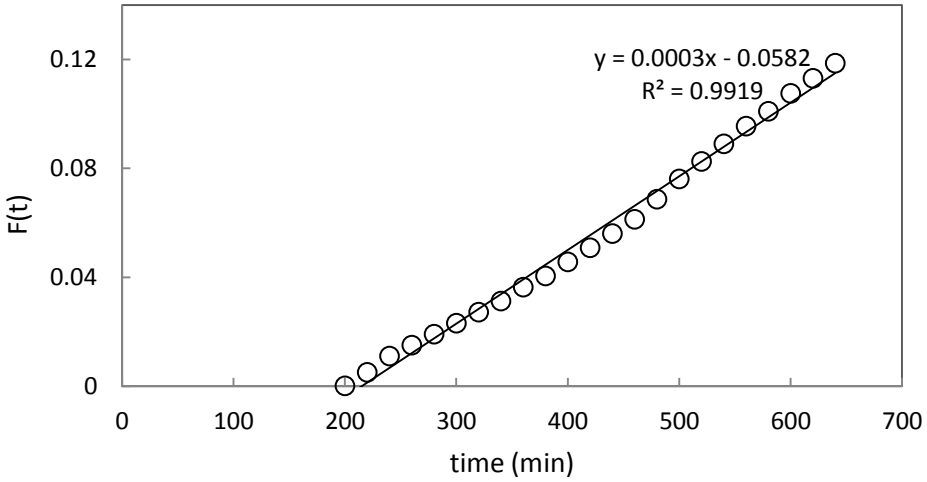

Figure 6-6 long-time permeation data. Ciprofloxacin-HCl : 300 ppm, sericin/chitosan 1:4, GA: 0.08%

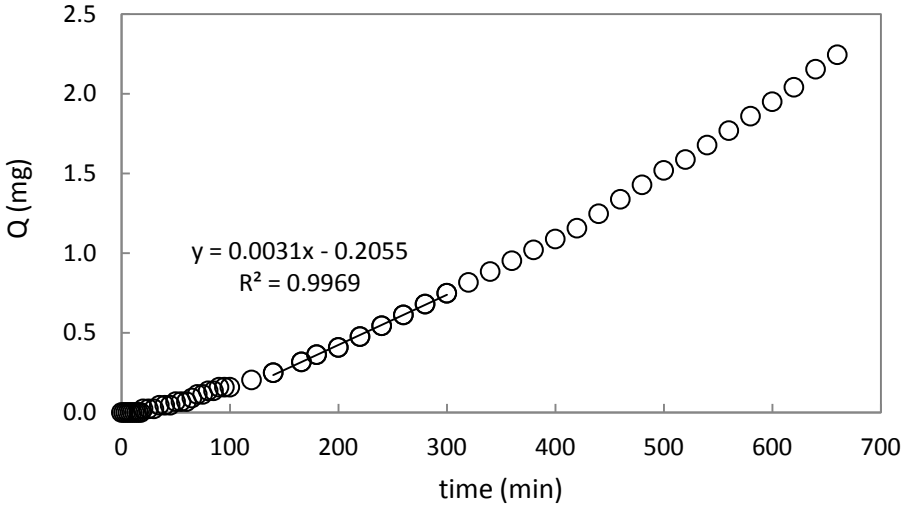

Figure 6-7 short-time permeation data, ciprofloxacin-HCl : 200 ppm, sericin/chitosan 1:4, GA: 0.08%

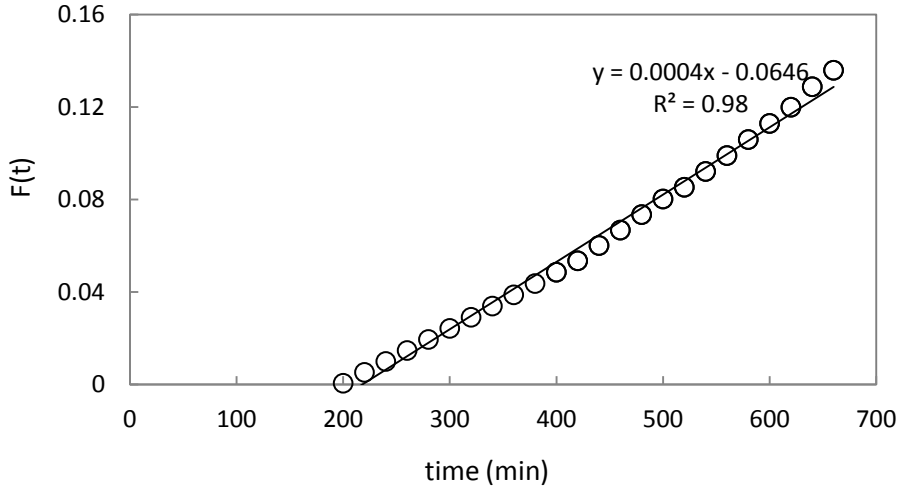

Figure 6-8 long-time permeation data Ciprofloxacin-HCl : 200 ppm, sericin/chitosan 1:4, GA: 0.08%

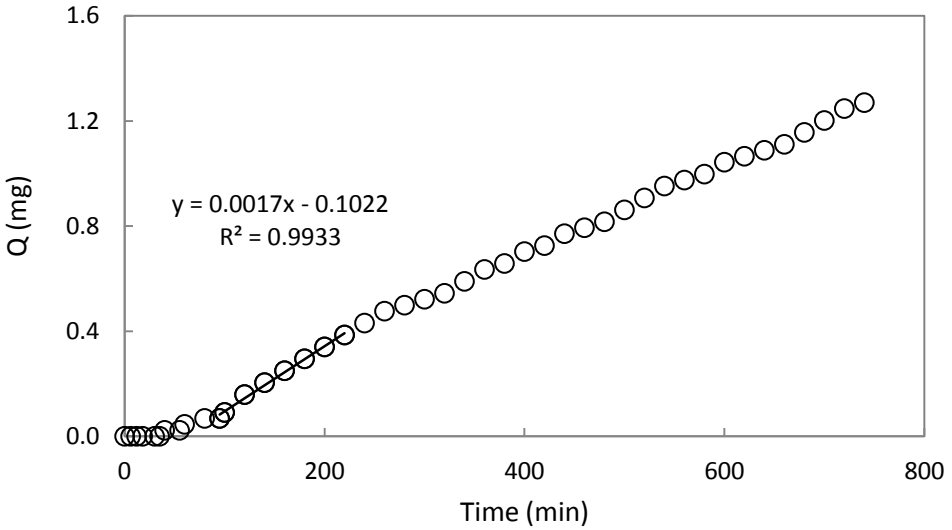

Figure 6-9 short-time permeation data Ciprofloxacin-HCl : 100 ppm, sericin/chitosan 1:4, GA: 0.08%

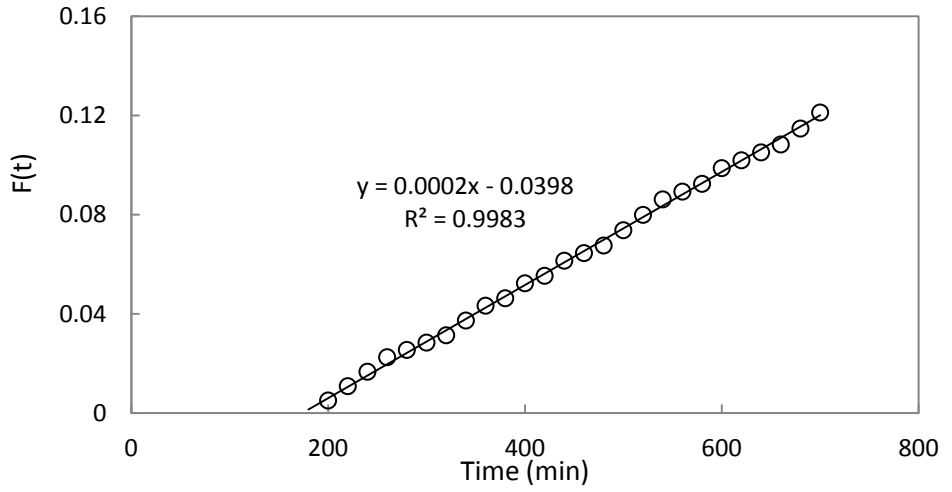

Figure 6-10 long-time permeation data Ciprofloxacin-HCl : 100 ppm, sericin/chitosan 1:4, GA: 0.08%

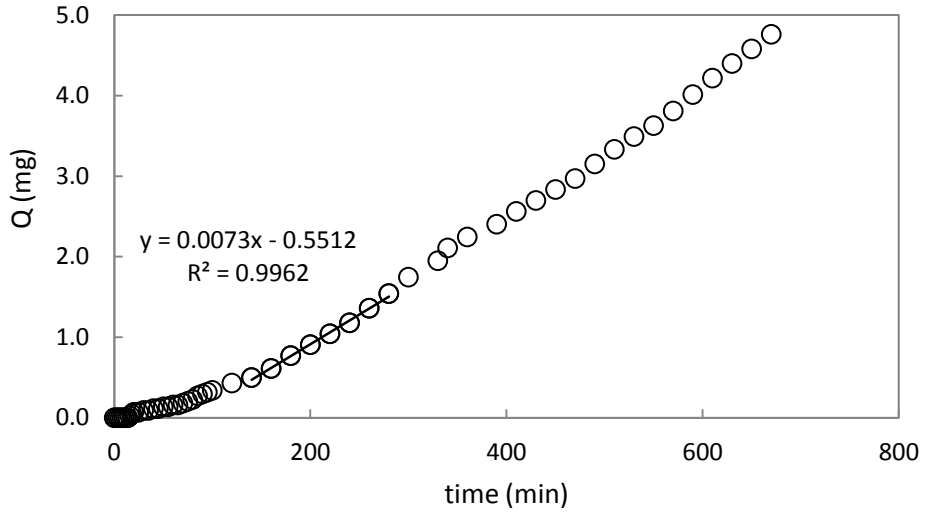

Figure 6-11 short-time permeation data Ciprofloxacin-HCl : 400 ppm, sericin/chitosan 1:4, GA: 0.16%

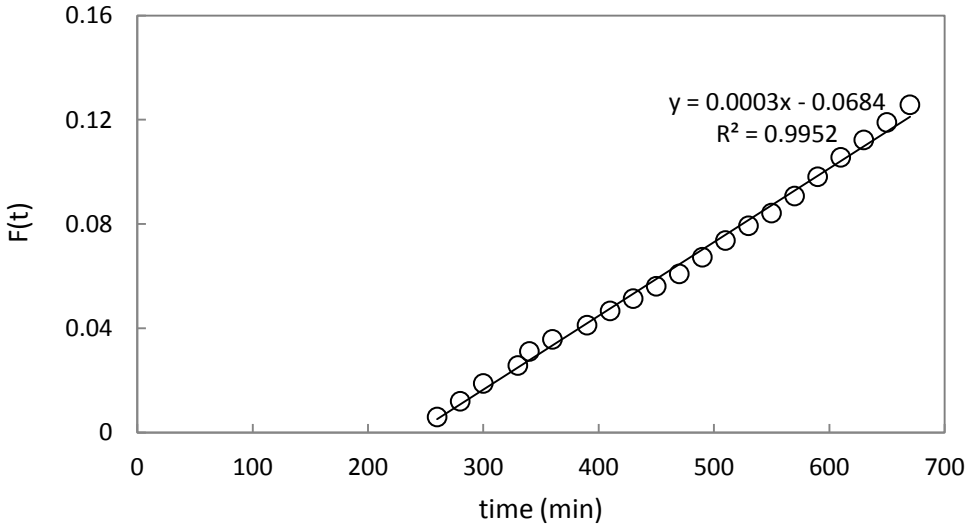

Figure 6-12 long-time permeation data Ciprofloxacin-HCl : 400 ppm, sericin/chitosan 1:4, GA: 0.16%

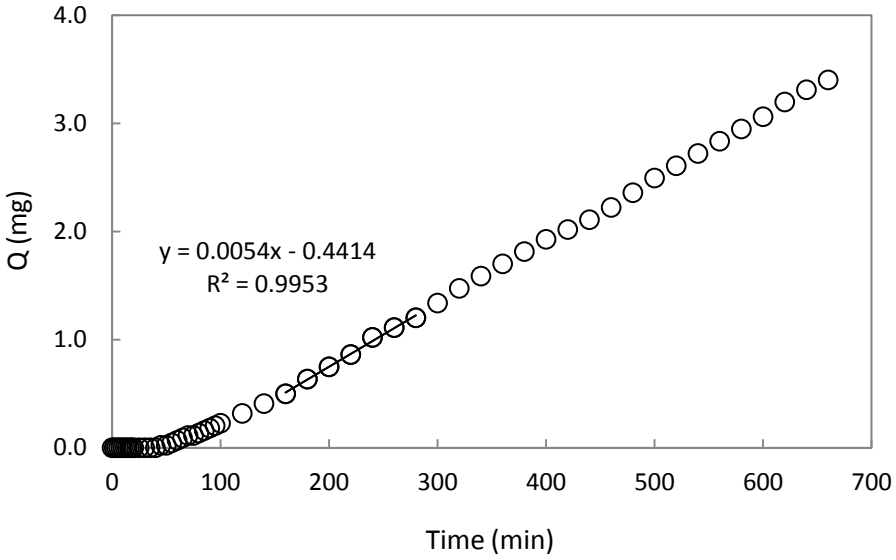

Figure 6-13 short-time permeation data Ciprofloxacin-HCl : 300 ppm, sericin/chitosan 1:4, GA: 0.16%

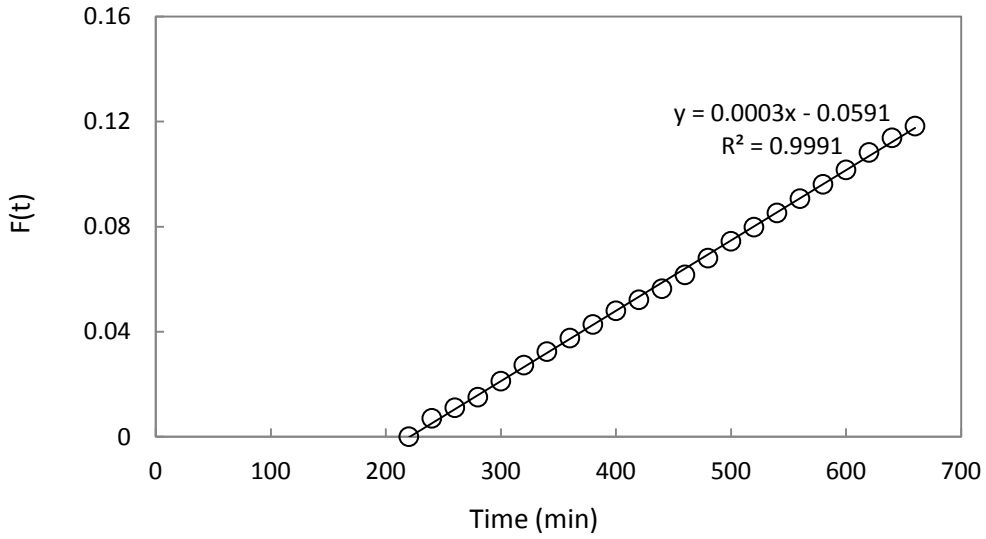

Figure 6-14 long-time permeation data Ciprofloxacin-HCl : 300 ppm, sericin/chitosan 1:4, GA: 0.16%

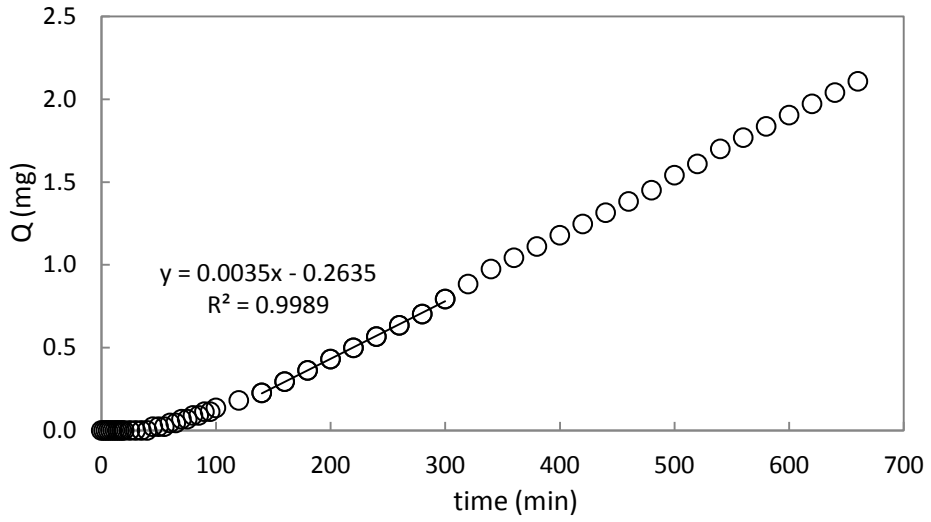

Figure 6-15 short-time permeation data Ciprofloxacin-HCl : 200 ppm, sericin/chitosan 1:4, GA: 0.16%

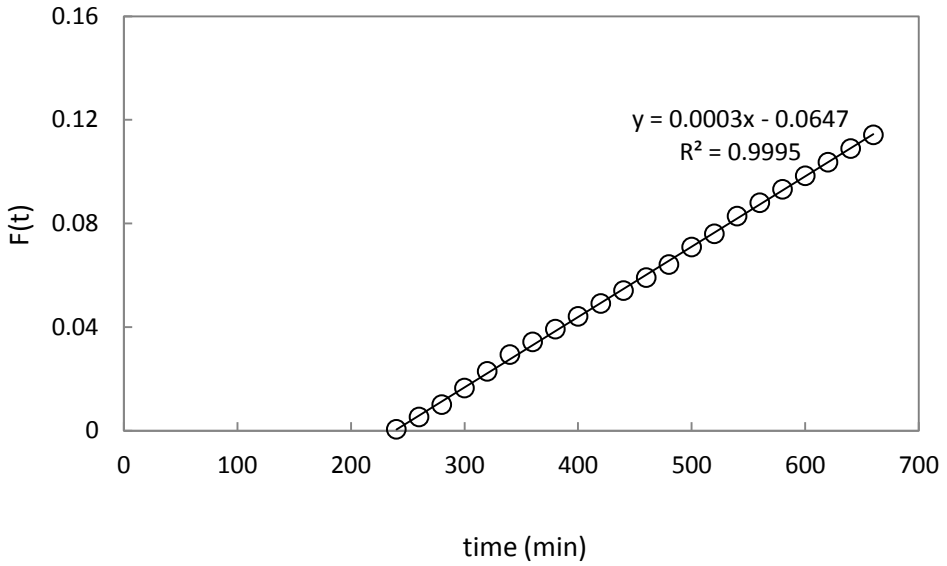

Figure 6-16 long-time permeation data Ciprofloxacin-HCl : 200 ppm, sericin/chitosan 1:4, GA: 0.16%

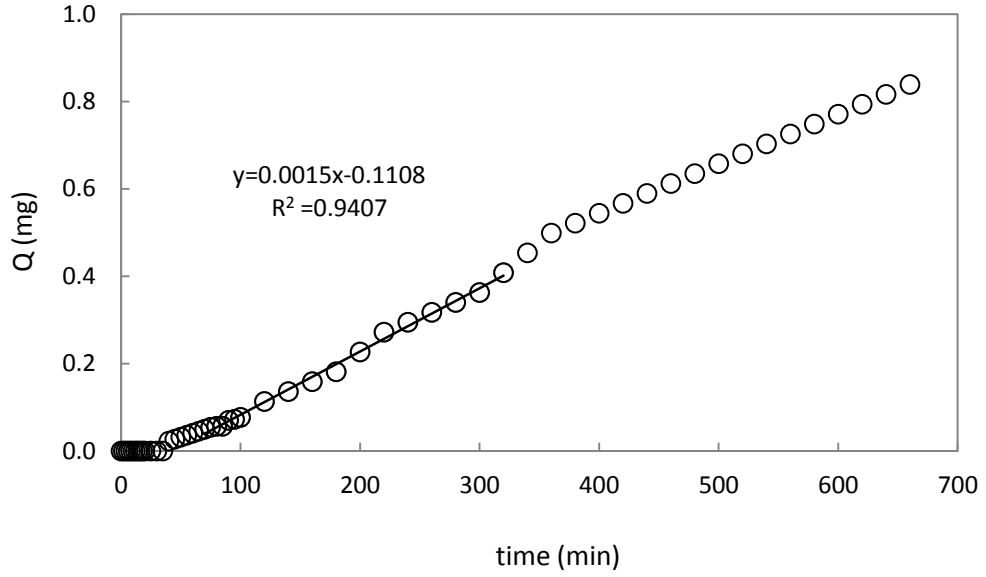

Figure 6-17 short-time permeation data Ciprofloxacin-HCl : 100 ppm, sericin/chitosan 1:4, GA: 0.16%

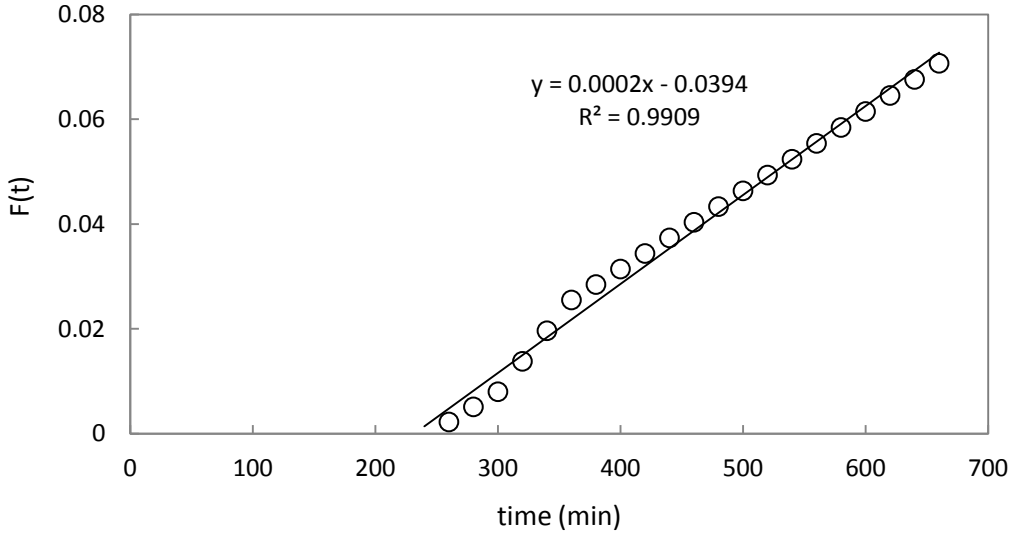

Figure 6-18 long-time permeation data Ciprofloxacin-HCl : 100 ppm, sericin/chitosan 1:4, GA: 0.16%

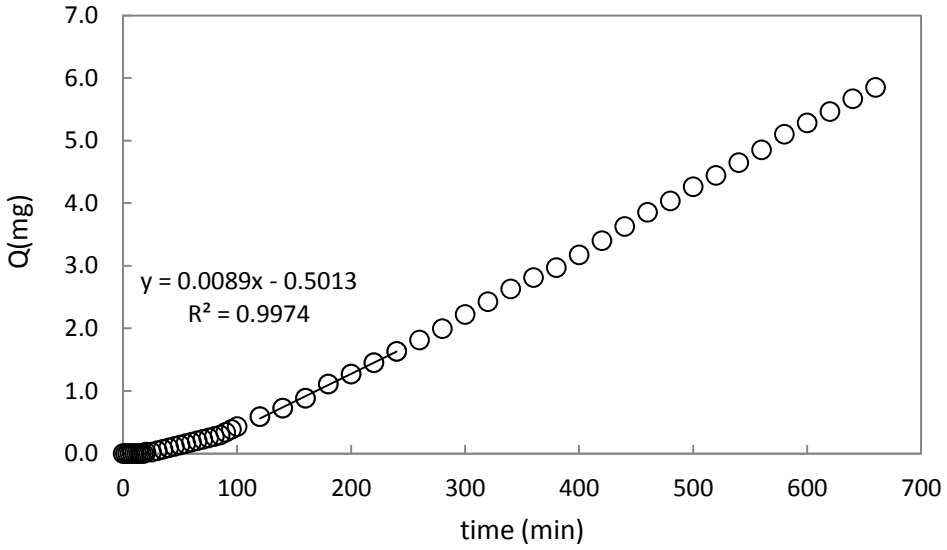

Figure 6-19 short-time permeation data Ciprofloxacin-HCl : 400 ppm, sericin/chitosan 1:4, GA: 0.24%

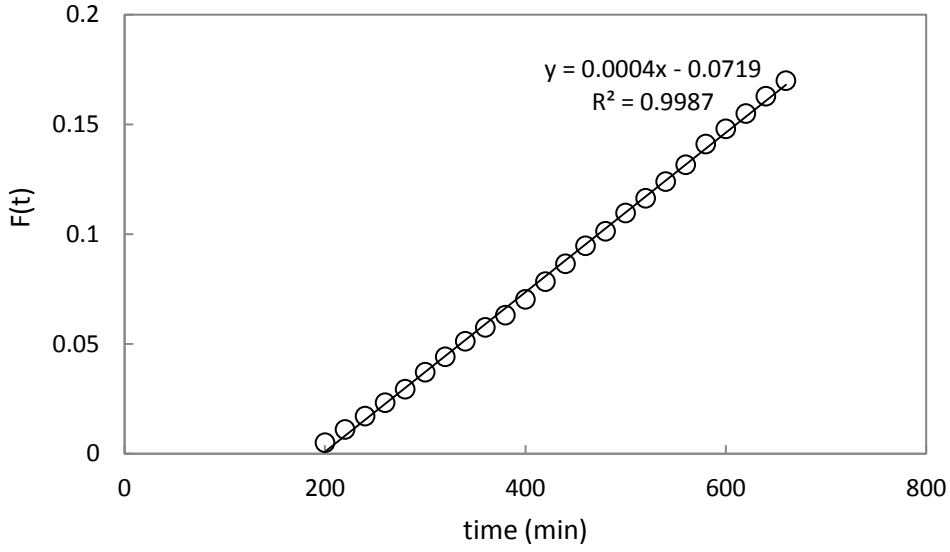

Figure 6-20 long-time permeation data Ciprofloxacin-HCl : 400 ppm, sericin/chitosan 1:4, GA: 0.24%

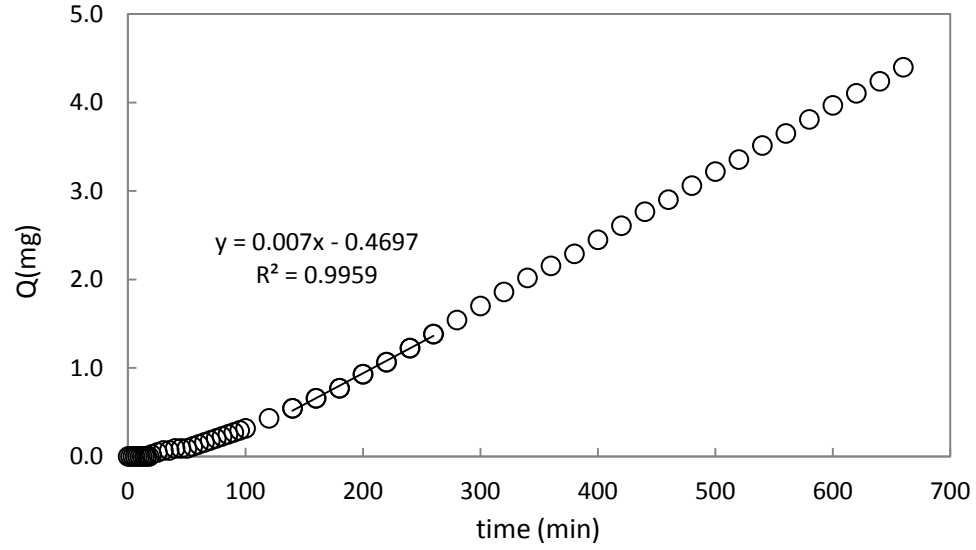

Figure 6-21 short-time permeation data Ciprofloxacin-HCl : 300 ppm, sericin/chitosan 1:4, GA: 0.24%

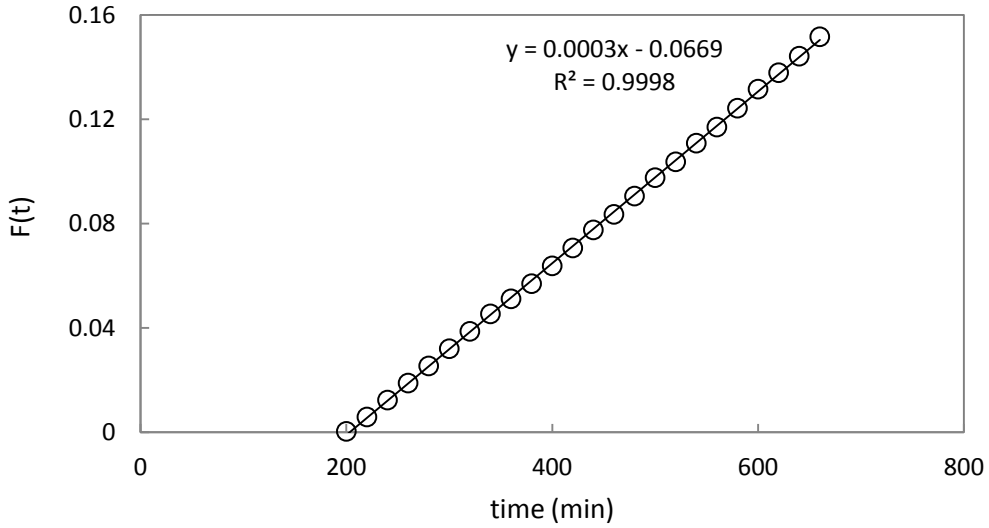

Figure 6-22 long-time permeation data Ciprofloxacin-HCl : 300 ppm, sericin/chitosan 1:4, GA: 0.24%

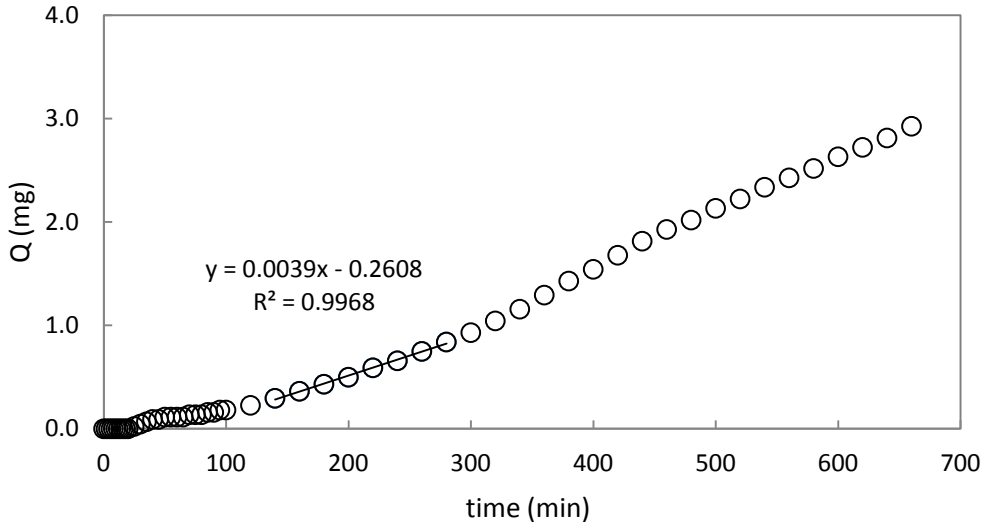

Figure 6-23 short-time permeation data Ciprofloxacin-HCl : 200 ppm, sericin/chitosan 1:4, GA: 0.24%

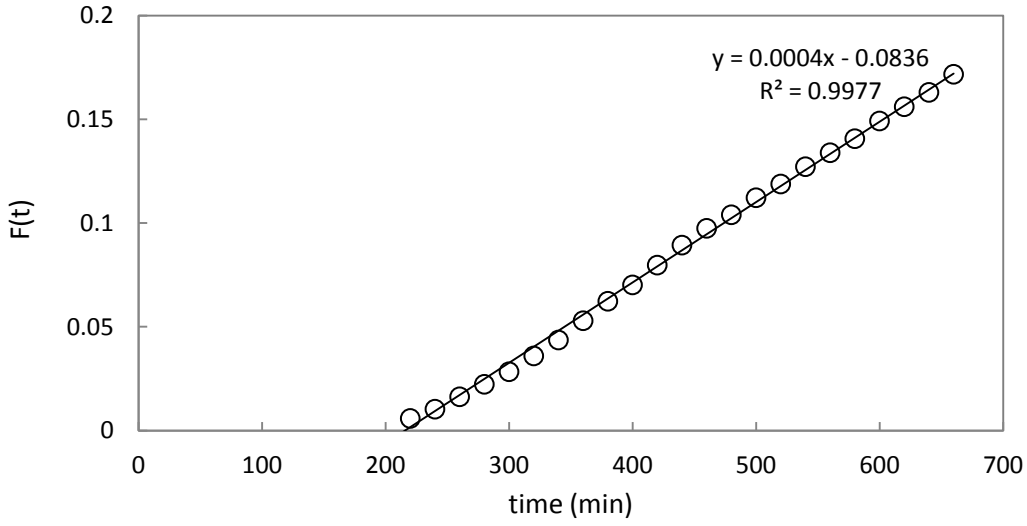

Figure 6-24 long-time permeation data Ciprofloxacin-HCl : 200 ppm, sericin/chitosan 1:4, GA: 0.24%

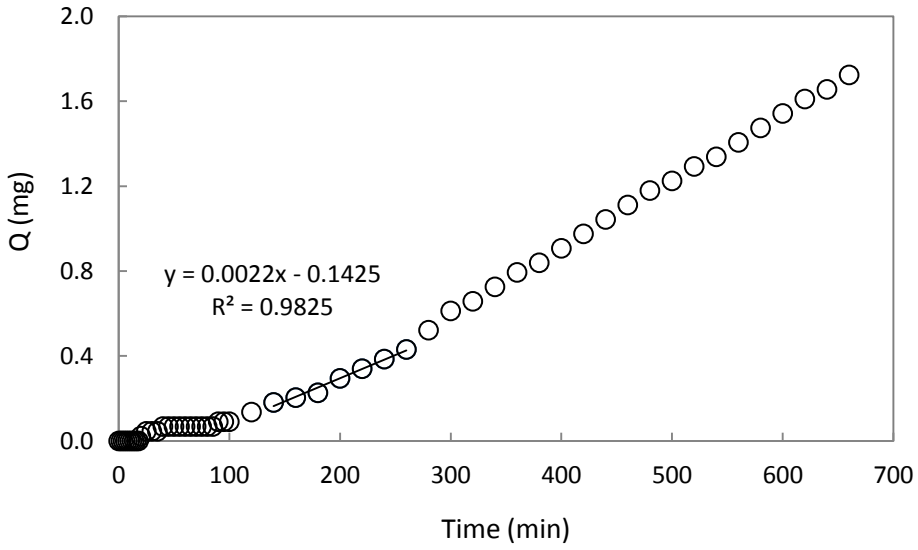

Figure 6-25 short-time permeation data Ciprofloxacin-HCl : 100 ppm, sericin/chitosan 1:4, GA: 0.24%

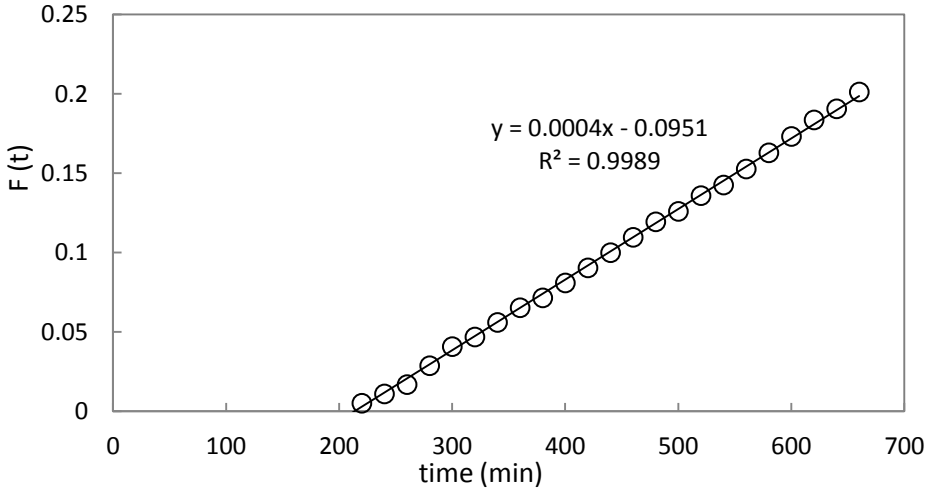

Figure 6-26 long-time permeation data Ciprofloxacin-HCl : 100 ppm, sericin/chitosan 1:4, GA: 0.24%

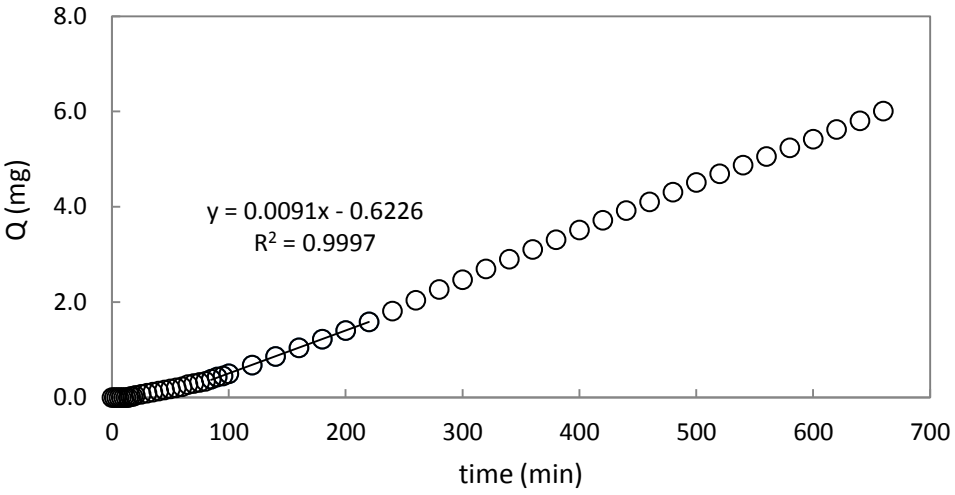

Figure 6-27 short-time permeation data Ciprofloxacin-HCl : 400 ppm, sericin/chitosan 1:4, GA: 0.40%

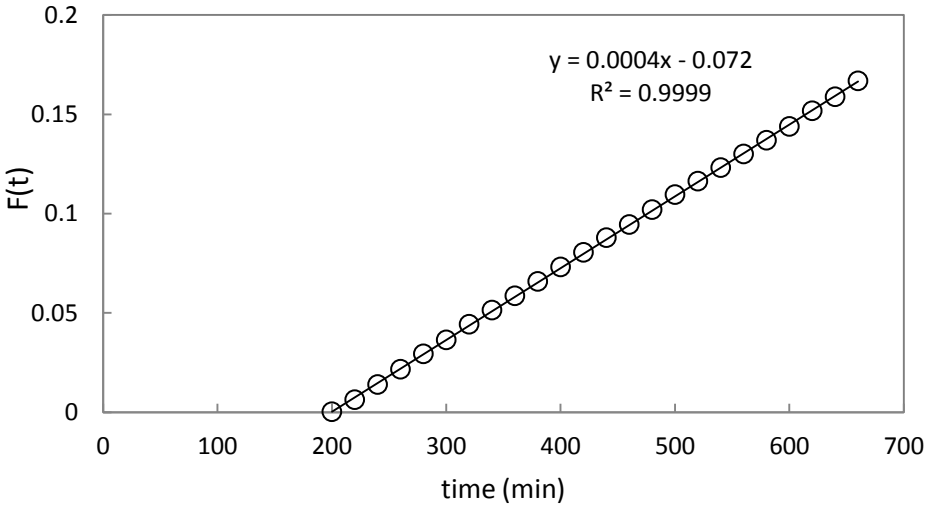

Figure 6-28 long-time permeation data Ciprofloxacin-HCl : 400 ppm, sericin/chitosan 1:4, GA: 0.40%

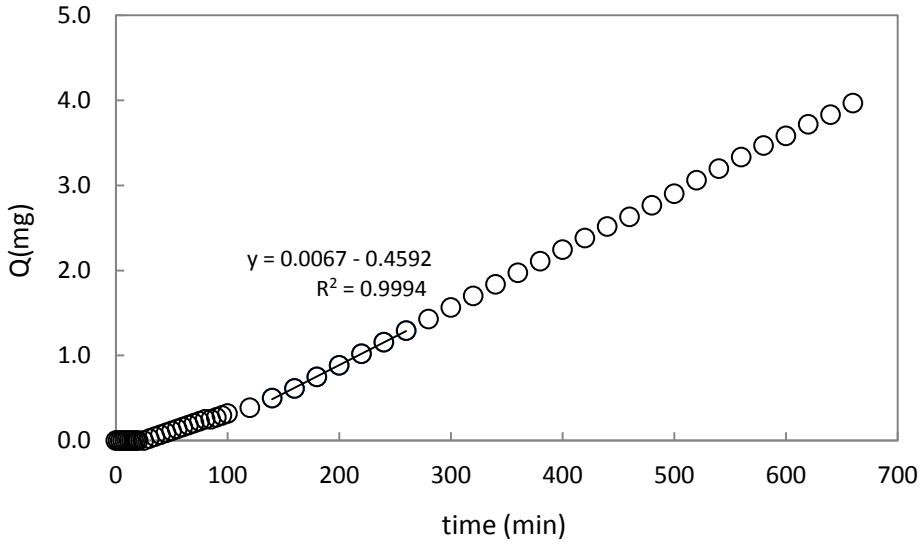

Figure 6-29 short-time permeation data Ciprofloxacin-HCl : 300 ppm, sericin/chitosan 1:4, GA: 0.40%

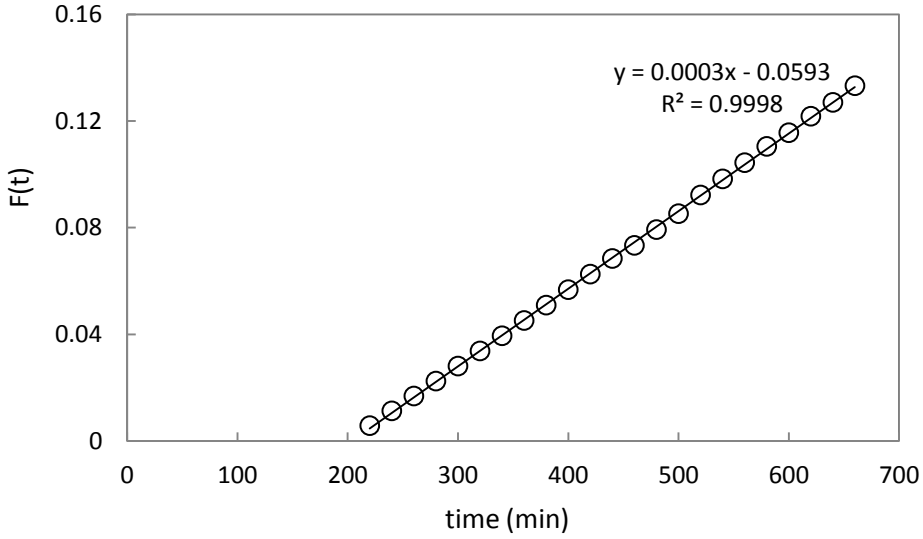

Figure 6-30 long-time permeation data Ciprofloxacin-HCl : 300 ppm, sericin/chitosan 1:4, GA: 0.40%

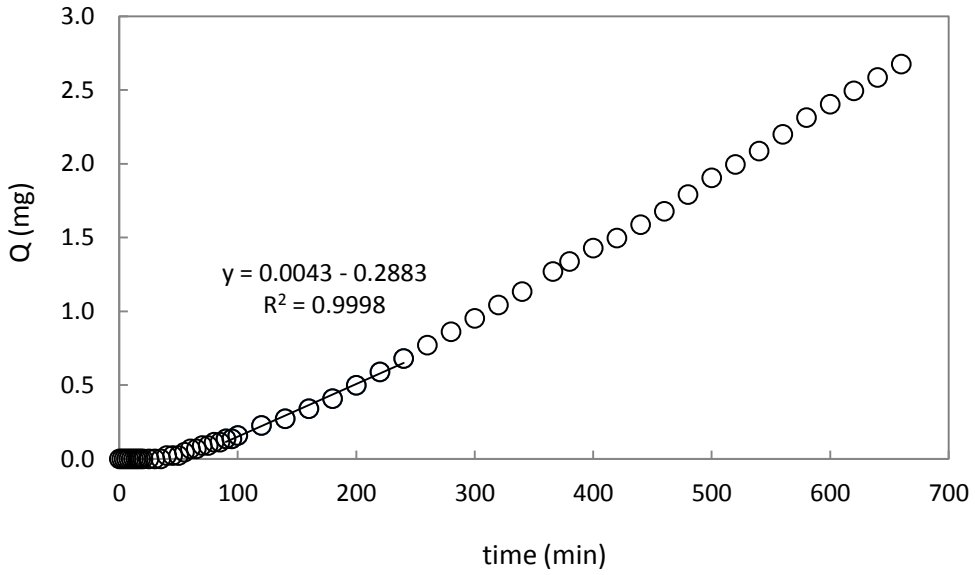

Figure 6-31 short-time permeation data Ciprofloxacin-HCl : 200 ppm, sericin/chitosan 1:4, GA: 0.40%

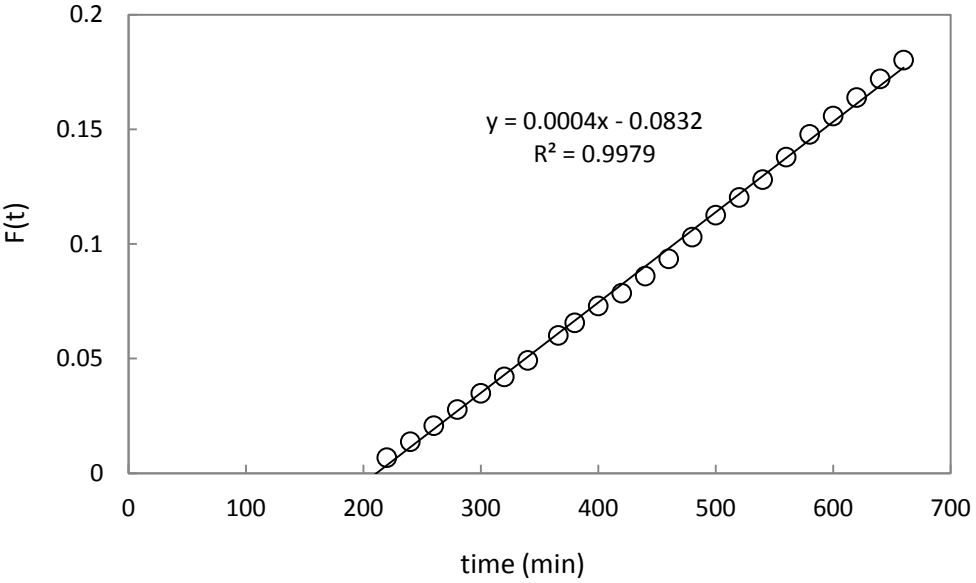

Figure 6-32 long-time permeation data Ciprofloxacin-HCl : 200 ppm, sericin/chitosan 1:4, GA: 0.40%

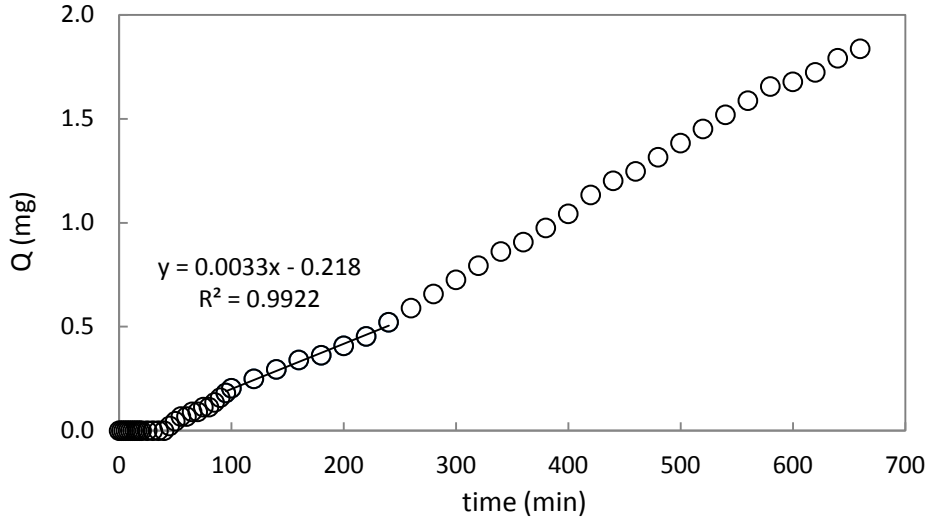

Figure 6-33 short-time permeation data Ciprofloxacin-HCl : 100 ppm, sericin/chitosan 1:4, GA: 0.40%

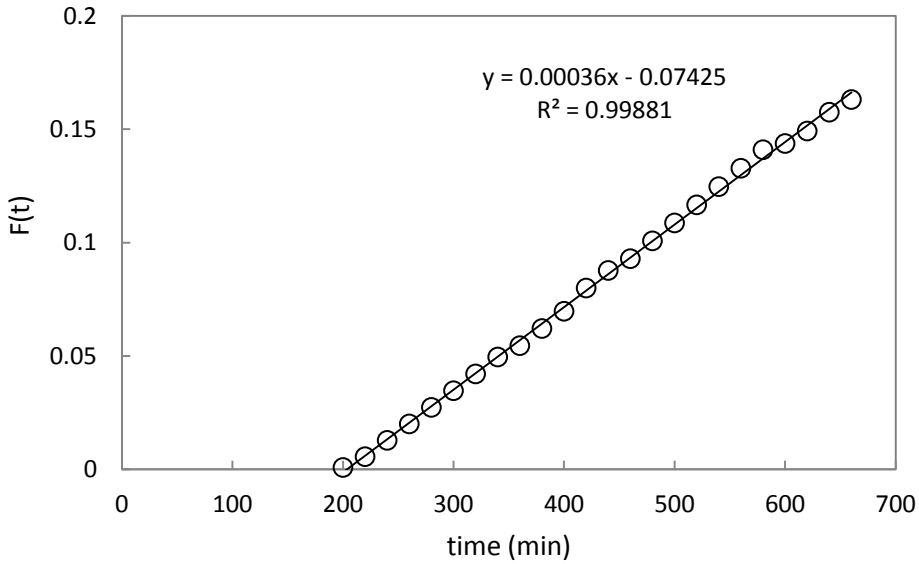

Figure 6-34 long-time permeation data Ciprofloxacin-HCl : 100 ppm, sericin/chitosan 1:4, GA: 0.40%

Table 6-2 Permeation parameters for Ciprofloxacin-HCl

GA%	Conc. (ppm)	Thickness (μ)	Time Lag (min)	D_T (cm^2/s)	P_T(cm^2/s)	P_M(cm^2/s)
0.08	100	76 ±5	60	2.67E-09	1.81E-07	1.62E-07
	200	76 ± 5	66	2.43E-09	1.69E-07	3.25E-07
	300	76 ± 5	62	2.59E-09	1.79E-07	2.65E-07
	400	76 ± 5	61	2.61E-09	1.80E-07	2.44E-07
0.16	100	77 ± 6	74	2.23E-09	1.51E-07	1.64E-07
	200	77 ± 6	75	2.19E-09	1.93E-07	2.47E-07
	300	77 ± 6	74	2.24E-09	1.89E-07	2.47E-07
	400	77 ± 6	76	2.18E-09	1.91E-07	2.80E-07
0.24	100	72 ± 4	65	2.22E-09	2.09E-07	3.08E-07
	200	72 ± 4	67	2.15E-09	1.89E-07	3.08E-07
	300	72 ± 4	67	2.15E-09	2.10E-07	2.31E-07
	400	72 ± 4	56	2.57E-09	2.18E-07	3.08E-07
0.40	100	70 ± 5	66	2.06E-09	2.48E-07	2.69E-07
	200	70 ± 5	67	2.03E-09	2.35E-07	2.99E-07
	300	70 ± 5	69	1.97E-09	1.95E-07	2.24E-07
	400	70 ± 5	68	2.00E-09	2.17E-07	2.70E-07

Diltiazem hydrochloride

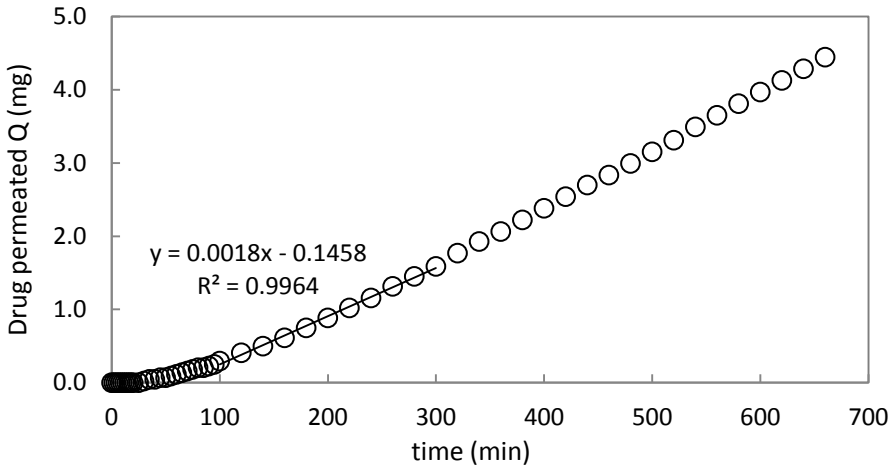

Figure 6-35 short-time permeation data, diltiazem-HCl: 400 ppm, sericin/chitosan 1:4, GA: 0.08%

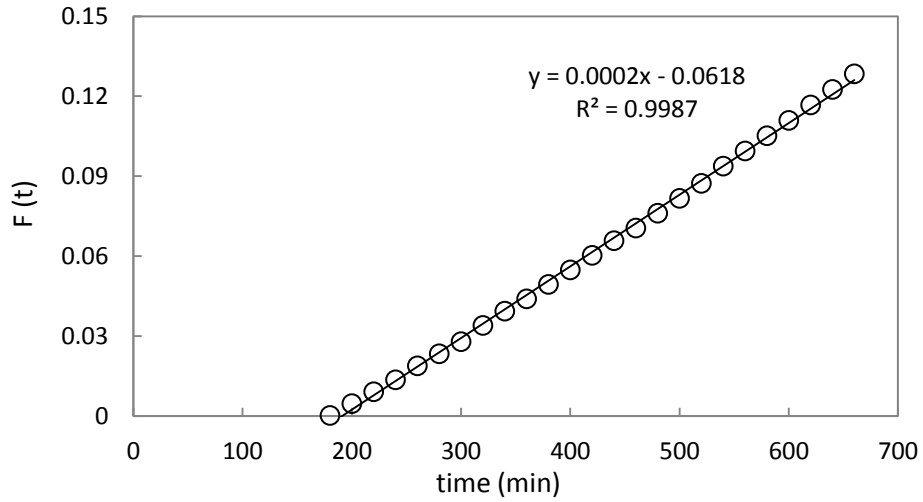

Figure 6-36 long-time permeation data. diltiazem -HCl : 400 ppm, sericin/chitosan 1:4, GA: 0.08%

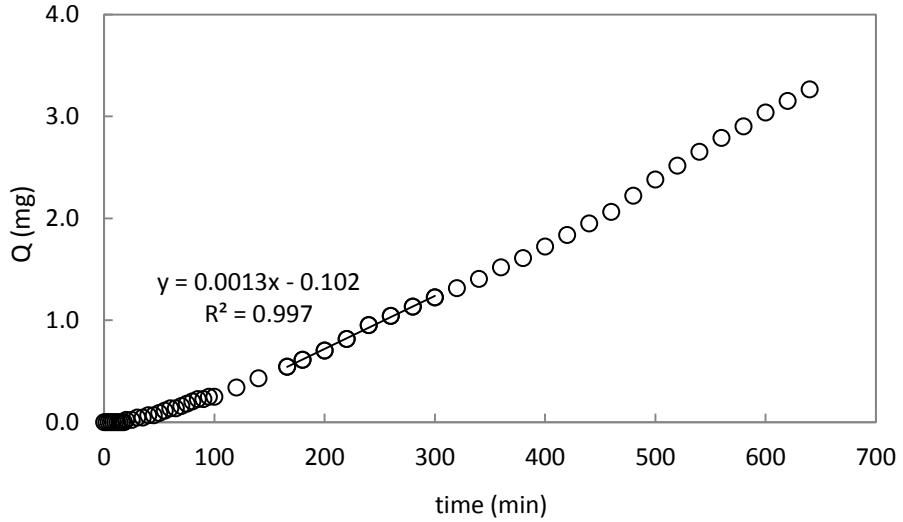

Figure 6-37 short-time permeation data, diltiazem -HCl : 300 ppm, sericin/chitosan 1:4, GA: 0.08%

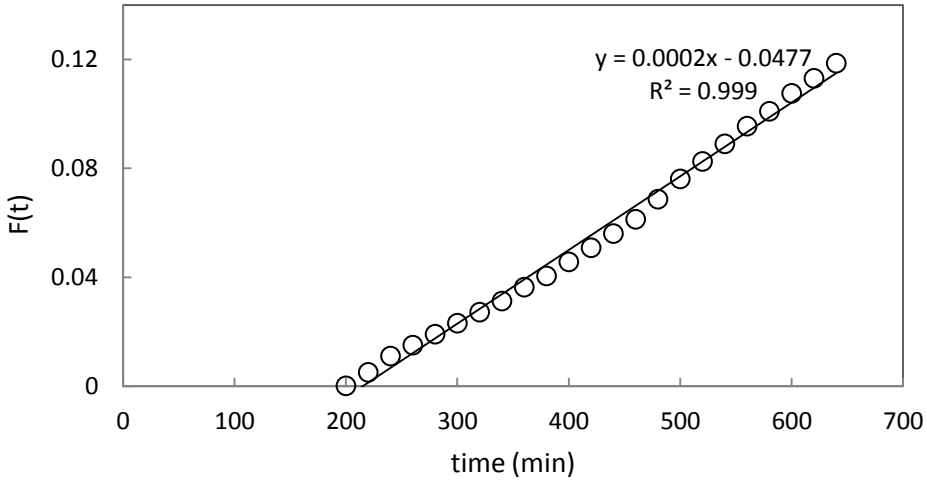

Figure 6-38 long-time permeation data diltiazem -HCl : 300 ppm, sericin/chitosan 1:4, GA: 0.08%

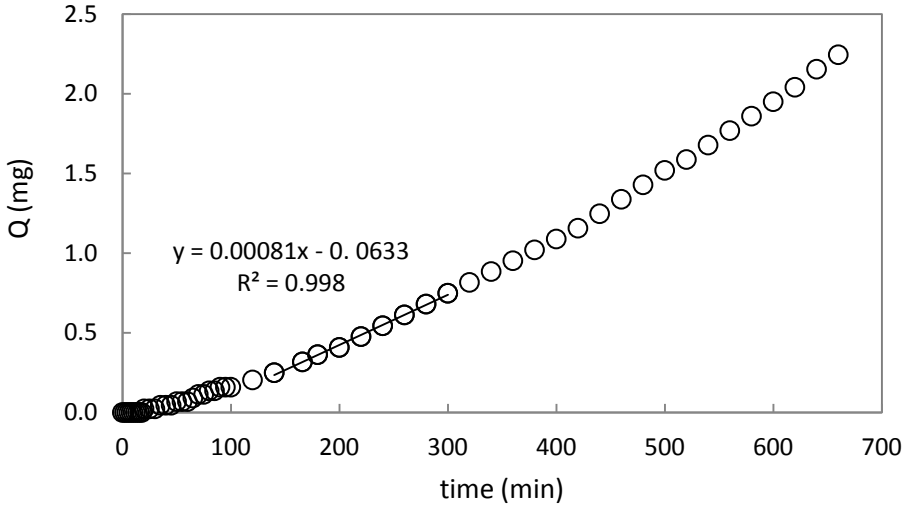

Figure 6-39 short-time permeation data, diltiazem -HCl : 200 ppm, sericin/chitosan 1:4, GA: 0.08%

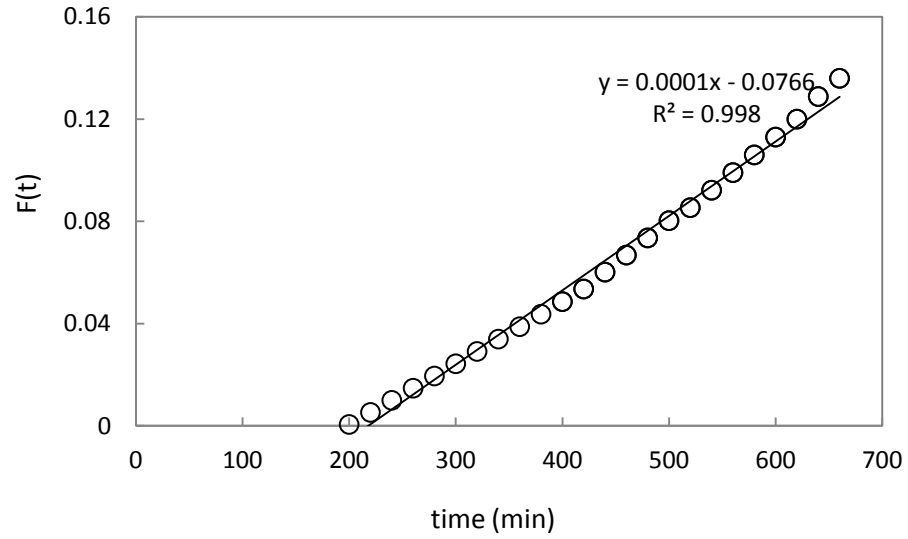

Figure 6-40 long-time permeation data diltiazem -HCl : 200 ppm, sericin/chitosan 1:4, GA: 0.08%

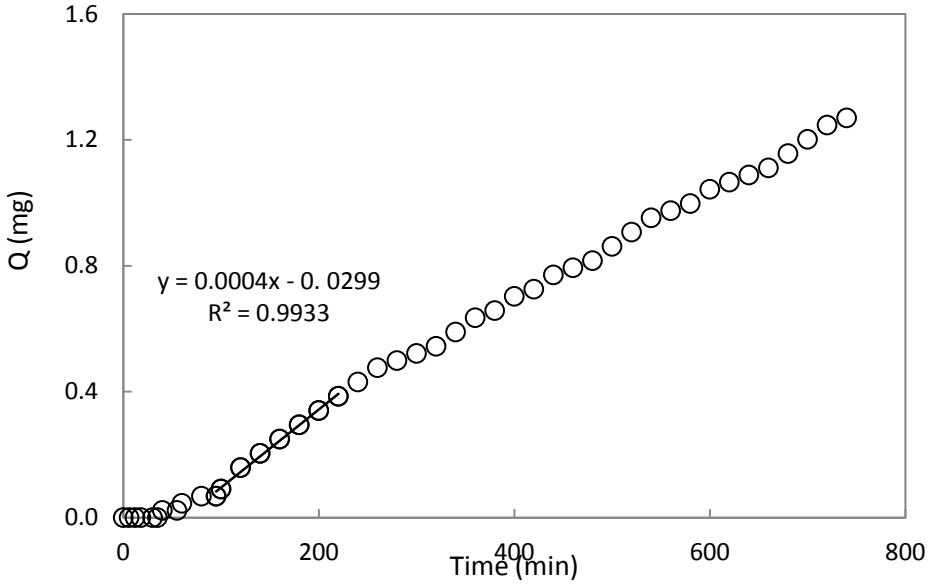

Figure 6-41 short-time permeation data diltiazem -HCl : 100 ppm, sericin/chitosan 1:4, GA: 0.08%

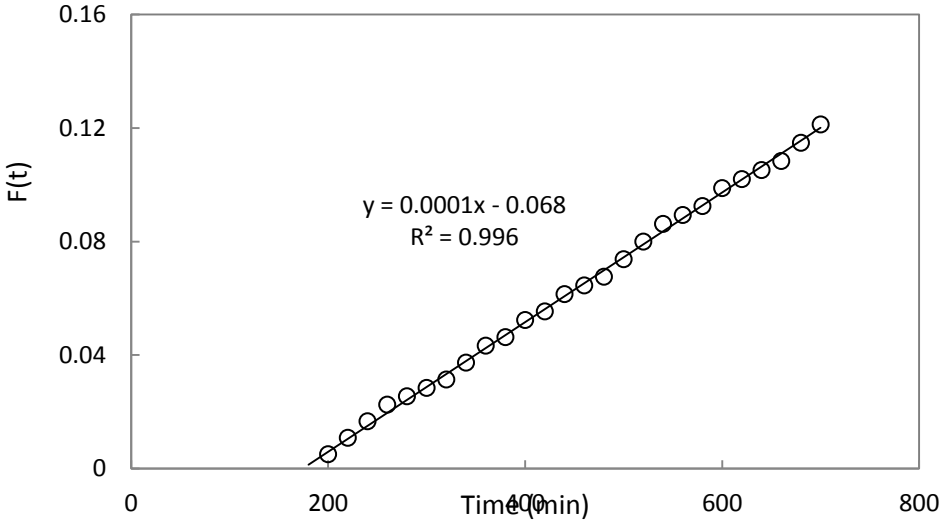

Figure 6-42 long-time permeation data diltiazem -HCl : 100 ppm, sericin/chitosan 1:4, GA: 0.08%

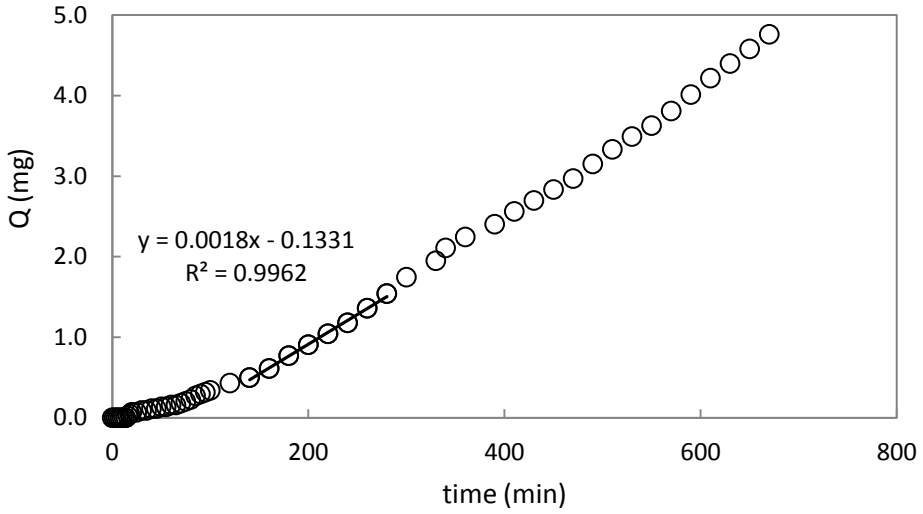

Figure 6-43 short-time permeation data diltiazem -HCl : 400 ppm, sericin/chitosan 1:4, GA: 0.16%

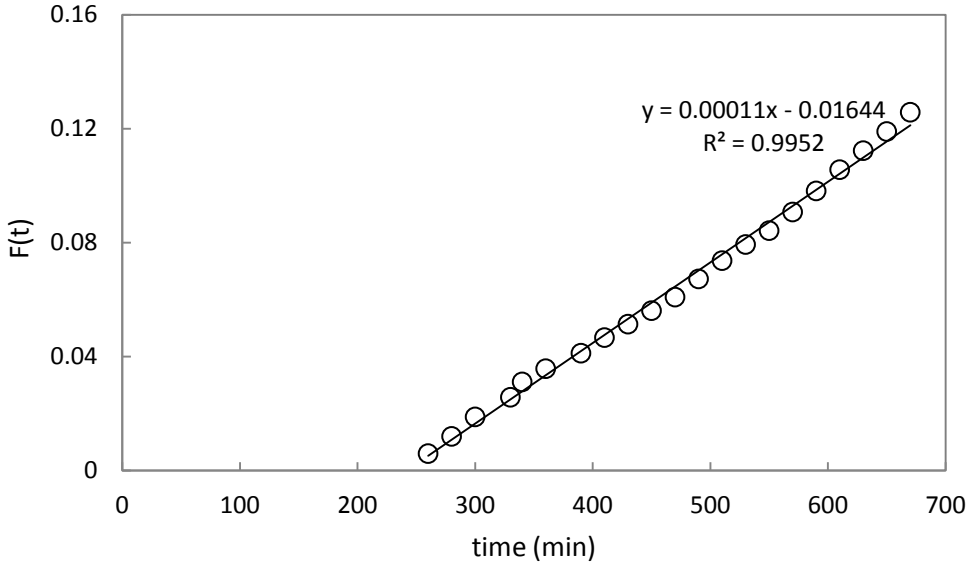

Figure 6-44 long-time permeation data diltiazem -HCl : 400 ppm, sericin/chitosan 1:4, GA: 0.16%

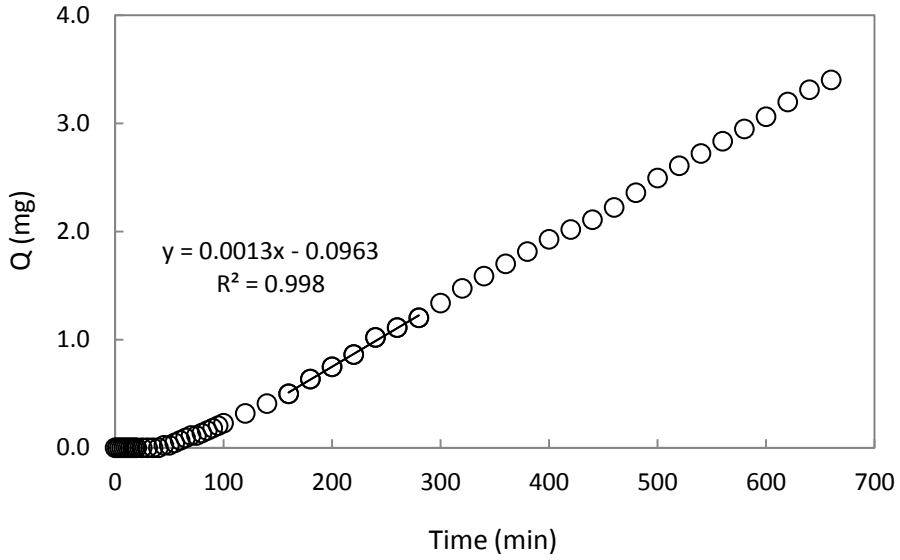

Figure 6-45 short-time permeation data diltiazem -HCl : 300 ppm, sericin/chitosan 1:4, GA: 0.16%

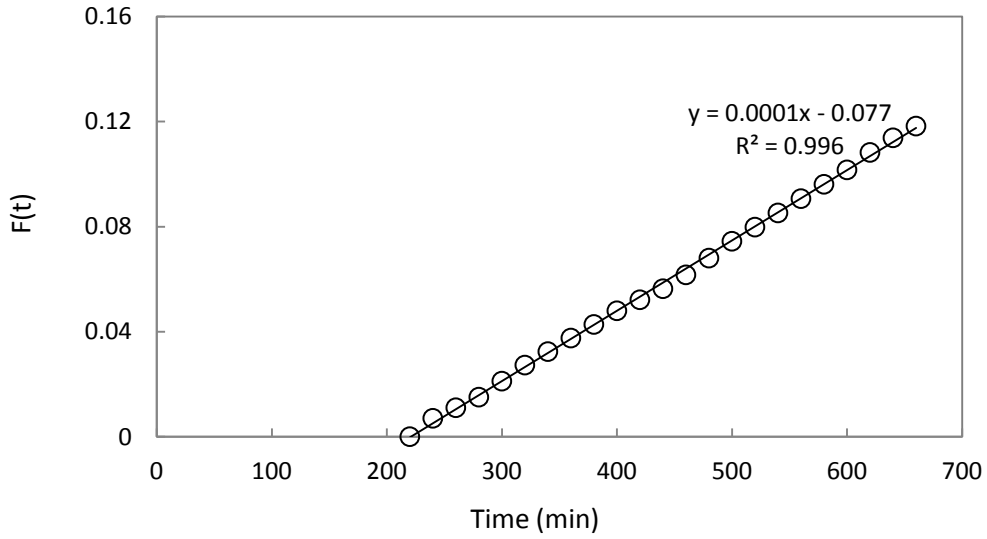

Figure 6-46 long-time permeation data diltiazem -HCl : 300 ppm, sericin/chitosan 1:4, GA: 0.16%

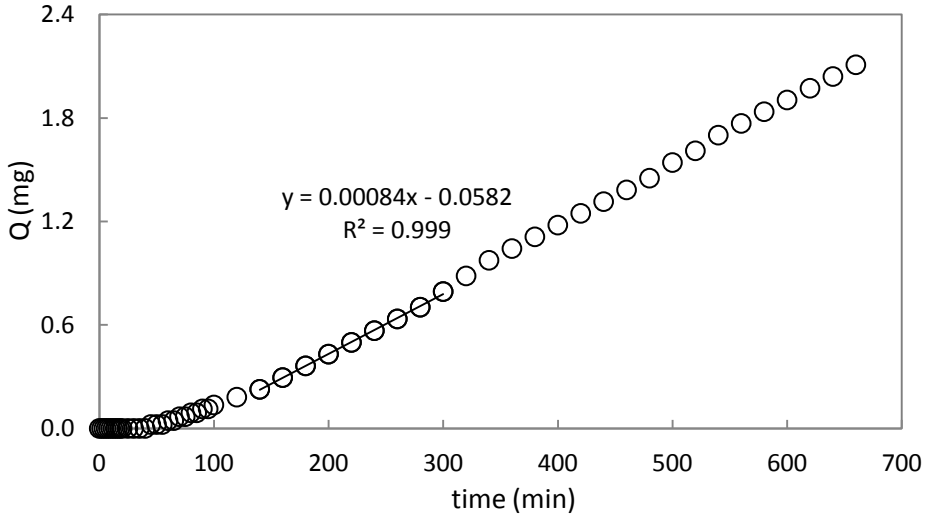

Figure 6-47 short-time permeation data diltiazem -HCl : 200 ppm, sericin/chitosan 1:4, GA: 0.16%

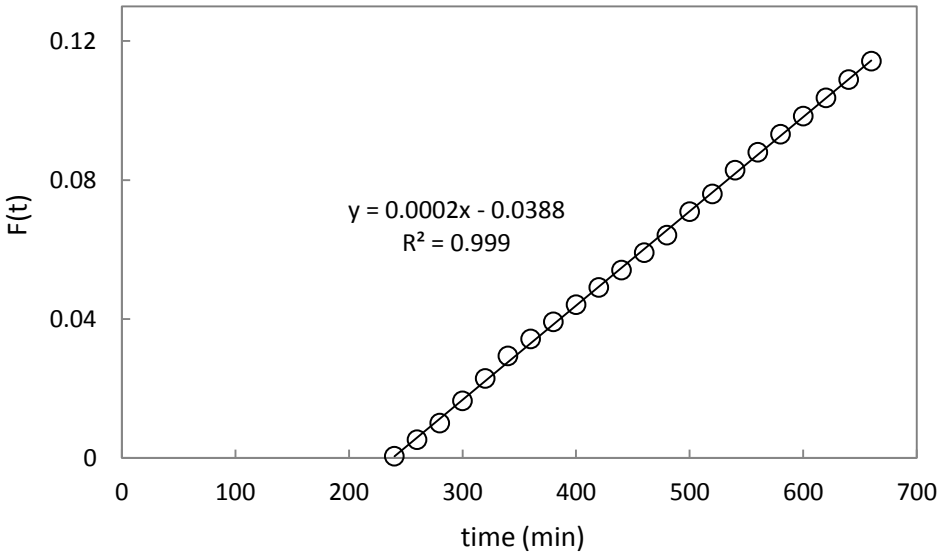

Figure 6-48 long-time permeation data diltiazem -HCl : 200 ppm, sericin/chitosan 1:4, GA: 0.16%

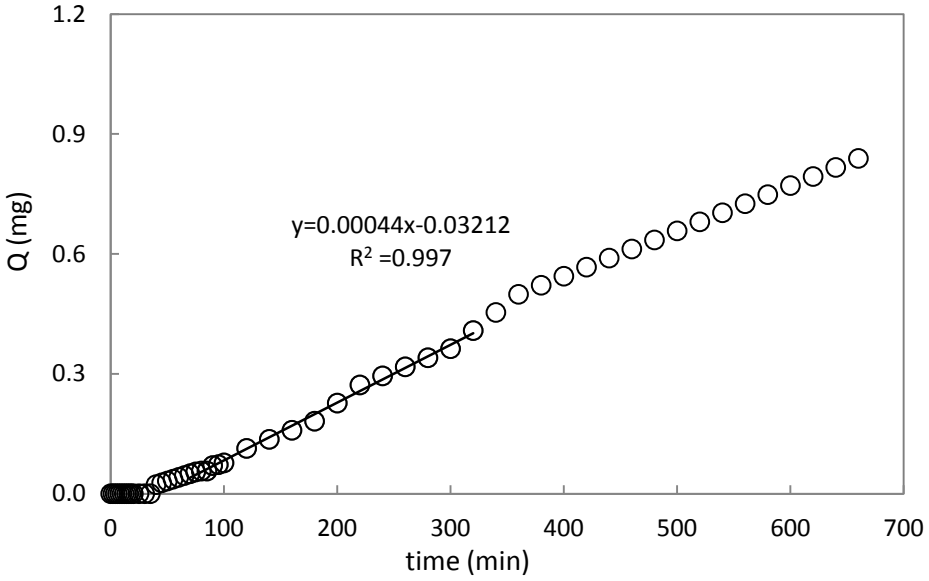

Figure 6-49 short-time permeation data diltiazem -HCl : 100 ppm, sericin/chitosan 1:4, GA: 0.16%

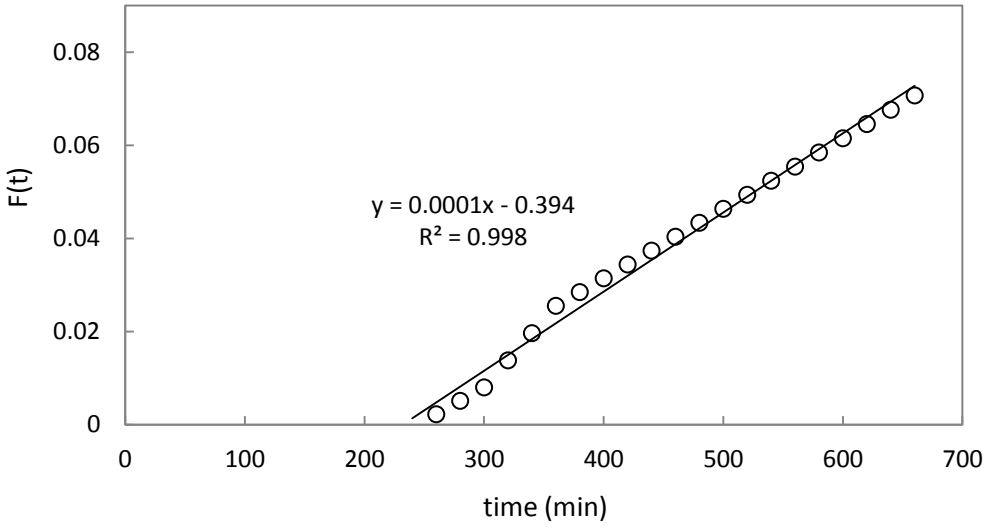

Figure 6-50 long-time permeation data diltiazem -HCl : 100 ppm, sericin/chitosan 1:4, GA: 0.16%

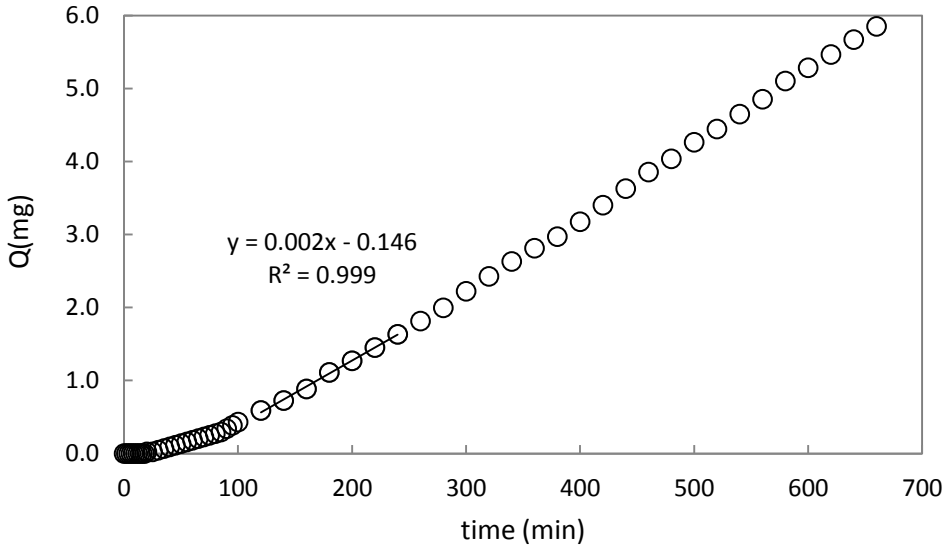

Figure 6-51 short-time permeation data diltiazem -HCl : 400 ppm, sericin/chitosan 1:4, GA: 0.24%

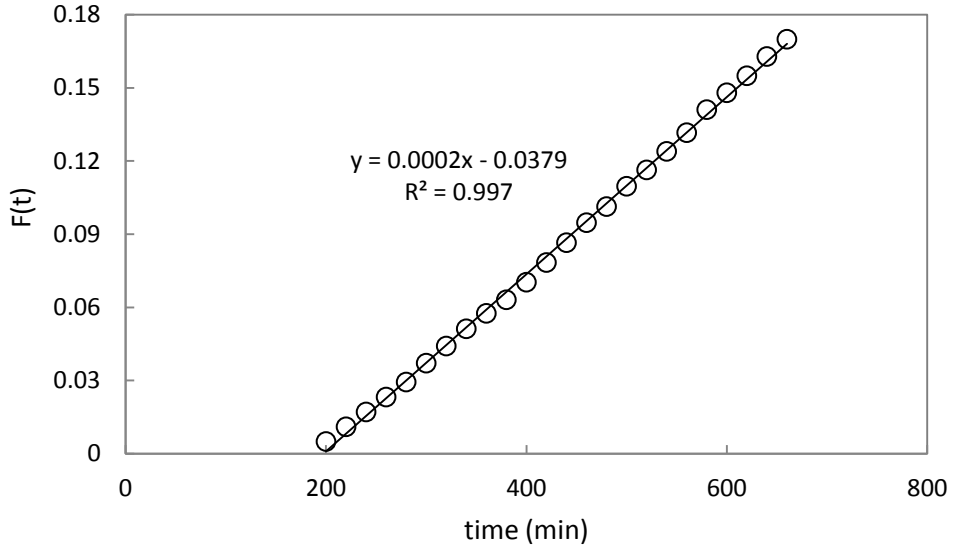

Figure 6-52 long-time permeation data diltiazem -HCl : 400 ppm, sericin/chitosan 1:4, GA: 0.24%

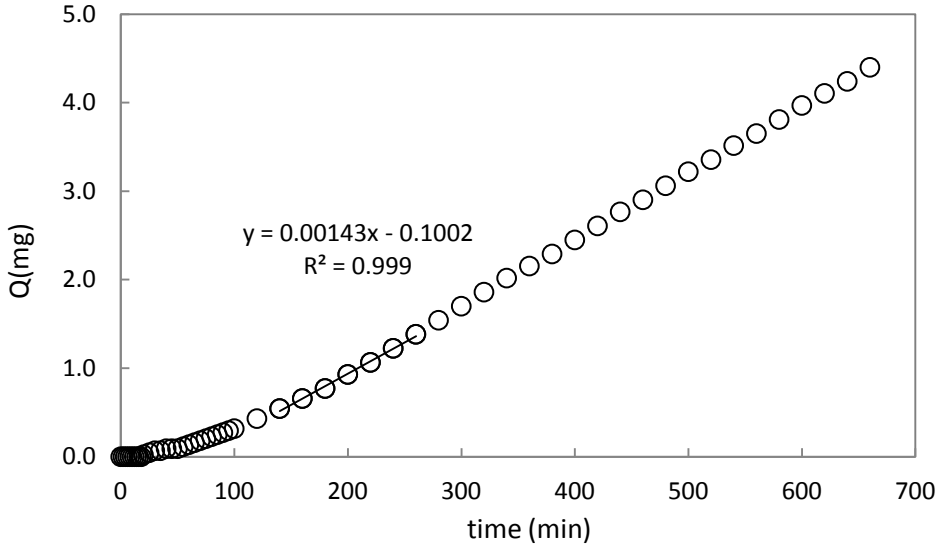

Figure 6-53 short-time permeation data diltiazem -HCl : 300 ppm, sericin/chitosan 1:4, GA: 0.24%

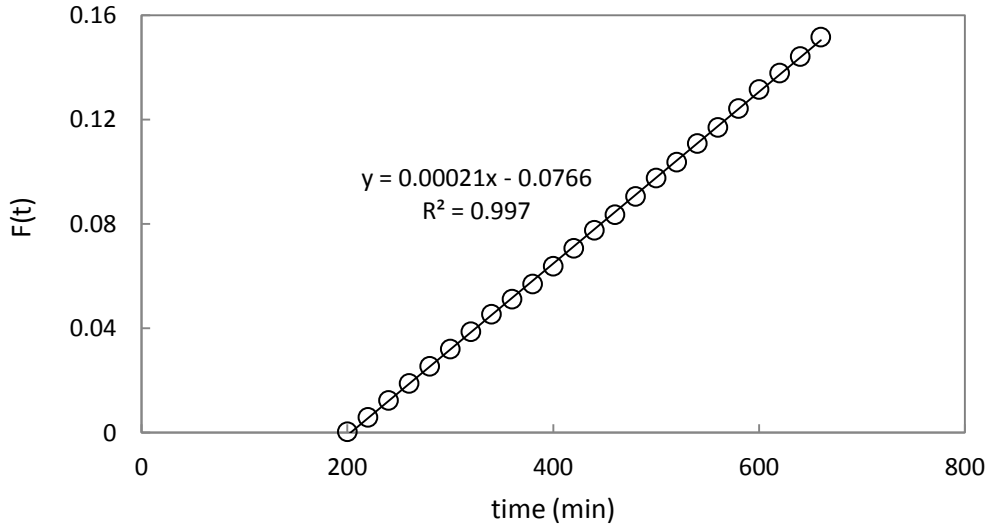

Figure 6-54 long-time permeation data diltiazem -HCl : 300 ppm, sericin/chitosan 1:4, GA: 0.24%

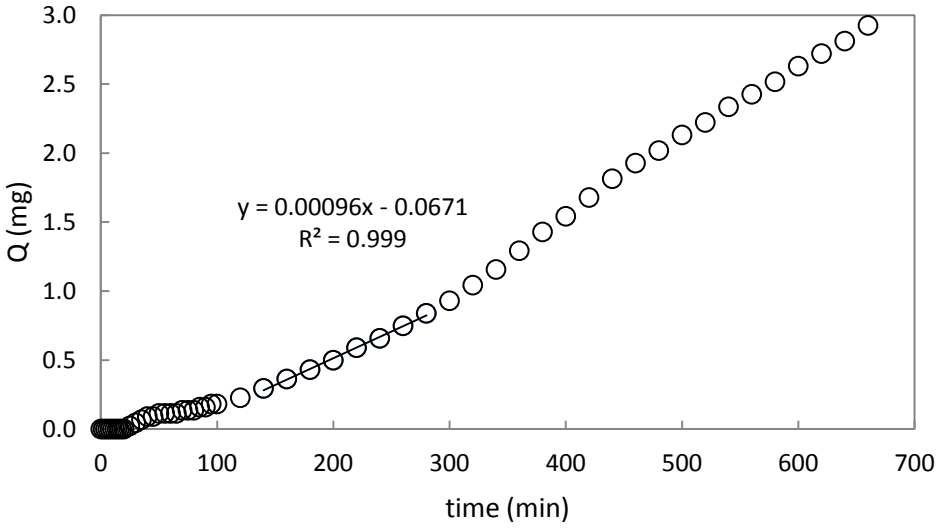

Figure 6-55 short-time permeation data diltiazem -HCl : 200 ppm, sericin/chitosan 1:4, GA: 0.24%

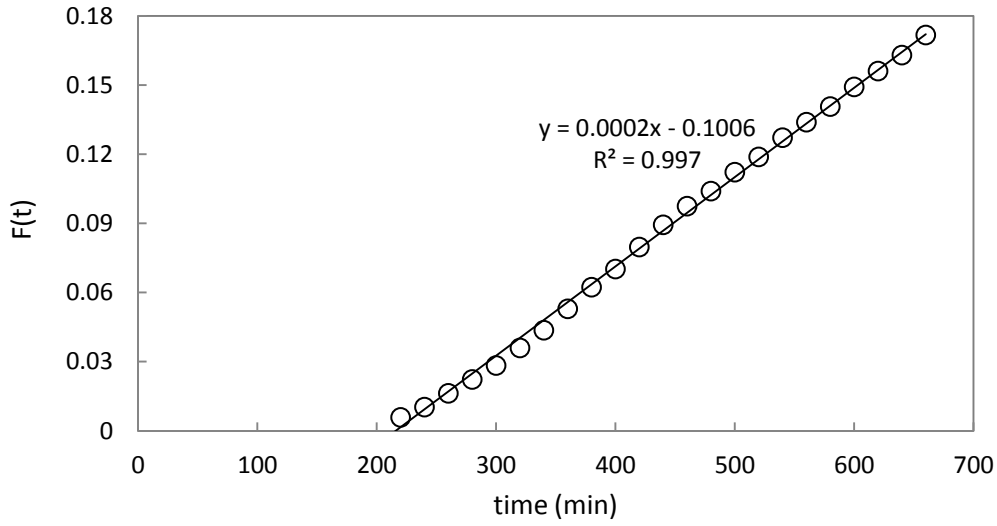

Figure 6-56 long-time permeation data diltiazem -HCl : 200 ppm, sericin/chitosan 1:4, GA: 0.24%

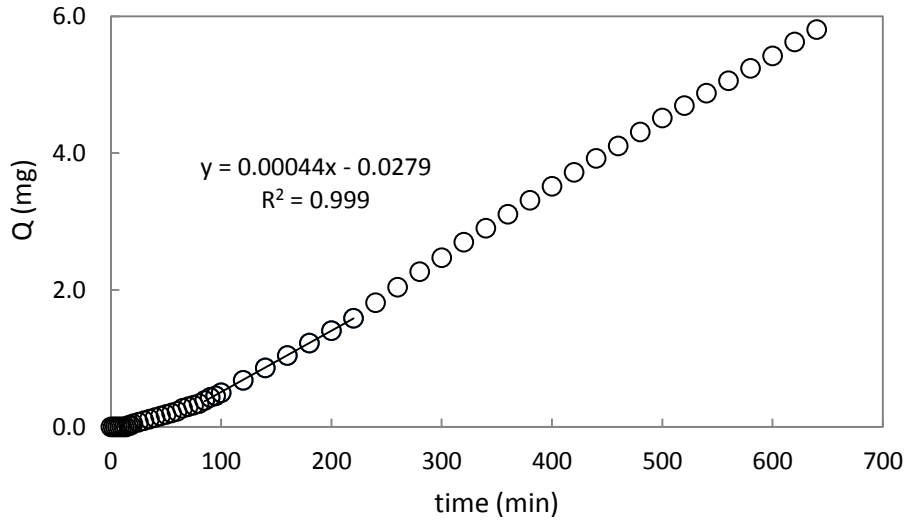

Figure 6-57 short-time permeation data diltiazem -HCl : 100 ppm, sericin/chitosan 1:4, GA: 0.24%

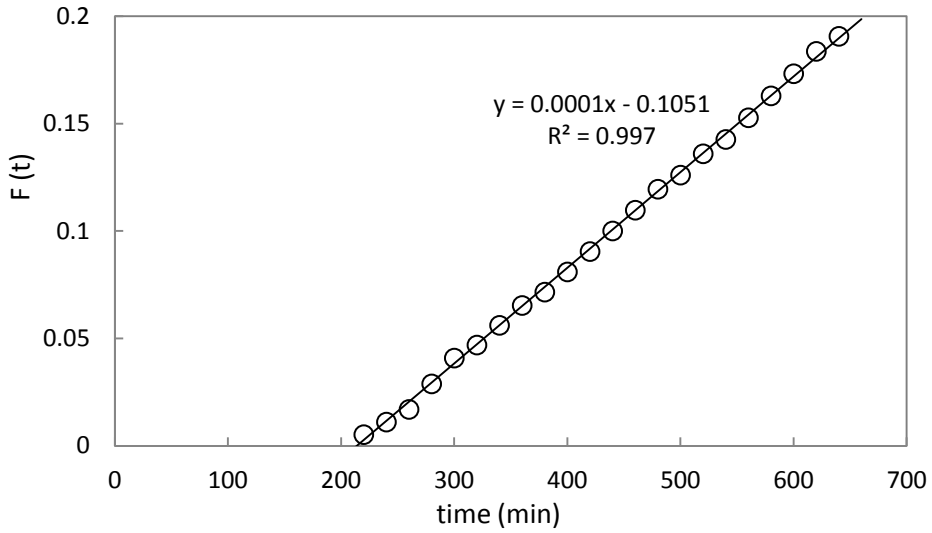

Figure 6-58 long-time permeation data diltiazem -HCl : 100 ppm, sericin/chitosan 1:4, GA: 0.24%

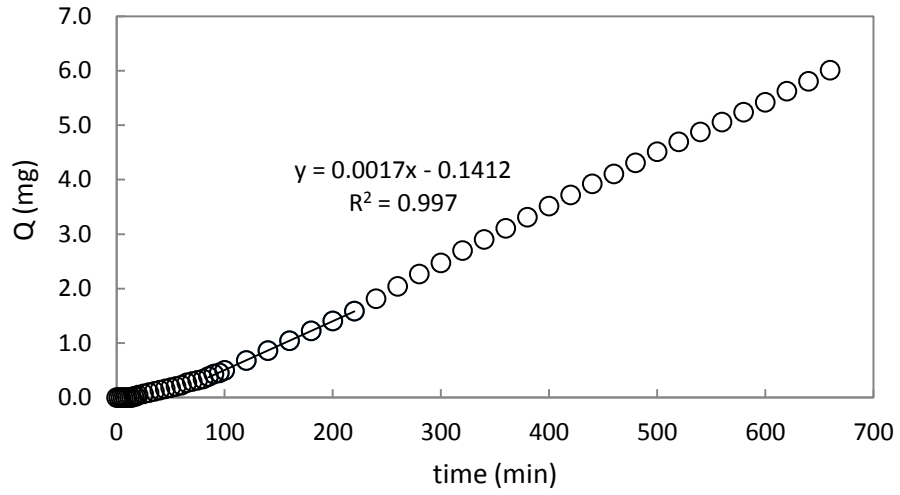

Figure 6-59 short-time permeation data diltiazem -HCl: 400 ppm, sericin/chitosan 1:4, GA: 0.40%

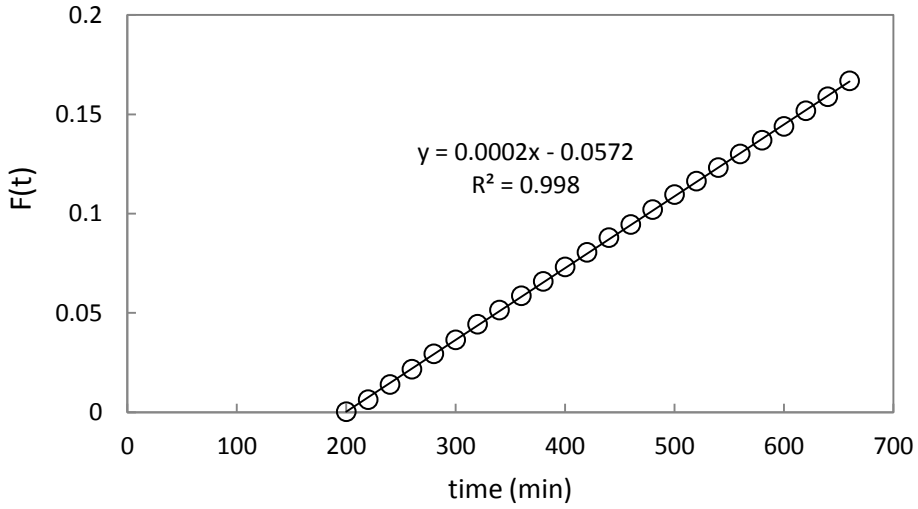

Figure 6-60 long-time permeation data diltiazem -HCl: 400 ppm, sericin/chitosan 1:4, GA: 0.40%

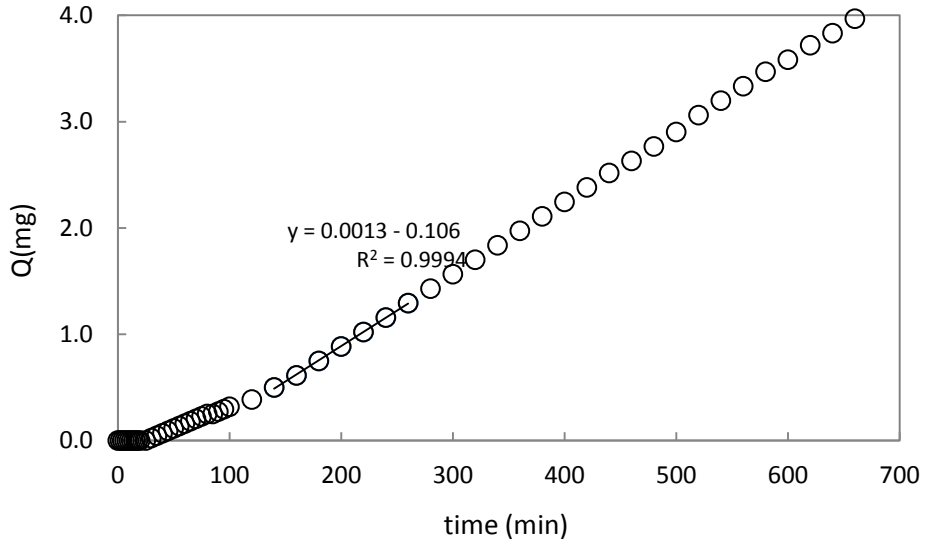

Figure 6-61 short-time permeation data diltiazem -HCl : 300 ppm, sericin/chitosan 1:4, GA: 0.40%

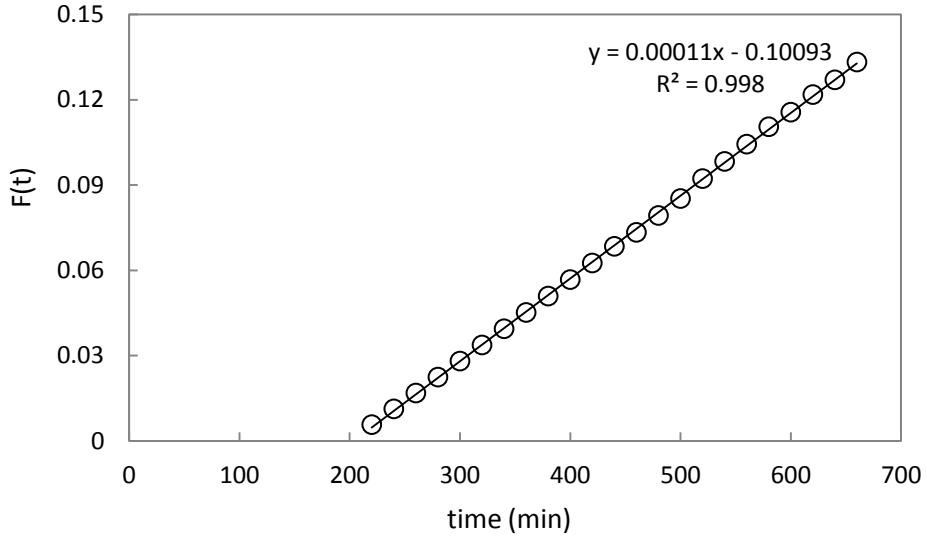

Figure 6-62 long-time permeation data diltiazem -HCl : 300 ppm, sericin/chitosan 1:4, GA: 0.40%

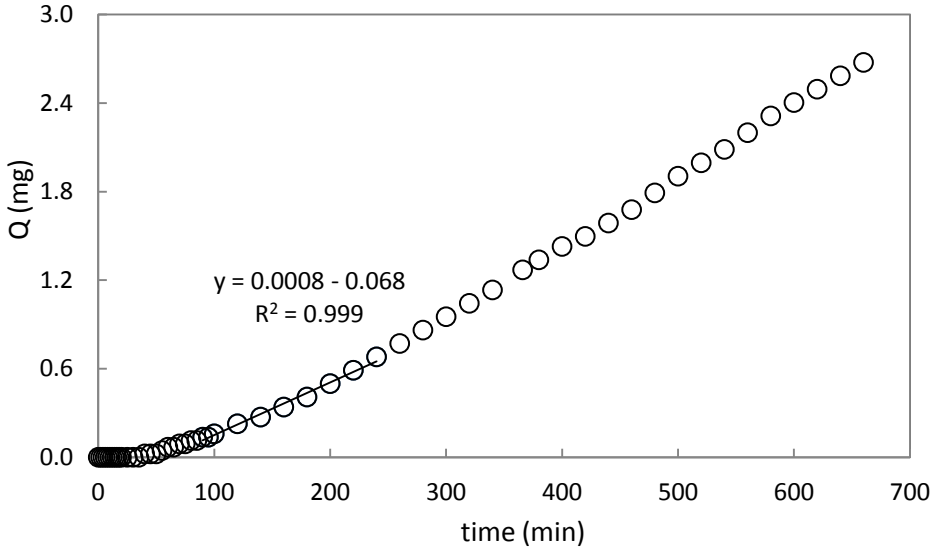

Figure 6-63 short-time permeation data diltiazem -HCl : 200 ppm, sericin/chitosan 1:4, GA: 0.40%

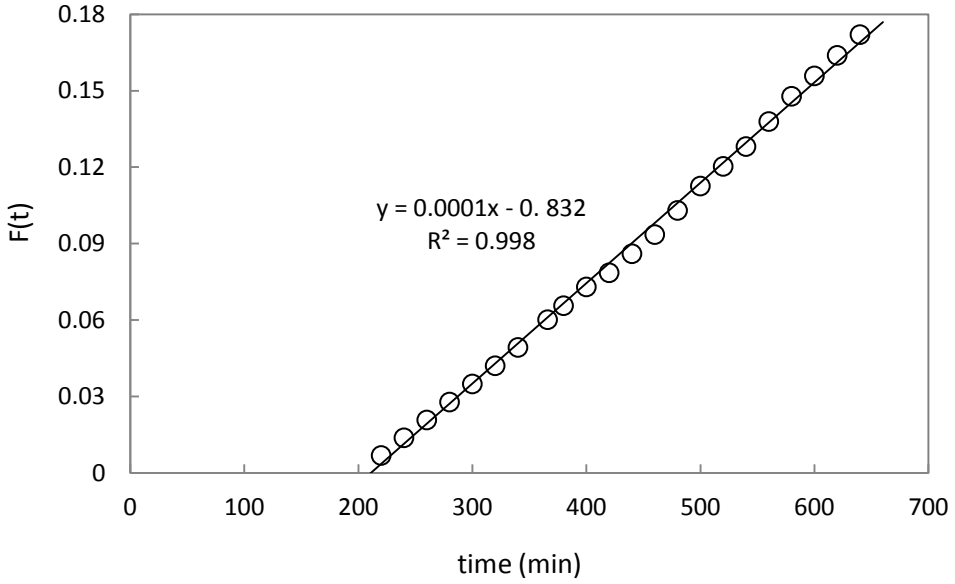

Figure 6-64 long-time permeation data diltiazem -HCl : 200 ppm, sericin/chitosan 1:4, GA: 0.40%

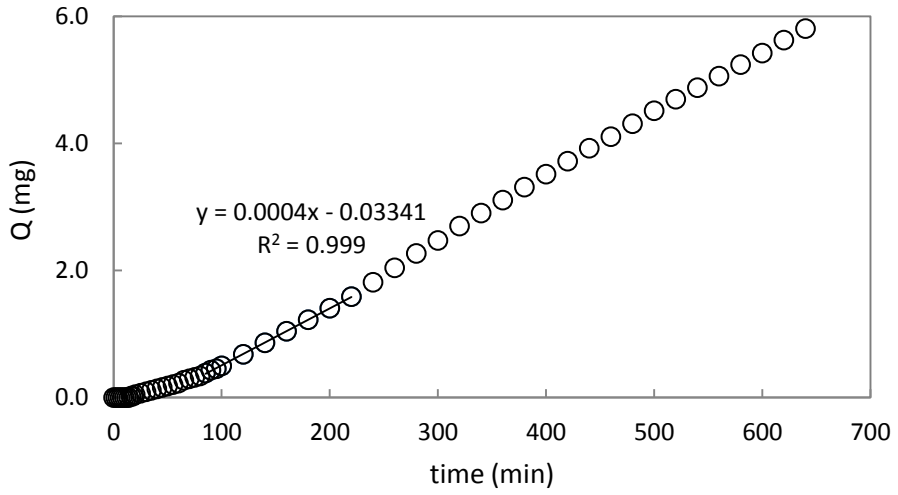

Figure 6-65 short-time permeation data diltiazem -HCl : 100 ppm, sericin/chitosan 1:4, GA: 0.40%

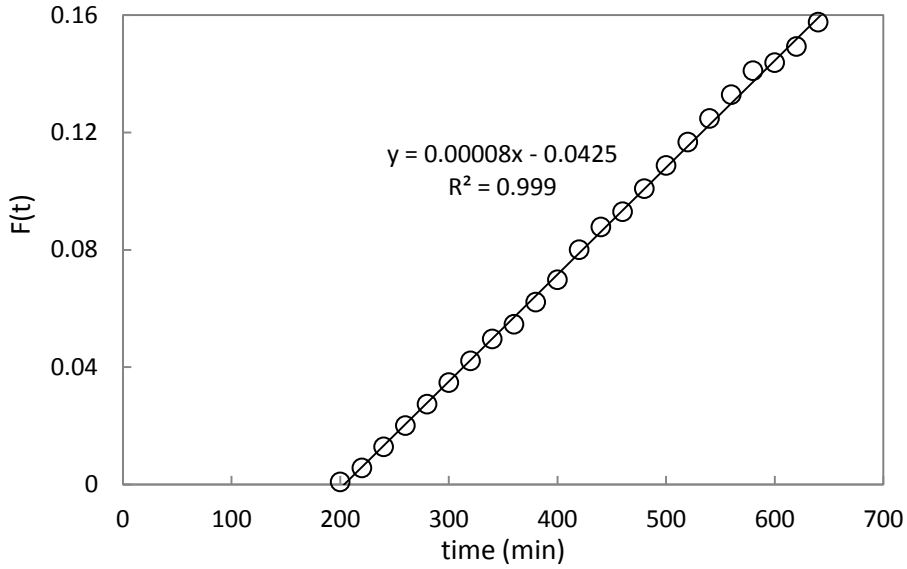

Figure 6-66 long-time permeation data diltiazem -HCl : 100 ppm, sericin/chitosan 1:4, GA: 0.40%

Table 6-2 Permeation parameters for Diltiazem-HCl

GA%	Initial drug conc. (ppm)	time-lag (min)	Thickness)	D_T **(cm^2/s)**	P_T **(cm^2/s)**	P_M **(cm^2/s)**
0.40	100	86	89	2.57E-09	4.89E-08	4.75E-08
	200	85	89	2.59E-09	4.90E-08	5.37E-08
	300	84	89	2.63E-09	5.20E-08	5.25E-08
	400	82	89	2.68E-09	5.32E-08	4.88E-08
0.24	100	63	78	2.67E-09	4.79E-08	4.69E-08
	200	70	78	2.42E-09	5.19E-08	5.17E-08
	300	70	78	2.41E-09	5.17E-08	5.15E-08
	400	73	78	2.33E-09	5.38E-08	5.38E-08
0.16	100	73	82	2.57E-09	4.99E-08	5.19E-08
	200	69	82	2.69E-09	4.80E-08	4.97E-08
	300	74	82	2.54E-09	4.94E-08	5.05E-08
	400	74	82	2.51E-09	5.12E-08	5.58E-08
0.08	100	76	84	2.57E-09	4.59E-08	4.79E-08
	200	79	84	2.49E-09	4.74E-08	5.27E-08
	300	79	84	2.49E-09	5.02E-08	4.85E-08
	400	81	84	2.43E-09	5.17E-08	5.28E-08

Nitrofurazon

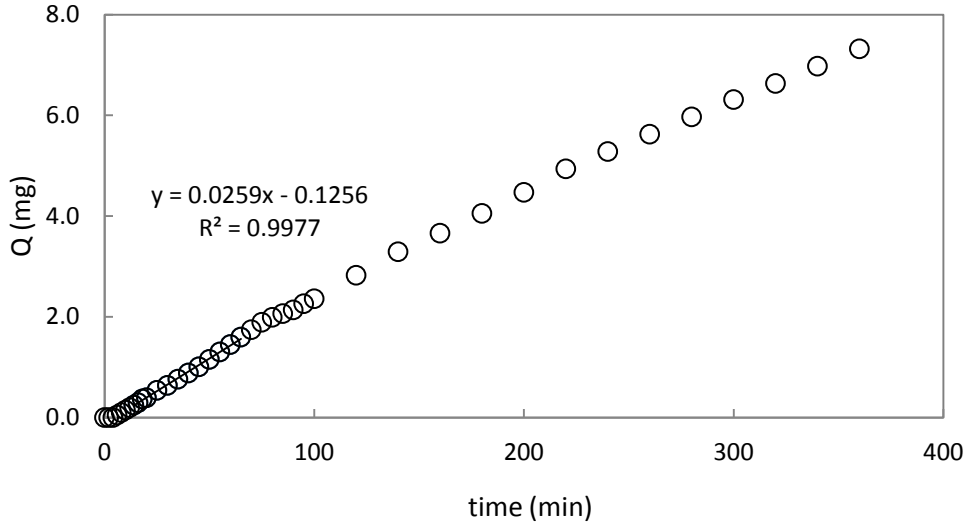

Figure 6-67 short-time permeation data, nitrofurazon: 400 ppm, sericin/chitosan 1:4, GA: 0.08%

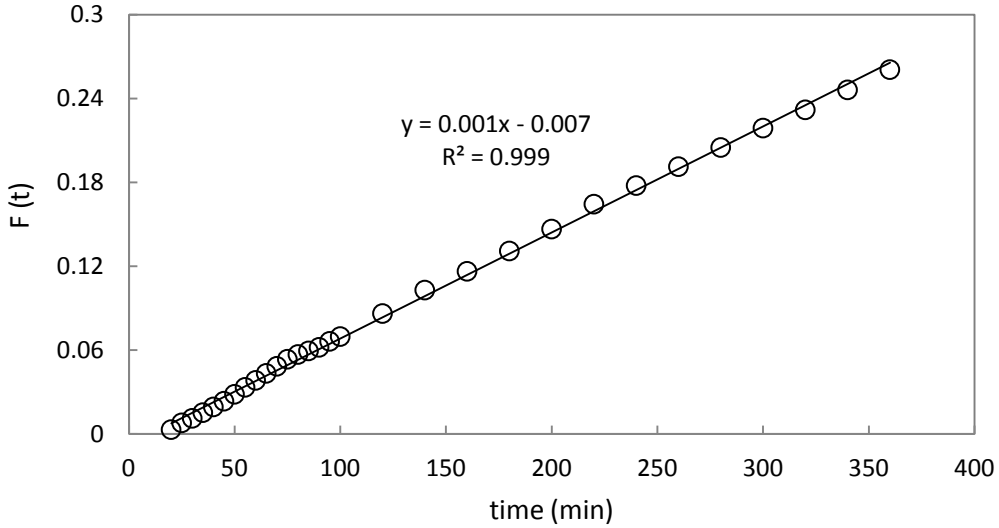

Figure 6-68 long-time permeation data, nitrofurazon: 400 ppm, sericin/chitosan 1:4, GA: 0.08%

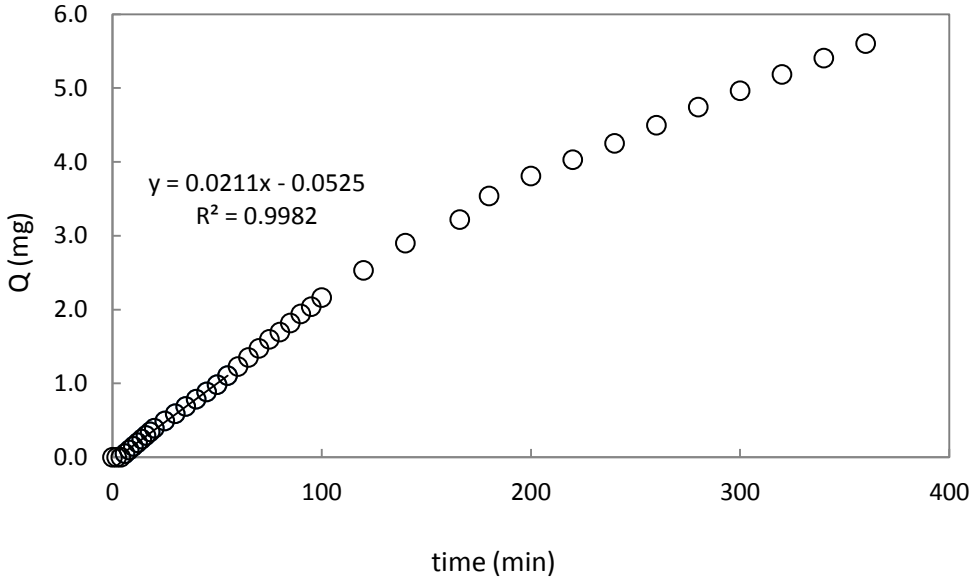

Figure 6-69 short-time permeation data, nitrofurazon: 300 ppm, sericin/chitosan 1:4, GA: 0.08%

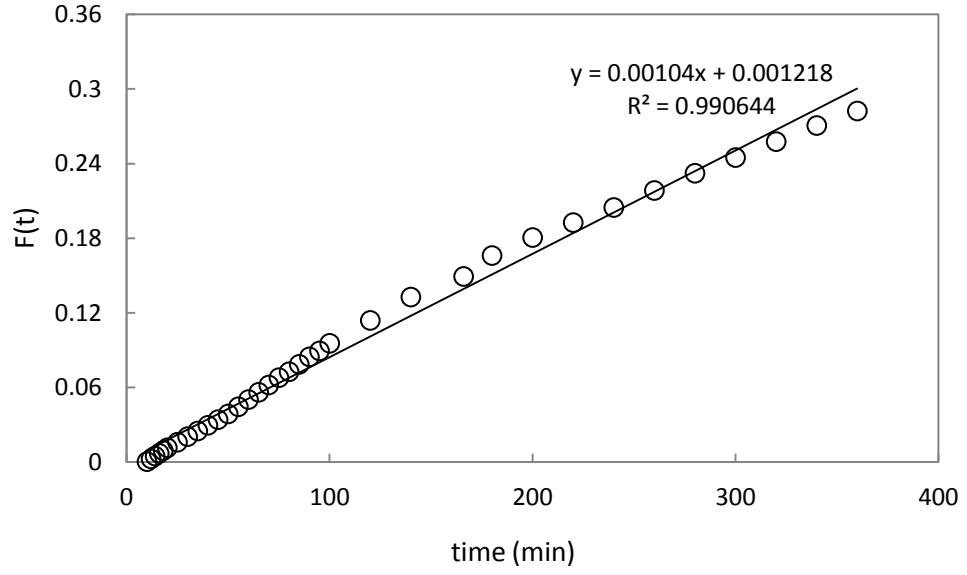

Figure 6-70 long-time permeation data, nitrofurazon: 300 ppm, sericin/chitosan 1:4, GA: 0.08%

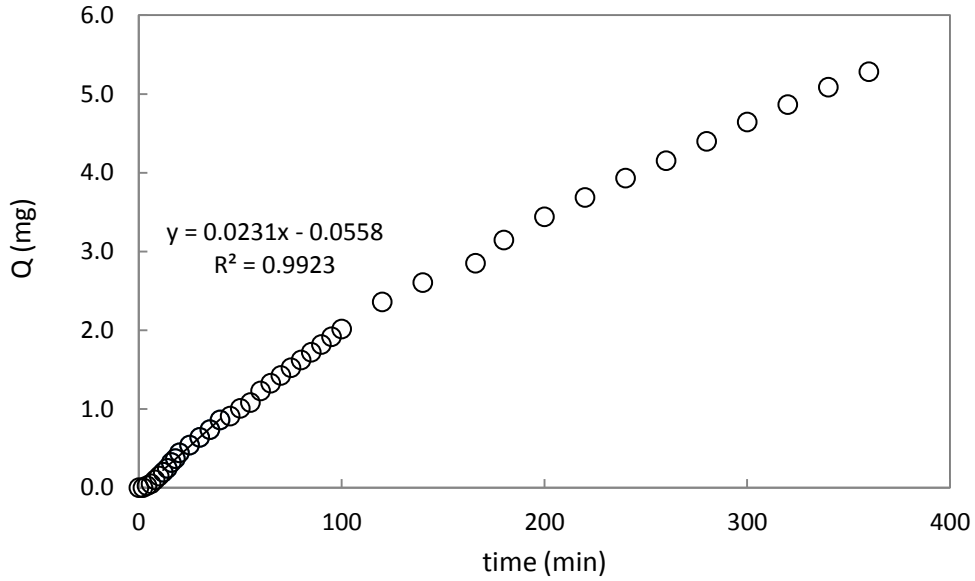

Figure 6-71 short-time permeation data, nitrofurazon: 200 ppm, sericin/chitosan 1:4, GA: 0.08%

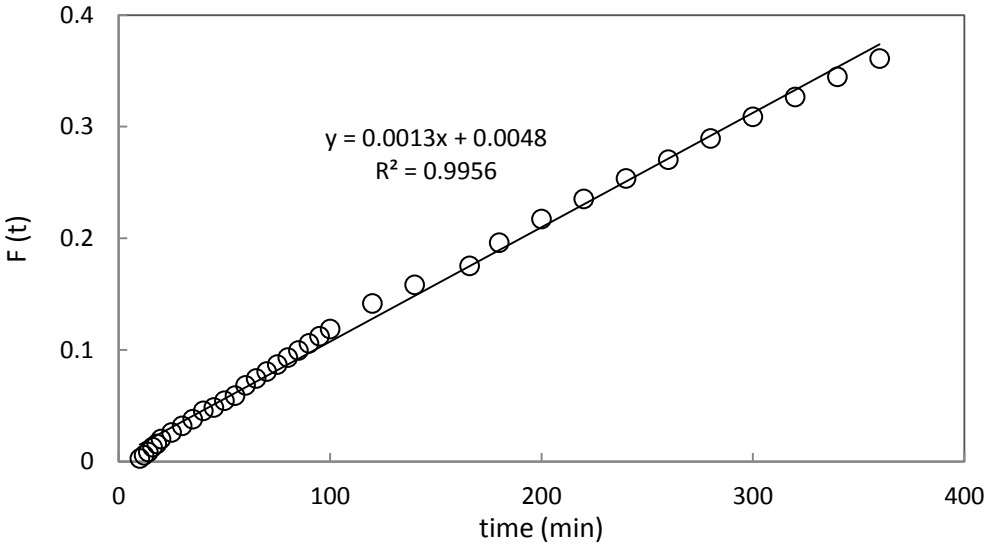

Figure 6-72 long-time permeation data, nitrofurazon: 200 ppm, sericin/chitosan 1:4, GA: 0.08%

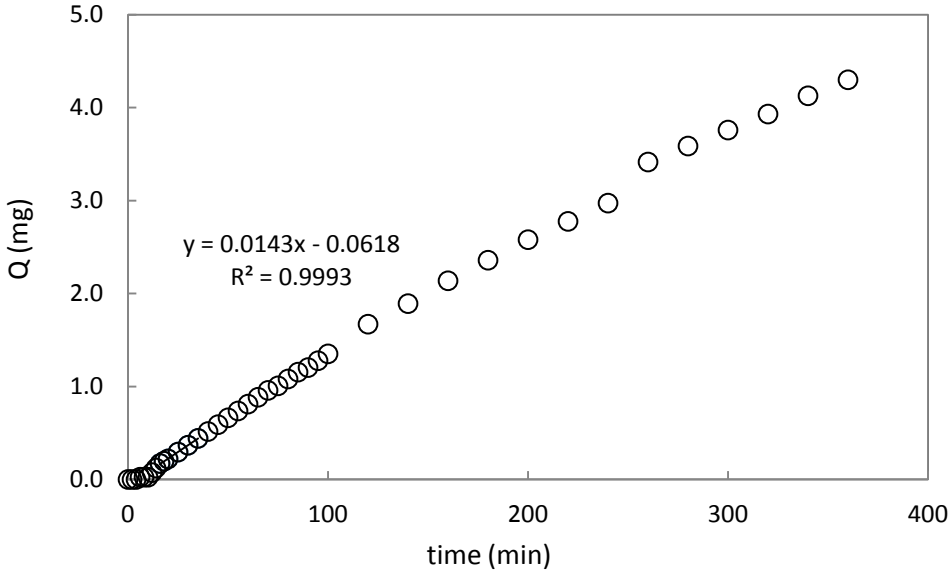

Figure 6-73 short-time permeation data, nitrofurazon: 100 ppm, sericin/chitosan 1:4, GA: 0.08%

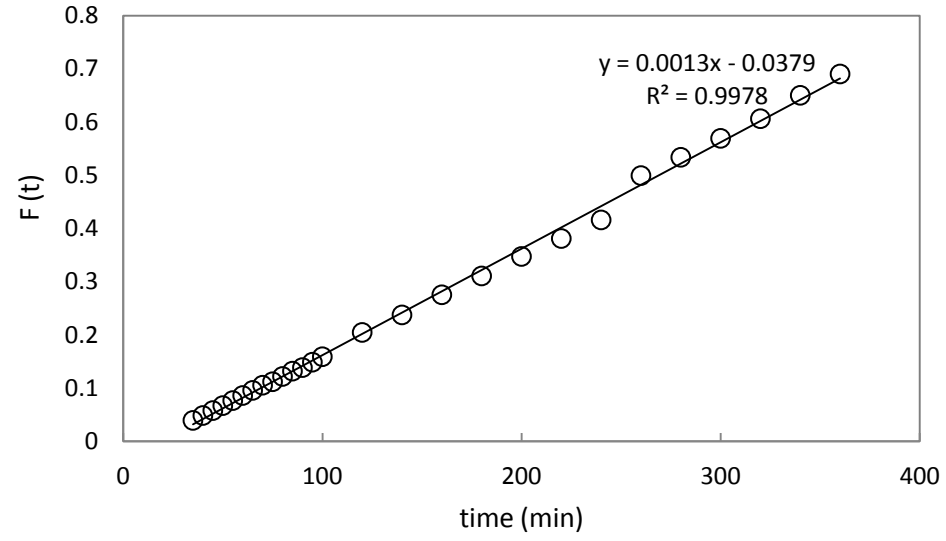

Figure 6-74 long-time permeation data, nitrofurazon: 100 ppm, sericin/chitosan 1:4, GA: 0.08%

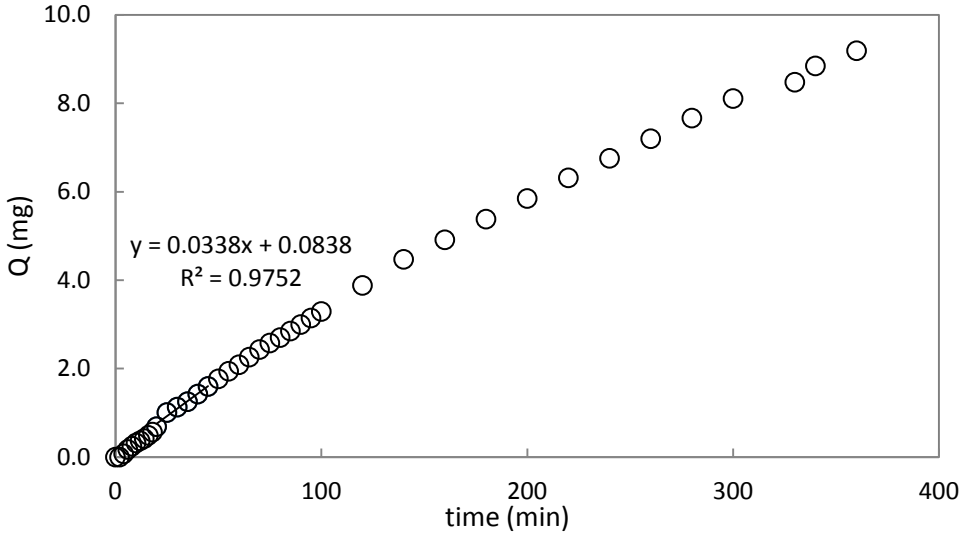

Figure 6-75 short-time permeation data, nitrofurazon: 400 ppm, sericin/chitosan 1:4, GA: 0.016%

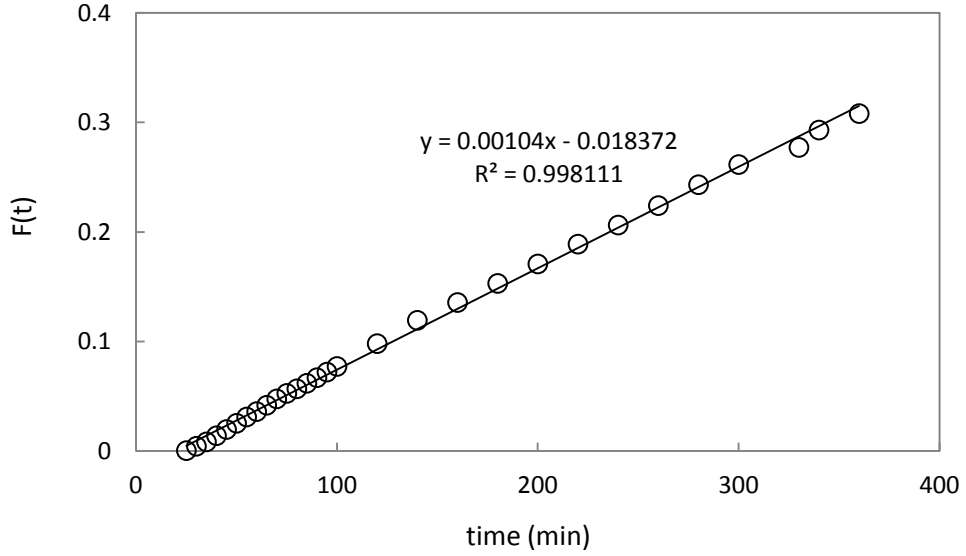

Figure 6-76 long-time permeation data, nitrofurazon: 400 ppm, sericin/chitosan 1:4, GA: 0.16%

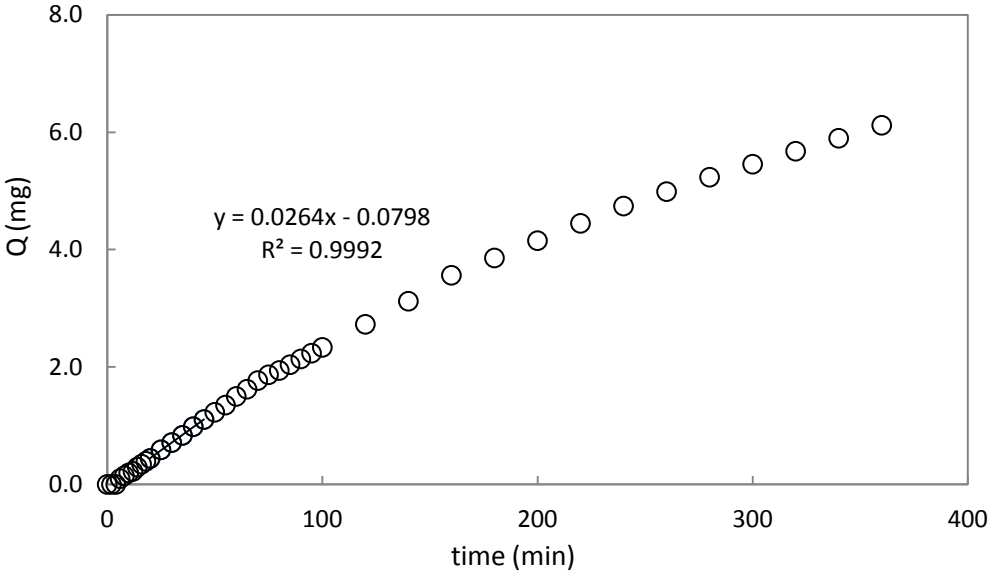

Figure 6-77 short-time permeation data, nitrofurazon: 300 ppm, sericin/chitosan 1:4, GA: 0.16%

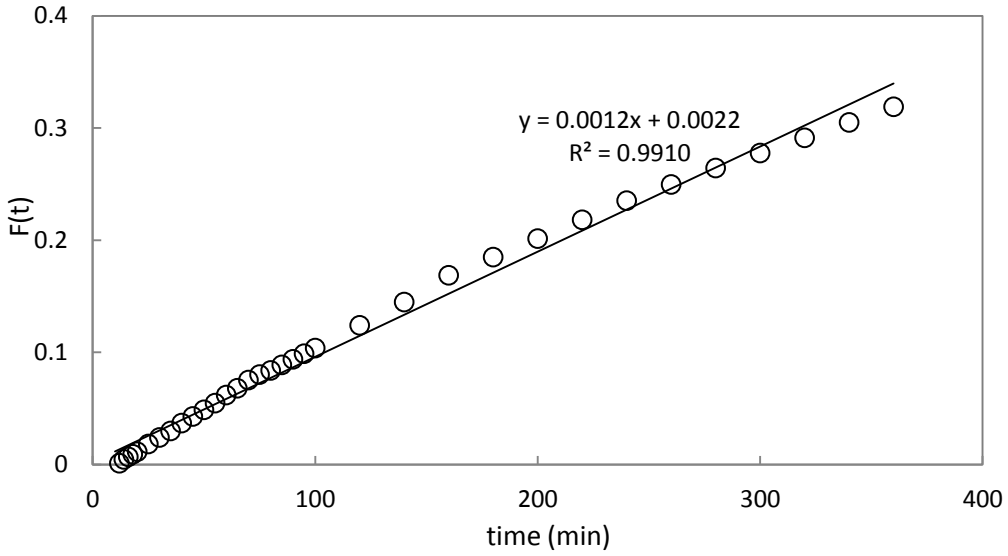

Figure 6-78 long-time permeation data, nitrofurazon: 300 ppm, sericin/chitosan 1:4, GA: 0.16%

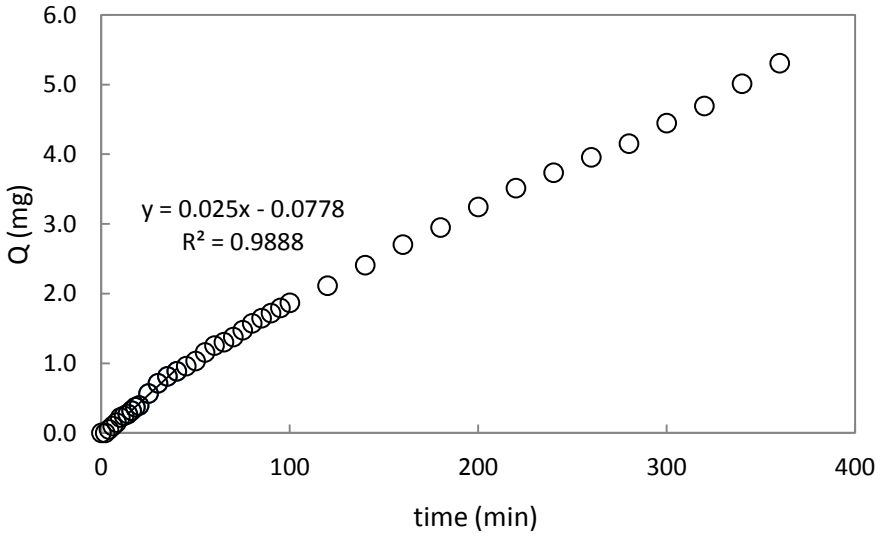

Figure 6-79 short-time permeation data, nitrofurazon: 200 ppm, sericin/chitosan 1:4, GA: 0.16%

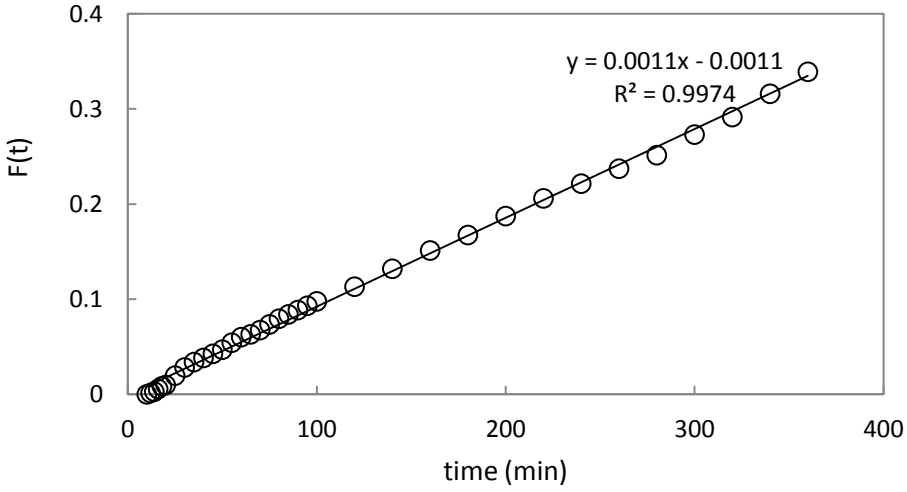

Figure 6-80 long-time permeation data, nitrofurazon: 200 ppm, sericin/chitosan 1:4, GA: 0.16%

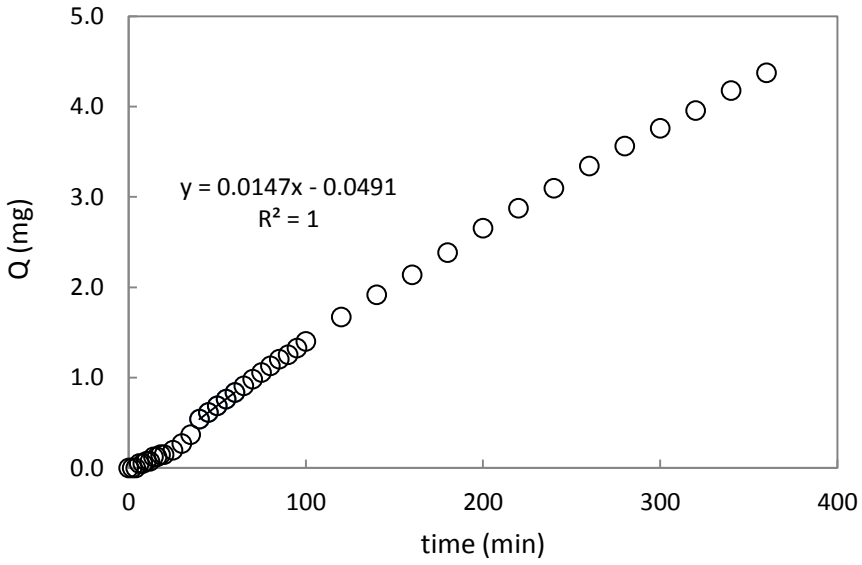

Figure 6-81 short-time permeation data, nitrofurazon: 100 ppm, sericin/chitosan 1:4, GA: 0.16%

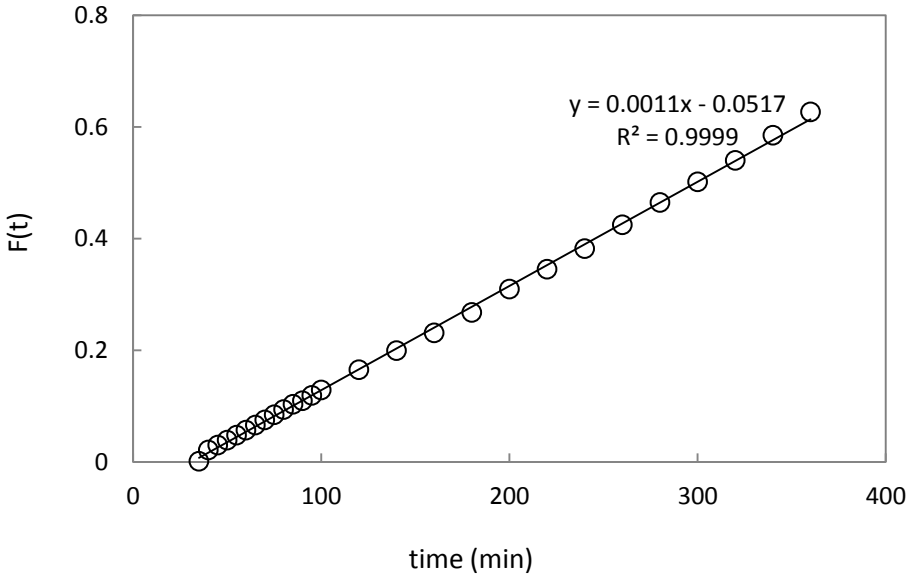

Figure 6-82 long-time permeation data, nitrofurazon: 100 ppm, sericin/chitosan 1:4, GA: 0.16%

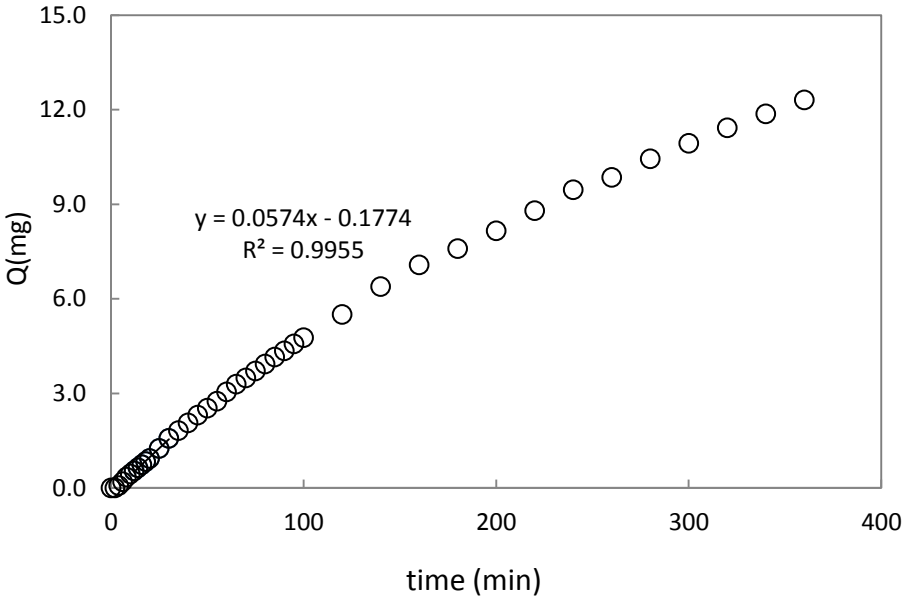

Figure 6-83 short-time permeation data, nitrofurazon: 400 ppm, sericin/chitosan 1:4, GA: 0.24%

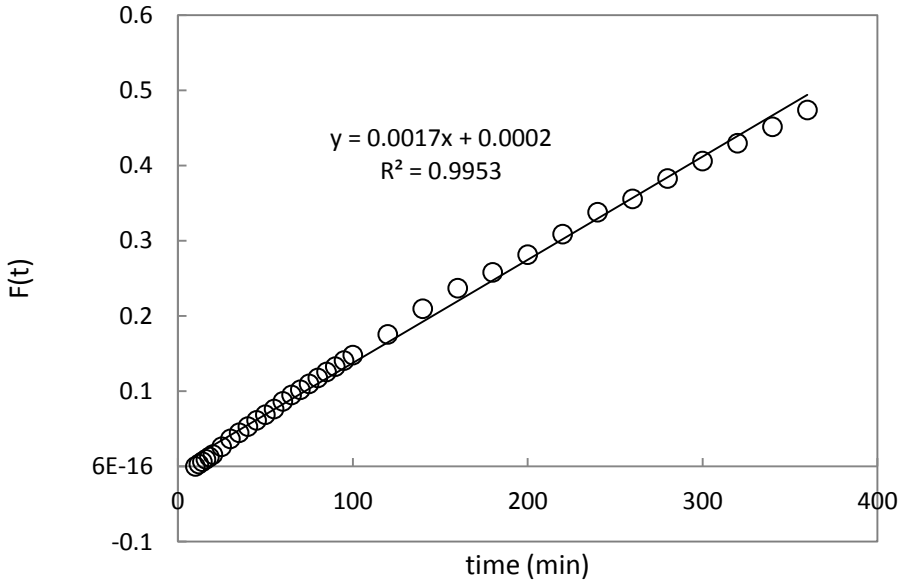

Figure 6-84 long-time permeation data, nitrofurazon: 400 ppm, sericin/chitosan 1:4, GA: 0.24%

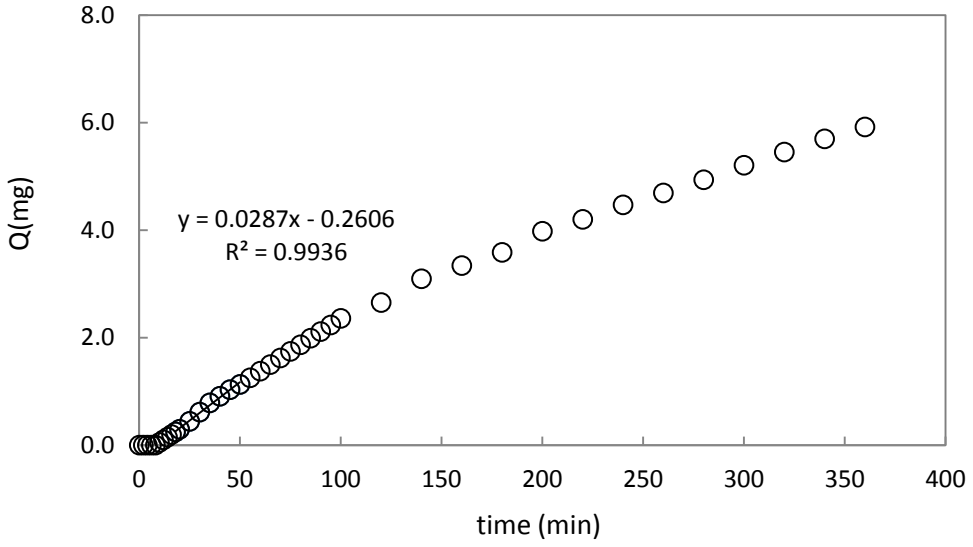

Figure 6-85 short-time permeation data, nitrofurazon: 300 ppm, sericin/chitosan 1:4, GA: 0.24%

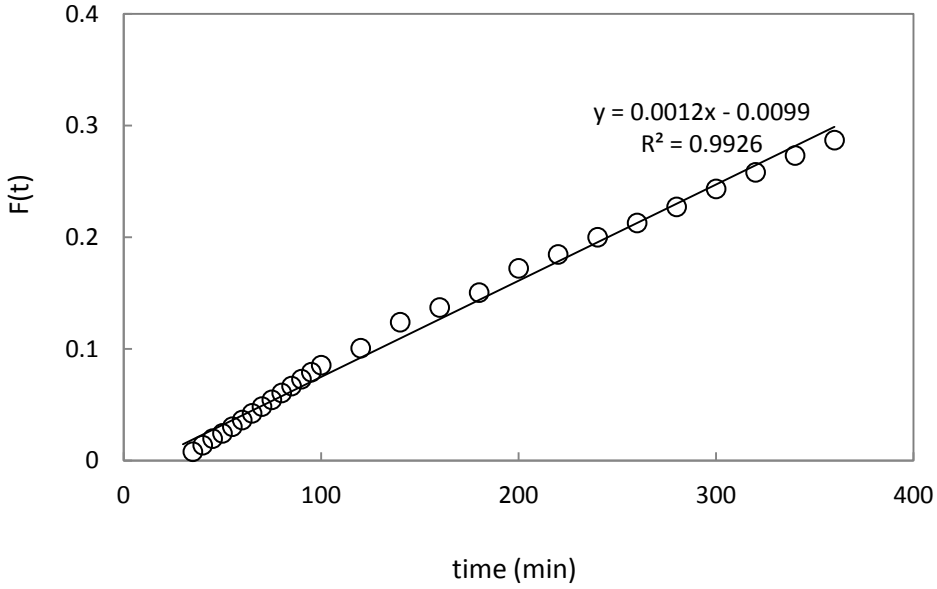

Figure 6-86 long-time permeation data, nitrofurazon: 300 ppm, sericin/chitosan 1:4, GA: 0.24%

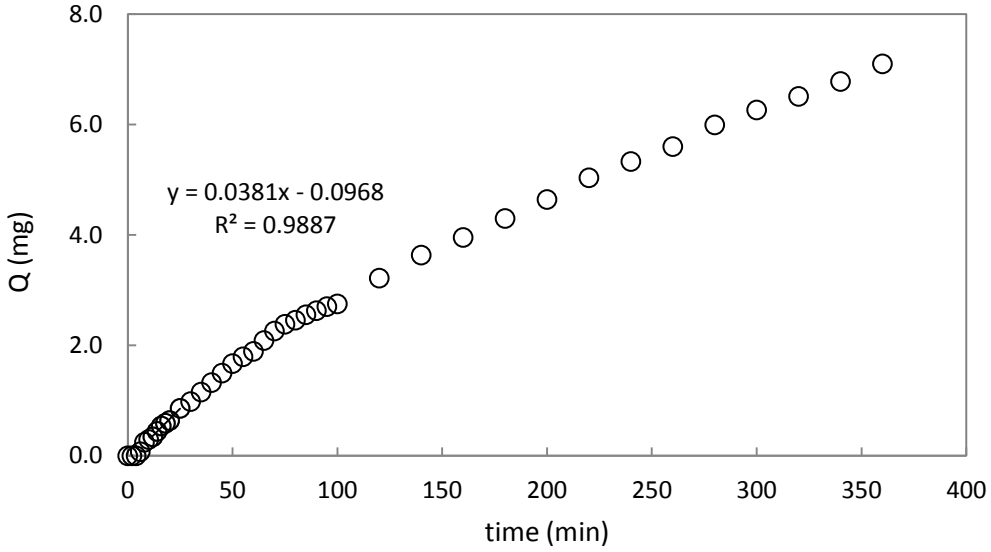

Figure 6-87 short-time permeation data, nitrofurazon: 200 ppm, sericin/chitosan 1:4, GA: 0.24%

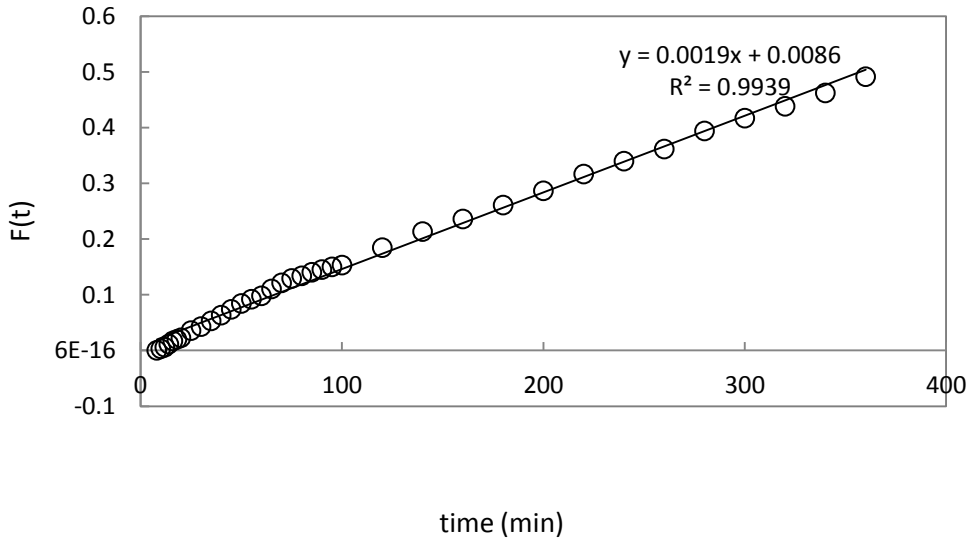

Figure 6-88 long-time permeation data, nitrofurazon: 200 ppm, sericin/chitosan 1:4, GA: 0.24%

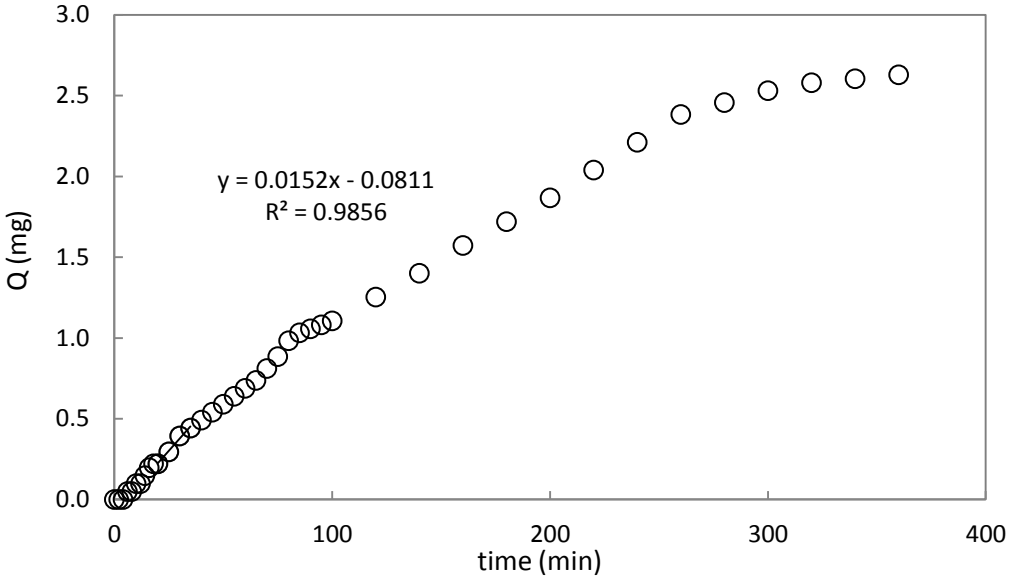

Figure 6-89 short-time permeation data, nitrofurazon: 100 ppm, sericin/chitosan 1:4, GA: 0.24%

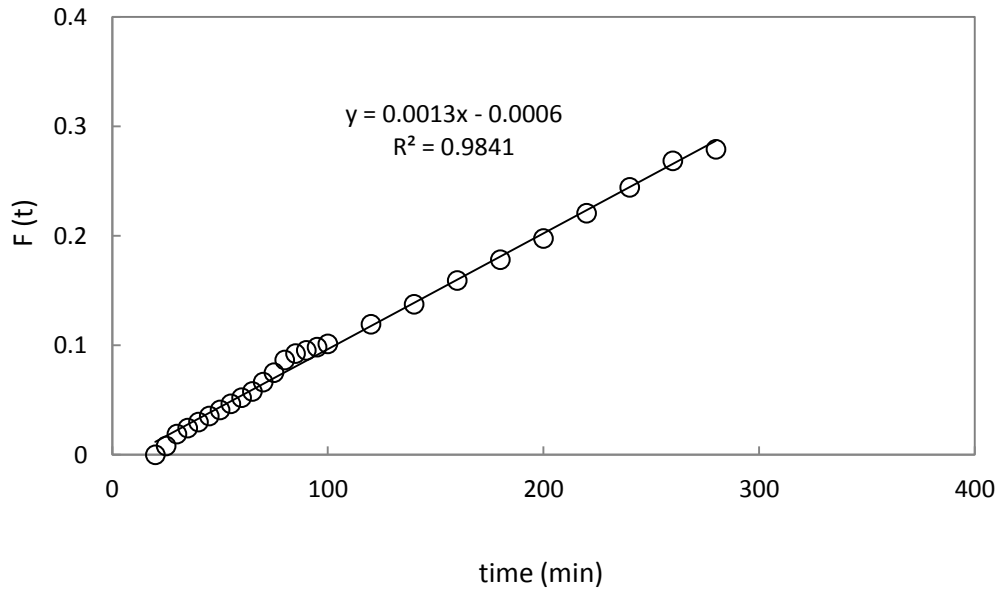

Figure 6-90 long-time permeation data, nitrofurazon: 100 ppm, sericin/chitosan 1:4, GA: 0.24%

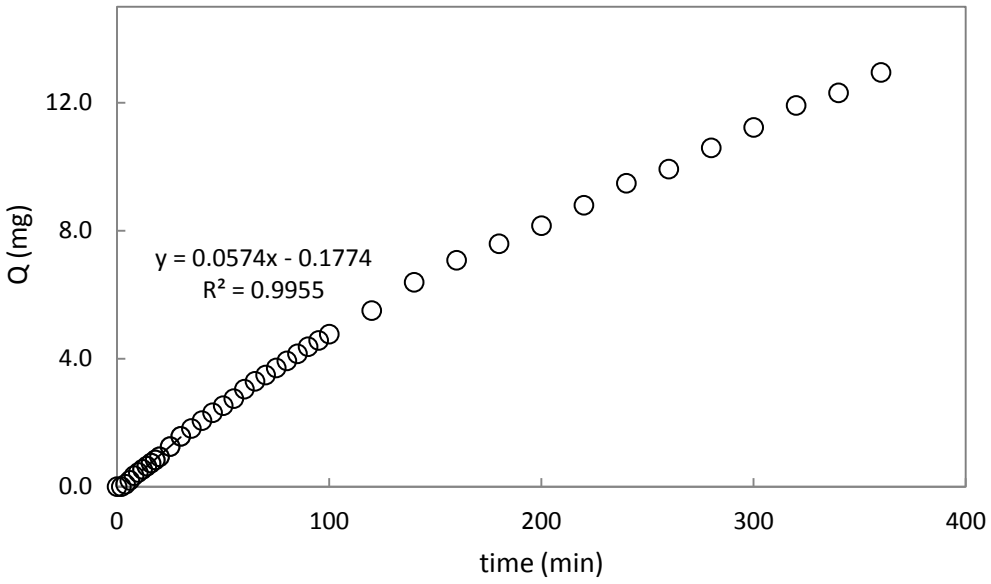

Figure 6-91 short-time permeation data, nitrofurazon: 400 ppm, sericin/chitosan 1:4, GA: 0. 40%

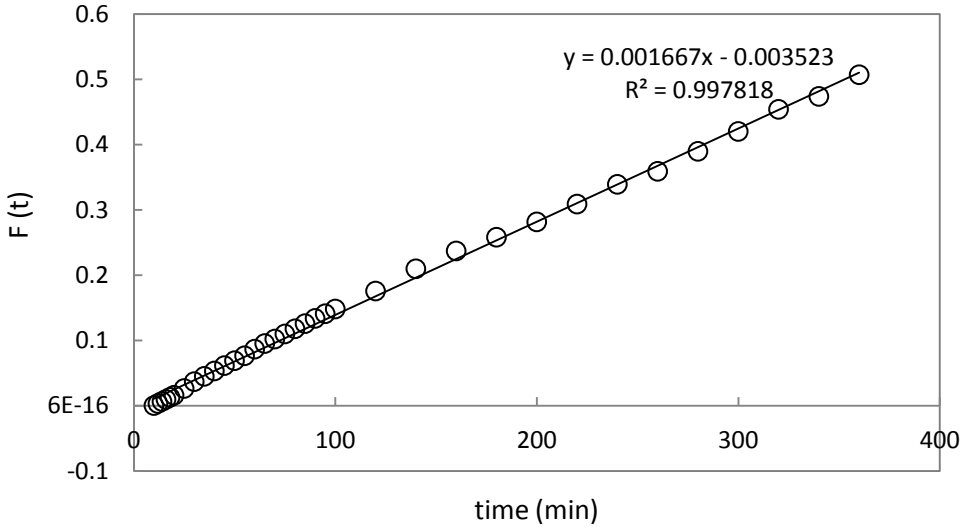

Figure 6-92 long-time permeation data, nitrofurazon: 400 ppm, sericin/chitosan 1:4, GA: 0. 40%

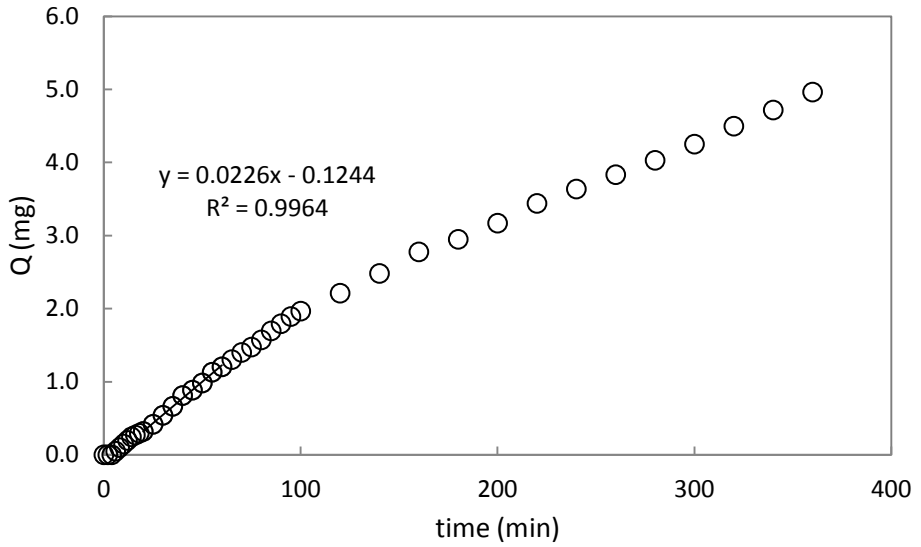

Figure 6-93 short-time permeation data, nitrofurazon: 300 ppm, sericin/chitosan 1:4, GA: 0. 40%

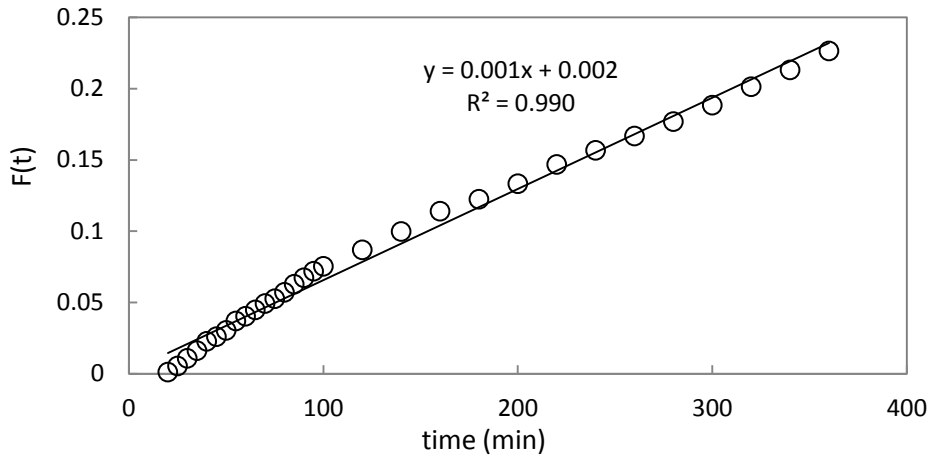

Figure 6-94 long-time permeation data, nitrofurazon: 300 ppm, sericin/chitosan 1:4, GA: 0. 40%

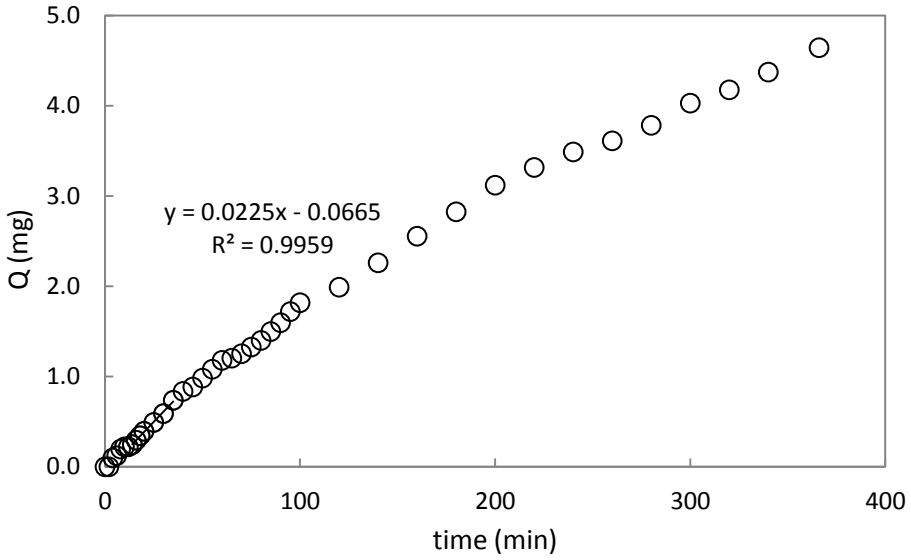

Figure 6-95 short-time permeation data, nitrofurazon: 200 ppm, sericin/chitosan 1:4, GA: 0. 40%

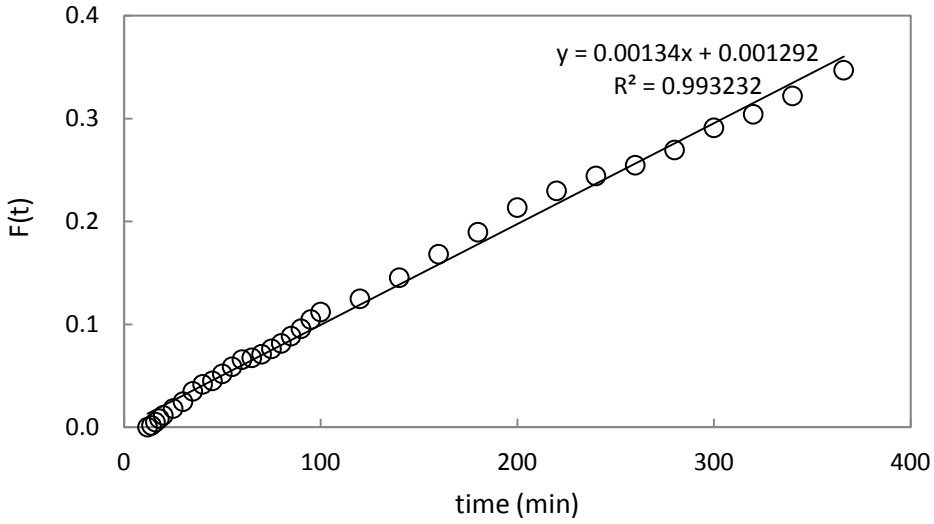

Figure 6-96 long-time permeation data, nitrofurazon: 200 ppm, sericin/chitosan 1:4, GA: 0. 40%

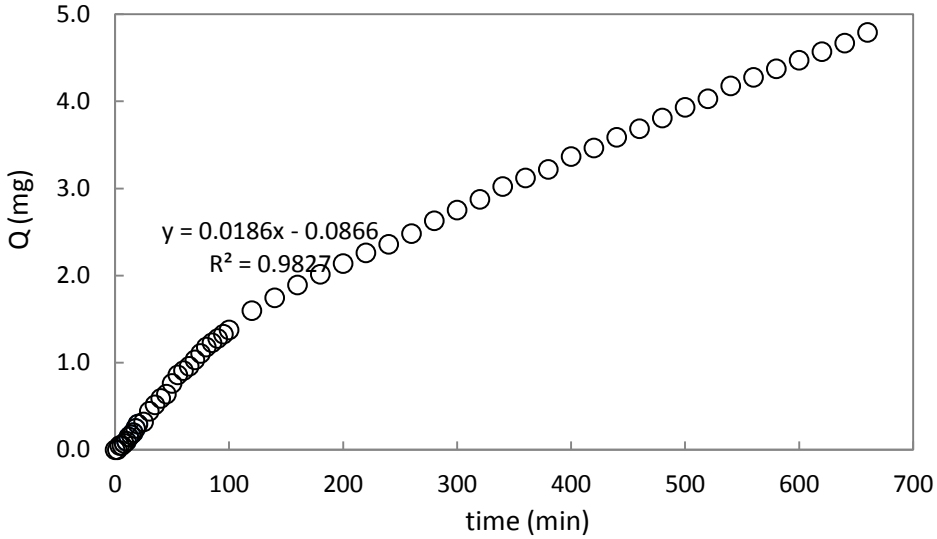

Figure 6-97 short-time permeation data, nitrofurazon: 100 ppm, sericin/chitosan 1:4, GA: 0. 40%

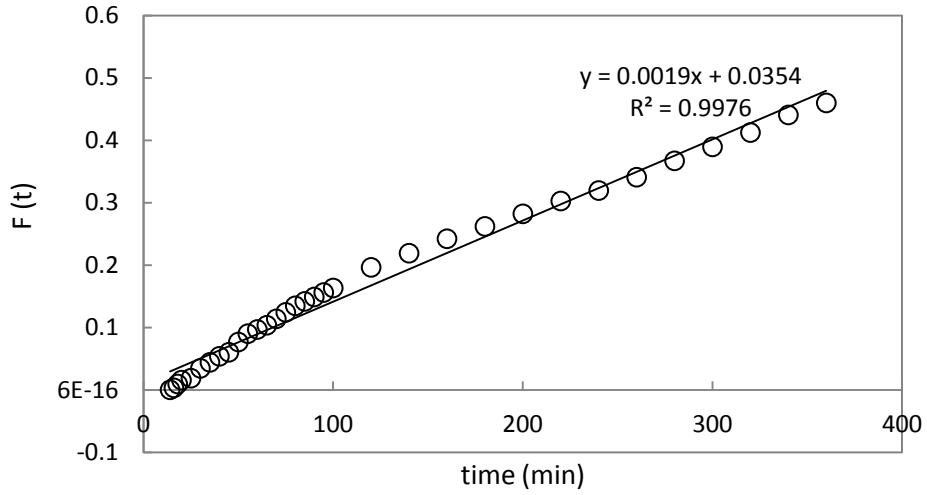

Figure 6-98 long-time permeation data, nitrofurazon: 100 ppm, sericin/chitosan 1:4, GA: 0. 40%

Table 6-3 Permeation parameters for nitrofurazon

GA %	Initial Drug Conc.	Time-Lag	Membrane Thickness	D_T	P_T	P_M
	(ppm)	(min)	(μ)	(cm^2/s)	(cm^2/s)	(cm^2/s)
0.08	100	4.3	110	7.82E-08	1.68E-06	1.53E-06
	200	2.5	110	1.34E-07	1.58E-06	1.53E-06
	300	2.5	110	1.34E-07	1.11E-06	1.22E-06
	400	4.8	110	7.00E-08	1.01E-06	1.18E-06
0.16	100	3.3	110	1.02E-07	1.92E-06	1.29E-06
	200	3	110	1.12E-07	1.64E-06	1.29E-06
	300	3	110	1.12E-07	1.42E-06	1.41E-06
	400	2.5	110	1.34E-07	1.13E-06	1.23E-06
0.24	100	5.3	114	6.81E-08	1.97E-06	1.58E-06
	200	2.5	86	8.22E-08	1.95E-06	1.75E-06
	300	9	111	3.80E-08	1.55E-06	1.42E-06
	400	3.1	110	1.08E-07	2.12E-06	2.01E-06
0.40	100	4.6	89	4.78E-08	2.16E-06	1.81E-06
	200	3	86	6.85E-08	1.35E-06	1.23E-06
	300	5.5	88	3.91E-08	9.12E-07	9.4E-07
	400	3	84	6.53E-08	1.62E-06	1.5E-06

7.1.4. Sorption and Desorption Experiments

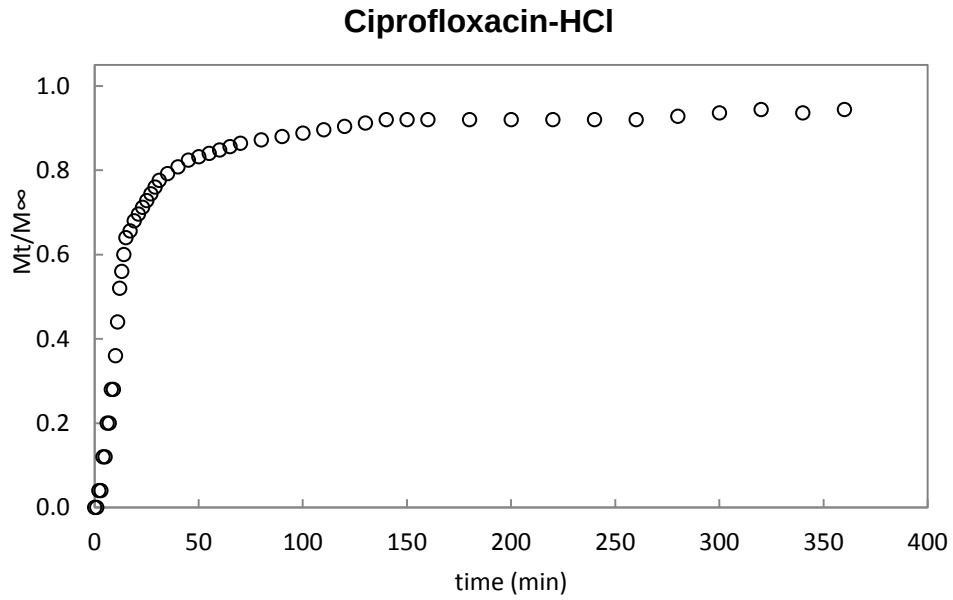

Figure 6-99 Sorption kinetics, ciprofloxacin-HCl: 100 ppm, GA: 0.40%

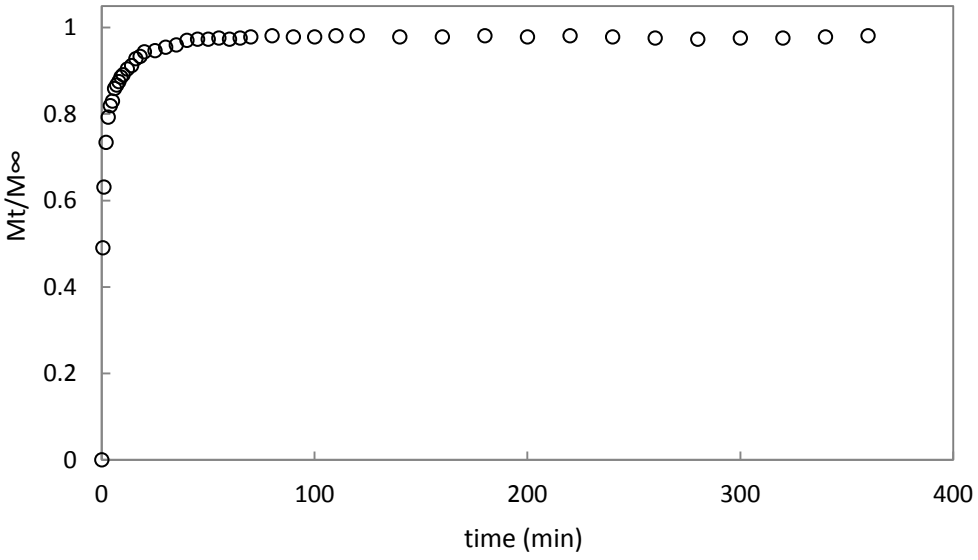

Figure 6-100 Desorption kinetics, ciprofloxacin-HCl: 100 ppm, GA: 0.40%

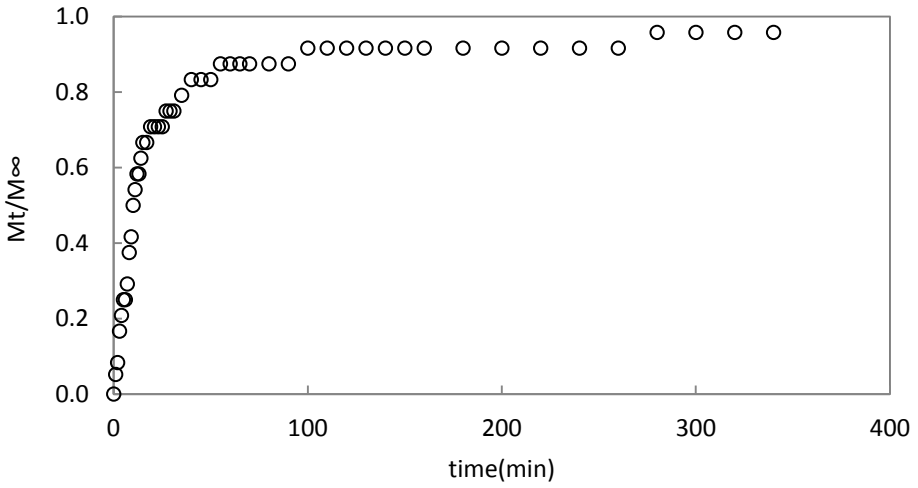

Figure 6-101 Sorption kinetics, ciprofloxacin-HCl: 200 ppm, GA: 0.40%

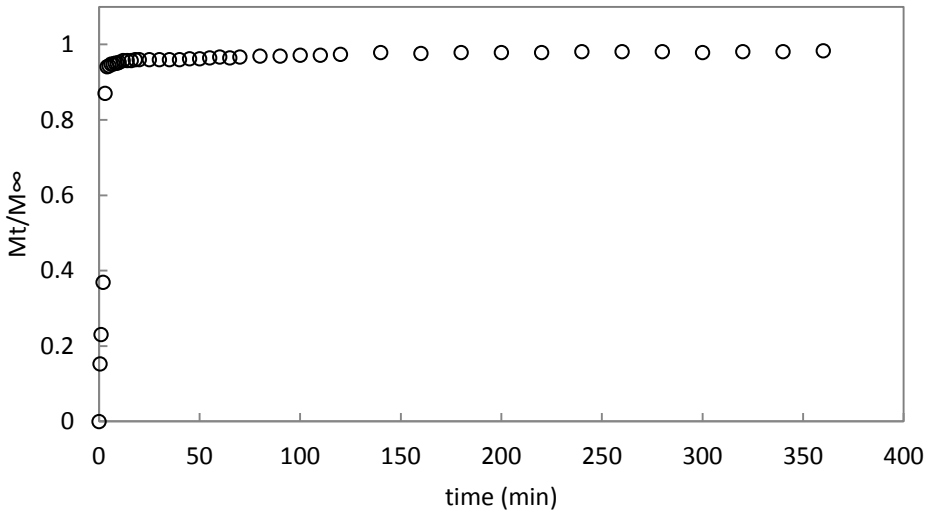

Figure 6-102 Desorption kinetics, ciprofloxacin-HCl: 200 ppm, GA: 0.40%

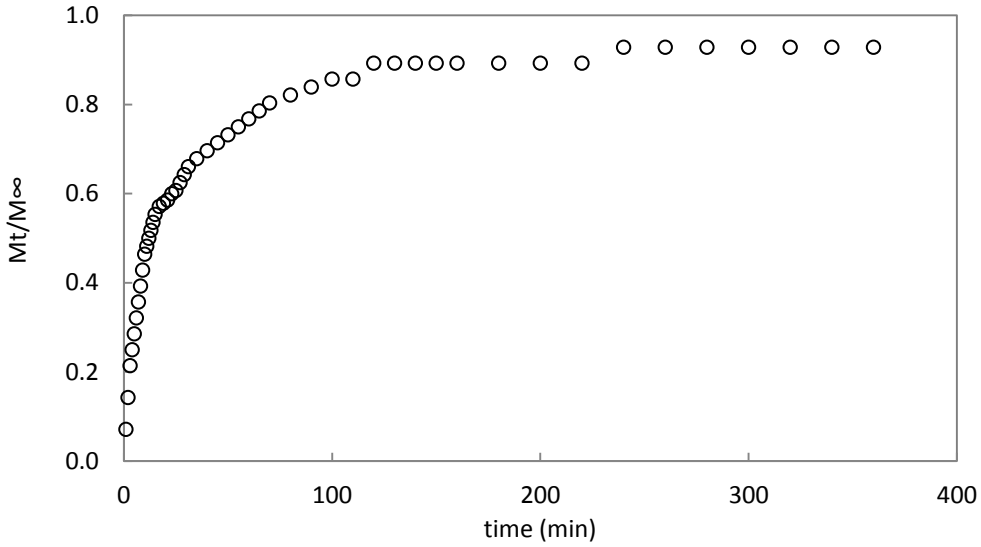

Figure 6-103 Sorption kinetics, ciprofloxacin-HCl: 300 ppm, GA: 0.40%

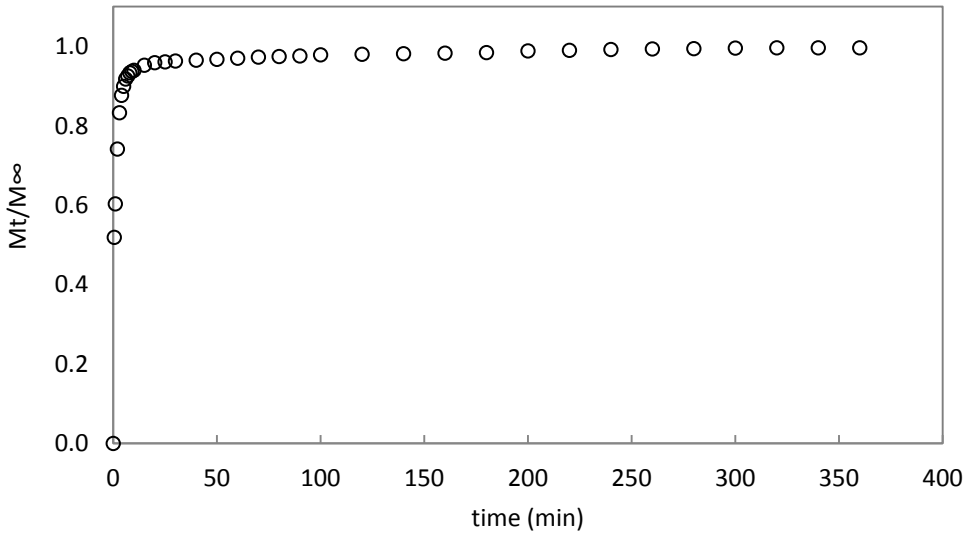

Figure 6-104 Desorption kinetics, ciprofloxacin-HCl: 300 ppm, GA: 0.40%

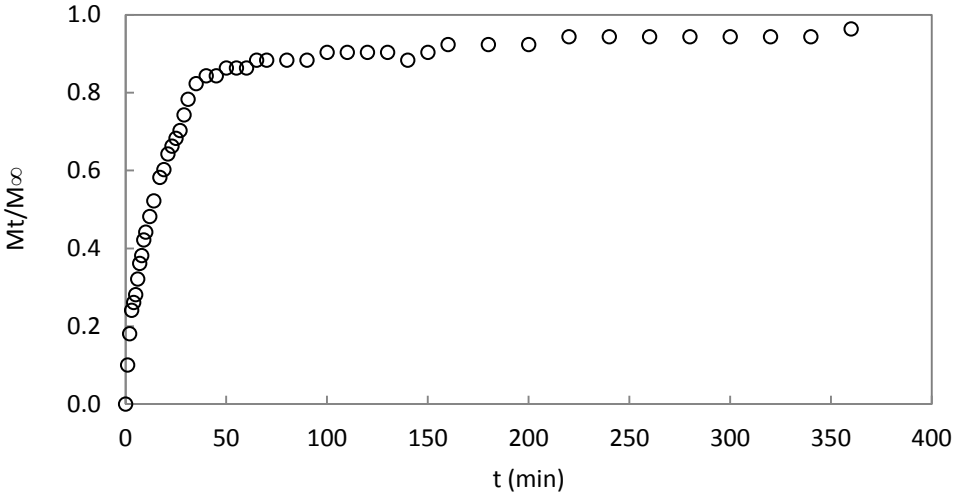

Figure 6-105 Sorption kinetics, ciprofloxacin-HCl: 400 ppm, GA: 0.40%

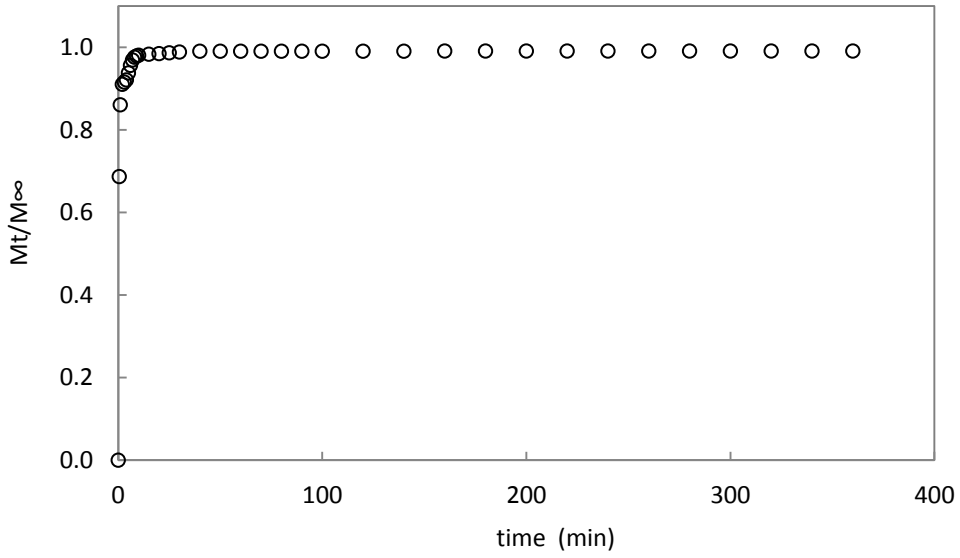

Figure 6-106 Desorption kinetics, ciprofloxacin-HCl: 400 ppm, GA: 0.40%

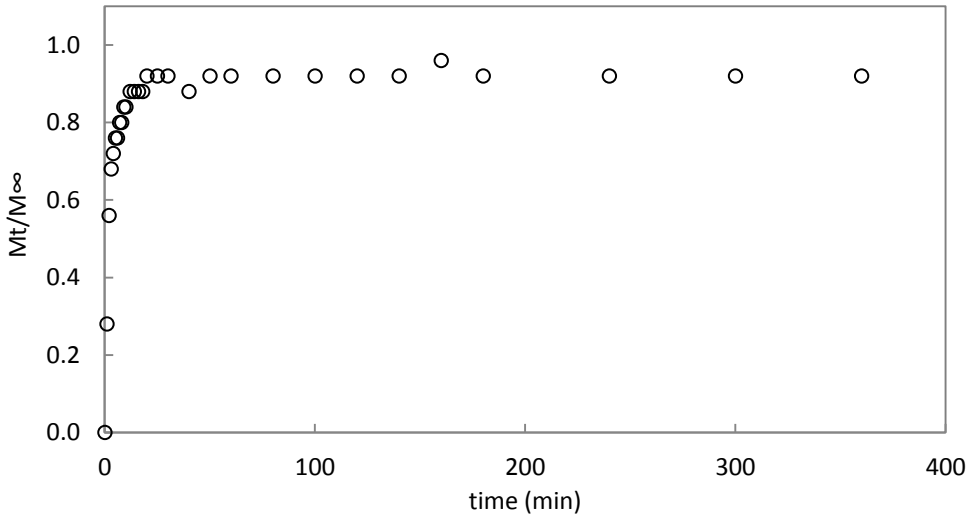

Figure 6-107 Sorption kinetics, ciprofloxacin-HCl: 400 ppm, GA: 0.24%

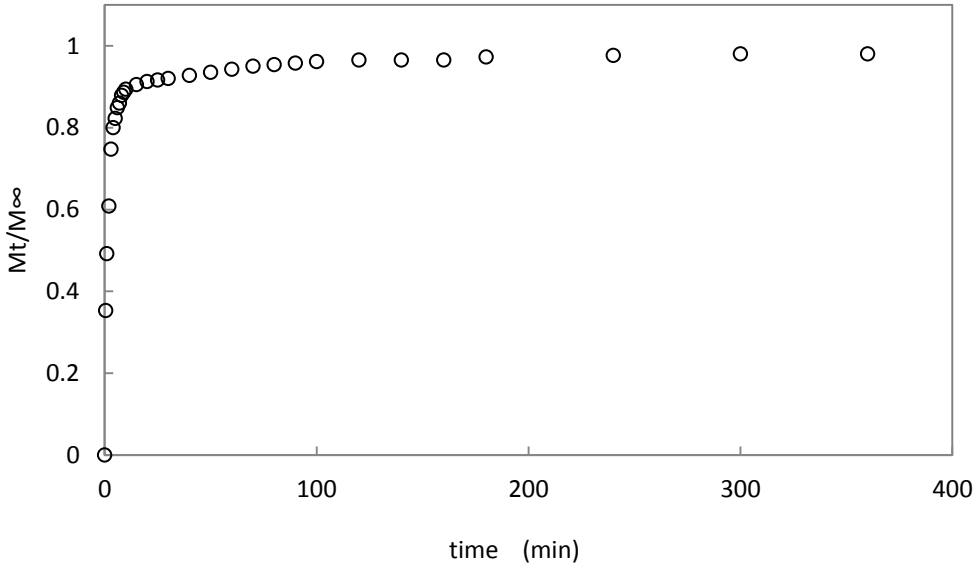

Figure 6-108 Desorption kinetics, ciprofloxacin-HCl: 400 ppm, GA: 0.24%

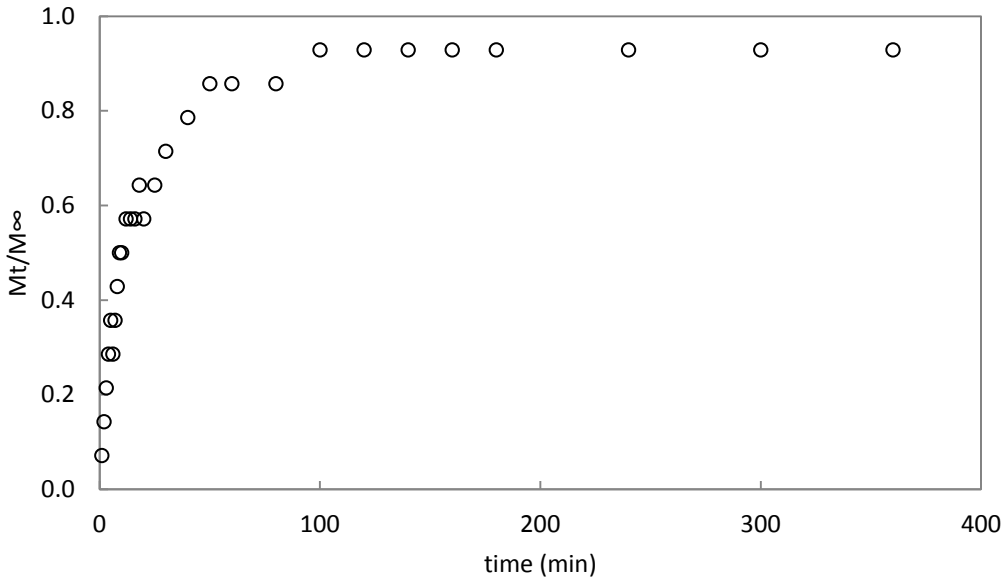

Figure 6-109 Sorption kinetics, ciprofloxacin-HCl: 300 ppm, GA: 0.24%

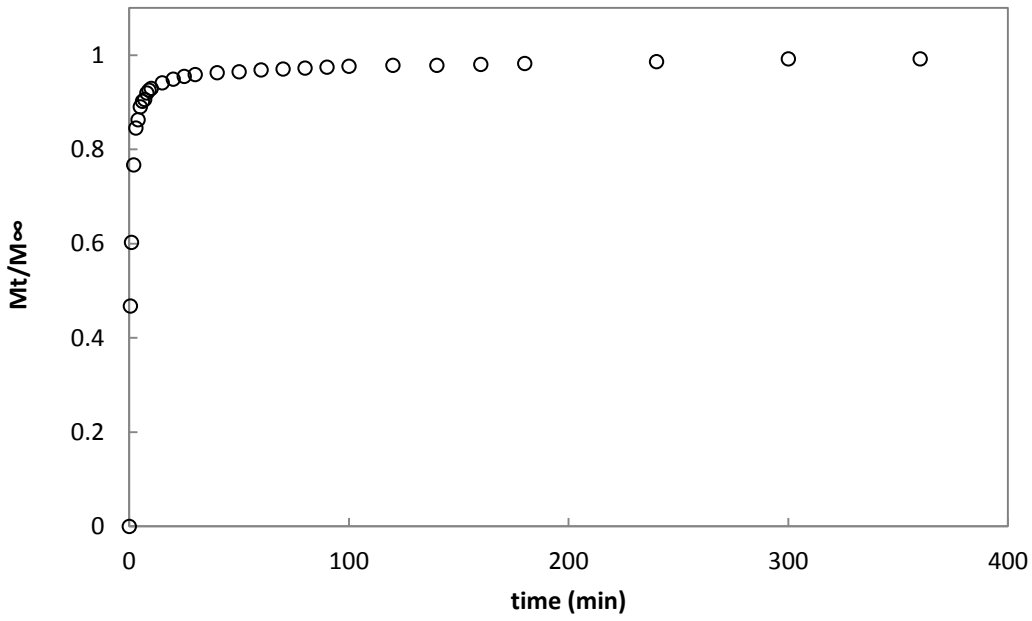

Figure 6-110 Desorption kinetics, ciprofloxacin-HCl: 300 ppm, GA: 0.24%

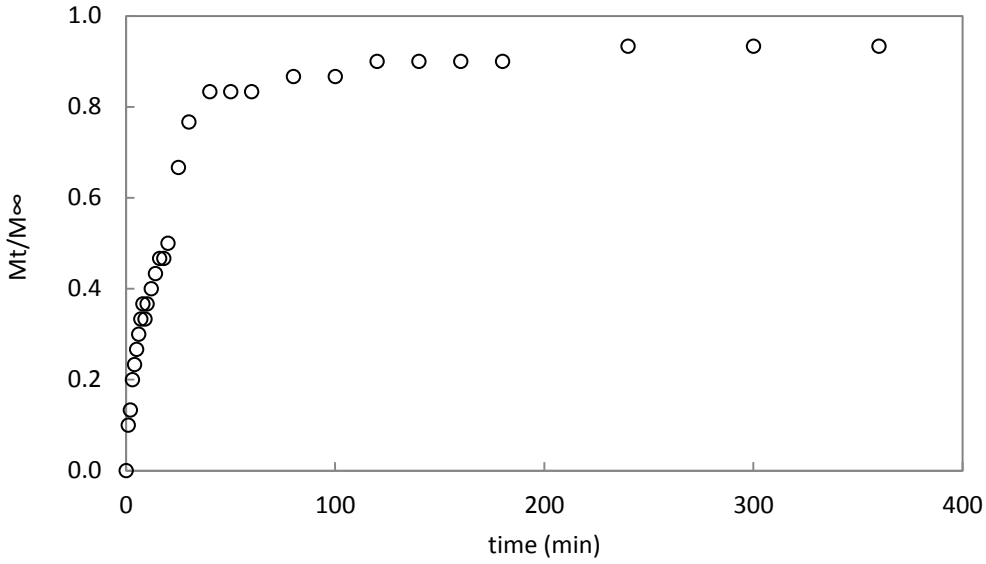

Figure 6-111 Sorption kinetics, ciprofloxacin-HCl: 200 ppm, GA: 0.24%

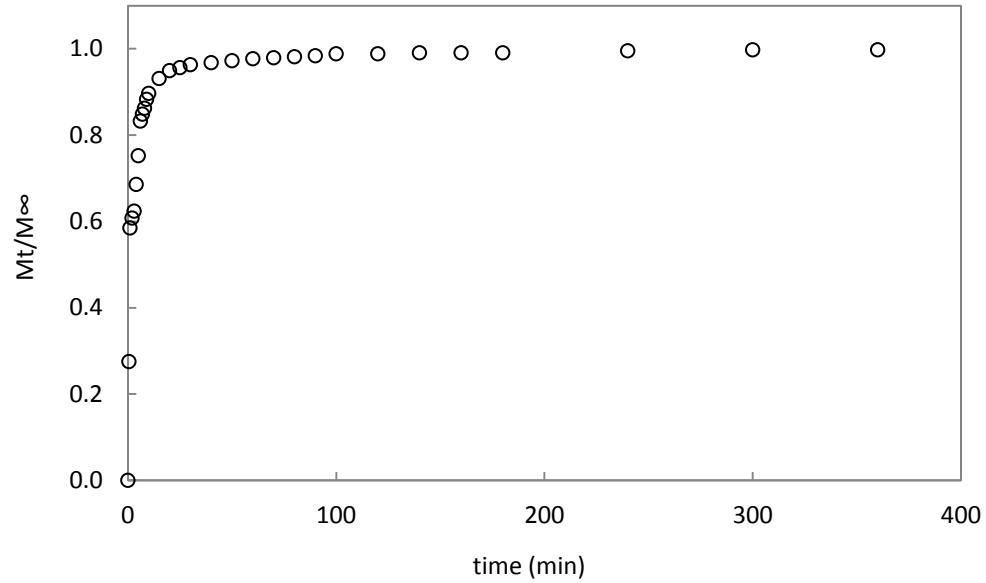

Figure 6-112 Desorption kinetics, ciprofloxacin-HCl: 200 ppm, GA: 0.24%

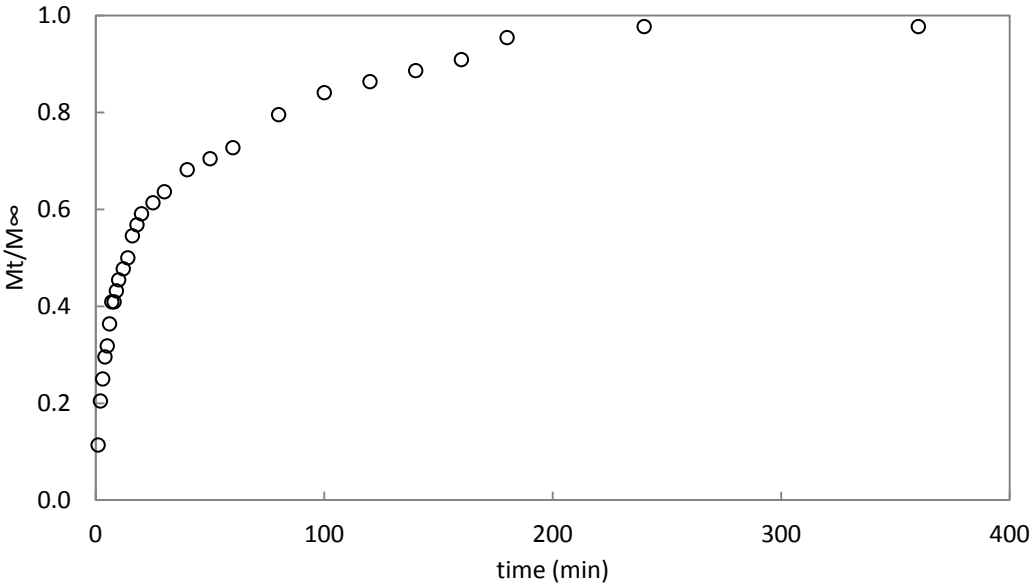

Figure 6-113 Sorption kinetics, ciprofloxacin-HCl: 100 ppm, GA: 0.24%

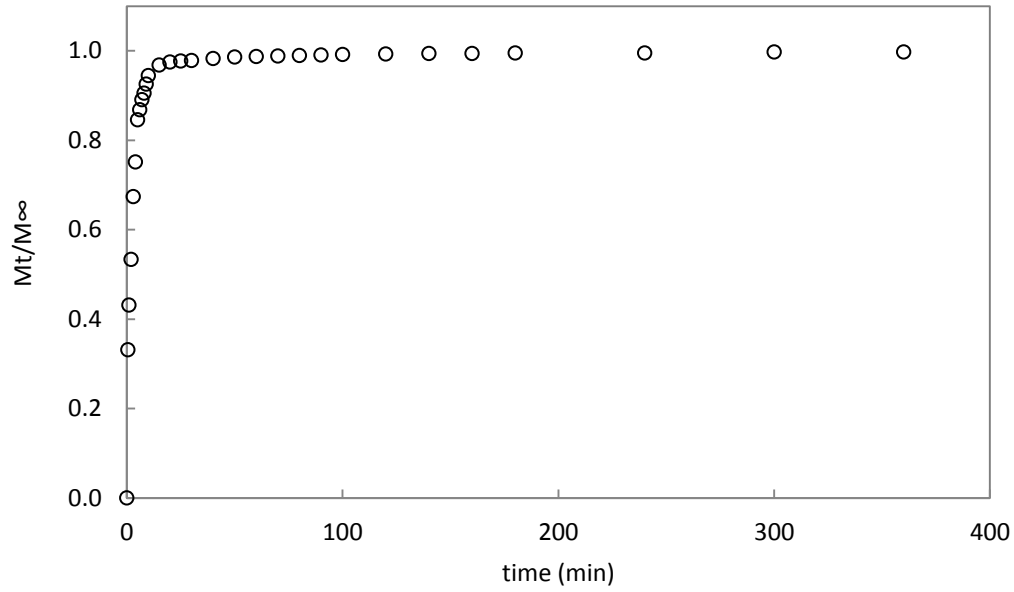

Figure 6-114 Desorption kinetics, ciprofloxacin-HCl: 100 ppm, GA: 0.24%

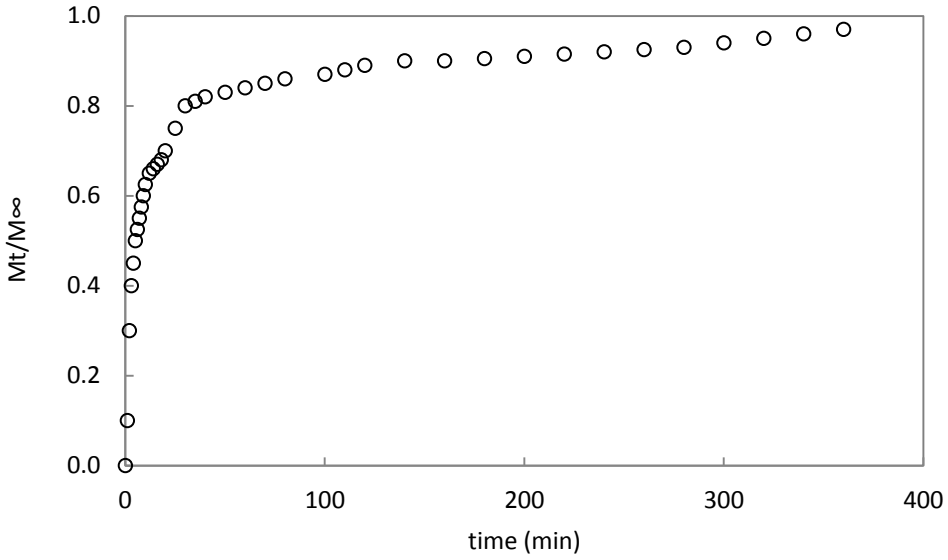

Figure 6-115 Sorption kinetics, ciprofloxacin-HCl: 400 ppm, GA: 0.16%

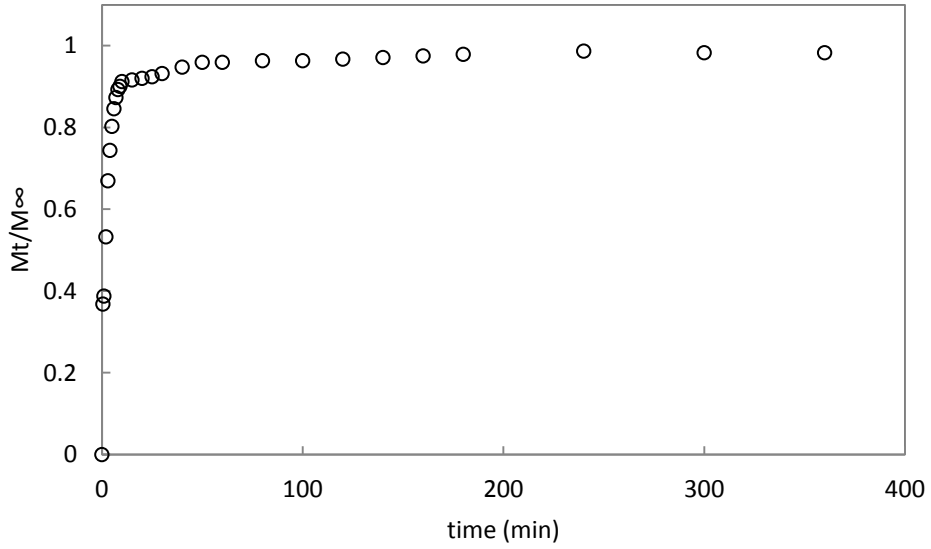

Figure 6-116 Desorption kinetics, ciprofloxacin-HCl: 400 ppm, GA: 0.16%

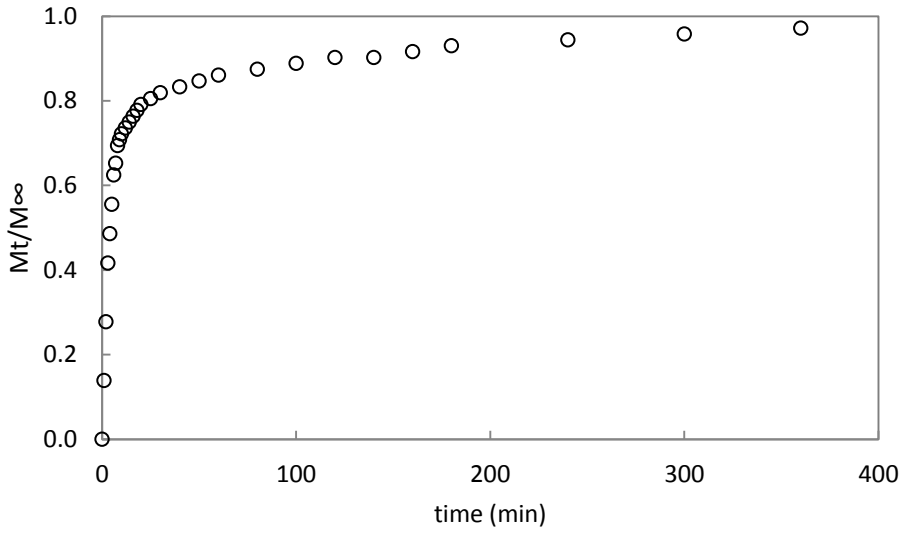

Figure 6-117 Sorption kinetics, ciprofloxacin-HCl: 300 ppm, GA: 0.16%

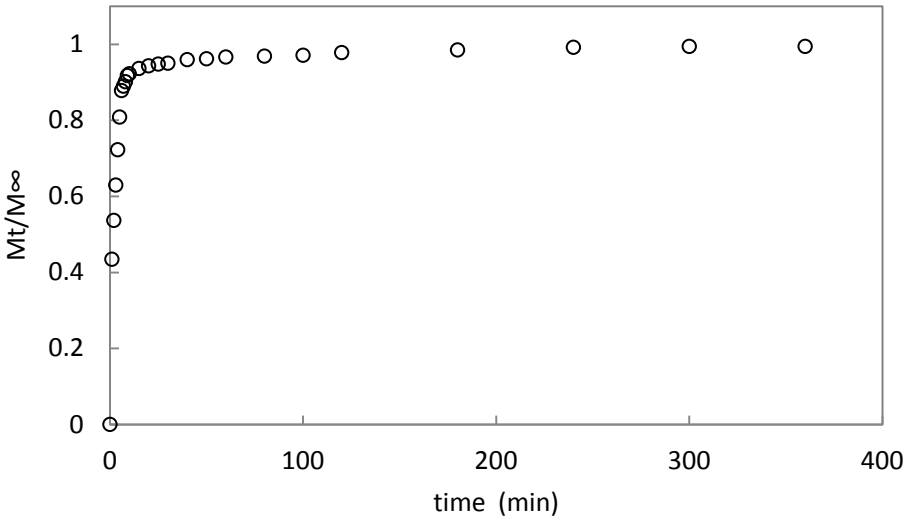

Figure 6-118 Desorption kinetics, ciprofloxacin-HCl: 300 ppm, GA: 0.16%

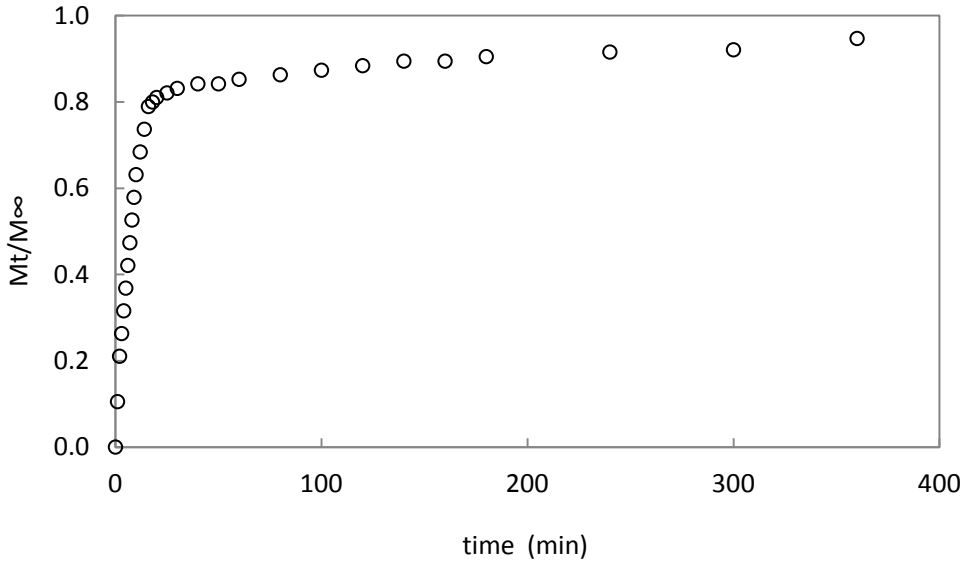

Figure 6-119 Sorption kinetics, ciprofloxacin-HCl: 200 ppm, GA: 0.16%

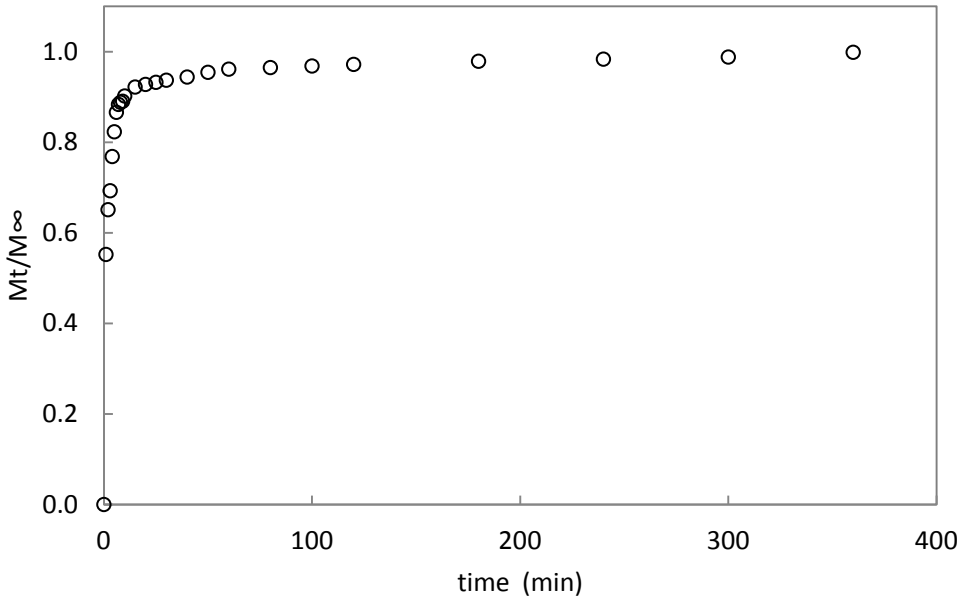

Figure 6-120 Desorption kinetics, ciprofloxacin-HCl: 200 ppm, GA: 0.16%

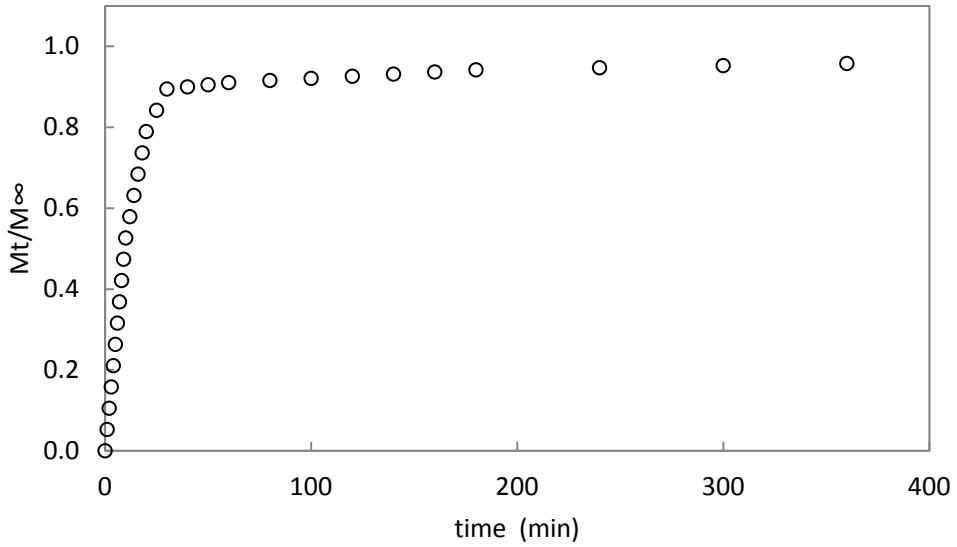

Figure 6-121 Sorption kinetics, ciprofloxacin-HCl: 100 ppm, GA: 0.16%

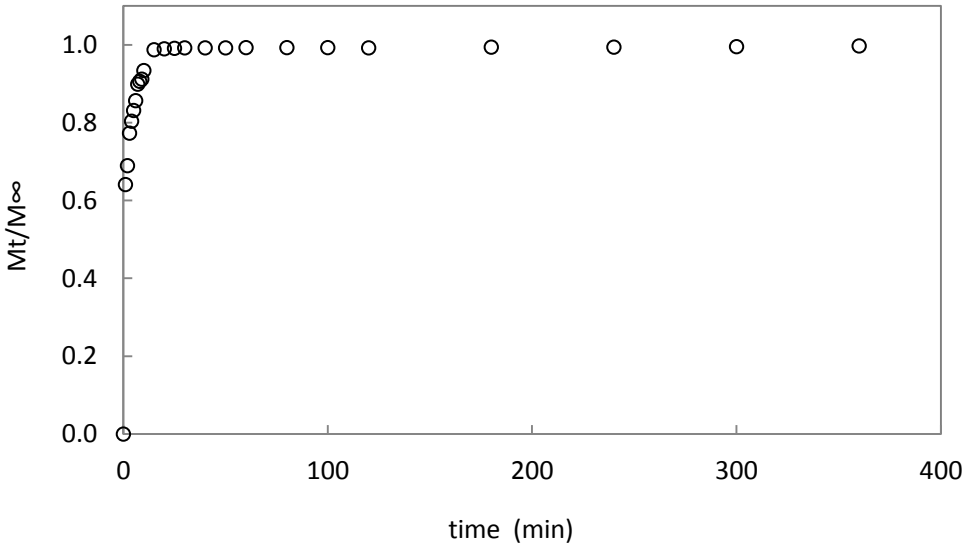

Figure 6-122 Desorption kinetics, ciprofloxacin-HCl: 100 ppm, GA: 0.16%

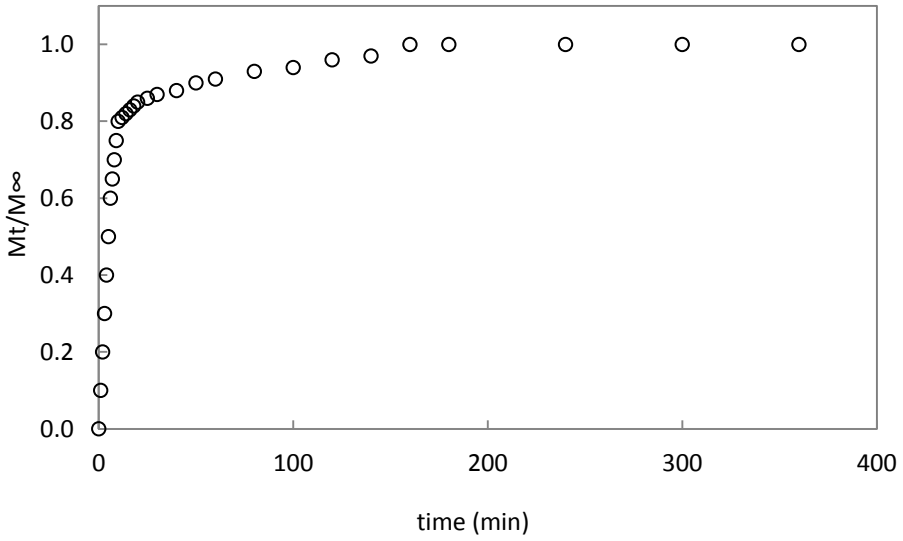

Figure 6-123 Sorption kinetics, ciprofloxacin-HCl: 400 ppm, GA: 0.08%

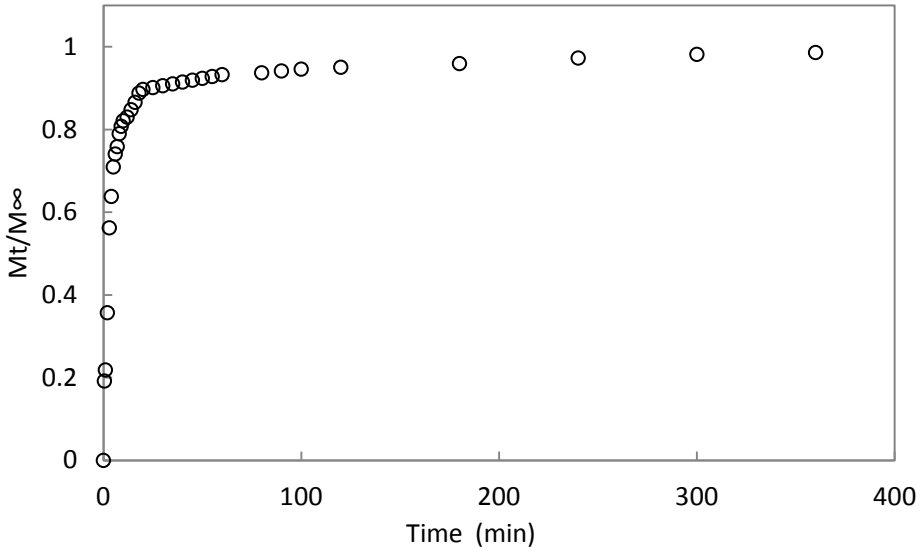

Figure 6-124 Desorption kinetics, ciprofloxacin-HCl: 400 ppm, GA: 0.08%

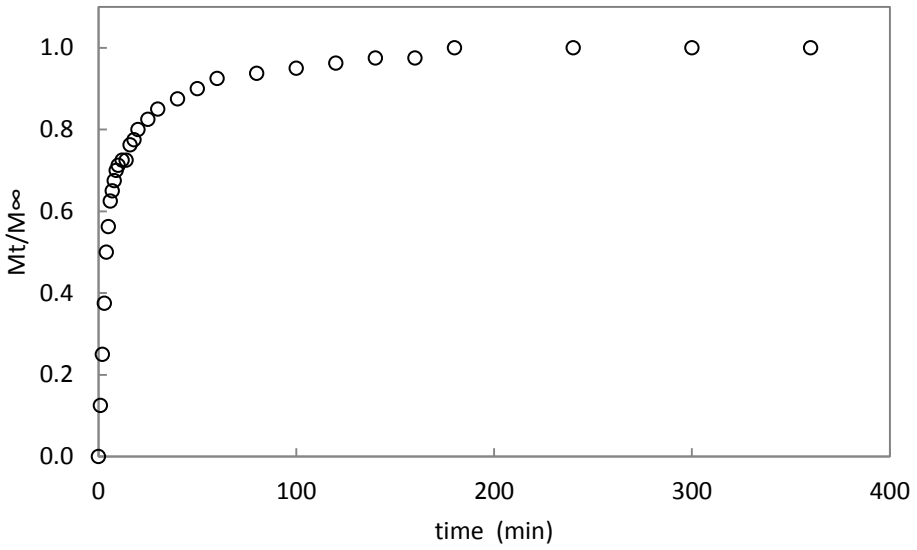

Figure 6-125 Sorption kinetics, ciprofloxacin-HCl: 300 ppm, GA: 0.08%

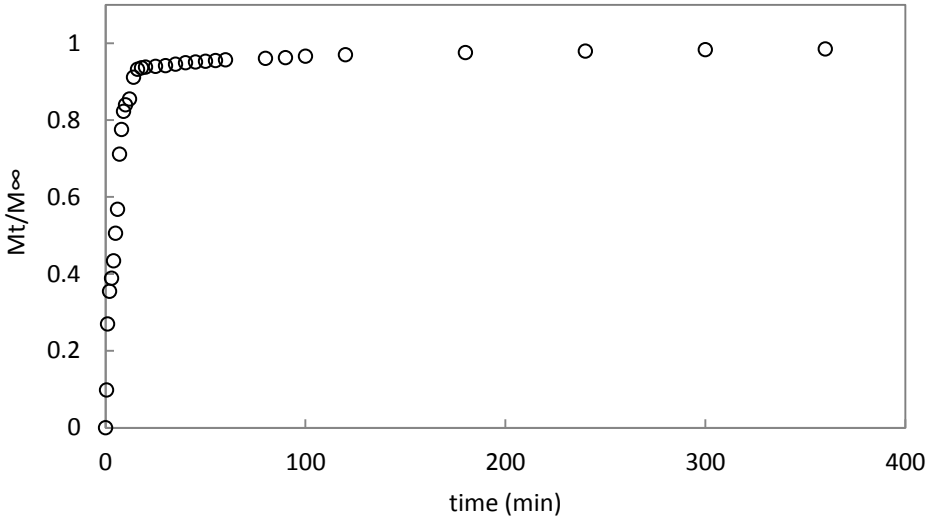

Figure 6-126 Desorption kinetics, ciprofloxacin-HCl: 300 ppm, GA: 0.08%

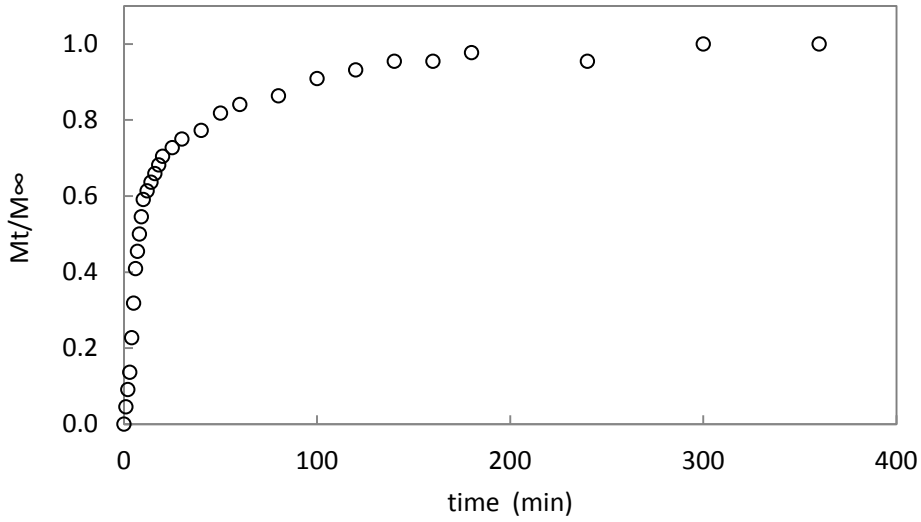

Figure 6-127 Sorption kinetics, ciprofloxacin-HCl: 200 ppm, GA: 0.08%

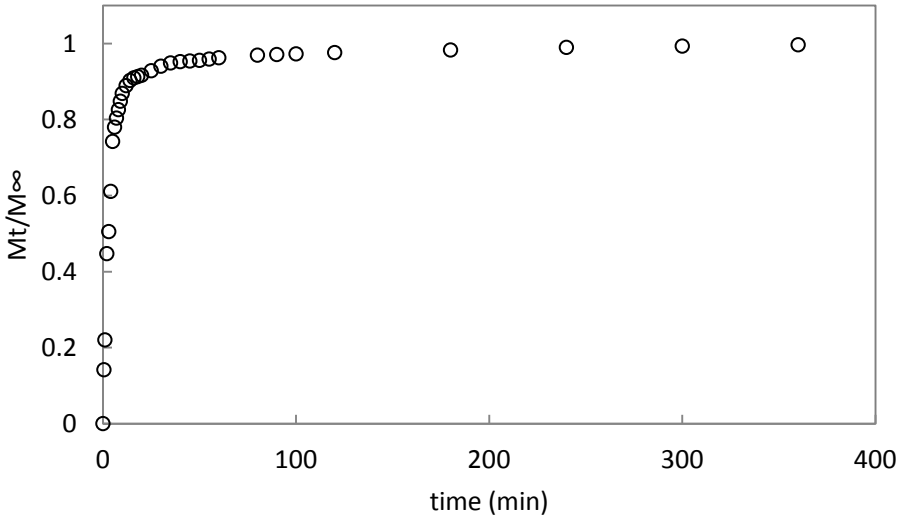

Figure 6-128 Desorption kinetics, ciprofloxacin-HCl: 200 ppm, GA: 0.08%

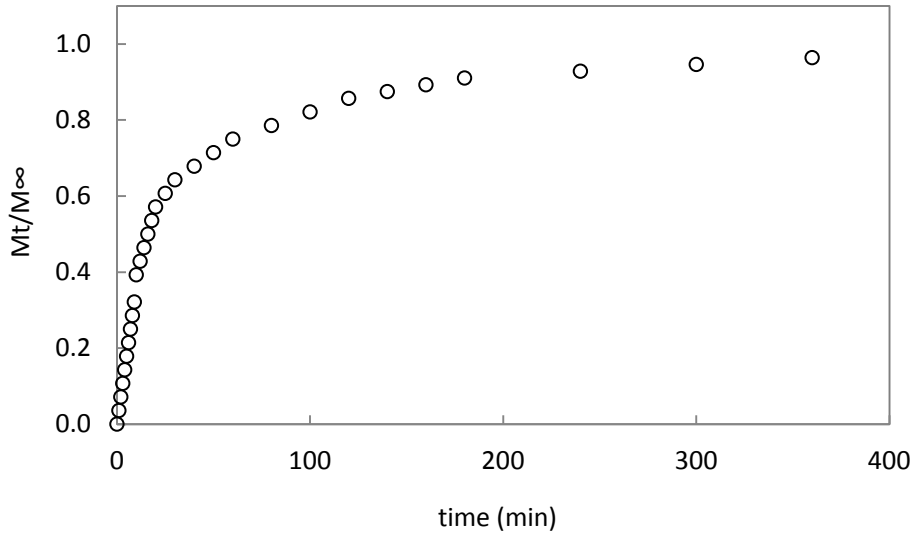

Figure 6-129 Sorption kinetics, ciprofloxacin-HCl: 100 ppm, GA: 0.08%

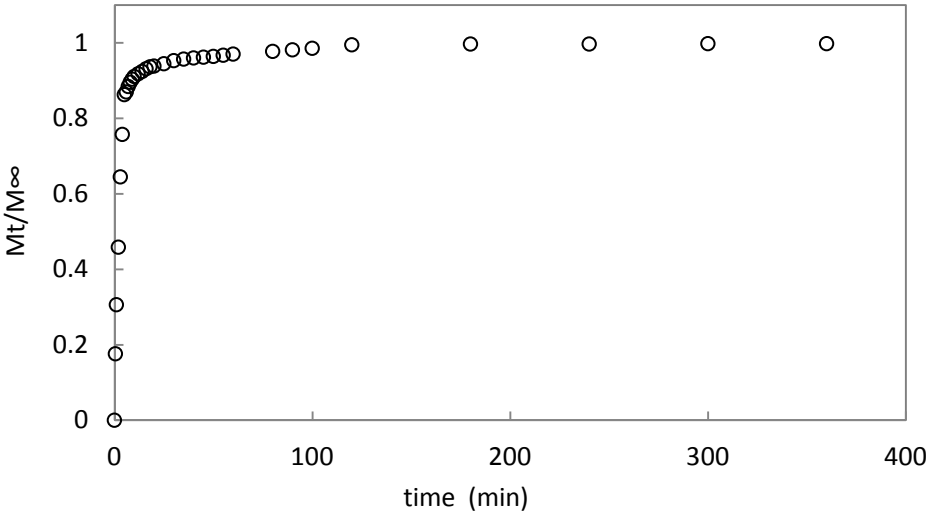

Figure 6-130 Desorption kinetics, ciprofloxacin-HCl: 100 ppm, GA: 0.08%

Diltiazem-HCl

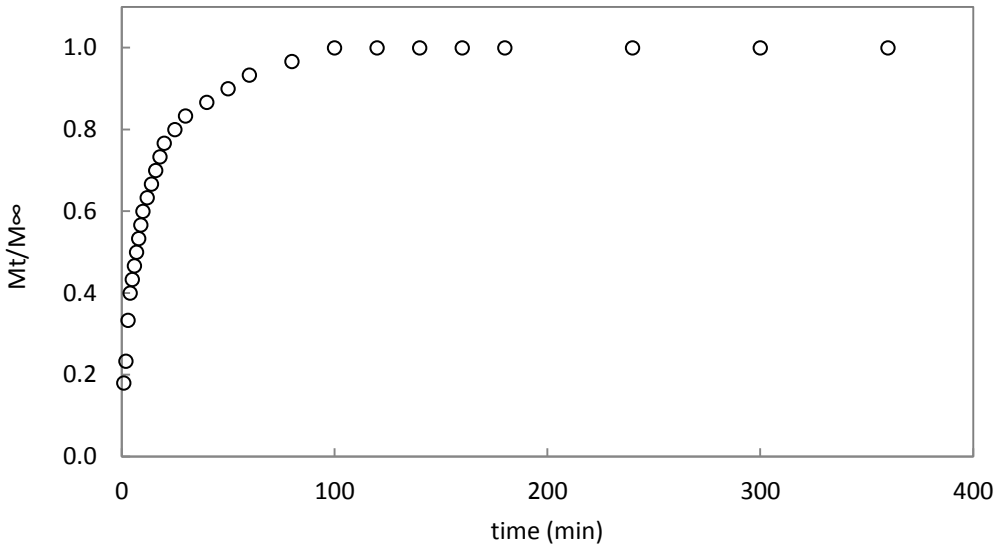

Figure 6-131 Sorption kinetics, diltiazem-HCl: 100 ppm, GA: 0.08%

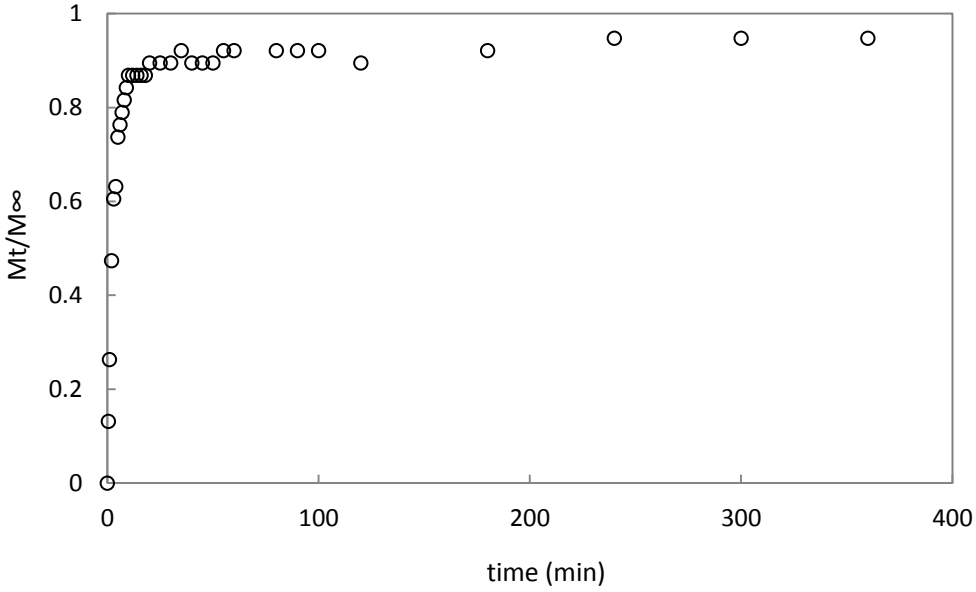

Figure 6-132 Desorption kinetics, diltiazem-HCl: 100 ppm, GA: 0.08%

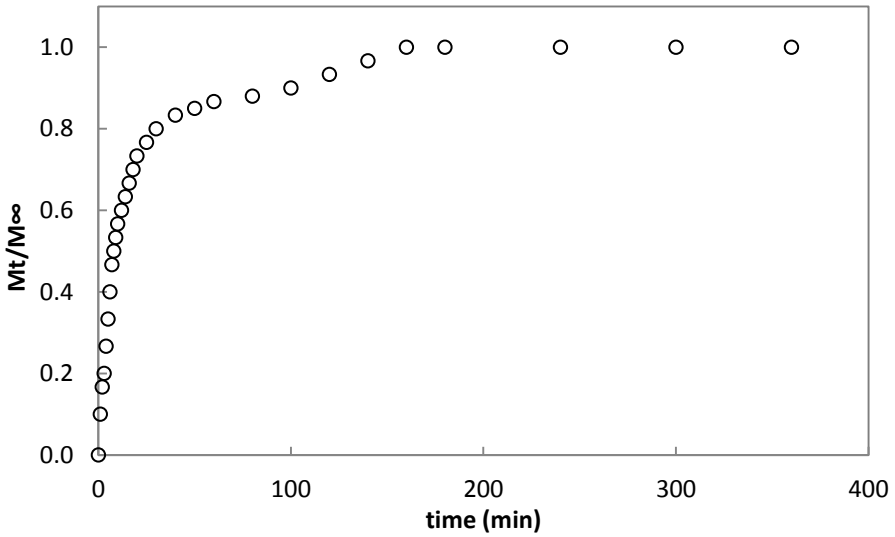

Figure 6-133 Sorption kinetics, diltiazem-HCl: 200 ppm, GA: 0.08%

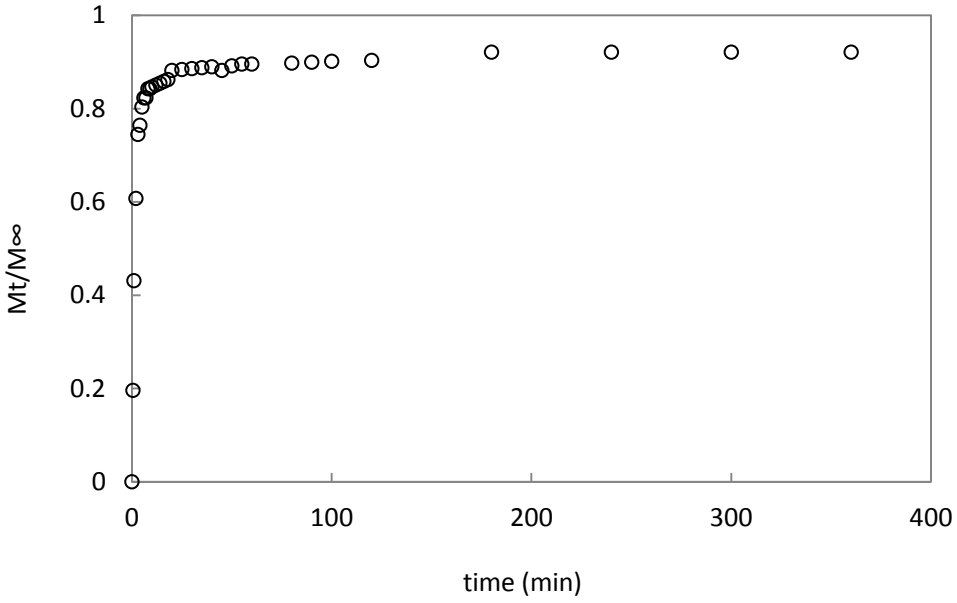

Figure 6-134 Desorption kinetics, diltiazem-HCl: 200 ppm, GA: 0.08%

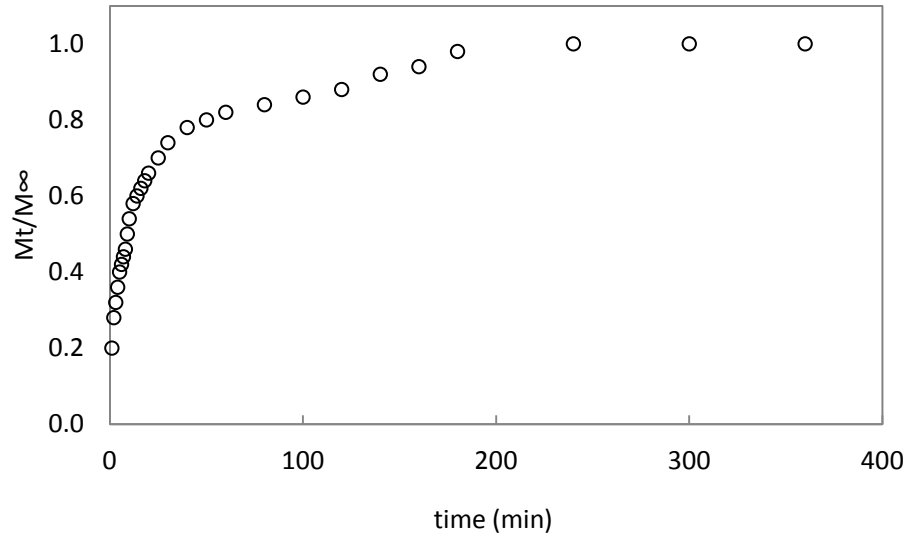

Figure 6-135 Sorption kinetics, diltiazem-HCl: 300 ppm, GA: 0.08%

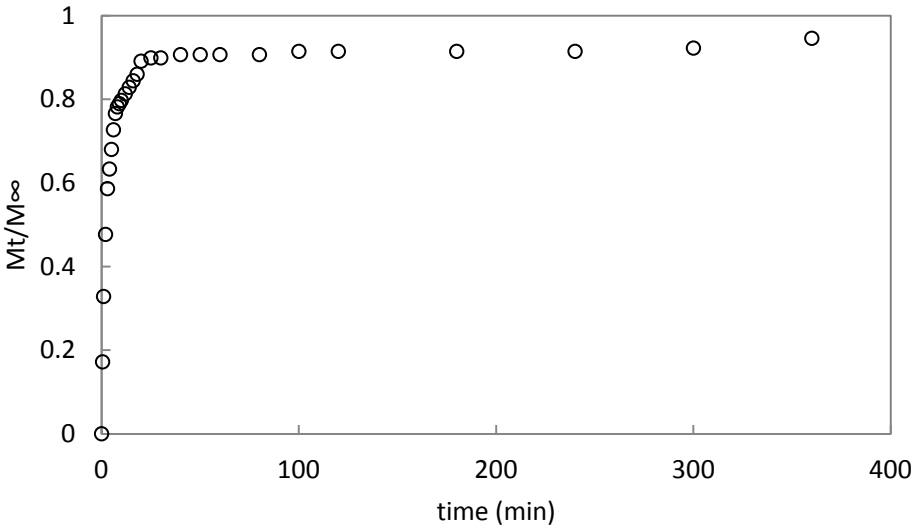

Figure 6-136 Desorption kinetics, diltiazem-HCl: 300 ppm, GA: 0.08%

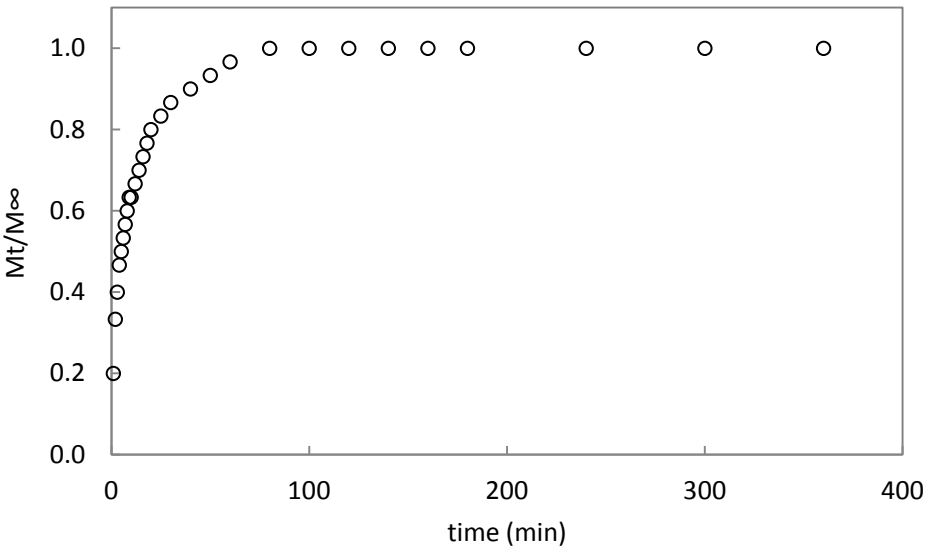

Figure 6-137 Sorption kinetics, diltiazem-HCl: 400 ppm, GA: 0.08%

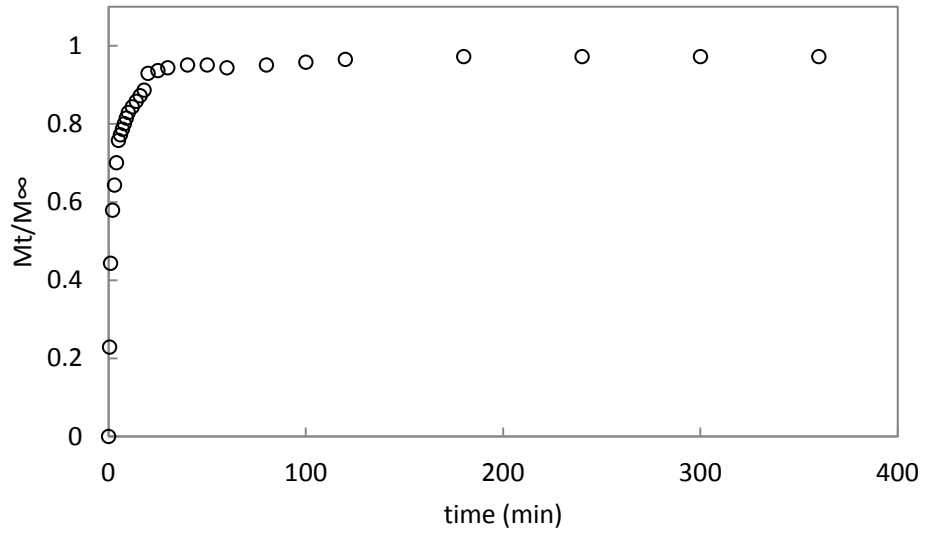

Figure 6-138 Desorption kinetics, diltiazem-HCl: 400 ppm, GA: 0.08%

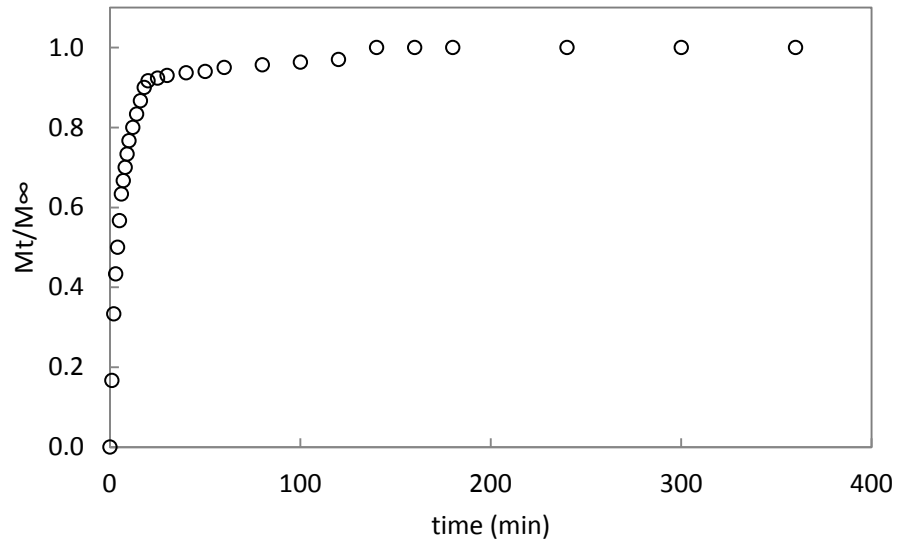

Figure 6-139 Sorption kinetics, diltiazem-HCl: 100 ppm, GA: 0.16%

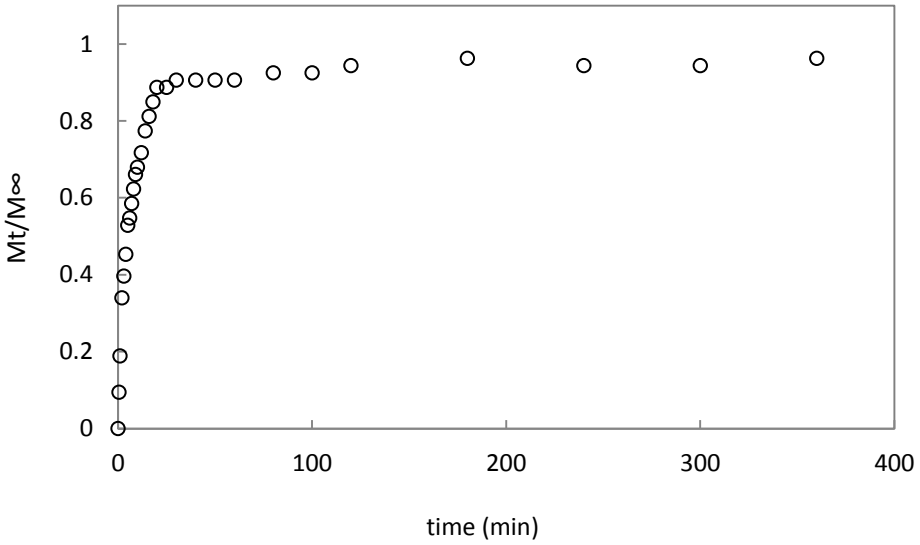

Figure 6-140 Desorption kinetics, diltiazem-HCl: 100 ppm, GA: 0.16%

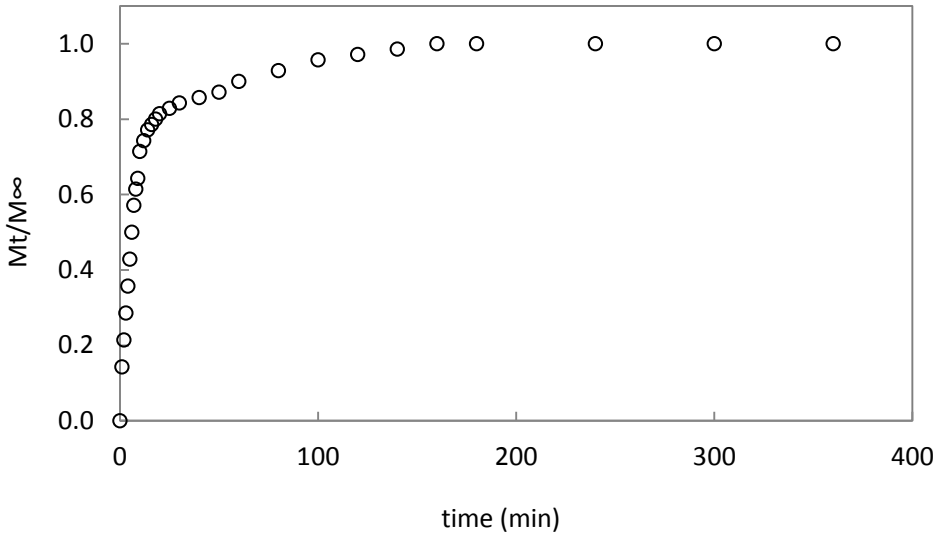

Figure 6-141 Sorption kinetics, diltiazem-HCl: 200 ppm, GA: 0.16%

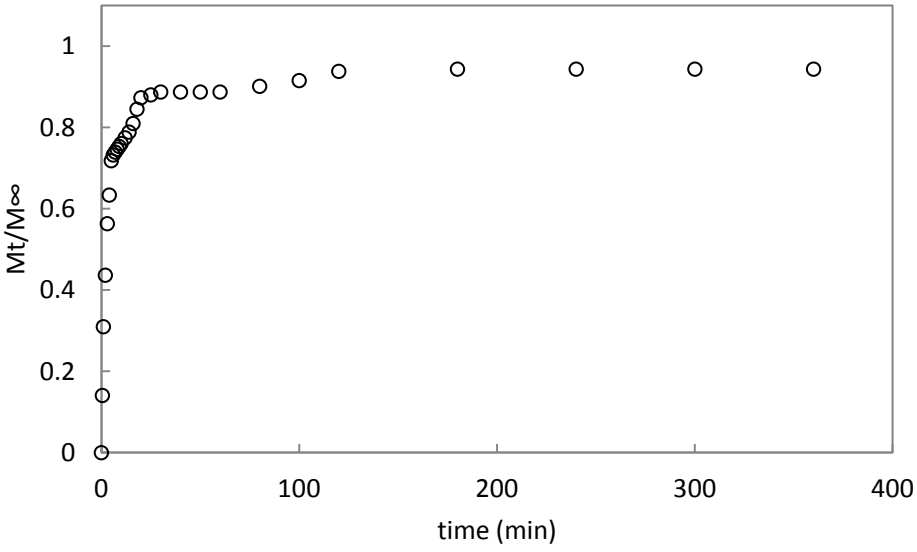

Figure 6-142 Desorption kinetics, diltiazem-HCl: 200 ppm, GA: 0.16%

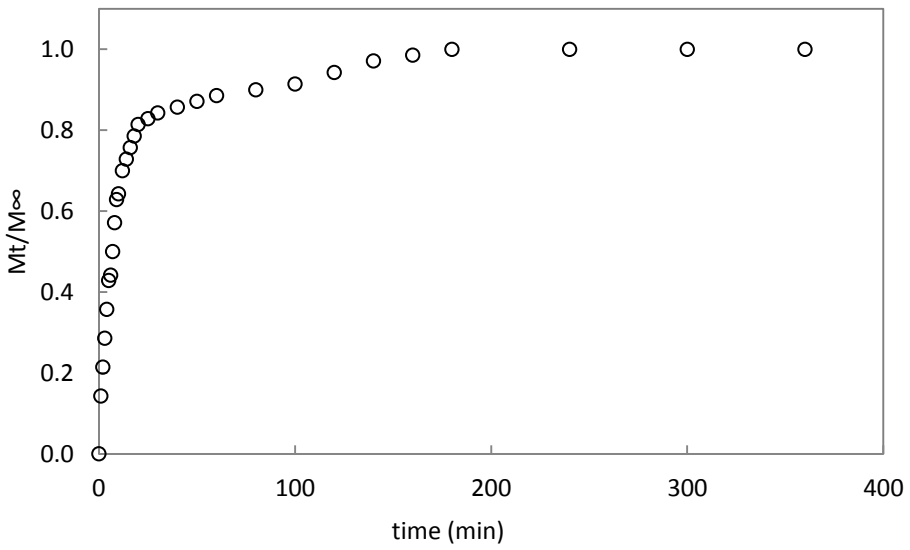

Figure 6-143 Sorption kinetics, diltiazem-HCl: 300 ppm, GA: 0.16%

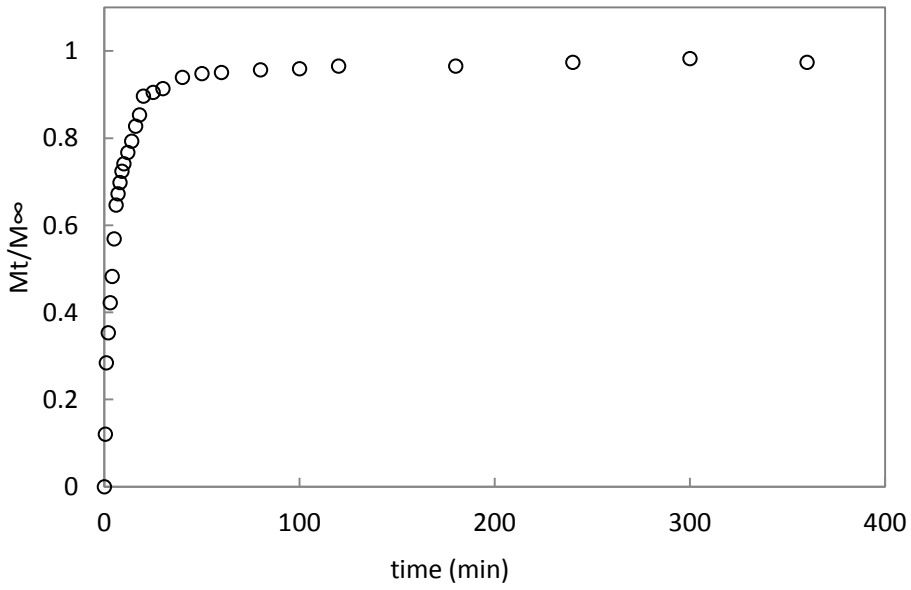

Figure 6-144 Desorption kinetics, diltiazem-HCl: 300 ppm, GA: 0.16%

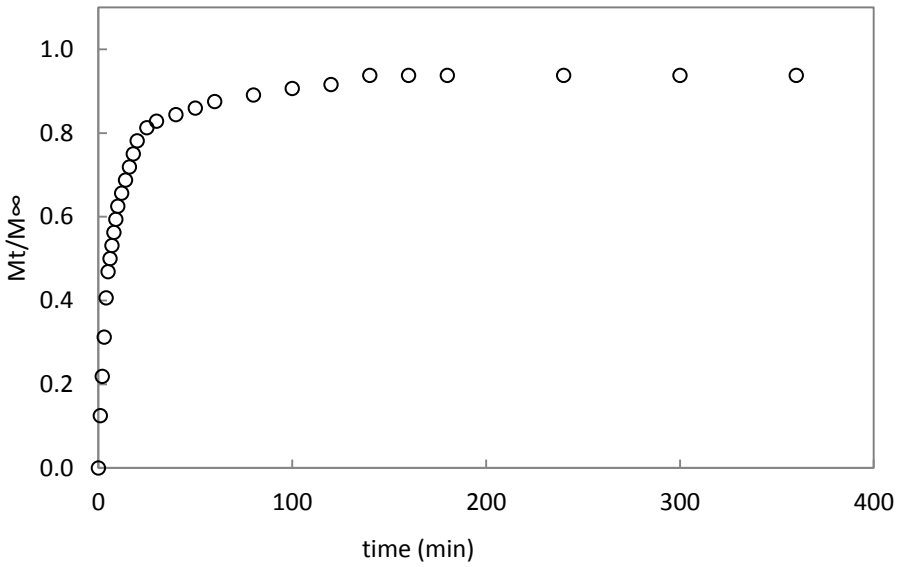

Figure 6-145 Sorption kinetics, diltiazem-HCl: 400 ppm, GA: 0.16%

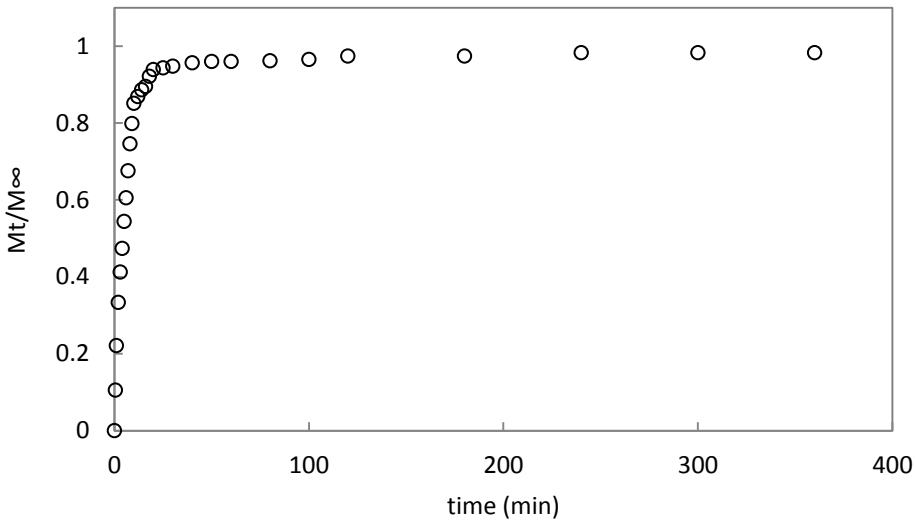

Figure 6-146 Desorption kinetics, diltiazem-HCl: 400 ppm, GA: 0.16%

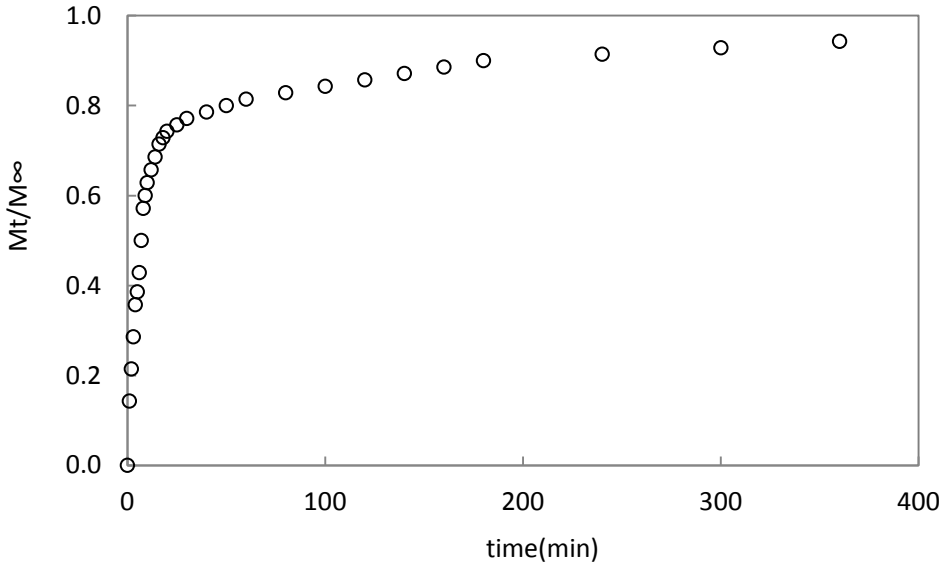

Figure 6-147 Sorption kinetics, diltiazem-HCl: 100 ppm, GA: 0.24%

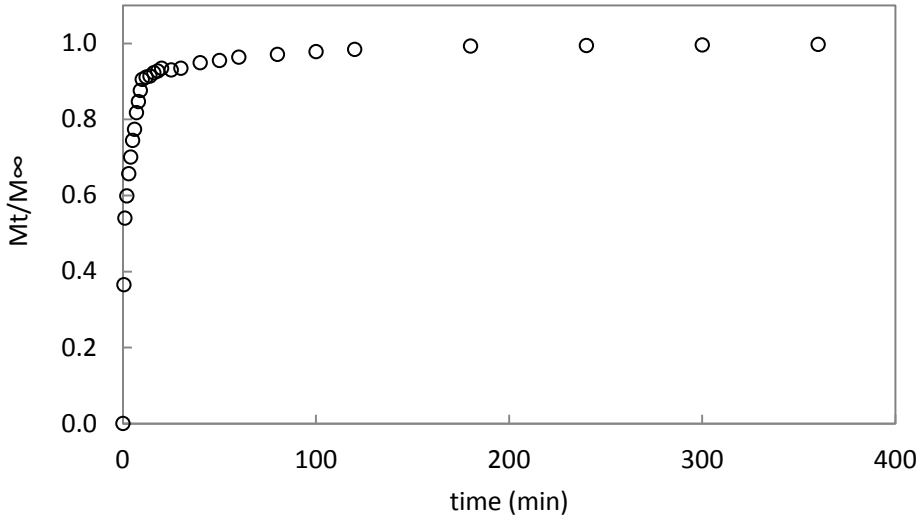

Figure 6-148 Desorption kinetics, diltiazem-HCl: 100 ppm, GA: 0.24%

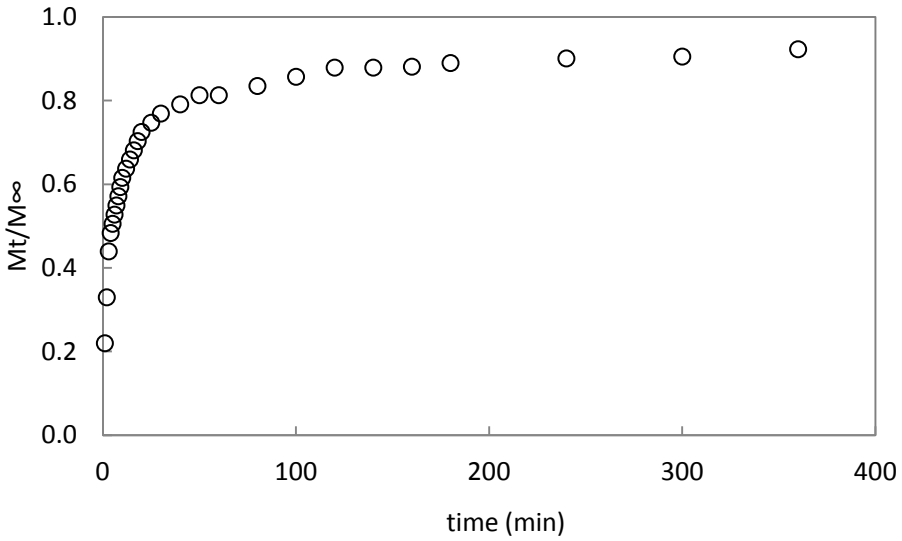

Figure 6-149 Sorption kinetics, diltiazem-HCl: 200 ppm, GA: 0.24%

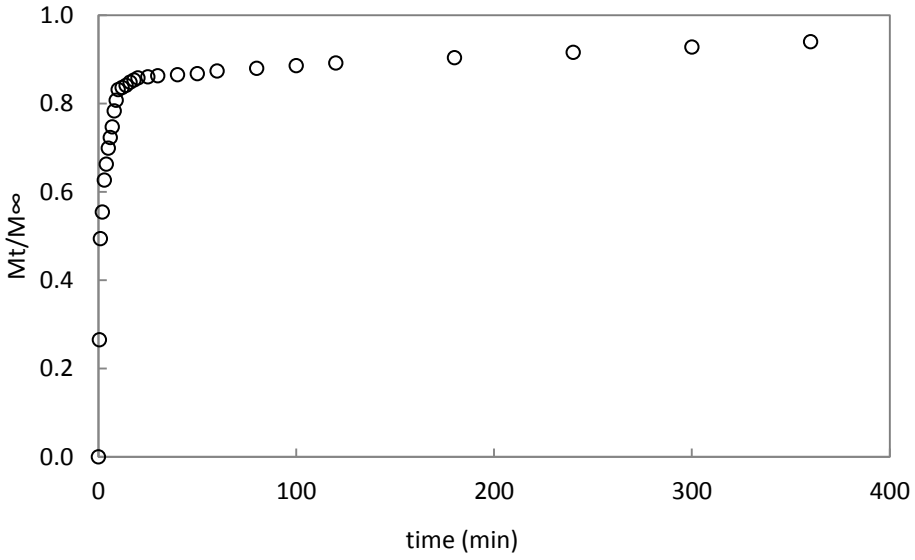

Figure 6-150 Desorption kinetics, diltiazem-HCl: 200 ppm, GA: 0.24%

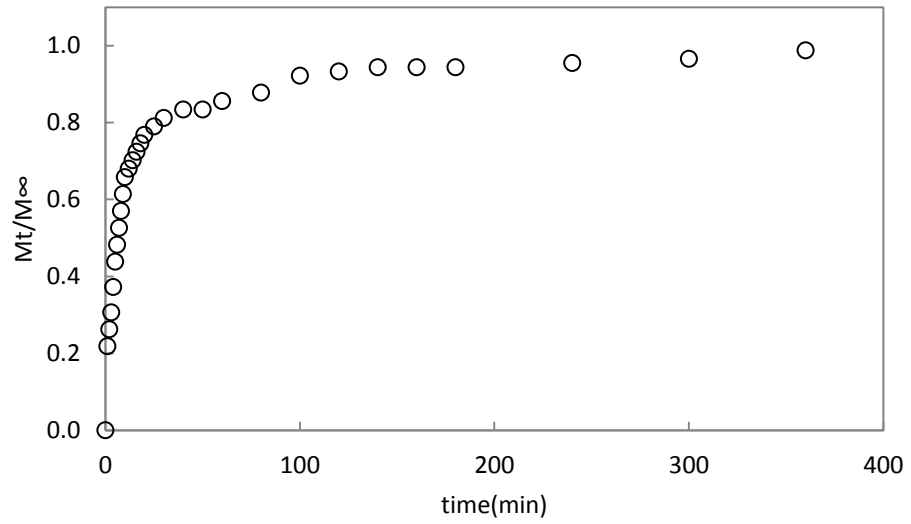

Figure 6-151 Sorption kinetics, diltiazem-HCl: 300 ppm, GA: 0.24%

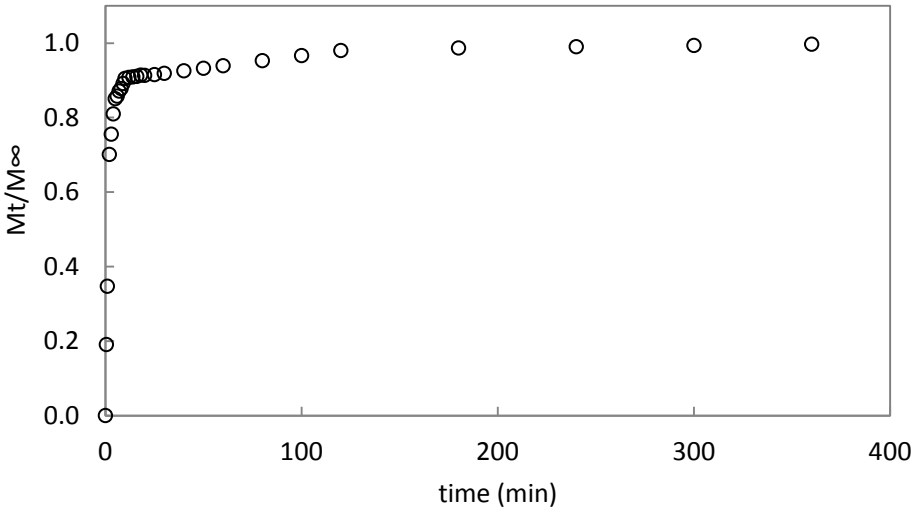

Figure 6-152 Desorption kinetics, diltiazem-HCl: 300 ppm, GA: 0.24%

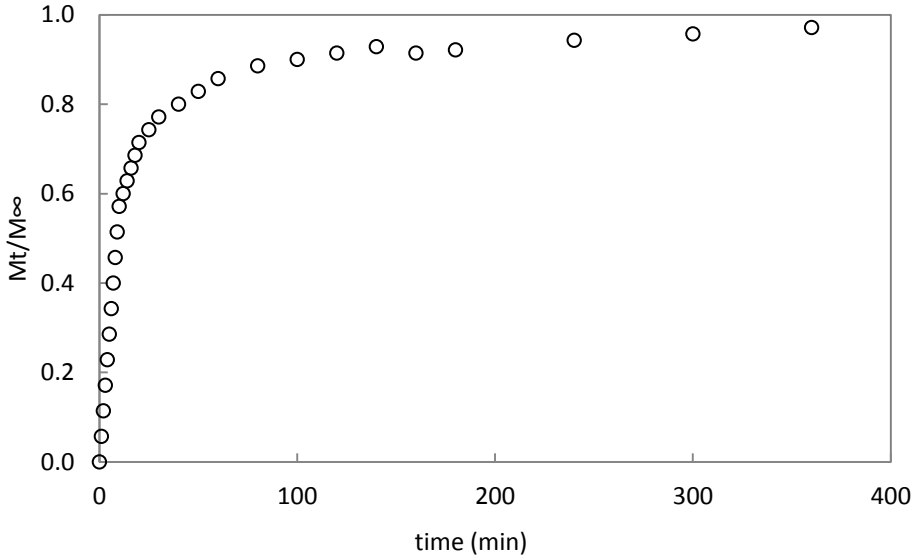

Figure 6-153 Sorption kinetics, diltiazem-HCl: 400 ppm, GA: 0.24%

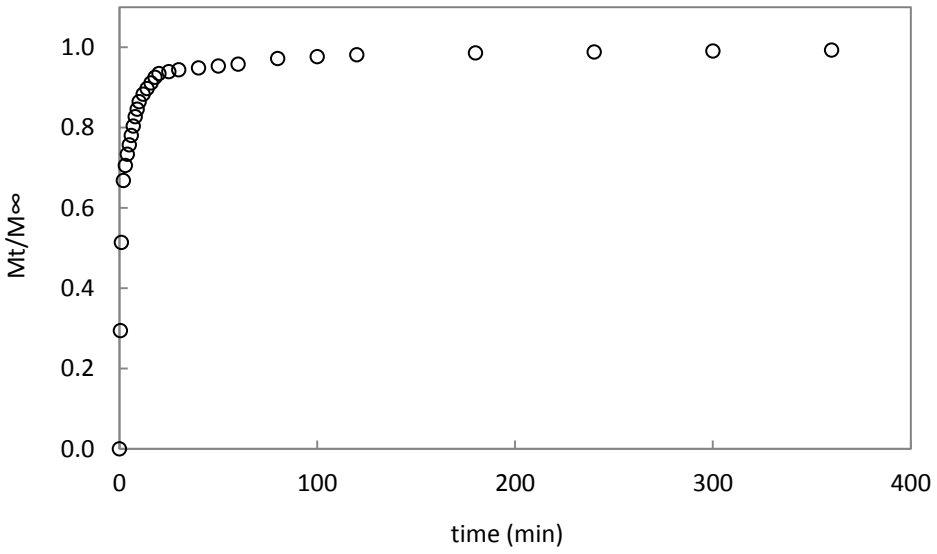

Figure 6-154 Desorption kinetics, diltiazem-HCl: 400 ppm, GA: 0.24%

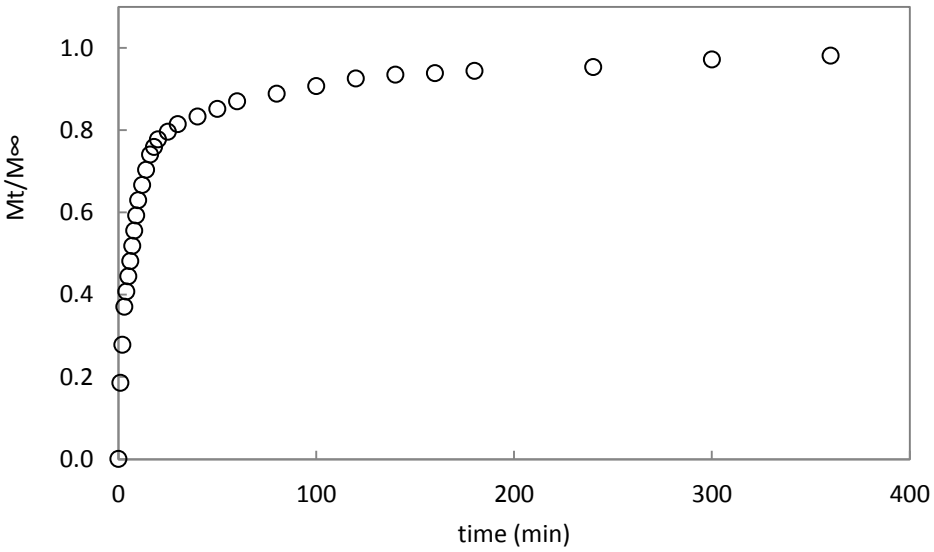

Figure 6-155 Sorption kinetics, diltiazem-HCl: 100 ppm, GA: 0.40%

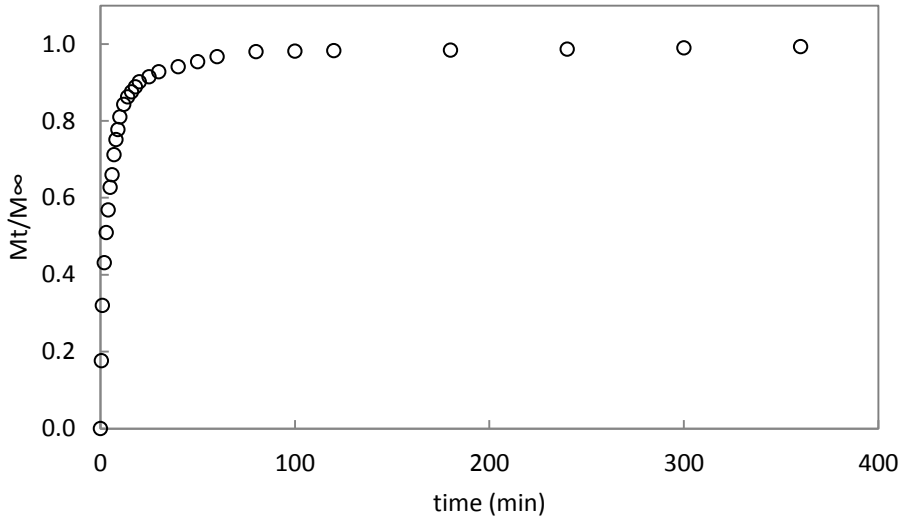

Figure 6-156 Desorption kinetics, diltiazem-HCl: 100 ppm, GA: 0.40%

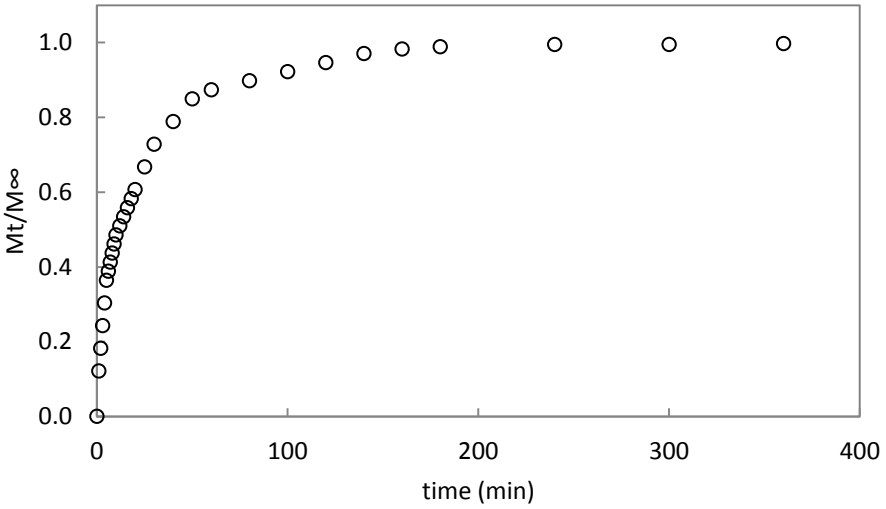

Figure 6-157 Sorption kinetics, diltiazem-HCl: 200 ppm, GA: 0.40%

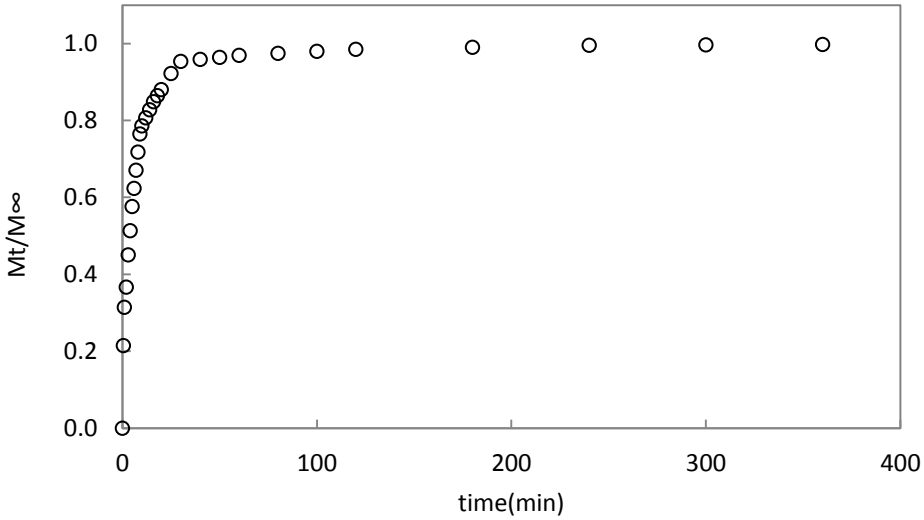

Figure 6-158 Desorption kinetics, diltiazem-HCl: 200 ppm, GA: 0.40%

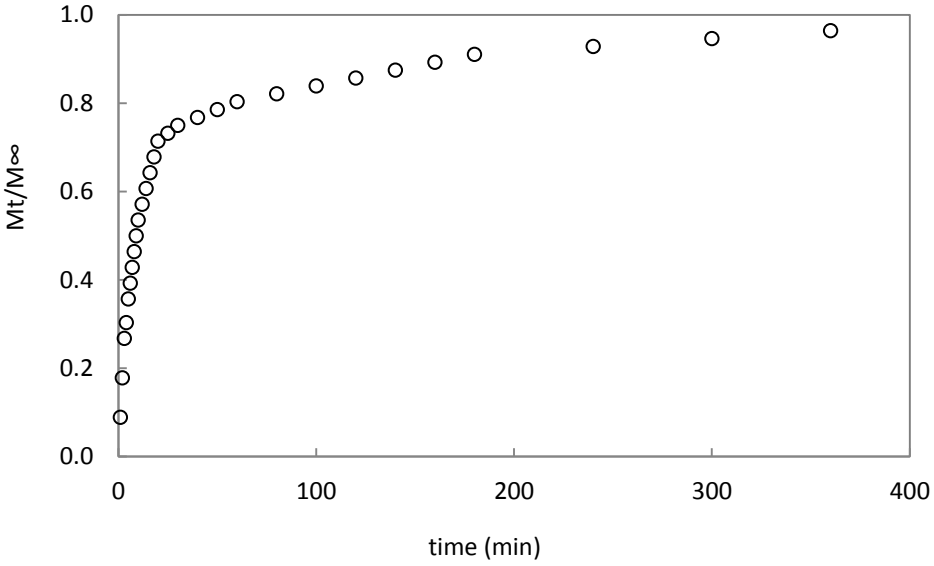

Figure 6-159 Sorption kinetics, diltiazem-HCl: 300 ppm, GA: 0.40%

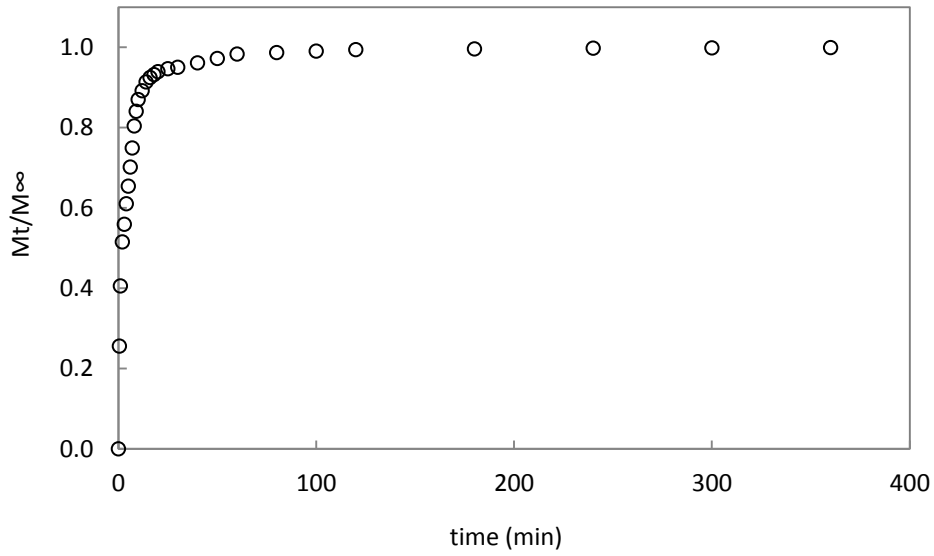

Figure 6-160 Desorption kinetics, diltiazem-HCl: 300 ppm, GA: 0.40%

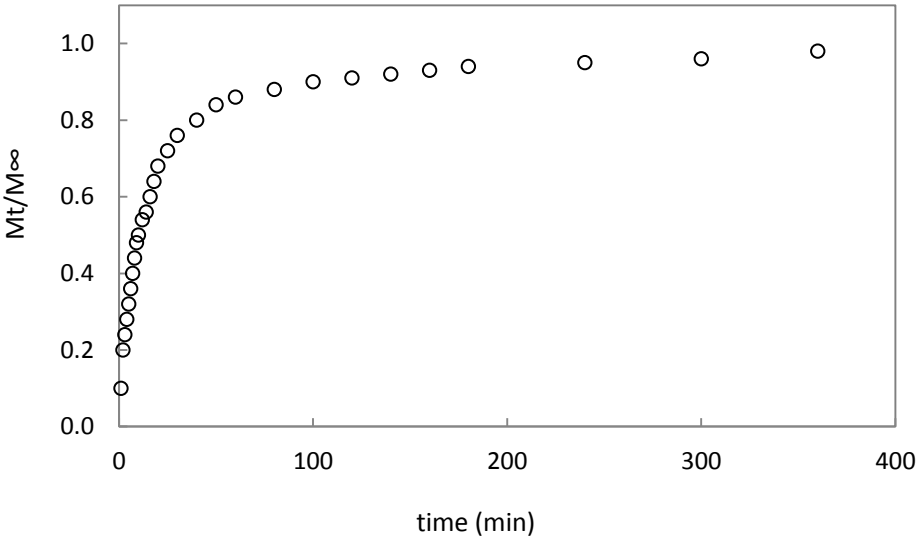

Figure 6-161 Sorption kinetics, diltiazem-HCl: 400 ppm, GA: 0.40%

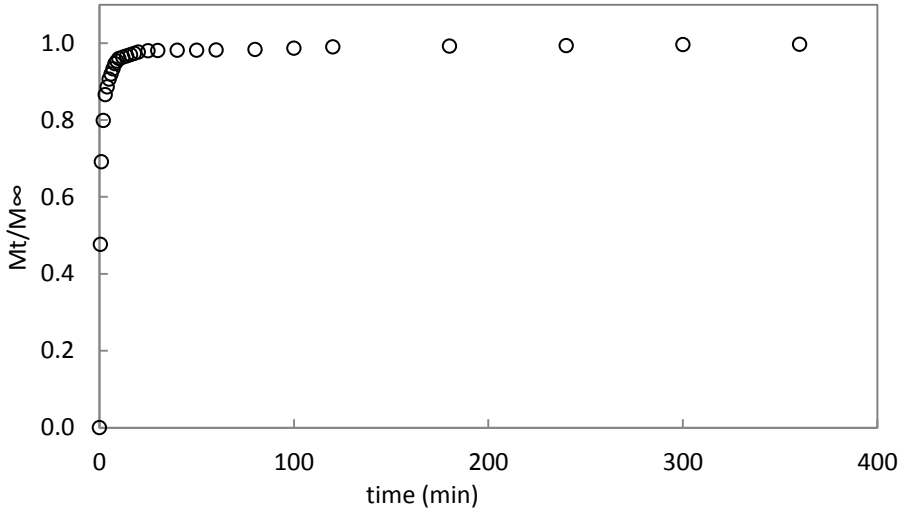

Figure 6-162 Desorption kinetics, diltiazem-HCl: 400 ppm, GA: 0.40%

Nitrofurazon

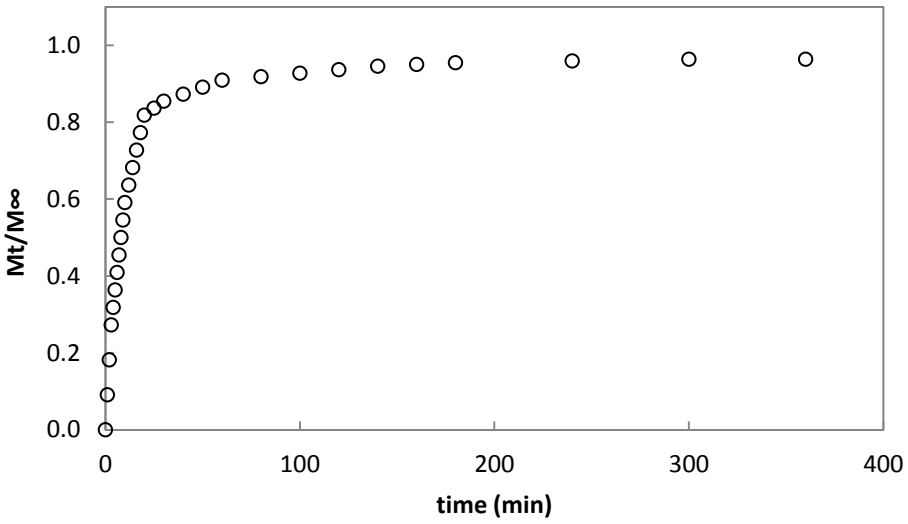

Figure 6-163 Sorption kinetics, nitrofurazon: 400 ppm, GA: 0.40%

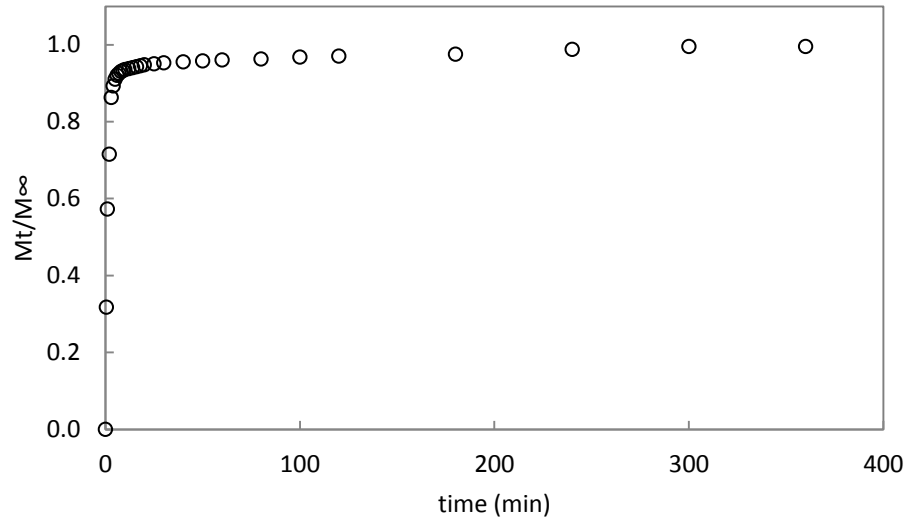

Figure 6-164 Desorption kinetics, nitrofurazon: 400 ppm, GA: 0.40%

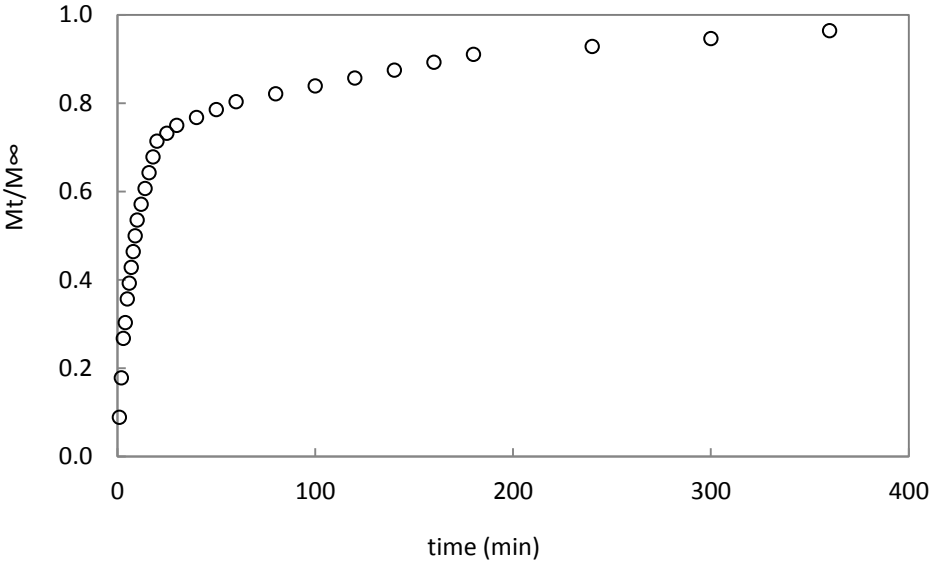

Figure 6-165 Sorption kinetics, nitrofurazon: 300 ppm, GA: 0.40%

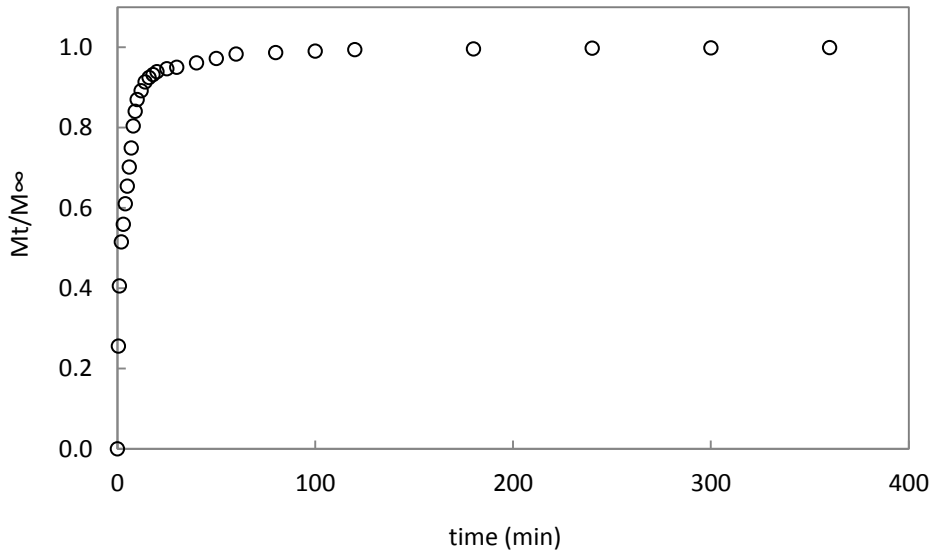

Figure 6-166 Desorption kinetics, nitrofurazon: 300 ppm, GA: 0.40%

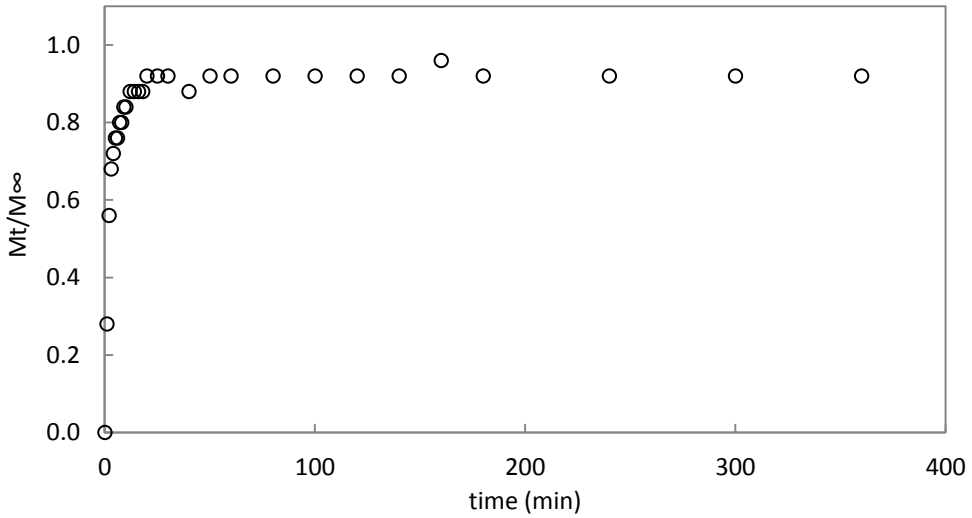

Figure 6-167 Sorption kinetics, nitrofurazon: 200 ppm, GA: 0. 40%

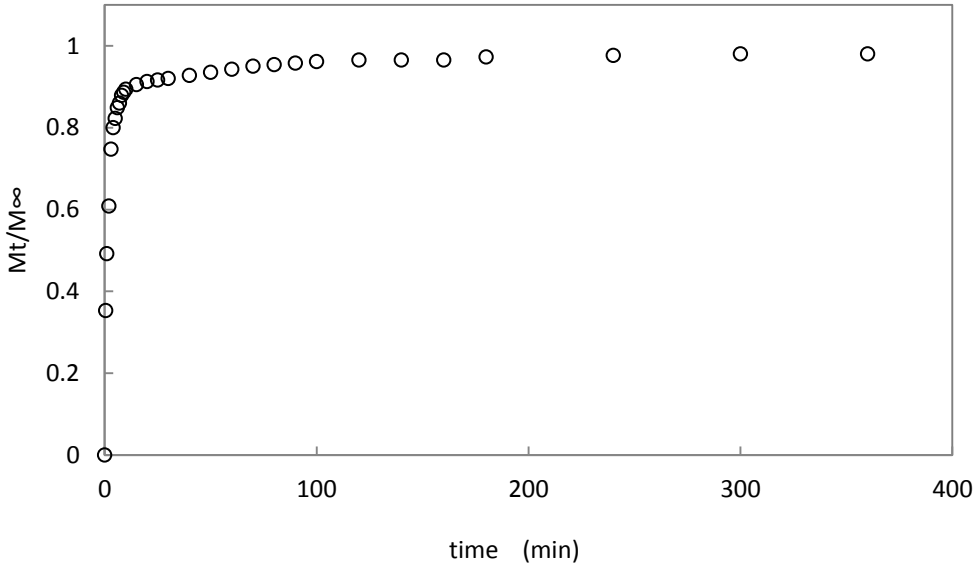

Figure 6-168 Desorption kinetics, nitrofurazon: 200 ppm, GA: 0. 40%

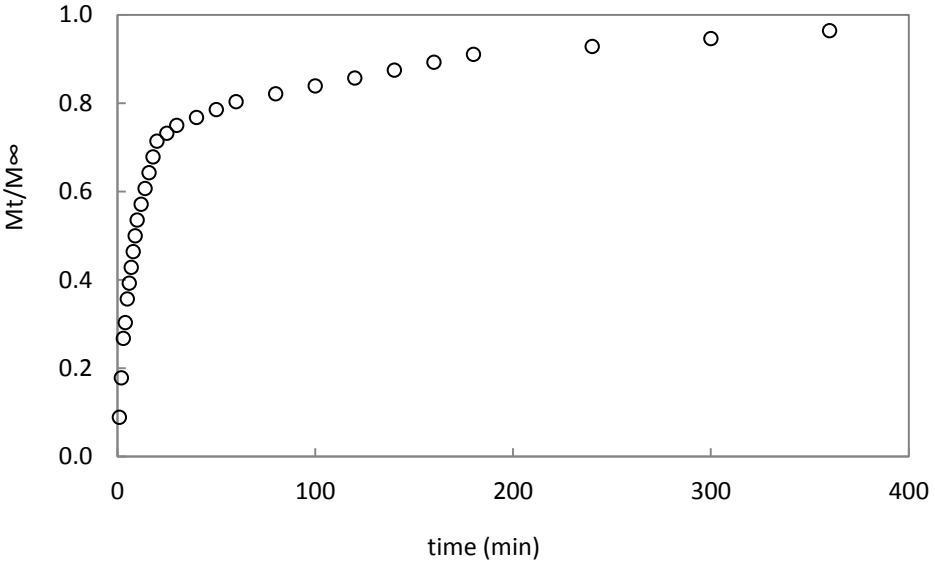

Figure 6-169 Sorption kinetics, nitrofurazon: 100 ppm, GA: 0.40%

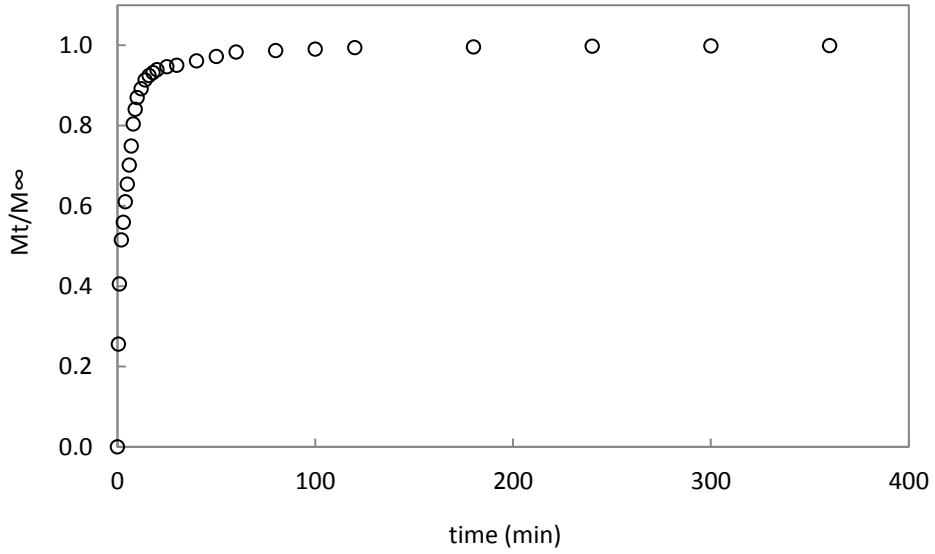

Figure 6-170 Desorption kinetics, nitrofurazon: 100 ppm, GA: 0.40%

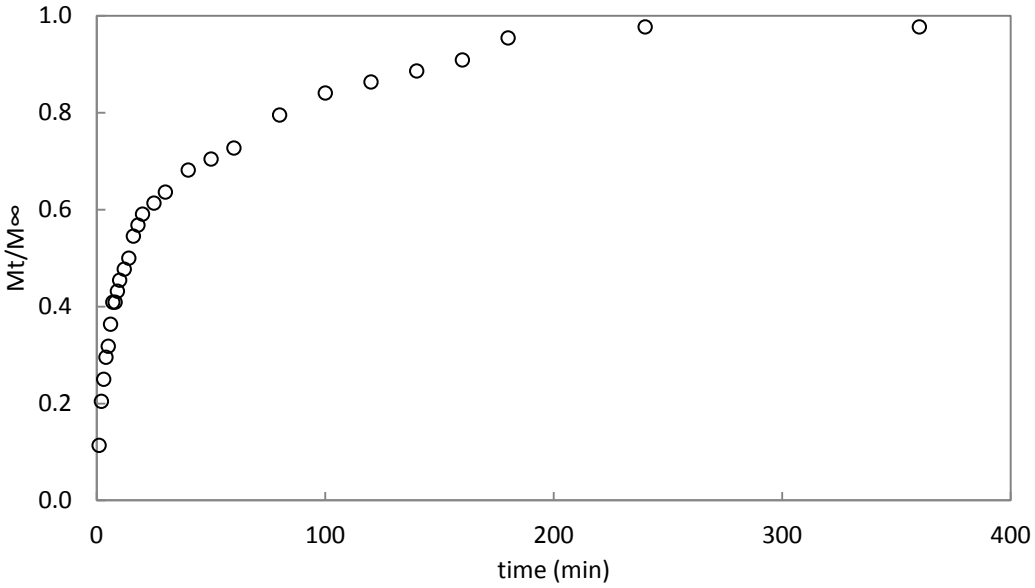

Figure 6-171 Sorption kinetics, nitrofurazon: 400 ppm, GA: 0.24%

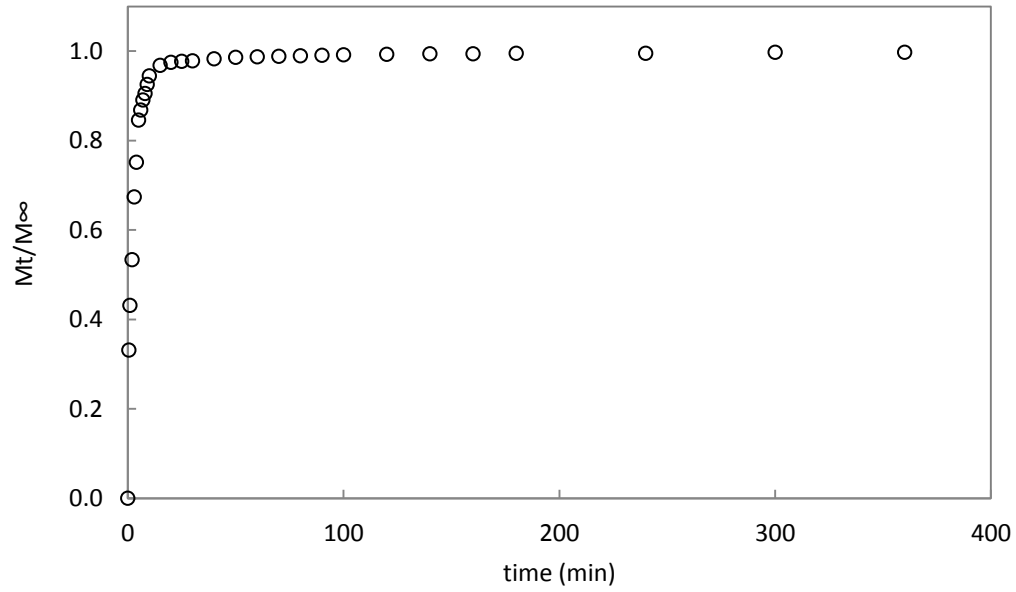

Figure 6-172 Desorption kinetics, nitrofurazon: 400 ppm, GA: 0.24%

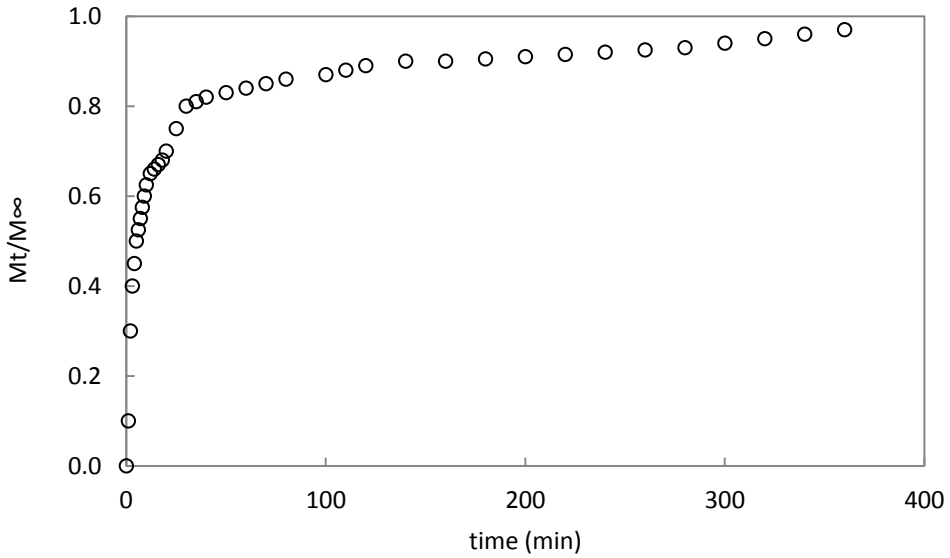

Figure 6-173 Sorption kinetics, nitrofurazon: 300 ppm, GA: 0.24%

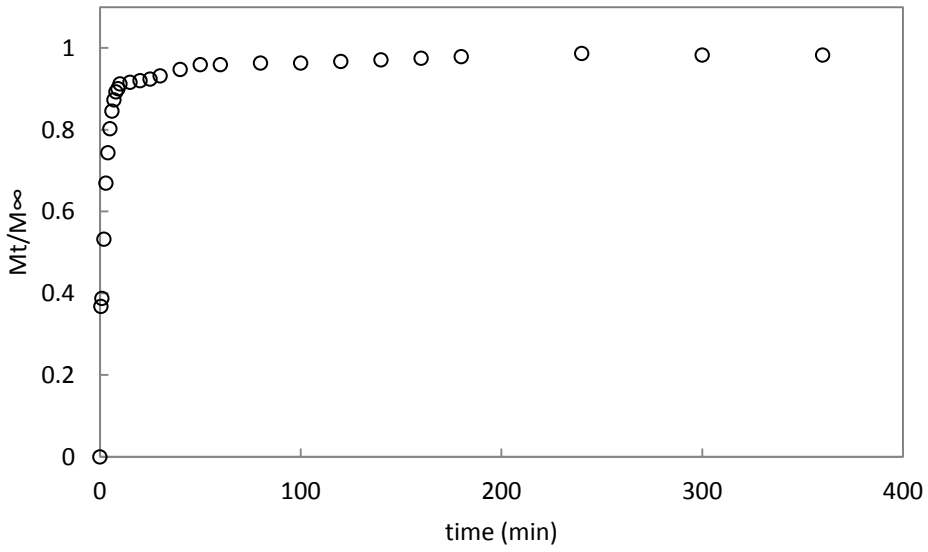

Figure 6-174 Desorption kinetics, nitrofurazon: 300 ppm, GA: 0.24%

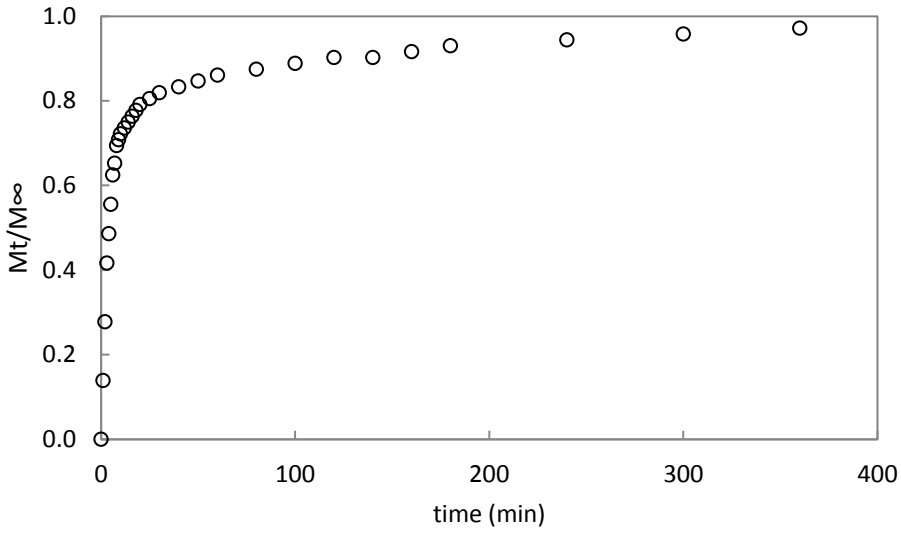

Figure 6-175 Sorption kinetics, nitrofurazon: 200 ppm, GA: GA: 0.24%

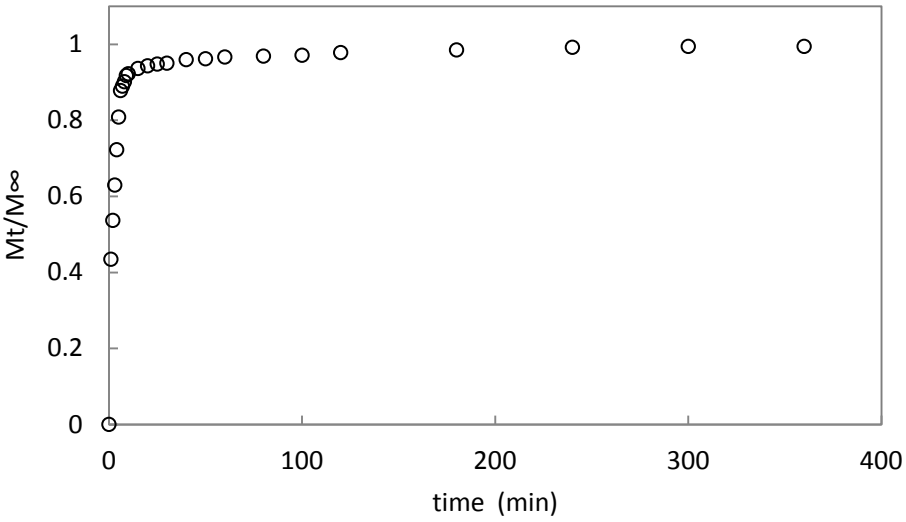

Figure 6-176 Desorption kinetics, nitrofurazon: 200 ppm, GA: 0.24%

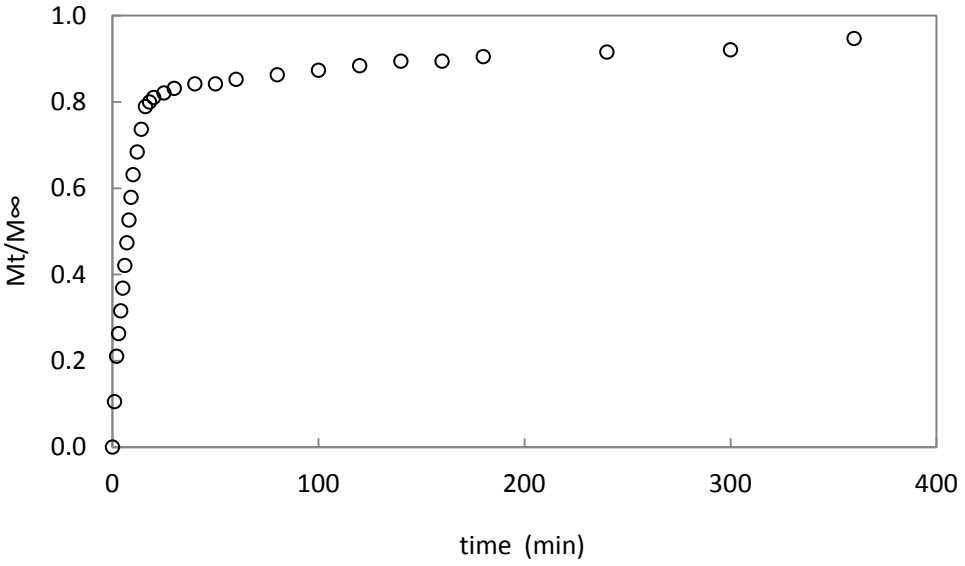

Figure 6-177 Sorption kinetics, nitrofurazon: 100 ppm, GA: 0.24%

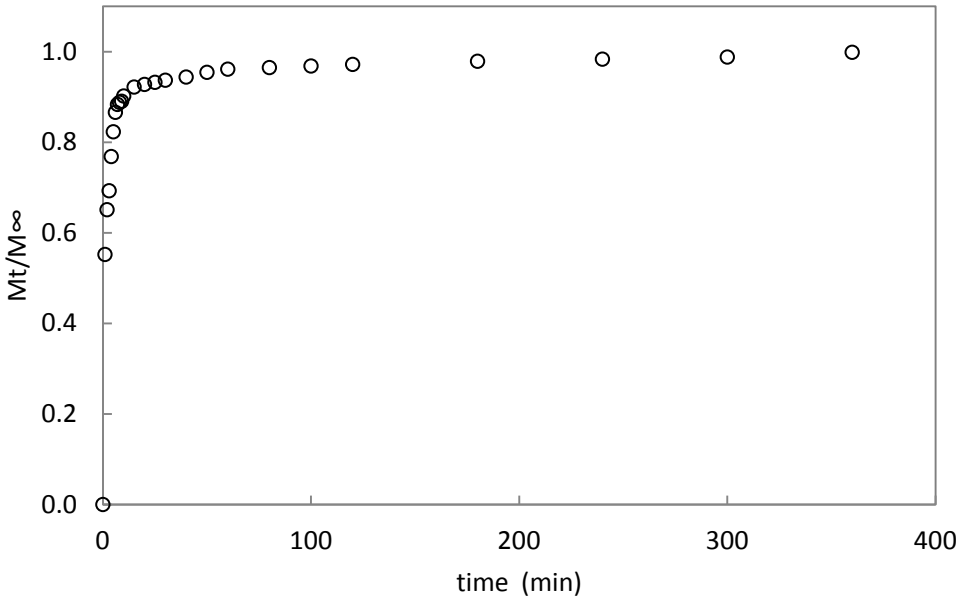

Figure 6-178 Desorption kinetics, nitrofurazon: 100 ppm, GA: 0.24%

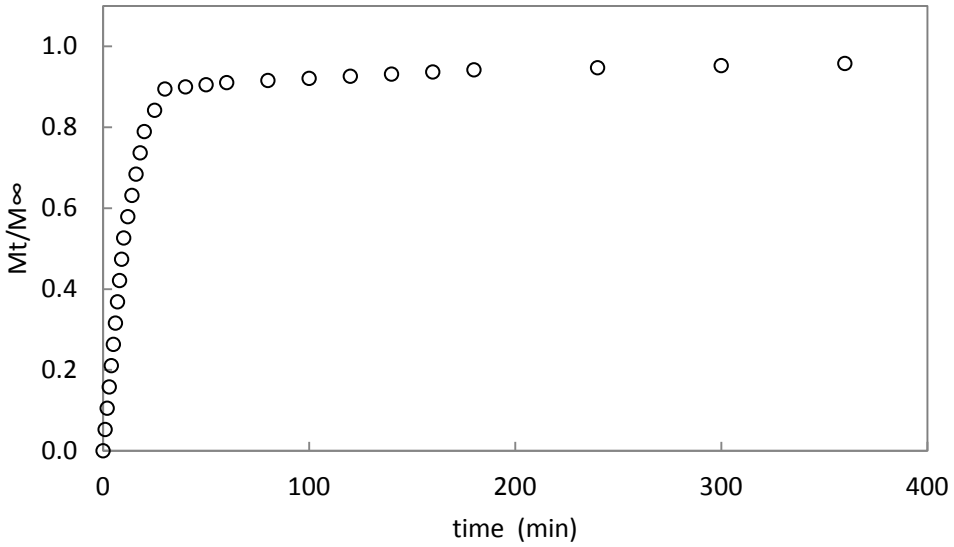

Figure 6-179 Sorption kinetics, nitrofurazon: 400 ppm, GA: 0.16%

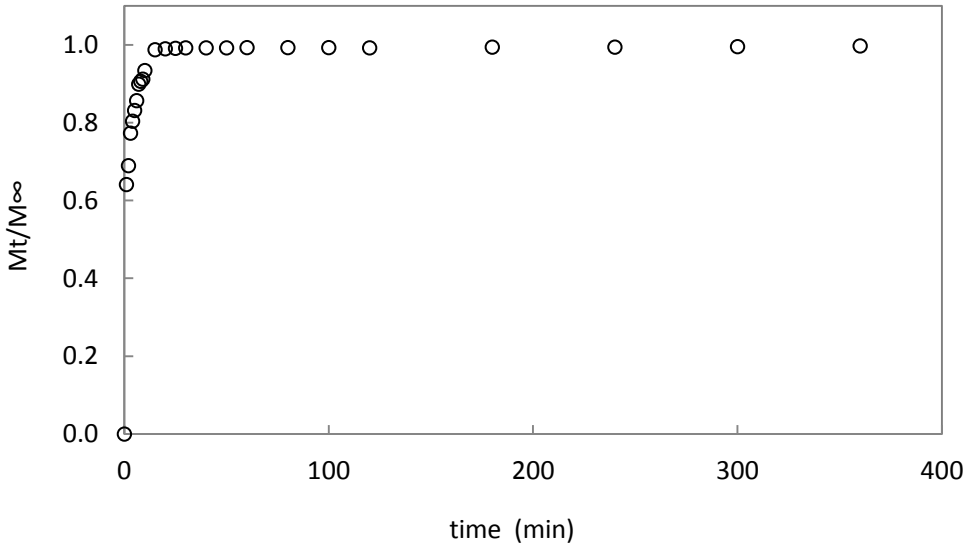

Figure 6-180 Desorption kinetics, nitrofurazon: 400 ppm, GA: 0.16%

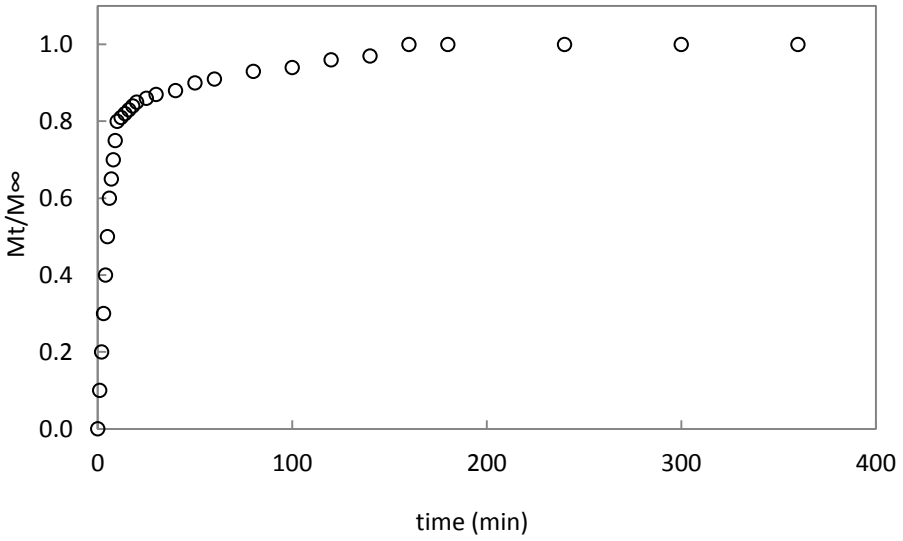

Figure 6-181 Sorption kinetics, nitrofurazon: 300 ppm, GA: 0.16%

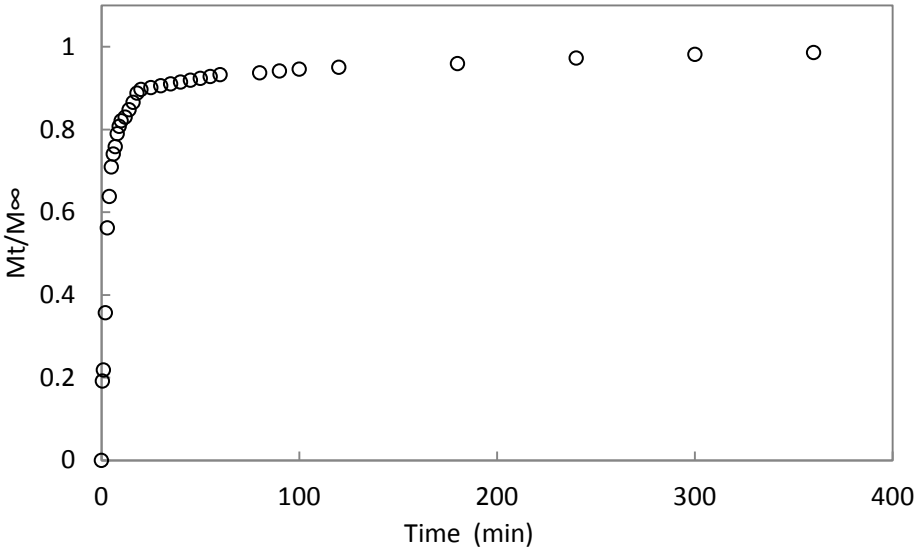

Figure 6-182 Desorption kinetics, nitrofurazon: 300 ppm, GA: 0.16%

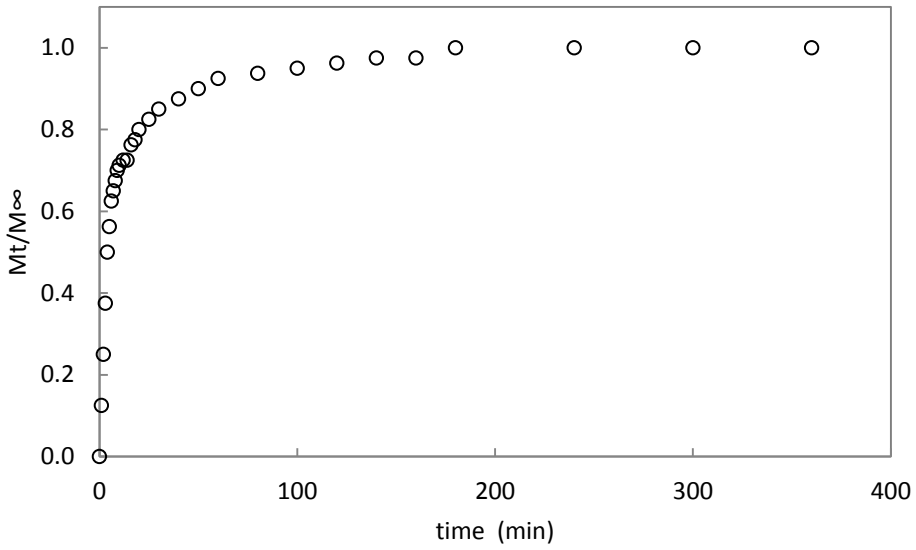

Figure 6-183 Sorption kinetics, nitrofurazon: 200 ppm, GA: 0.16%

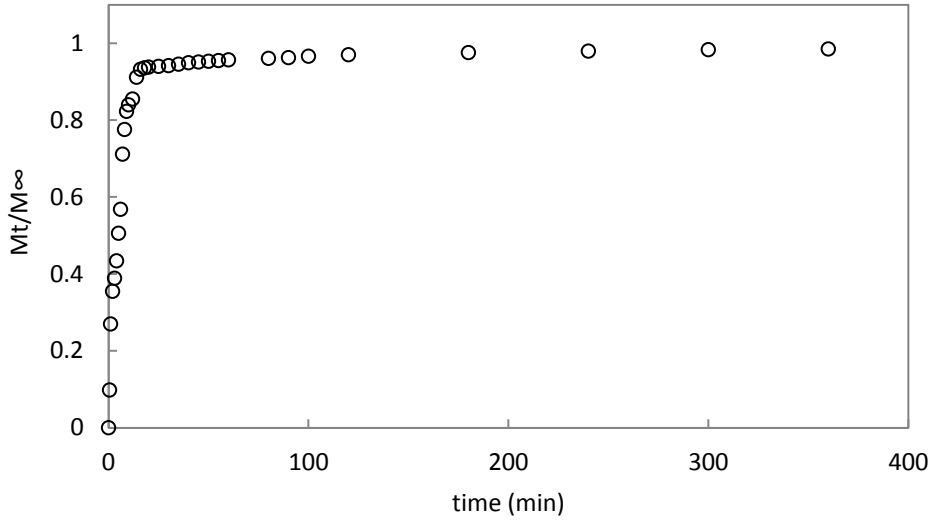

Figure 6-184 Desorption kinetics, nitrofurazon: 200 ppm, GA: 0.16%

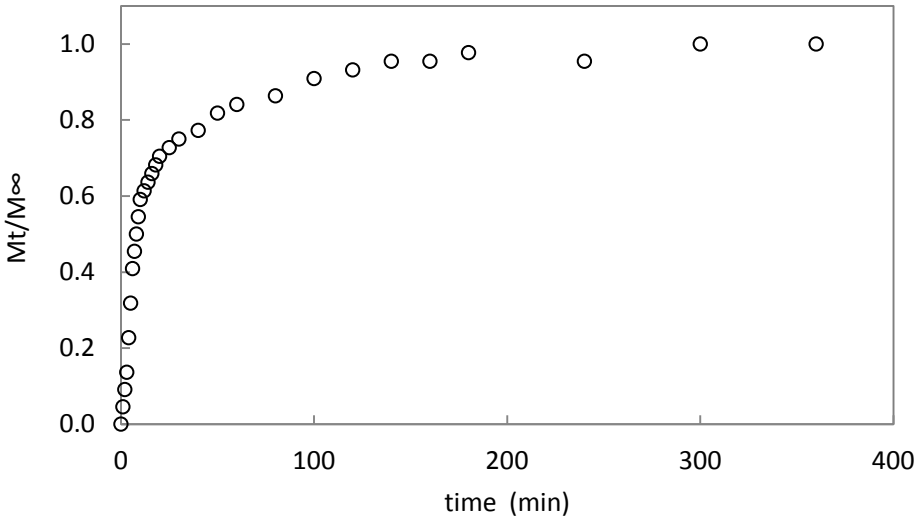

Figure 6-185 Sorption kinetics, nitrofurazon: 100 ppm, GA: 0.16%

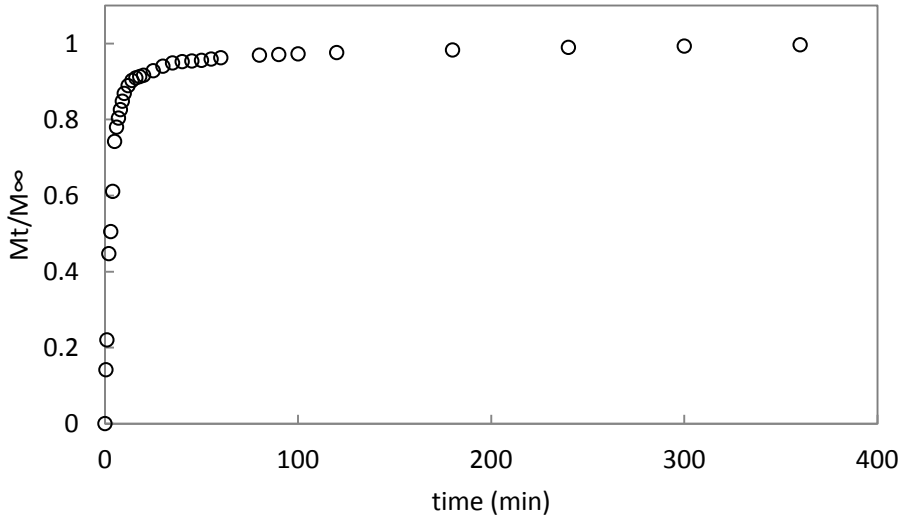

Figure 6-186 Desorption kinetics, nitrofurazon: 100 ppm, GA: 0.16%

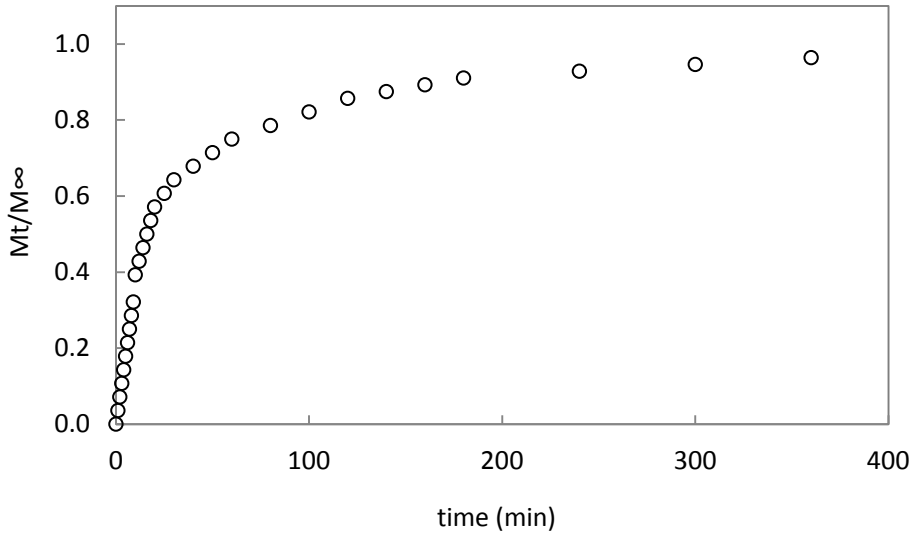

Figure 6-187 Sorption kinetics, nitrofurazon: 400 ppm, GA: 0.08%

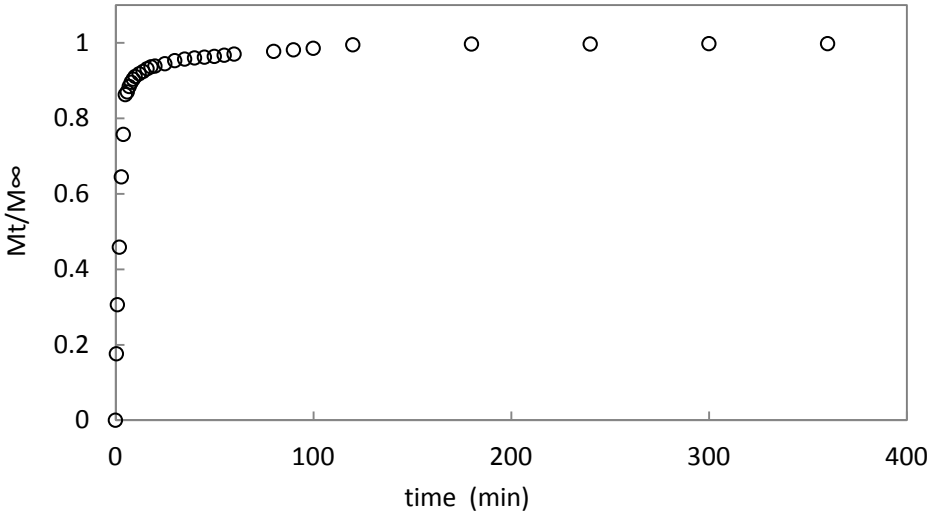

Figure 6-188 Desorption kinetics, nitrofurazon: 400 ppm, GA: 0.08%

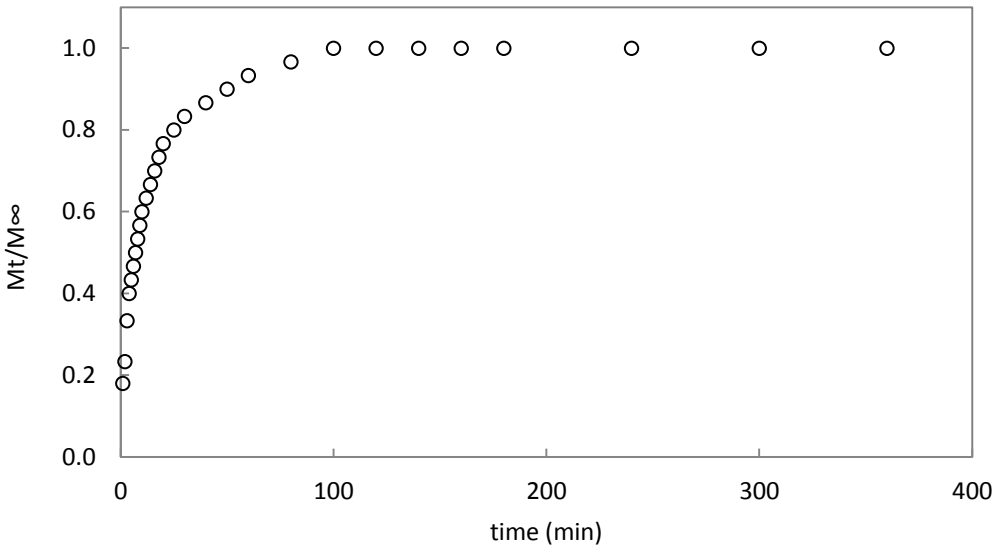

Figure 6-189 Sorption kinetics, nitrofurazon: 300 ppm, GA: 0.08%

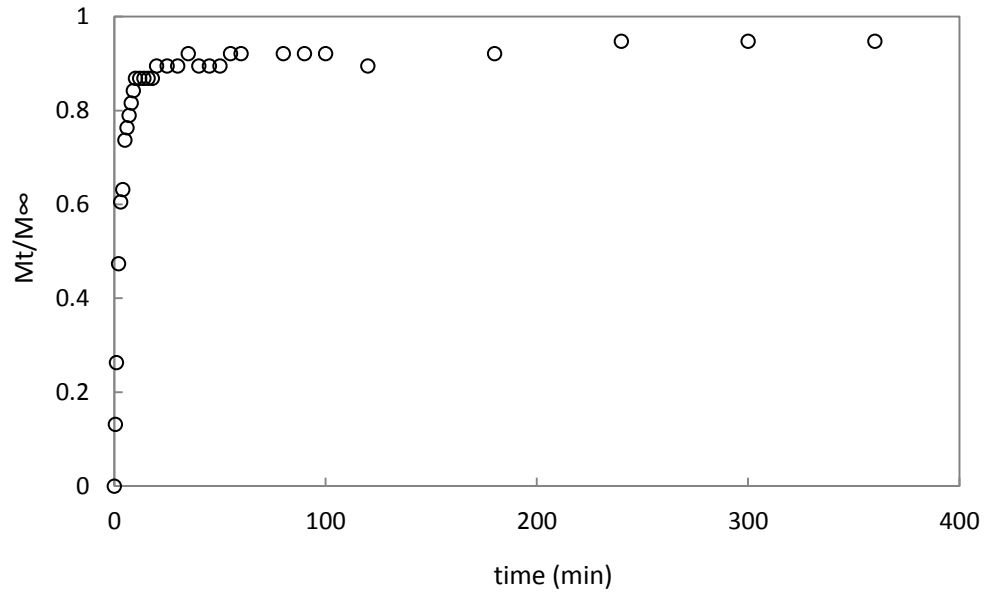

Figure 6-190 Desorption kinetics, nitrofurazon: 300 ppm, GA: 0.08%

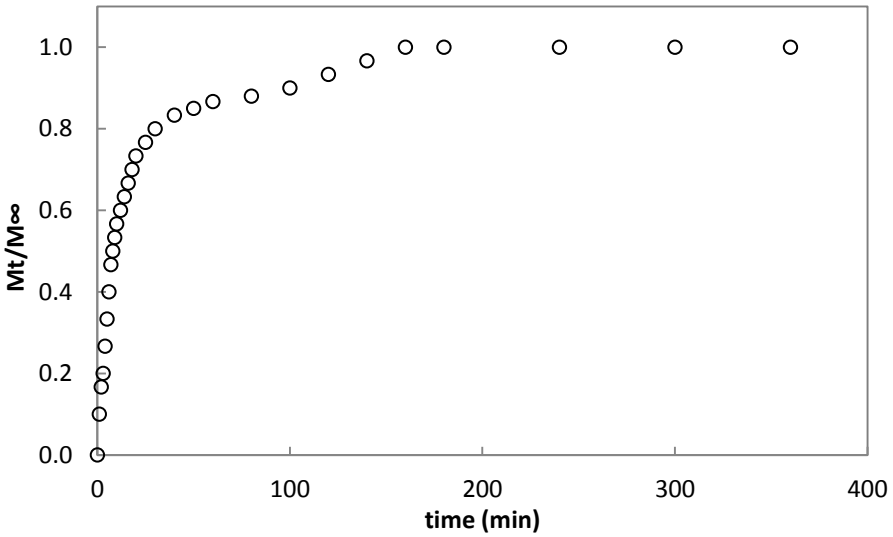

Figure 6-191 Sorption kinetics, nitrofurazon: 200 ppm, GA: 0.08%

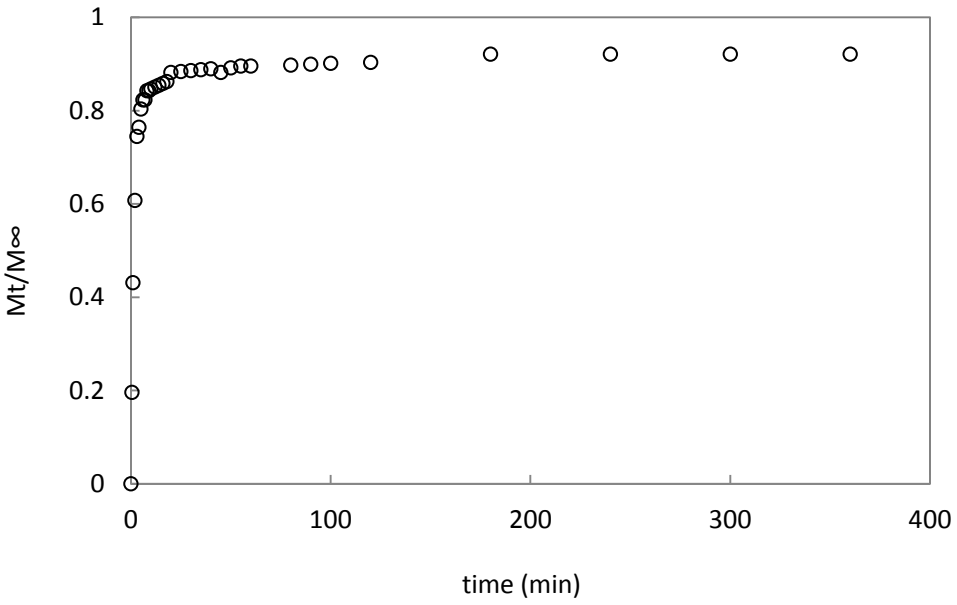

Figure 6-192 Desorption kinetics, nitrofurazon: 200 ppm, GA: 0.08%

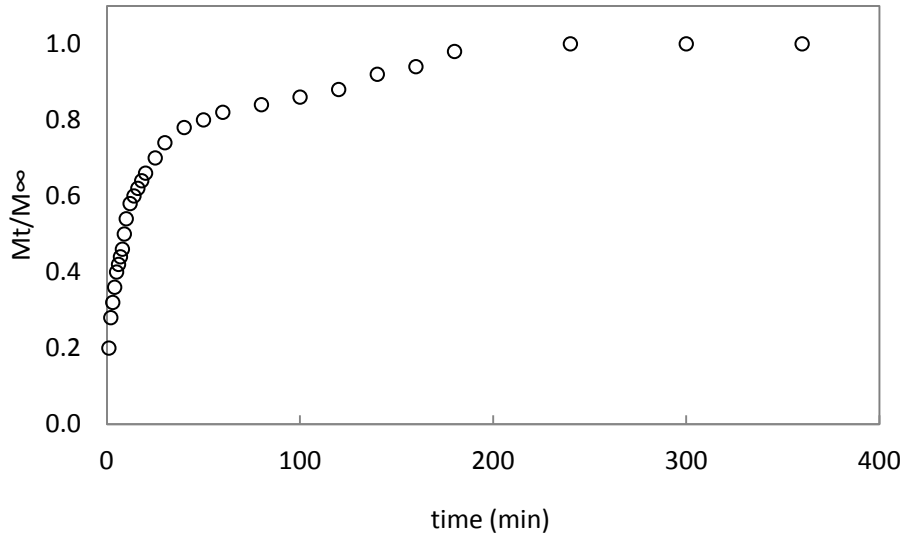

Figure 6-193 Sorption kinetics, nitrofurazon: 100 ppm, GA: 0.08%

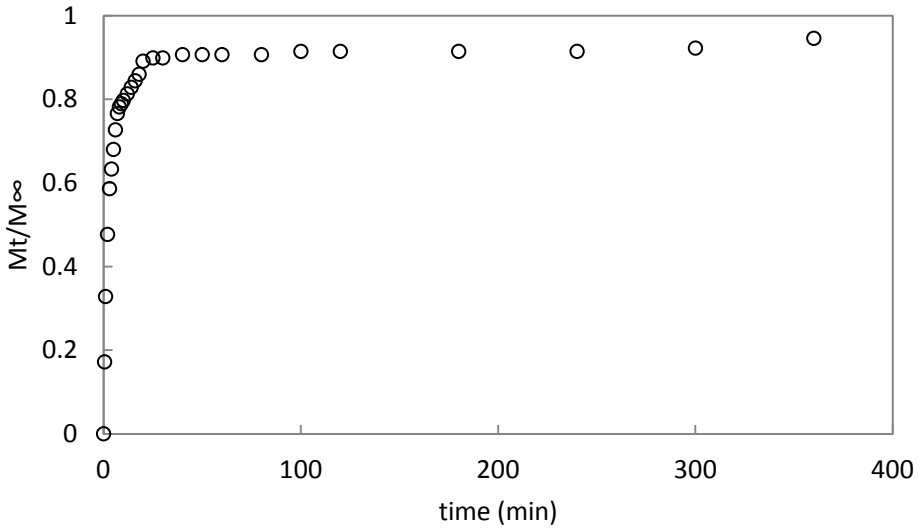

Figure 6-194 Desorption kinetics, nitrofurazon: 100 ppm, GA: 0.08%